

Eidgenössische Materialprüfungs- und Forschungsanstalt
Laboratoire fédéral d'essai des matériaux et de recherche
Laboratorio federale di prova dei materiali e di ricerca
Istituto federal da controlla da material e da retschertgas
Swiss Federal Laboratories for Materials Testing and Research

EMPA
Überlandstrasse 129
CH-8600 Dübendorf
Tel. +41-1-823 55 11
Fax +41-1-821 62 44



Swiss Contribution to Eureka Project Logchain Footprint E!2486

Schweizer Beitrag zu Eureka Project Logchain Footprint **E!2486**

Contribution Swiss à Eureka Project Logchain Footprint **E!2486**

Empa, Dübendorf, Switzerland

L. D. Poulikakos
P. Anderegg
M. Arraigada
R. Brönimman
K. Heutschi
R. Mastrangelo
G. Morgan
R. Muff
M.N. Partl
K. Sokolov
P. Soltic

RAPP Trans AG, Basel

P. Jordi
C. Petz

E. Doupal, RTSC
R. Calderara, Kistler Instrumente AG
I Schlachter, BAFU

Forschungs Auftrag:

ASTRA2004/008, BAFU TF 0111.03.04/ IDM 2003.1298, KTI P-Nr:6453.2 EUS-IW

July 2007

FORWARD

This report presents the results of the Swiss participation in a European cooperative project Eureka Logchain Footprint. Due to the multidisciplinary nature of the projects various experts have been brought together to contribute to the understanding of the environmental effect of heavy duty vehicles. The project on the European level addresses road and rail vehicles. Although this report focuses primarily on road vehicles it also addresses some common elements that are relevant to both.

In chapter 2 an overview of the relevant directives and international projects is presented. chapter 3 gives an overview of the Eureka Logchain Footprint. The Footprint Monitoring Site in Switzerland is described in chapter 4. Chapters 5 to 11 discuss various types of monitoring performed. Air pollutants are discussed in chapter 12. Chapter 13 describes the data acquisition system. Thresholds for environmentally friendly vehicles under discussion with other European partners is listed in chapter 14. A sample of collected data from WIM, noise and vibration of individual vehicles is presented and discussed in chapter 15 with data from two other footprint station outside Switzerland in chapter 16. The viscoelastic finite element model is presented in chapter 17. A report has been produced by the cost modeling work group on the European level. This report has been commented on and compared to a Swiss report addressing the same topic in chapter 18. In cooperation with the various partners from the federal departments current policy options discussed within the project is presented in chapter 19.

Various chapter have been authored by various experts in the field. Unless otherwise noted the author of the chapter is Lily Poulikakos. The document in its entirety has been edited by Lily Poulikakos and Manfred Partl.

Lily Poulikakos

Manfred Partl

July 2007

ABSTRACT

The European cooperative project Eureka Logchain Footprint E!2486 is an ongoing project that began in 2001 and it has been extended until 2008. This interim report has been prepared to document the status of Swiss participation in the project as of January 2007. The Footprint project aims to develop an innovative and cost effective method to identify road and rail vehicles by means of their environmental "footprint" as characterised by dynamic load, noise, ground borne vibration and gaseous emissions induced by the vehicle. There by producing a method for a 'true' bottom up allocation of effects of vehicles on infrastructure and environment. An important part of this project is the installation of road and rail Footprint Monitoring Sites (FMS) throughout Europe.

The first road FMS in Europe was built in June 2005 on the A1 motorway in Switzerland on a flexible asphalt pavement. This report presents the results of monitoring from this FMS and the data analysis using a finite element model. Additional information on Footprint Monitoring Sites in Austria and UK as well as information on other work groups working on the project such as cost modelling and policy options are summarized.

Dynamic loads are monitored using weigh in motion (**WIM**) sensors. The results of the WIM monitoring shows that the vast majority of the vehicles recorded on the A1 are considered to have pavement friendly axles in accordance to existing criteria i.e. < 10 t. This study focused on axle loads in excess of 10 t. The number of axles exceeding the 10 t limit is less than 6% of the total number of axles recorded by the WIM during the period under investigation.

The data from WIM of a selection of excessively loaded vehicles were further matched with the results from the stress in motion (**SIM**) sensor and used for further evaluation. These results appear largely insensitive to temperature, angle and speed of the passing vehicle.

Using a Finite Element model, stress distributions within the pavement for similar wheel loads were determined to vary from over/under-inflated Tyres by examination of the shape of the contact stress distribution under the Tyre and whether it had one peak ('n'-shaped) or two peaks ('m'-shaped). 'm'-shaped distributions resulted in higher stresses within the pavement leading to more damage.

The **acoustical** footprint of a vehicle passing by can be determined by evaluating the maximum sound pressure level received at a microphone in a distance of 7.5 m from the centre of the traffic lane. The validity of the measurement was checked by the 6 dB-down criterion. If this criterion was not fulfilled the interference stemming from neighbour vehicles was estimated and compensated for based on the level time history. A maximum correction of 6 dB(A) is allowed and if a higher correction was deemed necessary from the calculations, the measurement was categorised as invalid. Current

data from the FMS indicates that this procedure led to an increase of the percentage of pass-by events that could be evaluated successfully in the order of 95%. This result is for roads with dense traffic and an improvement can be expected for traffic that is less dense.

Ground borne **vibration** levels obtained during the measuring campaign at the FMS are not absolute as they depend on variables such as the road roughness, soil type, environmental conditions, etc. It is possible to make comparisons between vibrations produced by vehicles at this site as long as measurements are taken under the same conditions. Nevertheless, a simple comparison to reference values show that the measured vibration is low compared to the human perception threshold.

The **data acquisition** system has been a challenge while analogue and digital signals with quite different dynamics and sample rates had to be processed. They range from quasi static signals like temperature and humidity to the highly dynamic signals of wheel load distribution, which requires a sample rate of 8192 Hz to obtain reliable data at speeds up to 100 km/h. To gain readout speed, load measurement data were stored in binary form and analysed offline.

The process of matching data currently still requires considerable work and time. A way of automating the process further is required if data over longer periods needs to be efficiently matched. An alternative to improving the methods of matching the two clocks might be to ensure that the WIM and other data acquisition systems use the same clock in future. This would eliminate almost all errors due to matching, which would significantly improve the accuracy and reliability of the data.

The measurement of **gaseous emissions** in situ is not possible. Currently Euro engine ratings is used to identify the emissions of individual vehicles. However using the WIM, vehicle data and site data it is possible to obtain real life emissions data per vehicle using emissions models.

It is clear from analysis of the data that the heaviest vehicles are not necessarily the ones with the highest axle loads and causing the most damage to the pavement nor are they the noisiest or the ones causing the most vibrations. It is imperative that each vehicle is assessed separately for the various parameters that it causes. These parameters then should be compared against the environmental friendliness thresholds currently under discussion with other European partners.

A 'true' bottom up allocation of effects of vehicles on infrastructure and environment is only possible through a consistent charging scheme between the various modes of transport and between the various countries in Europe. In order to disaggregate costs so that they can be attributed countries will need to collect detailed records of maintenance and renewal expenditure, and costs due to accidents, congestion and pollution including



noise pollution and other external costs such as loss of property value and health. Further research is required on the impact transport has on the wear and tear of infrastructure and on society and the environment. To this end the current operating Footprint Monitoring Sites on the road and rail provide vital data.

ZUSAMMENFASSUNG

Das Europäisch kooperatives Project Eureka Logchain Footprint E!2486 ist ein laufendes Project das in 2001 begonnen hat und bis 2008 erweitert wurde. Dieser Zwischenbericht wurde der Status der Schweizerbeitrag an das Projekt bis Januar 2007 dokumentieren. Das Project Footprint wird innovative und kostengünstige Methode entwickeln womit Strassen- und Schienen- verkehr durch deren Umweltfussabdruck (Footprint) identifiziert werden können. Der „Footprint“ ist identifiziert als dynamischer Last, Lärm, Boden Vibrationen und Abgase die von Einzelfahrzeuge produziert wurde. Die Methode kann die Grundlagen zur Berücksichtigung der Effekte der verkehr an der Umwelt und Infrastruktur liefern. Ein wichtiger Teil des Projektes ist der Einbau von Footprint Messstationen (FMS) an verschiedenen Stellen in Europa.

Die erste Europäische FMS auf der Strasse wurde in Juni 2005 auf einen flexiblen Asphalt Belag auf der Nationalstrasse A1 im Kanton Aargau in der Schweiz gebaut. Diesem Bericht präsentiert die Monitoring Ergebnisse der FMS sowie die Daten Analyse mittels ein Finite Elemente Model. Zusätzlich wurden Informationen über andere FMS in Österreich und UK sowie die Arbeitsgruppen „Cost Modeling“ und „Policy Options“ zusammengefasst.

Der Monitoring von dynamischer Last wurde mit weigh in motion (**WIM**) Sensoren durchgeführt. Die Ergebnisse der WIM Monitoring zeigen das die Mehrheit der Fahrzeuge auf der A1 Infrastruktur freundliche Achslasten gemäss heutigen Kriterien d.h. < 10 t haben. Dieser Bericht fokussiert sich auf der Achslasten die über 10 t sind. Die WIM-Daten zeigen, dass während der Untersuchungsperiode 6% der Achslasten die 10 t Limite Überschritten hatten.

Die WIM- Daten von eine Reihe übergeladene Achsen wurde zusätzlich mit der stress in motion (**SIM**) Sensoren gematched und weiter analysiert. Diese Ergebnisse sind weitgehend gegen Temperatur, Winkel der fahrt und Geschwindigkeit unempfindlich.

Mittels der finite Elemente Model es wurde gesehen, dass Spannungsverteilung im Belag für ähnliche Radlast aber unterschiedlich gepumpte (überpumpt/unterpumpt) Pneus abhängig von Kontakt Spannungsform ist. Die Ergebnisse zeigen, dass die ein Peak Kontakt Spannungsverteilung (‘n’-formig) ergeben niedrigere Spannungen im Belag als die mit zwei Peaks (‘m’-formig) resultieren in mehr schaden im Belag.

The **acoustical** footprint of a vehicle passing by can be determined by evaluating the maximum sound pressure level received at a microphone in a distance of 7.5 m from the centre of the traffic lane. The validity of the measurement was checked by the 6 dB-down criterion. If this criterion was not fulfilled the interference stemming from neighbour vehicles was estimated and compensated for based on the level time history. A maximum correction of 6 dB(A) is allowed and if a higher correction was deemed

necessary from the calculations, the measurement was categorised as invalid. Current data from the FMS indicates that this procedure led to an increase of the percentage of pass-by events that could be evaluated successfully in the order of 95%. This result is for roads with dense traffic and an improvement can be expected for traffic that is less dense.

Die an der Messstelle gemessenen Boden **Beschleunigungen** sind nicht absolute weil sie von der Boden und Belag Eigenschaften wie Rauigkeit der Belag, Qualität der Erde, Umwelt, usw. abhängig sind. Die Vergleich zwischen den verschiedenen Fahrzeuge ist nur möglich wenn die Messungen unter gleiche Bedingungen aufgenommen sind. Eine Vergleich zwischen die gemessenen Daten und Referenzwerte zeigen, dass die Boden Beschleunigungen an dieser Messstelle unter spürbare Nivea für Menschen sind.

Die **Daten Erfassung** der FMS zeigt sich eine Herausforderung weil gleichzeitig analoge und digitale Signale mit unterschiedliche dynamisch und Erfassungsrate verarbeitet werden mussten. Die sind in quasi statischem Bereich wie in Fall von Temperatur und Feuchtigkeit bis zu sehr dynamischer Bereich wie im Fall von Kraftverteilung mit ein Aufnahme rate von 8192 Hz bei Geschwindigkeit bis zu 100 km/h sind. Für eine Beschleunigte Aufnahme die Daten wurden binär gespeichert und offline analysiert.

Den Prozess die Daten von verschiedenen Sensoren zu matchen sind noch sehr Zeit intensive. Um die Daten über eine längere Zeit zu aufnehmen muss dieser Prozess weiter durch die Anwendung der gleichen Uhr für WIM und andere Sensoren automatisiert werden. Das kann die Matching Fehler reduzieren und die Genauigkeit und Zuverlässigkeit der Datenaufnahme verbessern.

Die **Abgase Emissionen** wurden nicht in-situ gemessen. Zurzeit Euro Motor ratings wurde für die Abgase der einzelnen Fahrzeuge empfohlen. Es ist möglich mittels WIM Daten bessere Abgase Werte in Zusammenhang mit Emissionmodele zu kriegen.

Von den gemessenen Daten an der FMS ist es klar geworden, dass die schweren Fahrzeuge nicht immer derjenigen mit hohen Achslasten, hohe schaden an der Strassen verursachen oder hohe Lärmemissionen sind. Es ist nötig, dass jedes Fahrzeug für jeden Schadenparameter einzeln untersucht wurde. Dieser gemessenen Parametern sollen danach mit vorgegebenen umweltfreundliche Richtwerte vergleichen werden. Diese Richtwerte werden in Zusammenhang mit anderen Europäischen Partnern des Projektes definiert.

Eine gerechtfertige Verteilung der Effekte der Fahrzeuge auf der Infrastruktur und Umwelt ist nur möglich wenn ein konsequente „Charging“ Police zwischen die verschienen Transport mitteln und Europäischen Ländern existiert. Um die Kosten zu



unterteilen die verschiedenen Ländern müssen die Kosten von Unterhalt, Reparaturen, Unfälle, Stauung, Verschmutzung, Lärmbelastung und externe Kosten wie Gesundheitsschaden und Werteverlust von Liegenschaften in Detail dokumentieren. Weitere Forschung ist nötig, um die Wirkung von Fahrzeugen auf den Schaden an der Infrastruktur, Gesellschaft und Umwelt zu definieren. Die verschiedenen Footprint-Messstellen können für diese weiteren Datenaufnahme dienen.

RÉSUMÉ

Le projet européen Eurêka Logchain Footprint E!2486 est un projet en cours qui a débuté en 2001 et qui se prolongera jusqu'en 2008. Le présent rapport intermédiaire a été rédigé pour documenter l'état d'avancement au mois de janvier 2007 de la participation suisse à ce projet. Le projet Footprint a pour but de développer une méthode innovatrice et économique permettant d'identifier les véhicules routiers et ferroviaires au moyen de leur «empreinte environnementale» caractérisée par la charge dynamique, le bruit, les vibrations engendrées dans le sol et les émissions gazeuses. Ceci en développant une méthode de détection «bottom up» des effets des véhicules sur l'infrastructure et sur l'environnement. Une partie importante de ce projet est consacrée à l'installation de «Footprint Monitoring Sites» (FMS) sur des routes et des voies ferroviaires en l'Europe.

Le premier FMS routier a été installé en Suisse en juin 2005 sur l'autoroute A1 sur un revêtement bitumineux. Ce rapport présente les résultats du monitoring réalisé avec ce FMS et une analyse des résultats à l'aide d'un modèle éléments finis. Il fournit aussi des informations sur des sites de monitorages installés en Autriche et en Angleterre ainsi que sur d'autres groupes de travail du projet consacrés par exemple à la modélisation des coûts et aux options politiques.

Les charges dynamiques sont enregistrées à l'aide de capteurs de charge en mouvement **WIM** (Weight in Motion). Les résultats du monitoring WIM montrent que la grande majorité des véhicules enregistrés sur l'autoroute A1 peuvent être considérés comme ayant des charges par essieu ménageant le revêtement selon les critères existants, soit une charge < 10 t. Cette étude est centrée sur les charges par essieu dépassant 10 t. Le nombre d'essieux dont la charge dépasse la limite de 10 t. était inférieur aux 6% du nombre total d'essieux enregistrés par WIM durant la période étudiée.

Les données WIM de véhicules excessivement chargés ont encore été comparées avec les valeurs fournies par les capteurs de contraintes en mouvement **SIM** (stress in motion) et utilisées pour une évaluation plus poussée. Il apparaît que ces données sont largement indépendantes de la température ainsi que de l'angle et de la vitesse du véhicule lors de son passage.

En recourant à un modèle éléments finis on a déterminé la distribution des contraintes dans le revêtement pour des charges par roue similaires mais avec des pneumatiques sur-gonflés ou sous-gonflés en examinant la forme de la distribution des contraintes sous le pneumatique, cette distribution pouvant prendre deux formes, soit avec un pic (en forme de «n») soit avec deux pics (en forme de «m»). Il est apparu que les distributions en forme de «m» s'accompagnent de contraintes plus élevées dans le

revêtement et conduisent ainsi à des dommages plus importants.

L'empreinte **acoustique** d'un véhicule lors de son passage peut être déterminée en enregistrant le niveau de pression acoustique maximum reçu par un microphone placé à une distance de 7.5 m du milieu de la voie de circulation. La validité des mesures a été vérifiée à l'aide du critère «6 dB-down». Si ce critère n'était pas rempli, on estimait l'interférence provenant des véhicules voisins en se basant sur le déroulement temporel du niveau de bruit. Une correction de 6 dB (A) au maximum est permise et si une correction plus élevée est rendue nécessaire par le calcul, la mesure est considérée comme non valable. Les données courantes du FMS indiquent que cette procédure conduit à une augmentation à près de 95 % des passages pouvant être évalués avec succès. Ces résultats proviennent de routes à forte densité de trafic et une augmentation peut encore être attendue pour les densités de trafic moins élevées.

Les **vibrations** engendrées dans le sol mesurées sur le FMS au cours de la campagne ne sont pas des valeurs absolues dans la mesure où elles dépendent de variables telles que la rugosité de la chaussée, le type de sol, les conditions environnementales, etc. Il est possible de comparer les vibrations produites par les véhicules sur ce site de monitoring aussi longtemps que les mesures ont été réalisées dans les mêmes conditions. Néanmoins une simple comparaison avec des valeurs de référence montre que la fréquence des vibrations enregistrées est basse par rapport au seuil de perception humaine.

Le système **d'acquisition des données** a posé un véritable défi car il devait pouvoir traiter des signaux tant analogues que numériques avec des dynamiques et des fréquences d'échantillonnage fort différentes. Ces données vont des signaux quasi statiques tels que la température et l'humidité jusqu'aux signaux très fortement dynamiques de la distribution des charges par roue qui demandent une fréquence d'échantillonnage de 8192 Hz si l'on veut obtenir des données fiables à des vitesses atteignant jusqu'à 100 km/h. Afin d'accroître la vitesse de lecture, les données de mesure des charges ont été mises en mémoire sous forme binaire et analysées hors ligne.

La mise en correspondance de données est un processus qui demande normalement un travail et un temps considérable. Un moyen d'automatiser ce processus de mise en correspondance est de plus nécessaire si l'on veut mettre en correspondance efficacement des données récoltées sur une longue période. Une solution pour améliorer la méthode de mise en correspondance pourrait être d'assurer que le WIM et les autres systèmes d'acquisition de données fonctionnent dans le futur sur la même cadence d'horloge. Ceci éliminerait presque toutes les erreurs dues à la mise en correspondance des données et accroîtrait de manière significative leur précision et leur fiabilité.

La mesure des **émissions gazeuses** in situ n'est pas possible. Actuellement on utilise

la classification Euro des véhicules pour identifier les émissions des véhicules individuels. Toutefois, en utilisant les données WIM, les données sur le véhicule et les données d'immission sur le site, il est possible d'obtenir les émissions réelles par véhicules en utilisant des modèles d'émissions gazeuses.

L'analyse des résultats montre clairement que les véhicules les plus lourds ne sont pas nécessairement ceux qui présentent les charges par essieu les plus élevées ni ceux qui provoquent le plus de dommages sur le revêtement et qu'ils ne sont pas non plus forcément les plus bruyants ni ceux qui causent le plus de vibrations. Il est impératif d'évaluer les différents paramètres pour chaque véhicule séparément et de comparer les résultats avec les seuils de performances environnementales actuellement en discussion avec d'autres partenaires.

Une véritable détection «bottom up» des effets des véhicules sur l'infrastructure et l'environnement n'a de sens que s'il existe un schéma de taxation cohérent entre les différents modes de transport et les différents pays d'Europe. Pour pouvoir ventiler les coûts, les pays devront récolter des données détaillées sur les frais d'entretien et de réfection ainsi que sur les coûts provoqués par les accidents, les embouteillages, la pollution et d'autres coûts extérieur tels que la dégradation de la valeur foncière et de la santé. Des travaux de recherche supplémentaires sur l'usure des infrastructures et sur les effets sociaux et environnementaux seront encore nécessaires. Les sites de monitoring actuellement en place sur les routes et les voies ferroviaires fournissent des données indispensables pour cela.



TABLE OF CONTENTS

	Page
Forward	3
Abstract	4
Zusammenfassung	7
Résumé	10
Table of Contents	13
List of Figures	16
List of Tables	21
Abbreviations	22
1. Introduction	24
2. Overview of Relevant Directives and Projects	25
3. Overview of the Eureka Logchain Footprint Project; Partnership and Objectives	29
3.1. Background	29
3.2. Participation of Switzerland in Footprint	32
4. Footprint Monitoring Site in Switzerland (FMS)	34
4.1. Goals of the Footprint Monitoring Site	34
4.2. Overview	35
4.3. Inspection, Maintenance and Rehabilitation of the Footprint Monitoring Site	36
5. Weigh in Motion (WIM) Monitoring	37
5.1. Overview	37
5.2. WIM Data and Matching with other Sensors	38
5.3. Analysis of the WIM Data	44
5.4. Conclusions from the WIM Monitoring	46
6. Stress in Motion (SIM) Monitoring with the Modulas Sensor	47
6.1. Sensors Description	47
6.2. Data Acquisition (DAQ) and Analysis	47
6.3. Laboratory Experiments	54
6.4. Field Installation of the SIM	62
6.5. “Dummy” Replacement for Modulas	62
6.6. Sample Output	63
6.7. Statistical Analysis of the Road Data	64



6.8.	State of the Modulas Sensor End of 2006	67
6.9.	Conclusions and Further Work	68
7.	Deformation Monitoring	70
7.1.	Sensor Description	70
7.2.	Sample of Measurement Results	71
8.	Temperature Monitoring	73
8.1.	Sensors' Description	73
8.2.	Sample Output	73
9.	Humidity Monitoring	75
9.1.	Sensors Description	75
9.2.	Sample Output	75
10.	Acoustic Monitoring	77
10.1.	Preliminary Measurements on A2 in Reiden	77
10.2.	Strategies to Increase the Number of Valid Road Traffic Noise Events	81
10.3.	Measurements on A1 near Lenzburg (FMS)	85
10.4.	Conclusions	93
11.	Vibration Monitoring	94
11.1.	Basics of Ground Born Vibration	94
11.2.	Quantifying Vibration	96
11.3.	Vibration Measurements at the Footprint Monitoring Site	105
11.4.	Conclusions and Outlook	120
12.	Air Pollutants	121
12.1.	Background	121
12.2.	Measurement of Gaseous Emissions of Individual Road Vehicles	122
13.	Data Acquisition	125
14.	Thresholds for Environmentally Friendly Vehicles	129
15.	Sample Data of WIM, Noise, Vibration from September 2005	131
16.	Sample Data from other Footprint Monitoring Sites	136
16.1.	Rail FMS in Austria [Kalidova, M. (2006)]	136
16.2.	Road FMS in the UK [Lees, A. (2006)]	137
17.	Viscoelastic FE Pavement Model	142
17.1.	Creation of the Finite Element Model	142
17.2.	Material Properties	143
17.3.	Validation of the Finite Element Model	145
17.4.	Modelling the Road Data	152



17.5.	Potential Improvements to the Finite Element Model	161
17.6.	Conclusions and Suggestions for Further Study	162
18.	Cost Modeling	164
18.1.	Structure of Costs	165
18.2.	External Costs of Transport	166
18.3.	Summary	171
18.4.	Different Charging Regimes in Europe	172
18.5.	Conclusions	174
19.	Policy Options	175
20.	Summary, Conclusions and Outlook	178
21.	Acknowledgements	181
22.	References	182
Appendix I: Visuelle Beurteilung der Footprint-Messstelle (Vissual inspection of the FMS)		188
Appendix II: SANITY TEST MODULAS SENSOREN (6.6.2006)		190
Appendix III : Swiss 10 Vehicle Classification		193
Appendix IV : Vehicle Information used for Validation Passes		194
Appendix V : Summary Septemper 2005 Data WIM, Noise, Vibration		197
Appendix VI : Swiss Partners' Contribution to Mayer et al [2007] Status March 2007		199
	Road Weigh in Motion (WIM)	199
	Environmental noise measurements	203
	Footprint vibration measurements	213
	Definition of terms	217
	Data collection and on-line analysis	223

LIST OF FIGURES

Figure 1. 1: Alpine modal split in tones in France, Switzerland and Austria (Status 2004) where Strasse= Road and Schiene=Rail (source: www.are.admin.ch)	24
Figure 3. 1; Swiss Domestic (schweizerisch) and foreign (ausländisch) road freight vehicles (source: www.are.admin.ch)	32
Figure 3. 2: Organizational chart indicating Swiss participation in Eureka logchain Footprint where WG= Work Group	33
Figure 4. 1: Schema of the footprint monitoring site in Switzerland	35
Figure 5. 1: Lineas WIM Sensor (courtesy Kistler instrumente AG)	38
Figure 5. 2: Sample image from graphic matching of WIM and Modulas events. Vertical black line indicates an event in seconds, diagonal blue lines represent the number of centiseconds after the black line	38
Figure 5. 3: Screenshot of the Modulas and WIM event matching program in operation. Matching Vertical black line indicates a matching event in seconds, matching diagonal blue lines represent the number of centiseconds after the black line	39
Figure 5. 4: Normalized frequency plot of all wheel loads recorded by the WIM system in September 2005, compared to wheel loads which have been matched to the Modulas data.	41
Figure 5. 5: Normalized frequency plot of all speeds recorded by the WIM system in September 2005, compared to speeds which have been matched to the Modulas data.	41
Figure 5. 6: Frequency plot of speed/load combinations recorded by the WIM system	42
Figure 5. 7: Histogram of axle weights recorded by WIM during September 2005	44
Figure 6. 1: Stress in Motion (SIM) sensor Modulas with 32 channels top; schema of the cross section of the sensor, bottom	48
Figure 6. 2: Schematic of the sensor arrangement	48
Figure 6. 3: Physical interpretation of some terms from Equation [1]: a Tyre on one sensor element	49
Figure 6. 4: Example of the type of approximation made by using the Pz force distribution	50
Figure 6. 5: Graphical interpretation of Equation [1]	50
Figure 6. 6: Three-dimensional visualization of the Pz force distribution showing smooth surface and no data after the Tyre pass	52
Figure 6. 7: Three-dimensional visualization of the Fz force distribution showing more detailed surface and residual periodic error	52
Figure 6. 8: Lateral partial contact	53
Figure 6. 9: The SIM sensor embedded in a concrete slab and trafficked using	

the MMLS3	55
Figure 6. 10: Example “footprints” from the MMLS3	59
Figure 6. 11: 3D representation of force distributions in the footprints of MMLS3 Tyres at 2 bar with »m« shape distribution (top) and 6 bar »n« shape distribution (bottom), traffic direction is perpendicular to the channels	60
Figure 6. 12: Reinforcement and steel frame of the concrete element (left) and the modulas installed in the concrete element (right)	62
Figure 6. 13: Modulas replacement “Dummy” placed in the concrete element	63
Figure 6. 14: An example of load distribution of unevenly inflated dual Tyres (top) and a closely-spaced dual Tyre (bottom)	64
Figure 6. 15: Plot of wheel loads on the A1 (Sept. '06) as measured by the WIM system and as calculated from the Modulas data.	65
Figure 6. 16: Plot of wheel loads on the A1 (Sept. '06) as measured by the WIM system and as calculated from the Modulas data with 20% boundaries	66
Figure 6. 17: Plot of wheel loads on the A1 (Sept. '06) as measured by the WIM system and as calculated from the Modulas data with events colour coded by number of active channels	67
Figure 6. 18: By of end of 2006 the channels shown in blue were malfunctioning	67
Figure 6. 19: Channel Activity on the Modulas Sensor for all events in 2005	68
Figure 7. 1: Layout and principle of the installed sensors with the position of the magnets M1 ... M3	70
Figure 7. 2: Sample of deformations within the pavement most likely from a two axle vehicle passing over sensor 2	72
Figure 8. 1: Photograph from installation of temperature sensors showing their location in the pavement	73
Figure 8. 2: Figure Sample of temperature variation at three layers of the pavement at the FMS: Surface = 4 cm deep, Mid-layer = 12 cm deep and Deep = 22 cm deep from both sets of sensors	74
Figure 9. 1: Humidity sensors	75
Figure 9. 2: example of humidity monitoring at the FMS	76
Figure 10. 1: Cross sectional view of the measurement location Reiden with $d_1 = 2.55$ m, $d_2 = 6.2$ m, $d_3 = 10.9$ m, $d_4 = 12.7$ m and microphone height $h_m = 3.5$ m	78
Figure 10. 2: Measurement location Reiden. The microphone is protected with a grid basket	78
Figure 10. 3: Percentage of valid single truck measurements at station Reiden as a function of number of total vehicles (for intervals of 10 vehicles/h) on the two lanes heading south. The applied criteria are the above mentioned 6 dB down rule and a time frame of +/- 1 sec without any other vehicle on the two lanes south	80
Figure 10. 4: Percentage of valid single truck measurements at station Reiden as a function of number of total vehicles (for intervals of 10 vehicles/h)	

on the two lanes heading south. The applied criterion is the above mentioned 6 dB down rule	81
Figure 10. 5: Single pass-by measurements of passenger cars. The maximum pass-by level is shown as a function of vehicle speed	84
Figure 10. 6: Cumulative frequency distribution of the error in estimating the sound power level of a truck by compensating for the disturbing effect of a car with a level 5 dB below that of the truck	84
Figure 10. 7: Measurement location Lenzburg showing the microphone position 3 m above road level	86
Figure 10. 8: Evaluation of the percentage of events that fulfilled a 6, 5 or 4 dB down criterion.	87
Figure 10. 9: Strategy to compensate for the interfering effect of a disturbing vehicle, shown for simulated level time curves (see text). Note that only the total sound pressure can be observed by the microphone	88
Figure 10. 10: Statistics of corrections applied to the measured max values in the Lenzburg measurements. 50% of the data fulfilled the 6 dB down criterion and needed no correction. 28.4% of the data were corrected for 0 to 1 dB, etc.	89
Figure 10. 11: Statistical distribution of the evaluated maximum levels of category 5 vehicles, delivery pick ups (Lieferwagen) at Lenzburg	90
Figure 10. 12: Statistical distribution of the evaluated maximum levels of category 6 vehicles, delivery pick ups with trailer (Lieferwagen mit Anhänger) at Lenzburg	90
Figure 10. 13: Statistics of the evaluated maximum levels of category 7 vehicles, articulated delivery truck with semi-trailer (Lieferwagen mit Auflieger) at Lenzburg	91
Figure 10. 14: Statistics of the evaluated maximum levels of category 8 vehicles, freight truck (Lastwagen) at Lenzburg	91
Figure 10. 15: Statistics of the evaluated maximum levels of category 9 vehicles, freight trucks with trailers (Lastenzug) at Lenzburg	92
Figure 10. 16: Statistics of the evaluated maximum levels of category 10 vehicles, articulated freight truck with semi-trailer (Sattelzug) at Lenzburg	92
Figure 11. 1: Vehicle as source of vibration of different frequencies	95
Figure 11. 2: Propagation of the vibration in form of different waves	96
Figure 11. 3: Typical attenuation curve of the vibration amplitude (Hendriks 1996)	101
Figure 11. 4: Location and mounting of the velocity sensor at the Footprint site, A1 highway.	108
Figure 11. 5: Comparison of the vibration and WIM time stamps during a day	109
Figure 11. 6: Detailed comparison of the vibration and WIM time stamps	110
Figure 11. 7: Typical vibration signal produced by a passing by vehicle	111

Figure 11. 8: Histogram of PPV obtained during two month measuring campaign	112
Figure 11. 9: Vehicle class composition of valid measurements	113
Figure 11. 10: Intensity map of GVW and vehicle speed for vehicle class. Frequency distribution of PPV produced by each class during the two months measuring campaign.	114
Figure 11. 11: Box plot of PPV during the two months measuring campaign	116
Figure 11. 12: Summary of PPV levels of each vehicle class	117
Figure 11. 13: GVW and speed distribution of vehicles during the two months measuring campaign	118
Figure 11. 14: correlation between PPV to GVW and vehicle speed	119
Figure 11. 15: PPV correlation to GVW	119
Figure 12. 1: PM10 emissions ba category (Gehrig, 2007)	122
Figure 13. 1: Overview of the Data Acquisition System on the Swiss Motorway	125
Figure 13. 2: Data reduction in this passage by a factor of approximately 60	127
Figure 13. 3: Reference truck with total weight of 14.5 t	127
Figure 13. 4: Distribution of Tyre contact pressure in the single front Tyre (left) and the double rear Tyre (right)	128
Figure 15. 1: Maximum Gross Vehicle Weight (GVW) per day. CI=vehicle Swiss 10 class, AL=axle load	134
Figure 15. 2: Maximum Axle load per day. CI=vehicle Swiss 10 class, AL=axle load	134
Figure 15. 3: Maximum vibration per day for a single vehicle presented as peak particle velocity (PPV)	135
Figure 15. 4: Maximum noise emission per day for a single vehicle	135
Figure 16. 1: Nordbahn, track 2 @ km 14.6 north of Vienna	136
Figure 16. 2: Figure Sample of data from FMS Austria from the Acramos data acquisition system (Courtesy psiA-Consult GmbH)	137
Figure 16. 3: Figure Sample of data from FMS Austria from the Acramos data acquisition system (Courtesy psiA-Consult GmbH)	137
Figure 16. 4: Average noise level dB(A) from the FMS in the UK in November 2006 (Courtesy Department of Transport UK)	138
Figure 16. 5: Traffic vs. average noise level (Courtesy UK Department of Transportation)	139
Figure 16. 6: heaviest vehicles and heaviest axles per day in November 2006 (Courtesy UK Department of Transportation)	140
Figure 16. 7: Noise level produced by 6 axle artics vs. GVW	141
Figure 16. 8: Noise level produced by 6 axle artics vs. speed	141
Figure 17. 1: The finite element model, showing the geometry and mesh	145
Figure 17. 2: Vehicles used in the finite element model validation with the	

lengths and wheel loads shown	146
Figure 17. 3: Comparative plots of the finite element model results (run 021) and the measured data	148
Figure 17. 4: Comparative plots of the finite element model static deflection and the measured data.	150
Figure 17. 5: Comparative deflection maps constructed from simulated and measured deflection.	151
Figure 17. 6: Vertical stress distributions in a cross-section of the pavement under the Tyre (5 t)	154
Figure 17. 7: Maximum principal log(strain) distributions in a cross section of the pavement under the Tyre (5 t)	156
Figure 17. 8: Vertical stress (left) and maximum principal log(strain) (right) distributions in a cross section of the pavement under the Tyre (>7 t)	157
Figure 17. 9: Vertical stress distributions in a cross section under the Tyre (anomalies)	159
Figure 17. 10: Maximum principal log(strain) distributions in a cross section of the pavement under the Tyre (anomalies)	159
Figure 17. 11: Pz force distribution under a dual 'm'-shaped Tyre with very uneven inflation (run 67)	160
Figure 18. 1: Cost structure of the land transport sector in Switzerland in 2003 where pkm=person km and tkm=tonne km [Swiss Fed Statistical Office, ARE]	167
Figure 18. 2: Noise costs for different traffic situations (UNITE)	168
Figure 18. 3: schematic diagram of costs of climate changes (UNFCCC (http://unfccc.int/))	170
Figure 18. 4: External costs of transport in comparison between CH and the EU17 where PT=public transport (Doran et al 2005 ref?)	172
Figure A. 1: Lineas WIM Sensor (courtesy Kistler instrumente AG)	200
Figure A. 2: Geometry used by to measure noise	206
Figure A. 3: Example of the level-time history of a road vehicle pass-by event.	208
Figure A. 4: Example of the level-time history of a passing train	209
Figure A. 5: Outcome of noise measurements of a passing train	209
Figure A. 6: Vehicle as source of vibration of different frequencies	213
Figure A. 7: Propagation of the vibration in form of different waves	214
Figure A. 8: Transmission path from source to receiver	215
Figure A. 9: Measured signal, PPV and RMS (source (1))	217
Figure A. 10: Vibration versus frequency	220
Figure A. 11: Overview of the Data Acquisition System on the Swiss Motorway	225

LIST OF TABLES

Table 2. 1: Swiss allowable gross vehicle weights (GVW) and axle loads [www.admin.ch/ch/d/sr/741_11/a67.html]	27
Table 2. 2: LSVA vs. Footprint	28
Table 2. 1: Swiss allowable gross vehicle weights (GVW) and axle loads [www.admin.ch/ch/d/sr/741_11/a67.html]	27
Table 2. 2: LSVA vs. Footprint	28
Table 5. 1: Statistical summary of WIM data	45
Table 5. 2: The "Swiss 10" Vehicle Classification System (also see Appendix III)	45
Table 6. 1: Calculated Wheel Load	57
Table 6. 2: Specification of the Modulas "Dummy" element	63
Table 6. 3: Advantages and disadvantages of the different stress distribution calculation methods	69
Table 10. 1: Median and standard deviations of the statistics of maximum pass- by levels and of vehicle speed for each vehicle class	93
Table 11. 1: Main characteristics of geophones and accelerometers	99
Table 11. 2: Reaction of people and damage to buildings according to TRRL (Whiffen A. C. 1971)	103
Table 11. 3: Ground Borne Vibration limits according to US DOT (ANSI S3.29- 1983)	103
Table 11. 4: Desired specifications and specification of the vibration sensors in the A1 Footprint site	106
Table 12. 1: Description of the Euro emission ratings	123
Table 17. 1: Viscoelastic data used in the finite element model.	144
Table 17. 2: List of the events which have been used in the finite element model	153
Table 17. 3: Maximum principal stresses from the FEM (5 t)	155
Table 17. 4: Maximum principal strains from the FEM (5 t)	155
Table 17. 5: Maximum principal stresses from the FEM (>7 t)	157
Table 17. 6: Maximum principal strains from the FEM (>7 t)	158
Table 17. 7: Maximum principal stresses from the FEM (anomalies)	159
Table 17. 8: Maximum principal strains from the FEM (anomalies)	160
Table 18. 1: Overview of cost structure in both studies (change subgroup to work group)	166
Table A. 1: Minimum Data needed from a WIM System	201
Table A. 2: Factors influencing ground borne vibration values	214
Table A. 3: Specifications of the measurement equipment	221

ABBREVIATIONS

$a \rightarrow b$	defines all the Modulas active channels
API	Application programming interface
A_s	Area of each Modulas channel (=L _s B _s)
BAFU	Swiss Agency for the Environment
BAV	Federal Office of Transport
B_s	Modulas Channel width=0.015mm
C1 and C2	Parameters of the WLF shift function
FEDRO/ASTRA	Swiss Federal Roads Office
FMS	Footprint Monitoring Station
$F_z(t)$	Calculated contact force time history for Modulas
$F_{z\text{tot}}$	Total wheel force for Modulas
$G'(\omega)$ and $G''(\omega)$	the storage and loss modulus respectively
GVW	Gross Vehicle Weights
HGV	Heavy Goods Vehicles
L_s	Modulas Channel length=0.05m
LSVA	(Leistungsabhängige Schwerverkehr Abgabe) or heavy vehicle fee
N	number of discrete samples or number of terms used to approximate the results
pkm	Passenger kilometres
PT	Public Transport
P_{Tyre}	Tyre inflation pressure for Modulas
P_{Tyre}	Inflation pressure
$P_z(t)$	direct measurement of vertical contact force time history for Modulas
SD	Standard Deviation for Modulas
SIM	Stress in Motion
tkm	Tonne kilometres
TSI	Technical specifications for Interoperability
u_x	Speed for Modulas



Greek symbols

g_j , G_0 and τ_i

The prony series parameters used in ABACUS

α_θ

shift function

δt

Latch time for Modulas. This was defined as the total time, during a pass by a wheel, for which any channel was recording values of over 30 N or f-1 recording the timestep for Modulas

θ and θ_0

Temperature and the reference temperature, respectively

ω

Angular frequency

1. INTRODUCTION

The movement of additional goods associated with a single market in Europe will increase freight traffic and the resulting road maintenance costs. To reduce this impact, a better understanding of the dynamic interaction between freight vehicles and the infrastructure is required. The European cooperative project Eureka Logchain Footprint E!2486, hereafter referred to as Footprint, aims to develop an **innovative** and cost effective method to identify road and rail vehicles by means of their environmental "footprint" as characterized by **dynamic load, noise, ground borne vibration and gaseous emissions** induced by the vehicle. Eureka is a market oriented European cooperative research, and Logchain is an umbrella organization about freight movement currently comprising of 20 projects. Reducing the environmental impact of transport has a priority in Switzerland and local laws promote this policy. The result is that, as shown in Figure 1. 1, most freight in Switzerland (here shown in the alpine region) is transported via rail which is not the case in France, and Austria. This report documents the status of Swiss participation in Footprint as of January 2007.

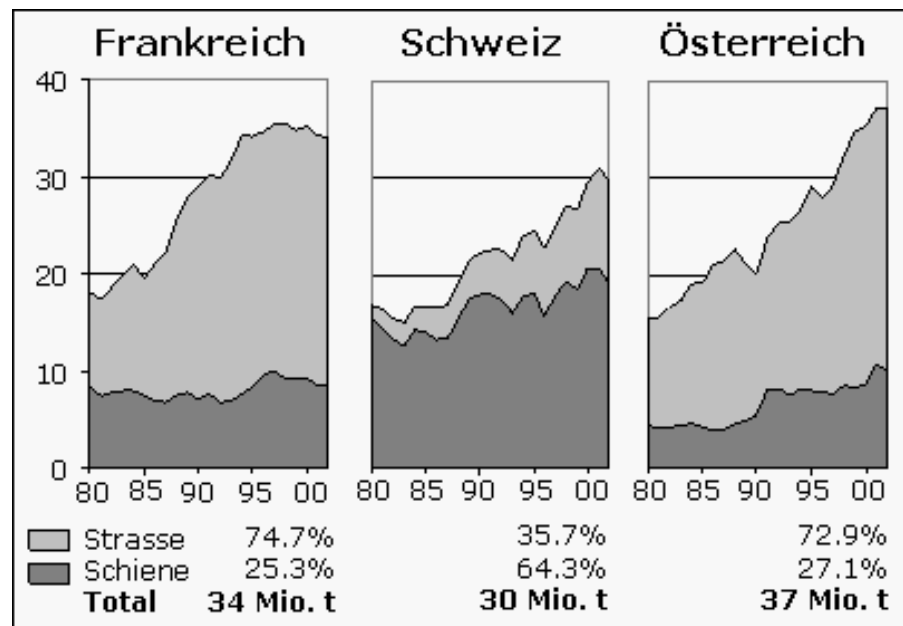


Figure 1. 1: Alpine modal split in tonnes in France, Switzerland and Austria (Status 2004) where Strasse= Road and Schiene=Rail (source: www.are.admin.ch)

2. OVERVIEW OF RELEVANT DIRECTIVES AND PROJECTS

Various European directives aim to reduce the environmental effect of freight transport. For example the directive from the European Parliament and Council on assessment and management of environmental noise was adopted in June 2002. As part of their implementation of the directive, the individual member states have to draw up strategic noise maps and action plans aimed at preventing and reducing environmental noise. This is noise from road traffic, railways, aircraft, and industrial plant. The directive contains four elements [2002/49/EC]:

- The harmonization of noise indicators and assessment methods for environmental noise.
- The collection of information about noise exposure in the form of noise maps.
- The preparation of action plans.
- Informing and consulting residents.

The European Union has also introduced the Eurovignette directive [1999/62/EC] which harmonizes levy systems vehicle taxes, tolls and charges relating to the use of road infrastructure and establishes fair mechanisms for charging infrastructure costs to haulers.

REORIENT is a project sponsored by DG-TREN of the European Commission that is aimed at enhancing the integration of European freight railway systems [www.reorient.org.uk]. As part of this project, the documents and data collected and generated are being brought together in an integrated Knowledge Base to enhance the project and to improve access to and transfer of the knowledge resources created in the course of the project.

At this half-way stage of the project, REORIENT is providing an opportunity for interested parties to learn about both the Internet-based data collection tools and the facilities in the knowledge base. These include extensive document searching, downloading of data, and some manipulation of data. In progress are thematic mapping and more visual explorations of the data.

The implementation of road access charging has been a major priority as Switzerland is a transit country. The trend in the modal split shown in Figure 1. 1 continues. In 2005 80% of freight movement through the alps moved via rail. The objective is to use true cost of transport for access charging including external costs in order to preserve the alpine region. Maximum allowable gross vehicle weight was set at 28t. This value was increased in 2005 to 40t in line with the EU as part of a bilateral treaty. The goal was to keep the price per ton for road and rail the same. The revenue has been used to update tunnels. The principle is to replace the flat fee with a non discriminate method based on distance travelled on all roads.

The LSVA (**L**eistungsabhängige **S**chwerverkehr **A**bgabe) or heavy vehicle fee was introduced in Jan 1st 2001 set at 1.1€/tkm. This value was increased in Jan 1st 2005 to 1.5 €/tkm at the same time that the maximum gross vehicle weight (GVW) was increase to 40 t. There is however a further classification as listed in Table 2. 2 according to number of axles and their configuration (www.admin.ch/ch/d/sr/741_11/a67.html). As shown in this table provisions are made for environmentally friendly vehicles. For example a vehicle with three axles is allowed to carry more if it has double axles or air suspension. Essentially all vehicles capable of carrying more that 3.5 t are charged based on the following [Krebs, 2004; Ohry, 2005]:

1. Distance travelled
2. Capacity regardless of whether the vehicle is empty or full
3. Gaseous emission Euro rating

These parameters are recorded based on available vehicle data in conjunction with an on board unit (OBU) mostly used for domestic vehicles or an electronic ID card, primarily used for foreign vehicles.

The net revenue has been considerably more than the costs. The impact of the LSVA has been overwhelmingly positive and is summarized below [Ohry, 2005]:

- Fleet adaptation
- Reduction of mileage
- Stabilization of transit
- Little change in modal split

Table 2. 1 shows how parameter considered in LSVA differ from those considered in Footprint. Both systems consider gaseous emissions and weight; LSVA considers capacity where Footprint considers weigh in motion (WIM). Distance travelled is considered by LSVA where noise and vibration are considered in Footprint. A Footprint Monitoring Station (FMS) will provide the actual environmental impact however, Implementation of an access charge based on Footprint data can be more complicated than the LSVA.

Table 2. 1: Swiss allowable gross vehicle weights (GVW) and axle loads
 [www.admin.ch/ch/d/sr/741_11/a67.html]

Configuration	Allowable GVW [t]	Special provisions
More than 4 axles	40	44
4 axles	32	
3 axle trolley bus	28	
3 axle	25...26	26 with double axle / air-suspension/ or similar
2 axle	18	
Configuration	Allowable Axle Load [t]	Vehicle in operation before 1.10.1997
Single axle	10...11.5	12
Double axle (<1.00m apart)	11.5	
Double axle (between 1.0 and 1.3m apart)	16	
Double axle (between 1.3 and 1.80m apart)	18	
Double axle (between 1.3 and 1.80m apart w. springs)	19	20
Double axle (>1.8m apart)	20	
Triple axle (<1.3m apart)	21	
Triple axle (Between 1.3m and 1.4m apart)	21	
Triple axle (>1.4m apart)	27	

The Technical Specification for Interoperability (TSI) sets threshold limits for all new build of railway vehicles and suggests imposing limits on existing vehicles whose life could be up to 40 years. In addition, the TSI sets restrictive conditions on the track profile [TSI, 2005].

**Table 2. 2: LSVA vs. Footprint**

	LSVA	Footprint
Weight	capacity	WIM
Distance traveled	considered	not considered yet
Gaseous emissions	Euro engine rating	probably Euro engine rating
Noise	not considered yet	considered
Vibration	not considered yet	considered



3. OVERVIEW OF THE EUREKA LOGCHAIN FOOTPRINT PROJECT; PARTNERSHIP AND OBJECTIVES

3.1. Background

The European cooperative project Eureka Logchain Footprint E!2486 is an ongoing project that began in 2001 and it has been extended until 2009. It aims to develop an innovative and cost effective method to identify road and rail vehicles by means of their environmental "footprint" as characterized by dynamic load, noise, ground borne vibration and gaseous emissions induced by the vehicle. The goal is to relate this footprint to the cost of maintaining the infrastructure in line with current Swiss and European policy listed in chapter 2. As of 2006, the project has 27 partners from Austria, Czech Republic, France, Hungary, Netherlands, Poland and Switzerland, with Rayner Mayer of the United Kingdom coordinating the project (www.eureka.be).

In summary, the project is innovative in the following ways:

- Use of novel data acquisition systems comprising of sensors or measuring techniques
- Identifying which vehicle types produce greatest vehicle/infrastructure interaction
- Identifying policy options which are cost effective to reduce interaction at source
- Making direct comparisons between road and rail transport modes

The work plan at the European level of Footprint is divided into six phases each comprising a number of tasks. A brief description of each phase and expected outputs are listed below:

Phase1- Analysis of existing knowledge

Expected Outputs

- Typical data characterizing infrastructure and vehicle interaction.
- Working definition of a vehicle's environmental indices

Phase 2- Modeling

- Track/vehicle interactions-The objective of this phase is computer simulation of track/vehicle interactions to establish damage to infrastructure. The models will be used to explore the range of parameters identified in phase 1 and to predict the influence of vehicle, suspension and infrastructure alignment for vehicles to be tested in phase 3.
- Acoustics-Algorithms will be developed to identify the acoustical emission of single vehicles. The main problem is to estimate and suppress the signals from the

neighbour vehicles. Specifically, mathematical computer simulation of the time history of the microphone signal located at a distance of 7.5 m and 1.2 m above ground for different configurations of vehicle chains. One crucial point is the uncertainty regarding the directivity of the sources. Implementation and evaluation of algorithms for the separation of sub-sources and suppression of the interfering effects of the neighbour vehicles. Estimation of the limits of the method.

Expected Outputs

- Models for predicting vehicle/infrastructure interactions.
- Critical vehicle and environment parameters which influence their dynamic interaction.

Phase 3- Measurements of the dynamic interaction and footprint

The objective of this phase is to develop novel ways of measuring the dynamic interaction and footprint of a vehicle with the infrastructure.

Expected Outputs

- Data base for better understanding of the damage mechanism between a vehicle and the infrastructure.
- Validation of models for simulating vehicle/track interaction.
- Methodology for measuring a vehicle's footprint for type approval and in service.
- Validation of the algorithms to separate the acoustical emissions of single vehicles. Estimation of the limit of the method.

Phase 4- Life cycle costs

The objective is to incorporate vehicle/infrastructure into a life cycle model. Using existing life cycle cost (LCC) models for roads with new data from the FMS and to develop a transparent pricing regime which reflects the external cost of the dynamic interaction.

Expected Outputs

- Data base to assess contribution of vehicle type to life cycle costs
- Data base to assess contribution of infrastructure quality to life cycle costs
- Internalize external costs and apportion amongst road users

Phase 5-Reducing the environmental impact of freight transport

The goal of this phase is to assess the options for increasing the efficiency of freight transport in terms of vehicle parameters, such as axle mass, vehicle speed, and suspension characteristics, and infrastructure parameters such as road or track alignment. The ability to convey freight by road and rail will be examined in order to optimize use of existing infrastructure capacity. The significance will be assessed of investing in long life, low maintenance infrastructure and what limits should be set on

vehicle/infrastructure interactions.

The concept of environmental indices will be refined and agreed. Criteria will be proposed for setting various classes of environmental friendliness. A range of suitable incentives will be examined in order to assess the likely impact of transforming the market for environmentally friendly vehicles and infrastructure.

Objectives

- To develop criteria for classes of environmental friendliness of vehicles and infrastructures
- To strategic options for enhancing capacity and making optimum use of existing road and rail infrastructure
- To explore options for encouraging shift of freight from road to rail

Expected Outputs

- Optimizing the use of existing infrastructure to enhance the capacity for conveying freight by rail and road
- Strategies for enhancing intermodal capability between road and rail
- Develop an outline label for vehicles and infrastructures
- Propose suitable incentives for operators and infrastructure maintainers

Phase 6- Discussions, recommendations and dissemination

Expected Outputs

- Definition of a vehicle's environmental footprint and a methodology for measurement.
- Recommendations for reducing environmental impact of freight traffic and encouraging intermodality between road and rail.
- Interim and final report

An important part of the project is monitoring of the vehicle infrastructure interaction and measuring the specific parameters listed above in a reliable, reproducible and costs effective manner. To this end Footprint Monitoring Stations (FMS), on the road and on the rail have been installed. As of 2006 there are three rail FMS in the Netherlands. The first rail Footprint station is located in Zevenhuizen in the Netherlands. This is a fully functional Footprint station using fibre optic rail Weigh in Motion (WIM), vibration and acoustic sensors (Moor '03). In the Netherlands 90% of rail vehicles are tagged and are monitored at 40 rail WIM stations.

Currently there are three road FMS' one in Switzerland and two in the UK. The first road Footprint station was built in spring 2005 in Canton Aargau in Switzerland on the major east-west motorway A1 between Zürich and Bern. Details of this monitoring site are presented in chapters 4 to 11 and chapter 15. Chapter 16 gives a summary of the UK site.

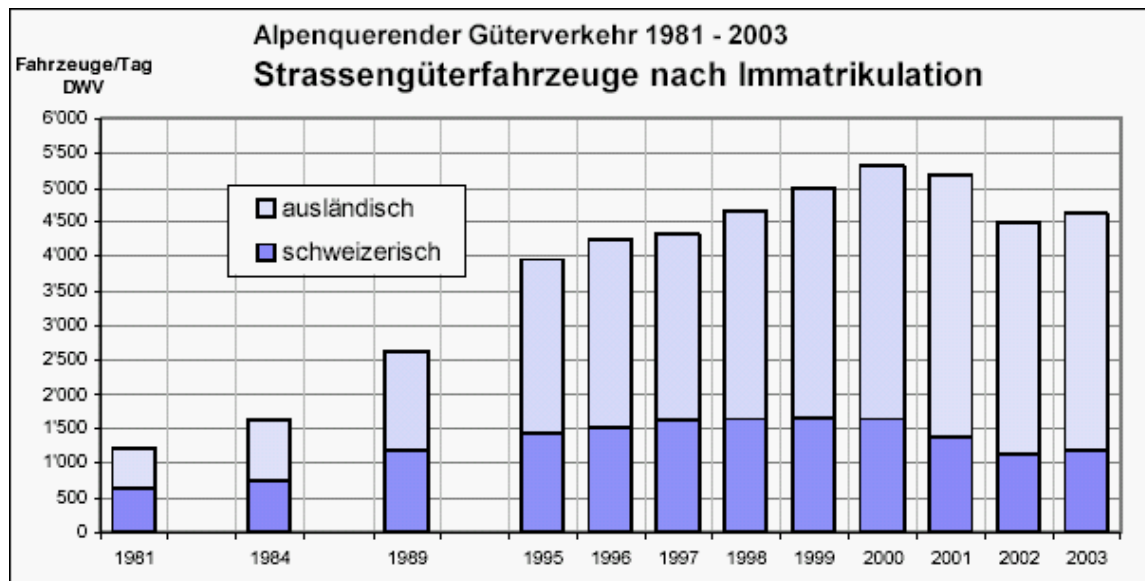


Figure 3. 1: Swiss Domestic (schweizerisch) and foreign (ausländisch) road freight vehicles (source: www.are.admin.ch)

3.2. Participation of Switzerland in Footprint

Figure 3. 1 shows the number of alpine domestic and foreign freight vehicles per day (Fahrzeug/Tag) per year. It can be seen that most of the freight through the alpine region in Switzerland is foreign. There is significant political and economic interest in determining the environmental effect of these vehicles as they pass through Switzerland. Preserving the alpine region and encouraging freight from road to rail are policies that are in place in Switzerland and the Footprint project promises to make contributions in this direction.

Vital synergies were brought together in order to make a significant contribution to all phases of this project as defined above, at the European level. Three laboratories at Empa; Road Engineering/Sealing Components, Electronics/Metrology and Acoustics, three federal departments (Swiss Federal Roads Office, FEDRO/ASTRA, Swiss Agency for the Environment, BAFU, Federal Office of Transport, BAV) and two private firms (Kistler, RTSC) are partners in the project. Six work groups (WG), listed below, have been formed to address the multidisciplinary problems addressed by Footprint. WG modelling aims to develop a vehicle infrastructure interaction model. WG FMS A1 is responsible for the installation of all the sensors of the FMS on the A1 motorway. WG policy is responsible for evaluating the policy options recommended by the European project. WG Modulas is responsible for the installation and data evaluation of the Modulas SIM sensor. WG acoustics is responsible for the acoustic monitoring and WG DAQ is responsible for the data acquisition in the project.

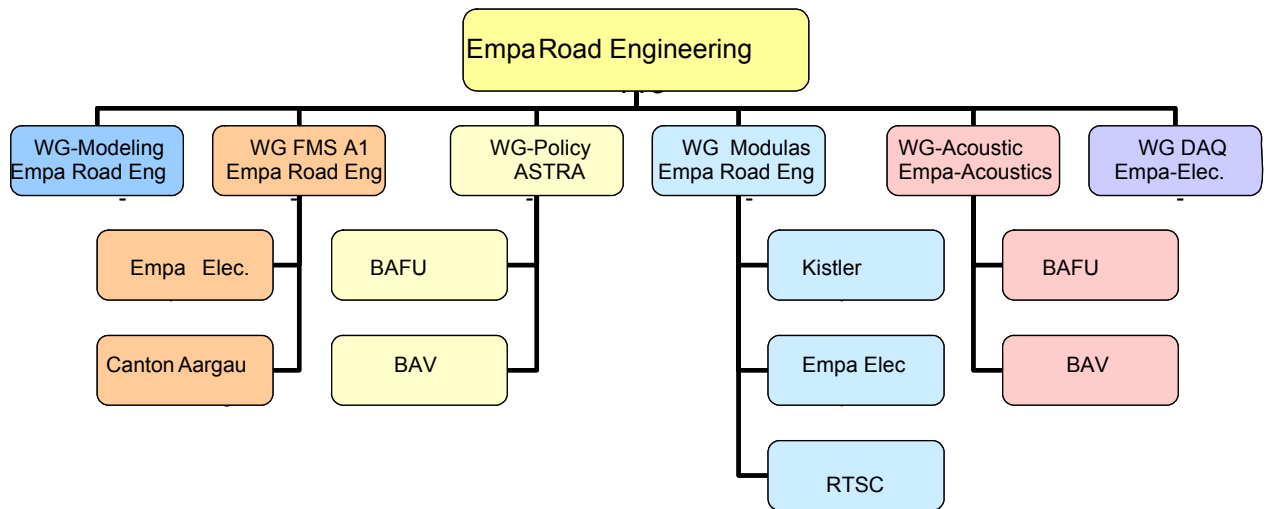


Figure 3. 2: Organizational chart indicating Swiss participation in Eureka logchain Footprint where WG= Work Group

4. FOOTPRINT MONITORING SITE IN SWITZERLAND (FMS)

4.1. Goals of the Footprint Monitoring Site

The goals of the FMS in Switzerland are the following:

1. Compile statistical data for the Eureka Logchain Footprint project.

To fulfil this goal WIM, noise and ground borne vibration (outside the road) data for heavy duty vehicles have been compiled. Noise data were acquired during a certain time interval. A threshold was set for WIM and vibration after initial measurements. The basis for this threshold was either one of or a combination of gross vehicle weight, axle load and a certain level of vibration. Only data over this threshold was stored. This data was re-evaluated and readjusted as needed within two months of the calibration date. WIM data was acquired from FEDRO/ASTRA every week via email.

2. Compile Modulas, deformation and vibration data which are relevant as input to the finite element model.

A sample based on a short term data acquisition period representing the following conditions was compiled. The model will provide the effect of the above variations on the pavement.

- Normal Tyre pressure
- Low Tyre pressure
- High Tyre pressure
- Double Tyres
- Single Tyres
- Wide vs. narrow Tyres
- Unbalanced load (left wheel vs. right wheel)

3. Evolution of plastic deformation of the pavement.

Deformation data is being extracted and stored at regular intervals.

4. Compare deformation data with vibration data.

Based on initial measurements a threshold was set to select vehicles.

5. Temperature and Humidity

A daily file is saved. The relevant data based on WIM is extracted from this file.

6. Statistical overview of pressure. Counting and classification of Tyre pressure.
Based on the results obtained in step 2, above, the need for this step will be evaluated.
7. Data storage
Daily files of WIM (from ASTRA, direction Bern) temperature and humidity and selected data as specified above will be stored on a PC at Empa for further analysis.

4.2. Overview

Several Footprint Monitoring Sites (FMS) have been built in Europe. A brief description of the FMS' outside of Switzerland is given in chapter 16. The first prototype road FMS in Europe (Figure 4. 1) was built on the A1 motorway on June 10th to 13th 2005 on a flexible asphalt pavement 3km from an existing Empa monitoring site [Raab '05]. In parallel, FEDRO/ASTRA has built a standard WIM station at this site and the on coming direction covering all four lanes using quartz-crystal WIM sensors (Doupal, Calderara '02). This site is located at a slight curve which makes it not ideal as a WIM station however it was chosen due to its proximity to a police station which could be used for static weighing and enforcement.

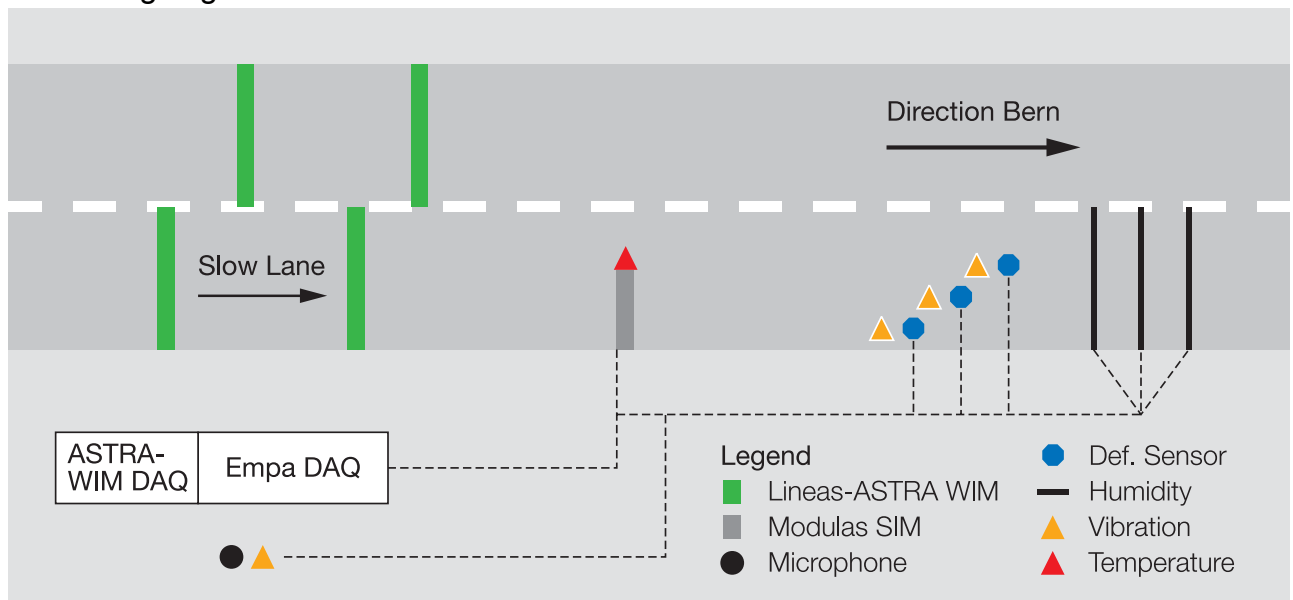


Figure 4. 1: Schema of the footprint monitoring site in Switzerland

The other Footprint sensors starting with the SIM sensor are installed 6m from the last WIM sensor on the slow lane in the direction Zürich-Bern as shown in the Figure. In addition to the prescribed Footprint parameters of dynamic load, vibration and noise also temperature, deformation and humidity at different depths of the pavement are

monitored. Gaseous emissions are not measured in situ and are not part of this monitoring site. Further details regarding the measurement of gaseous emissions are discussed in chapter 12 and are under discussion with other European partners. The deformation sensors are based on the magnetostrictive principle [Anderegg'02] and further discussed in chapter 7. Two types of vibration monitoring are done at this site. First, accelerometers were placed temporarily 4cm below the pavement. Second, one geophone is placed on the side of the road at the same location as the microphone as further discussed in chapter 11. The main purpose of the microphone and the geophone is to perform a comparison to rail emissions and therefore, the location of these sensors is based on the ISO standards, 7.5m from the centreline of the slow lane [EN ISO 11819-1, 1997].

An important part of this project is the installation of two prototype stress in motion (SIM) sensors, Modulas, that deliver the tyre footprint characteristics in terms of vertical contact pressure between tyre and road surface, as discussed in chapter 6. Noise, temperature and humidity monitoring are further discussed in chapters 10, 8 and 9 respectively.

4.3. Inspection, Maintenance and Rehabilitation of the Footprint Monitoring Site

Since its installation in June 2005 the FMS was inspected in April 2006 after heavy rainfall in the area. As shown in Appendix I the sensors and cables were found in good working condition. No excessive rutting or cracks that would affect the sensors were observed. Two screws on the SIM sensor had to be fastened.

The 64 channels of the SIM sensor were inspected by a "sanity test" using the available data as shown in Appendix II. In a first step the data from several results of each channel was added in order to establish if any channel registers systematically a lower signal. In a second step a representative result of each channel is checked for sensibility. Through the "sanity test" it was shown that as of spring 2006 the 64 channels of the SIM sensor were active without showing any systematic measurement deviations. Additionally, The WIM sensors are inspected and calibrated every year as discussed in chapter 5. The FMS has been and will be inspected at least once a year for the duration of its life.

5. WEIGH IN MOTION (WIM) MONITORING

(Authors: Gerald Morgan, Lily Poulikakos)

5.1. Overview

For WIM measurements Lineas sensors made from silicon-dioxide, SiO₂, and manufactured by Kistler are used. At the FMS site both lanes are covered each containing two rows of three sensors (Figure 4. 1, Figure 5. 1). In addition, the same set up is used for the traffic in the opposite direction (Bern to Zürich).

Quartz based sensors have shown unique qualities as they are electrically and mechanically stable, temperature influences are negligible, show uniform sensitivity over the entire sensor, display a wide measurement range and results are speed independent. The sensors are fully embedded in the pavement with no screws or frames, using a special grout consisting of a two component epoxy and quartz sand allowing decoupling from lateral forces. Lineas sensors can be ground flush if cracks or ruts occur in the pavement. A relatively small intrusion of 55 mm depth x 72 mm width in the pavement is needed. The length of the sensors can be 0.75 m or 1.0 m. At the FMS the sensors are 0.75 m.

A wheel rolling over the Lineas applies vertical forces to the quartz crystals in the sensor, with virtually no deformation. The piezoelectric quartz discs yield an electrical charge proportional to the forces applied (Figure 5. 1). The piezoelectric sensitivity is virtually independent of temperature, time and speed. The electric charge signals are converted by a charge amplifier into exactly proportional voltages that can be further processed as required. The accuracy of the measured wheel load is not influenced by Tyre type, Tyre quantity or Tyre pressure. In the case of dual Tyres, the Lineas measures one signal and expresses it as one wheel load, which is equal to the sum of both wheel loads (www.kistler.com).

The WIM sensors at this site record on the average 3700 heavy goods vehicles (HGV) per day and deliver axle load, gross vehicle weight (GVW), speed, axle distance and vehicle length with very good accuracy at this particular site. The sensors are calibrated once a year normally in the Fall as reported by Mastrangelo (2005, 2006). The accuracy class as defined by COST 323 (1999) for the FMS location in 2005 was B(10) and in 2006 A(5).

Detail of the data acquisition can be found in chapter 13.

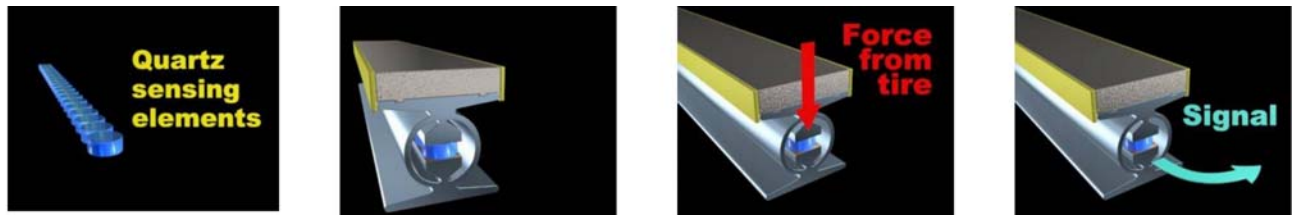


Figure 5. 1: Lineas WIM Sensor (courtesy Kistler instrumente AG)

5.2. WIM Data and Matching with other Sensors

While all the sensors such as the Modulas SIM sensor and the Balluff displacement sensors use a single data acquisition system maintained by Empa, the WIM uses the 'Marksman 660' vehicle categorization and data-logging system.

In order to record different parameters monitored for the same vehicle it is important to match the data produced by the various sensors. A problem was encountered when it came to matching the data recorded by these two systems as the data was recorded with reference to separate clocks which were moving at noticeably different speeds and being checked and corrected at different times. As the WIM data acquisition is separate from the rest of the sensors it was not possible to synchronize the clocks.

In order to match the data, a computer program was developed using Perl which was able to display the data visually, as a bitmap image such as Figure 5. 2. The images are produced at a resolution of 1 pixel to one second, allowing reasonable lengths of time to be visualized. If any given second contains an event, it is drawn as a vertical black line on the image. The finer matching is done using diagonal blue lines representing the number of centiseconds after the black line. For example, if an event occurs 77 centiseconds after a given second, the blue line will meet the black line 77% of the way up, and touch the edge of the image 77 pixels from the black line. Figure 5. 3 shows the program in operation.

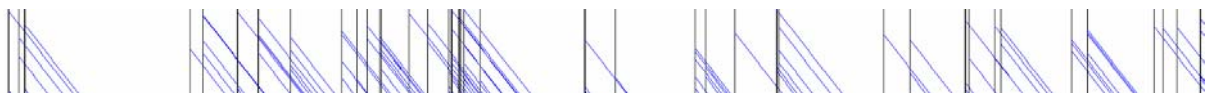


Figure 5. 2: Sample image from graphic matching of WIM and Modulas events. Vertical black line indicates an event in seconds, diagonal blue lines represent the number of centiseconds after the black line

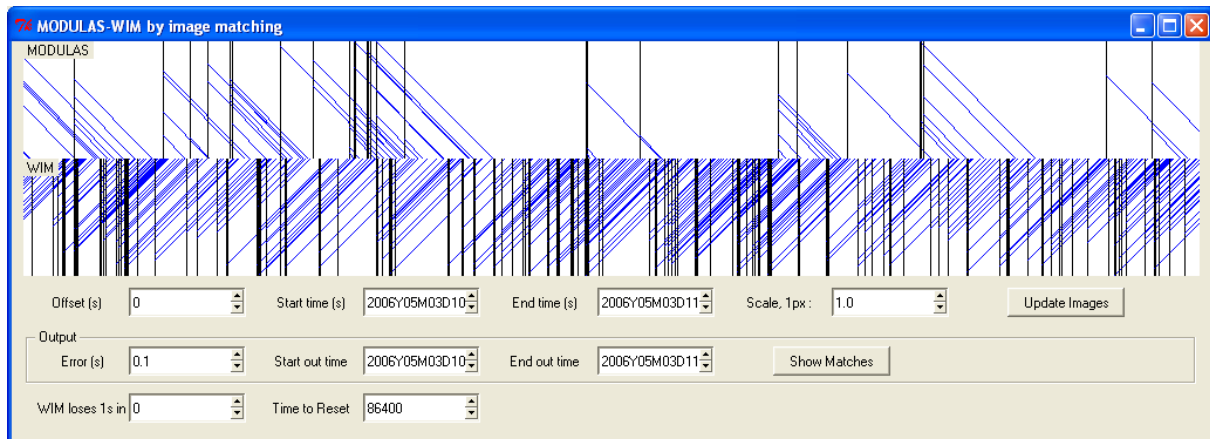


Figure 5. 3: Screenshot of the Modulas and WIM event matching program in operation. Matching Vertical black line indicates a matching event in seconds, matching diagonal blue lines represent the number of centiseconds after the black line

The problem was further complicated by the fact that the Modulas does not record all the events that the WIM does. There are several reasons for this:

- Both systems experience periods of downtime, repair and maintenance during which no events are recorded.
- The criteria by which the WIM system determines that an event should be logged are based on the gross vehicle weight whereas the criterion for Modulas events is the peak force on any channel.
- The Modulas discards any event in which either of the two outermost channels is active, as some of the wheel may not be on the sensor.

This third reason is perhaps the most critical and the problem is compounded by the fact that the Modulas sensor is considerably shorter than the WIM sensor (see Figure 4. 1). Additionally, this WIM station is also on a curve, and the Modulas is rather positioned, in that vehicles have a tendency to drift into the hard shoulder. On some occasions, vehicles have been shown to miss the sensor altogether.

Important consideration for the matching algorithm

The algorithm by which the data is matched does have a number of drawbacks. It assumes that neither clock is accelerating with respect to the other and that the WIM clock is always reset at midnight. While neither of these assumptions is actually true, the errors which they introduce are not significant. The WIM does, in fact, update itself once a day (although still not to the same clock as the Modulas) and this clock reset limits the effects of acceleration.

The algorithm also assumes that all vehicles take the same length of time to travel from

the WIM sensors to the Modulas sensors. Clearly, this will vary with vehicle speed. This is accounted for, to some extent, by allowing inexact matches: in this case, the first matching event in a window of ± 0.1 s around the time to be matched was used. There are two restrictions this places on the algorithm. First, in the case of double or triple axles, the algorithm will occasionally match the wrong wheel. Secondly, the algorithm will only be able to match vehicles within a certain range of speeds. In this case, with the window of ± 0.1 s, the theoretical limits are between about 17 and 41 m/s.

Validating the matching algorithm

It is very difficult to validate the matching procedure effectively, as no data exists with which to do it. However, some conclusions can be drawn from studying the relative frequencies at which certain events are recorded. While this clearly gives little indication of how many of the events are errors, it will show that every type of event is matched with approximately equal accuracy, within the restrictions imposed by the data.

Figure 5. 4 shows histograms (some of which have been rendered as lines, for ease of comparison) showing the frequency of certain wheel loads. The blue bars show the matched data while the lines show data for the whole month of September 2005. It is necessary to compare frequencies rather than numerical totals as the samples we are comparing have different sizes.

This method is also imperfect, as the thresholds of detection of each system are different. This explains why there is a poor match between the histograms for low wheel loads. In an attempt to mitigate this, the histogram for wheels over 15 kN has also been shown. It can be clearly seen that the shapes are comparable and, if the low values are excluded from the unmatched WIM histogram, the values are not dissimilar. It should be noted that the value of 15 kN used here is not entirely representative of the Modulas threshold. The Modulas detects vehicles with any channel loaded to over 1 kN—a threshold which is not directly comparable to that of the WIM.

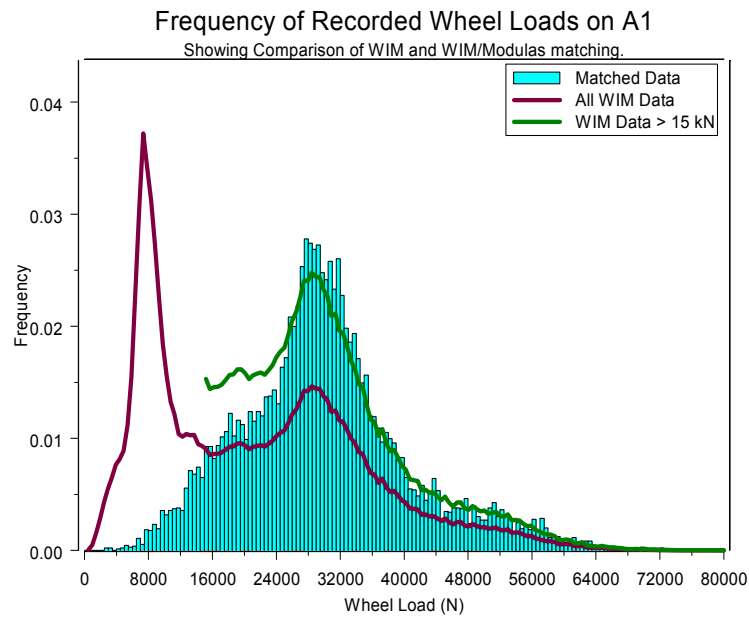


Figure 5. 4: Normalized frequency plot of all wheel loads recorded by the WIM system in September 2005, compared to wheel loads which have been matched to the Modulas data.

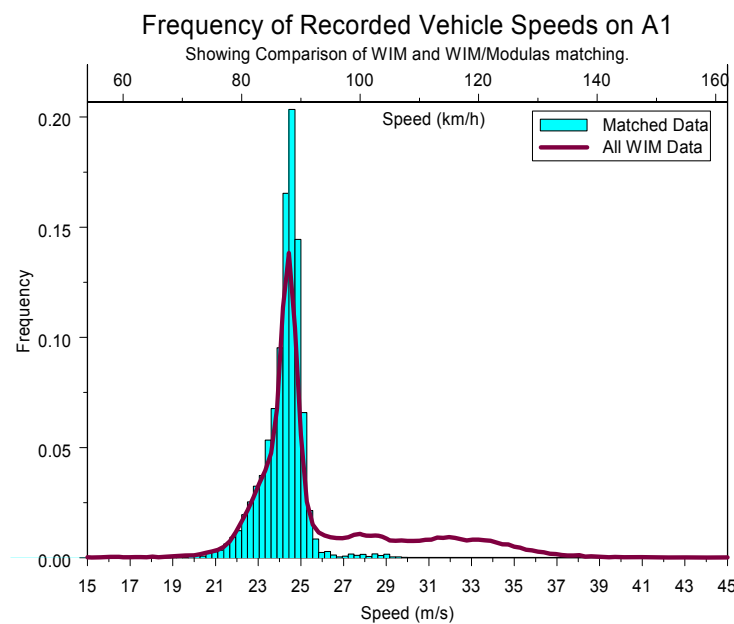


Figure 5. 5: Normalized frequency plot of all speeds recorded by the WIM system in September 2005, compared to speeds which have been matched to the Modulas data.

Figure 5. 5 shows the frequency of speeds recorded by the WIM system for the entire month of September 2005, and for only the available matched data. Once again, one histogram has been rendered as a line for ease of comparison. This shows that the WIM system is recording many more events at higher speeds than the algorithm appears to be matching. This can be explained however, by reference to Figure 5. 4, which shows

that the high speeds recorded by the WIM are almost exclusively related to light vehicles, below the threshold of detection of the Modulas.

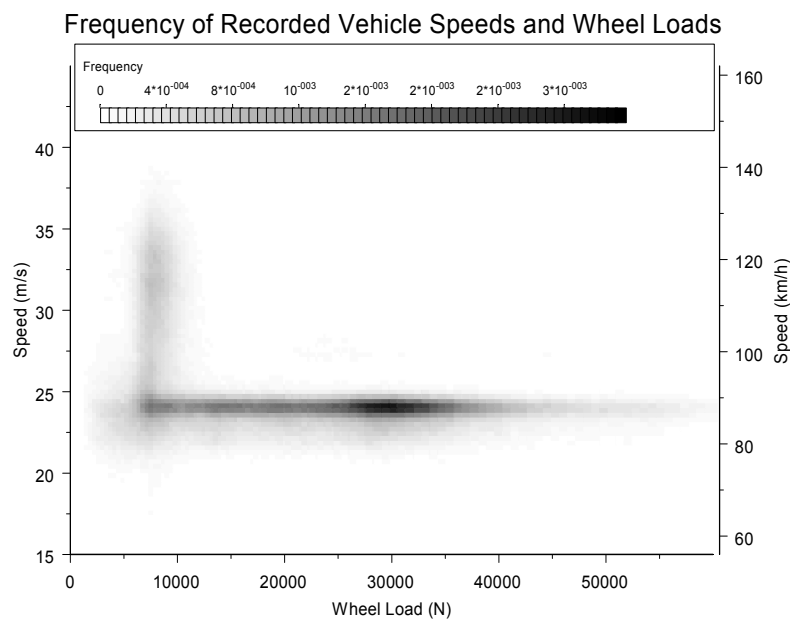


Figure 5. 6: Frequency plot of speed/load combinations recorded by the WIM system

Figure 5. 6 shows the frequency of wheels of a given load (to the nearest 5 kN), travelling at a given speed (to the nearest km/h).

To illustrate the number of events which are recorded by both systems, the first half of September 2005 was examined. From the first 17 days, 9½ days produced results from both systems which it was possible to match. From these 9½ days, the four days with the most matches were selected in order to minimize the effects of errors in the matching algorithm. These days were Friday 9th, Monday 12th, Wednesday 14th and Friday 16th. It was found that obtaining accurate matches during the weekends was very difficult due to the comparative lack of events from heavy goods vehicles. Also, the matching process is very difficult if a selection of matching events cannot be found in the early morning. This made matching data at weekends especially difficult.

These four days had 13574 Modulas events compared to a total of 56824 WIM events, meaning that roughly 23.9% of WIM events were also detected by the Modulas. For these four, well-matched days, 12913 matched events were obtained, although how many of those events are accurate matches is unknown.

All the other measurement devices recorded their results with reference to the same clock, however the nature of some of these sensors meant that matching their events to



Modulas events (and hence to WIM records) is still not trivial. For example, the Balluff displacement sensors, once triggered will output a full second of data, regardless of the number of events in that time. This means that one Balluff event may contain one or more Modulas events and, because of the length of one Balluff event, one pass may be split between 2 or more files. The files are also only recorded at a resolution of one second, making matching using the methods used for the Modulas impossible.

Conclusions and further work

The current position of the Modulas in the pavement and its relatively short length leads to a significant amount of data being missed. A further contributing factor to this is the location of the footprint monitoring site on a curve, although this is far harder to rectify.

The criterion used to determine if a WIM event is recorded is incompatible with that used to determine if a Modulas event is recorded. This leads to a significant number of events which are recorded on one, but not both, sensors.

It is clear that the matching algorithm is able to match the vast majority of events, although its error-rate is unknown.

There are several deficiencies in the matching algorithm which could be addressed which might reduce the number of erroneous matches and increase the number of correct ones. These include:

- Taking account of the time taken to travel between the two sensors, and incorporating this into the algorithm.
- Improving the process for selecting a match when more than one match is possible within the error window specified. For example, double and triple axle combinations are especially prone to matching the wrong wheel.
- Attempting to account for the acceleration of one clock with respect to the other over time.

The process of matching data currently still requires considerable work and time. A way of automating the process further is required if data over longer periods needs to be efficiently matched.

An alternative to improving the methods of matching the two clocks might be to ensure that the WIM and EMPA DAQ system use the same clock in future. This would eliminate almost all errors due to matching, which would significantly improve the accuracy and reliability of the data.

5.3. Analysis of the WIM Data

Statistical analysis

An important aspect of the footprint project is the determination of what constitutes an environmentally friendly vehicle. It is not practical to investigate every vehicle for which data has been recorded and determine the amount of damage and nuisance they cause on a case-by-case basis. The WIM data was therefore used in order to select vehicles from the traffic stream which should be investigated. A wide range of both typical and atypical vehicles had to be selected.

WIM data was examined for the month of September 2005. Figure 5. 7 shows the distribution of axle weights recorded by the WIM system during that month. It should be noted that the system only records vehicles with gross weights in excess of 3 tonnes, explaining the relatively small number of light axles.

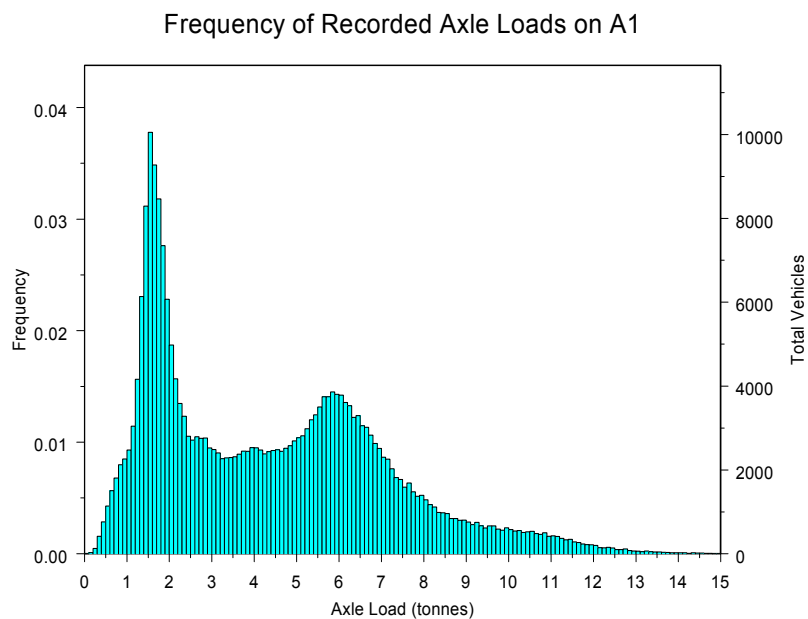


Figure 5. 7: Histogram of axle weights recorded by WIM during September 2005

Several vehicles were recorded with axle weights in excess of 15 tons, however they are too infrequent to be seen on the histogram plot. From close examination of the data, it is thought that axle loads up to approximately 21 tonnes have been accurately recorded during September. For further analysis of maximum axle loads see Figure 5. 7. It is probable that many of the vehicles with axle loads in excess of this are anomalous results. The histogram shows two clear peaks, at 1.5 tonnes—presumed to correspond

to an unladen truck, and at 5.8 tonnes—presumed to correspond to a laden truck. The distribution of recorded speeds was compared to these data, and the key values shown in Table 5. 1 were extracted.

Table 5. 1: Statistical summary of WIM data

Axle Load (tonnes)	Peak Speed (km/h)	Modal Speed (km/h)	Mean Speed (km/h)
1.5	255 ⁽¹⁾	88 ⁽²⁾	102
6.0 ⁽³⁾	107 ⁽⁴⁾	88	87

(1) This peak is clearly anomalous, but the distribution of the data is such that no clear point can be determined above which all results are definitely anomalous.

(2) A second peak was observed at 115 km/h.

(3) 6.0 tons was used as the peak at 5.8 tonnes was relatively flat and 6.0 tons was felt to be a conservative value.

(4) The peak speed recorded for this axle load was, in fact, 235 km/h. However as only one axle was recorded, this was deemed an anomaly, and the next lowest value was taken.

The Swiss classification system (Table 5. 2, Appendix III) currently considers vehicles with no axles over 10 tons in weight to be road-friendly as they are not required to pay a fee (Table 2. 1). This was partially adopted, and most of the study focused on axle loads in excess of 10 tons.

Table 5. 2: The "Swiss 10" Vehicle Classification System (also see Appendix III)

Class	German Designation	Vehicle Type
1	Bus	Buses and Coaches
2	Motorräder	Motorcycles
3	Personenwagen	Personal Cars
4	Personenwagen+ Anhänger	Personal Cars with Trailers
5	Lieferwagen	Delivery / Pick-up Trucks (< 3.5 t)
6	Lieferwagen+ Anhänger	Delivery / Pick-up Trucks with Trailers (< 3.5 t)
7	Lieferwagen+ Auflieger	Articulated Delivery / Pick-up Trucks with Semi-Trailers (< 3.5 t)
8	Lastwagen	Freight Trucks
9	Lastenzüge	Freight Trucks with Trailers



10	Sattelzüge	Articulated Freight Trucks with Semi-Trailers
----	------------	---

It can also be seen from Figure 5. 7 that the number of axles exceeding the 10 ton limit is quite small—less than 6% of the total number of axles recorded by the WIM.

5.4. Conclusions from the WIM Monitoring

The vast majority of the vehicles recorded on the A1 are considered to have environmentally friendly axles by the Swiss authorities. This report need only focus on the 6% of axles in excess of 10 tonnes.

The axles over 10 tonnes tend to fall into a limited range of speeds, and nearly all axles in this category are below 90 km/h. This limited speed range should reduce the errors in the matching algorithm in the area of interest. It should be noted that the speed limit for heavy goods vehicles on this road is 80 km/h.

6. STRESS IN MOTION (SIM) MONITORING WITH THE MODULAS SENSOR

(Authors: Gerald Morgan, Lily Poulikakos, Rico Muff, Manfred Partl, Emil Doupal, Reto Calderara)

6.1. Sensors Description

The modulas SIM sensor (Figure 6. 1) is a piezo quartz sensor array that measures the vertical forces exerted irrespective of the part of the Tyre which crosses the device and, as opposed to other SIM sensors (De Beer et al 1999, De Beer 2006, Owende et al 2001) at high and low vehicle speeds. Piezoquartz technology is advantageous in this case since it theoretically offers mechanical and electrical stability as well as no wear or fatigue. However this type of sensor is not suitable for static loading. Further details on the use of other quartz sensors and positive field experiences have been previously reported (Doupal et al 2002a, Doupal et al 2002b).

The Modulas is a reusable device, set flush with the road, and measures the vertical contact forces between tyre and pavement during vehicle crossings using 32 independent channels with less than 2% cross-talk and 15 mm spatial resolution (the width of each channel). The SIM sensor is capable of delivering the traditional WIM, parameters such as axle load, speed, and axle distance.

6.2. Data Acquisition (DAQ) and Analysis

A challenging and important part of this work is the data acquisition, reduction and analysis. To acquire the voltage signals from the SIM sensor charge amplifier, a 64 channel analogue input data acquisition card in combination with a National Instrument PXI controller. Details of the data acquisition can be found in chapter 13.

Assuming that the whole wheel is rolling over the sensor, each pass of a double Tyre with a width of 58.25 cm activates 39 channels and a single tyre with a width of 27 cm activates 18 channels. A delayed, offline calculation performs a reduction of the raw data and calculates the contact force-time history for each sensor. The recorded data from each pass was stored in a single file. This was then split into events by an algorithm which split the data at times when any channel was recording more than 1 kN. This threshold of detection was chosen based on the experimental data. In general, this threshold caught all the events in the files minimizing false events. Additionally the software combines 2 raw data files in order to guarantee one complete passing within one file. To calculate the force, the offset of each channel is calculated and corrected while the data reduction eliminates the zero values before and after the passing of a Tyre. Together with a data file that is readable from a spreadsheet, a plain text log file is generated that contains the results of the passage detection and the calculation.

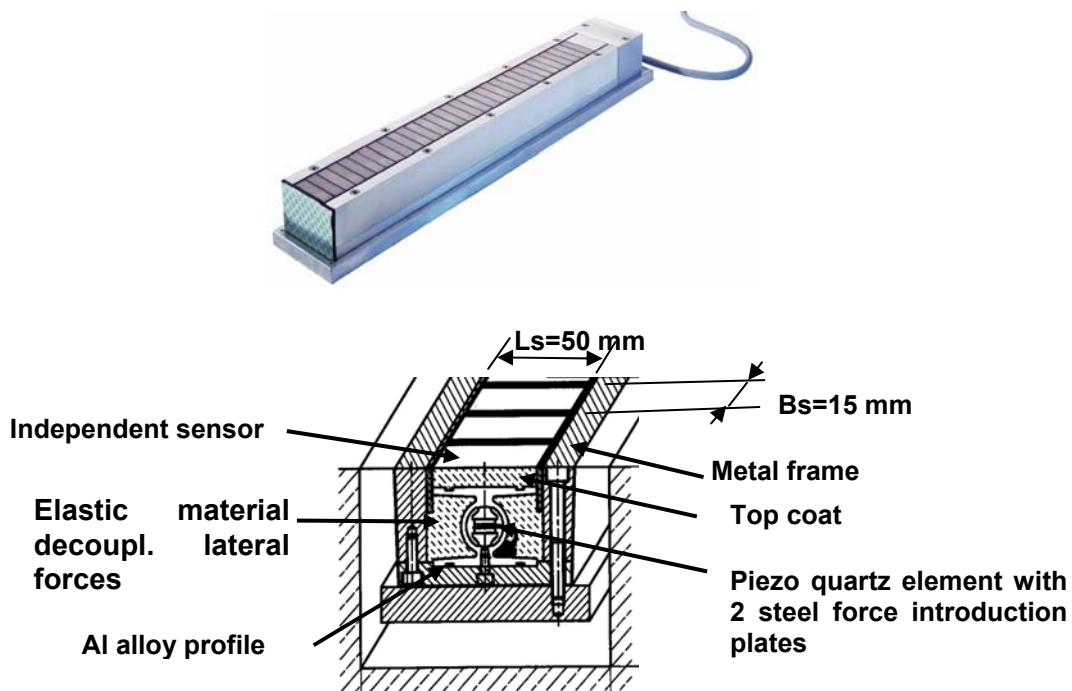


Figure 6. 1: Stress in Motion (SIM) sensor Modulas with 32 channels top; schema of the cross section of the sensor, bottom

The voltage data is converted to Newton [N] indicating the force-time history registered by the 32 independent channels. The details of the data analysis and practical conclusions are discussed below:

Theoretical analysis of recorded force distributions

The SIM sensor records the vertical force at time t , $P_z(t)$, on each of its channels with a frequency, f (the timestep, $\delta t = f^{-1}$). A wheel with a total vertical force $F_{z_{tot}}$ traverses the sensor at a speed u_x , as shown in Figure 6. 2. The sensor which records the force is of width B_s (0.015m) and length L_s (0.05m). L_s is considerably larger than the distance travelled by the wheel in one timestep, $\delta t \cdot u_x$.

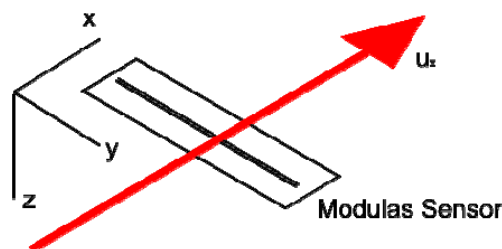


Figure 6. 2: Schematic of the sensor arrangement

To get a more detailed understanding of the contact force distribution (and hence the

contact stress distribution), the forces applied to an area defined by the width of one channel sensor and the distance travelled by the Tyre in one timestep must be considered. This force distribution, $F_z(t)$, can be calculated from the differences between the recorded forces as follows:

$$F_z(t + \delta t) = P_z(t + \delta t) - [P_z(t) - F_z(t - (L_s/u_x))] \tag{6.1}$$

In words, the force at time $t + \delta t$ is the difference between the last two recorded forces plus the force calculated L_s/u_x seconds previously. L_s/u_x represents the time taken for the wheel to travel the length of the sensor element. Figure 6. 3 and Figure 6. 4 illustrate the physics and mathematics behind Equation 6.1. Figure 6. 5 shows a Tyre rolling over a sensor element.

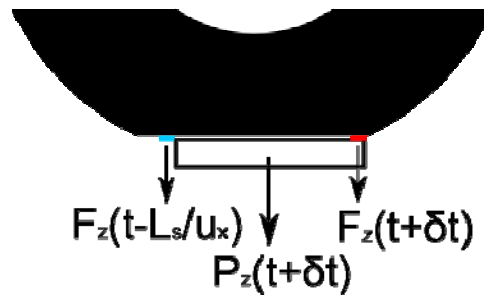


Figure 6. 3: Physical interpretation of some terms from Equation [1]: a Tyre on one sensor element

In any given timestep the wheel will add a force to the sensor. It will also remove a force. This method assumes that the removed force is the same as the force that was added at a time L_s/u_x seconds earlier, thus enabling to calculate the additional force. Figure 6. 5 shows a fictitious force distribution from a channel. As well as showing how the terms of Equation 6.1 can be interpreted graphically, it also shows several physical and practical problems that the model faces:

In order to use the SIM sensor array practically, in the field, a threshold of detection must be set in order to limit the amount of data recorded. The current field installation uses a threshold of 1000N for any channel. This threshold was set at 30 N for the laboratory measurements in order to get a strong signal to noise ratio. For this reason, Equation 6.1 can only be applied for areas of the graph above this detection threshold. The distribution below this threshold is not known.

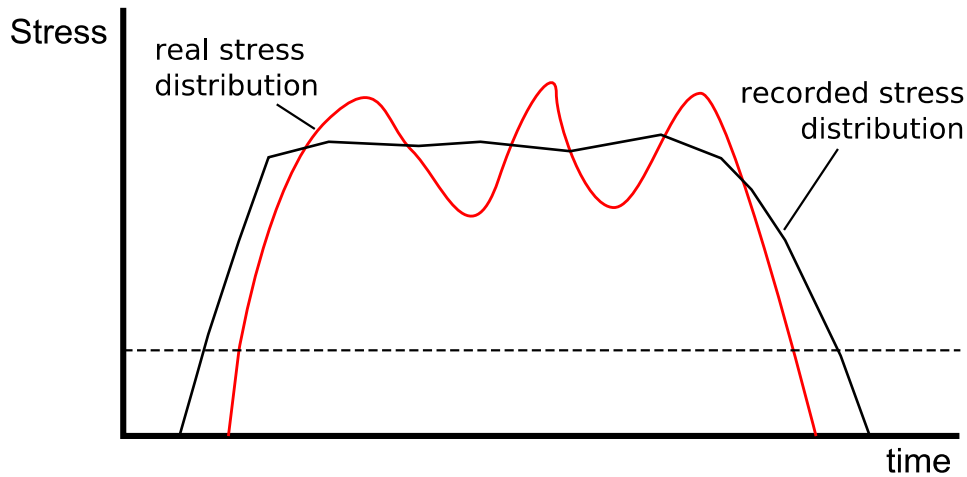


Figure 6. 4: Example of the type of approximation made by using the Pz force distribution

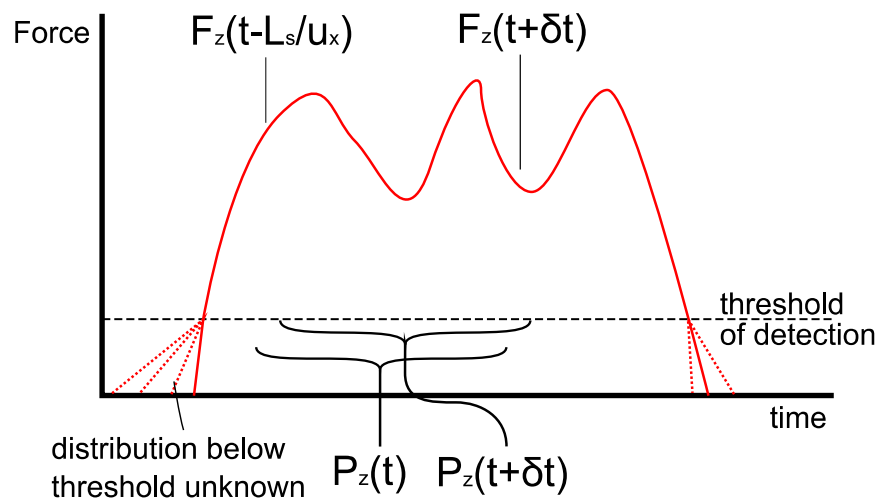


Figure 6. 5: Graphical interpretation of Equation [1]

It can be clearly seen that Equation 6.1 is a recursive formula using its own calculated values as an input. This not only allows for the propagation of errors through the footprint (errors will increase linearly with time) but also presents problems for calculation at the start of the footprint. Because the force distribution below the detection threshold is unknown, its values must be assumed in order to calculate the start of the footprint. This will introduce a small but significant periodic error (of L_s/u_x) which will propagate throughout the entire result, although some amount of correction is possible. The use of Equation 6.1 also presents an interpolation problem. The equation discretises the force function, F_z , into increments of time, δt , however there is no guarantee that $t - (L_s/u_x)$ will be a multiple of δt . For example, once installed in the road, a vehicle travelling at 90 km/h takes 16.4 timesteps to traverse the sensor when the sensor is recording at 8196 Hz. In this case, $F_z(t - (L_s/u_x))$ is unknown and must be

calculated by interpolation of the surrounding values, introducing further errors into the system.

Calculating the contact stress distribution

There are two possible sets of data which can be used to plot the contact stress distribution—the stress distribution felt by the pavement as the Tyre passes over it. The original recorded forces, P_z , can be used and converted to stresses p_z by dividing by the total channel sensor area, $B_s \cdot L_s$, or the calculated forces, F_z , can be used, converting by dividing by the ‘timestep area,’ $B_s \cdot u_x \cdot \delta t$.

$$p_z = P_z / (B_s \cdot L_s) \quad \text{or} \quad \sigma_z = F_z / (B_s \cdot u_x \cdot \delta t) \quad [6.2]$$

The stresses, p_z , calculated from P_z , shown in equation 6.2 and Figure 6. 6, represent the average stress over a number of timesteps (determined by the speed of the vehicle) and are therefore not conservative and not particularly accurate representation of the stress. They do, however, give a constant level of accuracy over the entire footprint, including the otherwise unknown start and end sections. The approximation made is not unlike that of a moving-average smoothing, as shown in Figure 6. 4.

The stresses, σ_z , calculated from F_z , (Figure 6. 7) represent the stress under the smallest area it is possible to measure with the SIM sensor recording at a given frequency. While they can be unconservative in some cases, the granularity is much finer than the p_z stresses, allowing a much closer representation of the “real” curve. However, they suffer from the progressive propagation of errors through the footprint, and there is no way of accounting for the area of the curve below the detection threshold.

For visualization purposes, the recorded p_z stresses were chosen. Their comparatively smooth surface make them easy to visualize and difficult to misinterpret. The high level of error present in the σ_z stresses, when combined with their apparent high resolution and periodic error, causes their plots to appear much more detailed than they actually are. Keeping in mind the ultimate goal to use the data from the SIM sensor in a finite element model, the recorded p_z stresses are recommended. The comparatively large area over which they are applied and their smoother shape both give significant advantages for model run time, allowing sparser meshes and higher timesteps. Additionally, as finite element models will also propagate some errors through their run time, it is preferable to use input data with a constant error to avoid the total error in the model becoming too great.

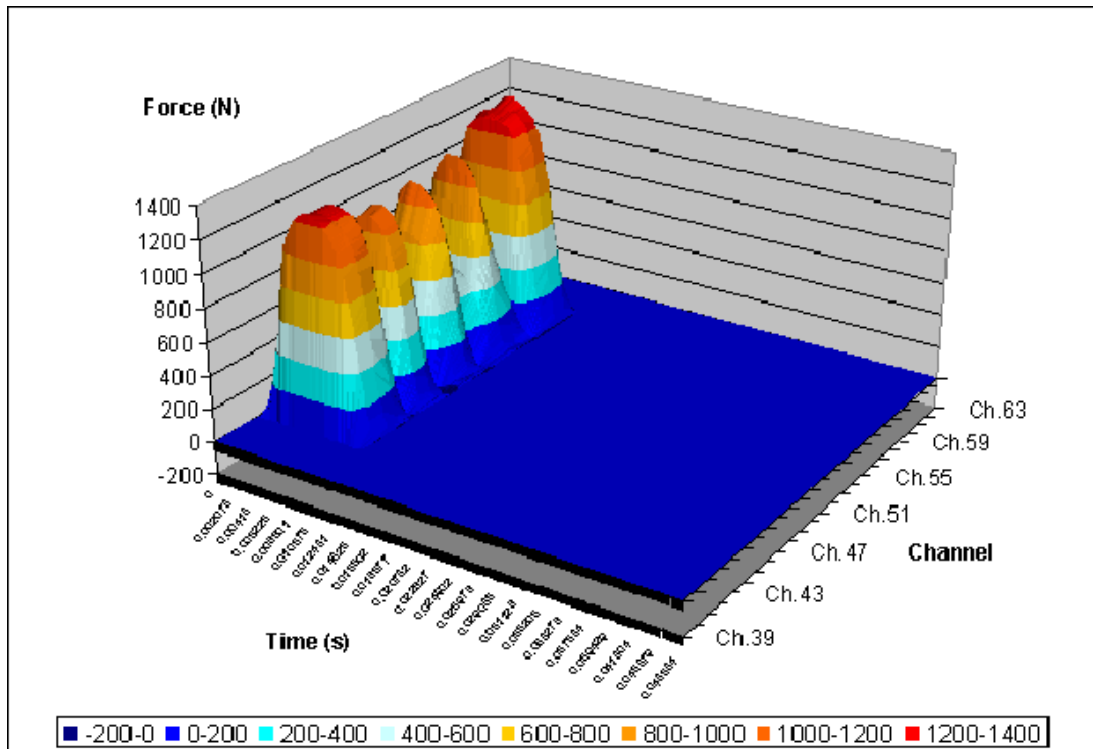


Figure 6. 6: Three-dimensional visualization of the Pz force distribution showing smooth surface and no data after the Tyre pass

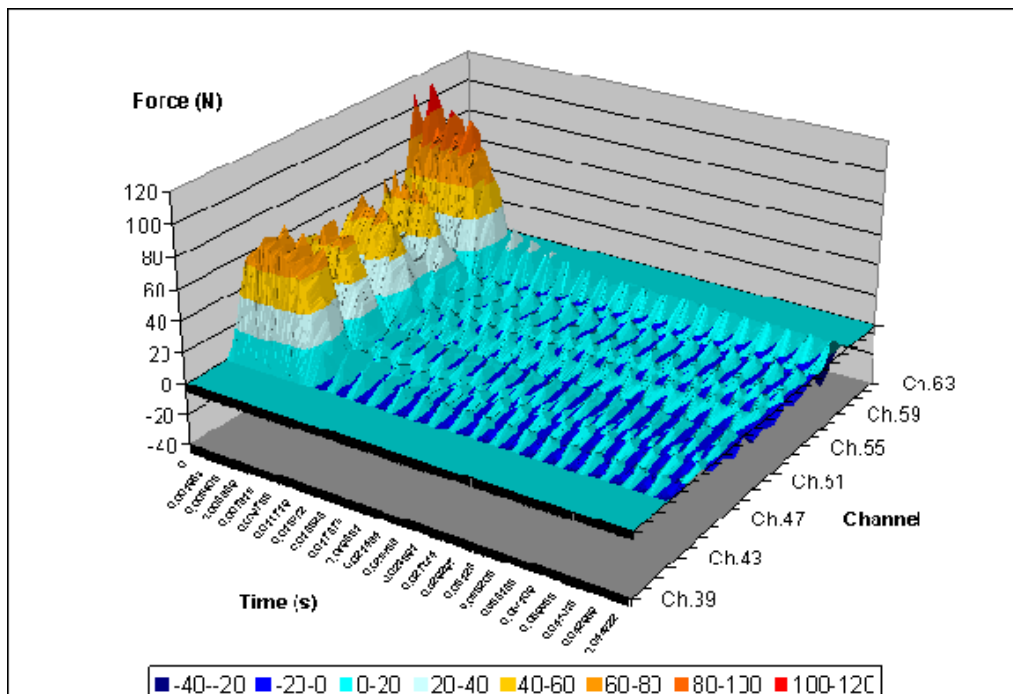


Figure 6. 7: Three-dimensional visualization of the Fz force distribution showing more detailed surface and residual periodic error

Calculating the total wheel load

Estimation of the total applied wheel load, $F_{z\text{tot}}$, using a set of forces, F_z , calculated from Equation [1] follows from the integral of the $F_z(t)$ function with respect to time. In order to minimize the calculation errors involved, however, an attempt was made to devise a method by which this quantity could be directly estimated from the recorded forces, P_z . The method adopted was to effectively scale the recorded force measurements by the ratio of the timestep to the pass-by time (L_s/u_x). This can be expressed mathematically as

$$\int_{t_0}^{t_{\text{end}}} P_z(t) \cdot (L_s/u_x)^{-1} \cdot dt \tag{6.3}$$

for each channel, where t_0 to t_{end} defines the whole event. This must be discretised and summed for all the SIM sensor channels to give Equation 4.

$$F_{z\text{tot}} = \delta t \cdot (u_x/L_s) \cdot \sum_a^b \sum_{n=0}^{n=N} P_z(n \cdot \delta t) \tag{6.4}$$

where $a \rightarrow b$ defines all the channels and N is the number of discrete samples.

Accounting for partial contact

The above discussion makes the assumption that the sensor is completely covered by the wheel, but there are areas of the stress distribution where that is not the case. Excluding partial coverage due to the tread grooves in the Tyre, there are two ways in which a channel sensor may be partially covered: laterally or longitudinally.

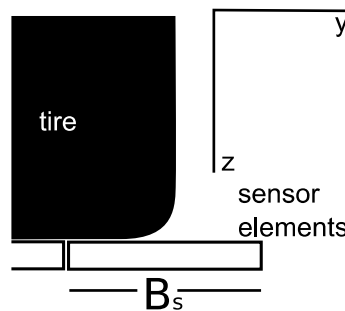


Figure 6. 8: Lateral partial contact

Only the two outermost channels of any Tyre need be considered for partial lateral coverage, giving two or four channels per footprint for single or dual Tyre arrangements respectively. The partial contact will not affect the force recorded by any given channel, so no errors will be introduced to either of the two force distributions $P_z(t)$ or $F_z(t)$. The stress distributions, $p_z(t)$ and $\sigma_z(t)$ will be affected, however. The area over which the force is being applied will vary from 100% to 0% of the actual channel area which is

used in the calculation. This over-estimation of contact area will result in a significant under-estimation of stress. The stress at the edges of the Tyres cannot be over-estimated by either method. It is not possible to know the amount of contact and it is therefore not possible to further quantify this error. Particularly as there is a wide variation in Tyre widths in practice.

Partial contact in the longitudinal direction is taken into account of by the F_z/σ_z method, as this uses the length of the timestep rather than the length of the sensor to determine its area. A correction can be made to the p_z stresses by scaling those which fall within the first and last (L_s/u_x) seconds of the event by the inverse of the proportion of sensor covered at that moment. However, this is difficult to do in practice due to the detection threshold. It is not known at exactly what time the wheel enters or leaves the sensor—effectively the same problem that the F_z/σ_z method experiences—and so it cannot be guaranteed that the corrections are being applied to the correct values.

As, in general, it is not possible to predict with any accuracy the errors due to partial contact no attempt has been made to account for or to correct them.

To investigate whether it is possible to estimate the inflation pressure, P_{Tyre} , various models were investigated. Equation 5 resulted in the best estimate of the inflation pressure as shown in the next section. It uses the integral of the force time history using all active channels and the entire passing time.

$$P_{\text{tire}} = \frac{\sum_a^b \frac{u_x}{L_s} \int_{t_0}^{t_{\text{end}}} P_z(t) dt}{\sum_a^b u_x \cdot \delta t \cdot B_s} = \frac{1}{L_s B_s} \frac{\sum_a^b \int_{t_0}^{t_{\text{end}}} P_z(t) dt}{\sum_a^b \delta t} \quad [6.5]$$

6.3. Laboratory Experiments

A series of laboratory experiments were conducted to optimize and calibrate the SIM sensor prior to its installation on the A1. The SIM sensor was temporarily built into a groove (130 mm wide x 85 mm deep) in a concrete slab of 1100 mm x 3750 mm x 200 mm (Figure 6. 9) and trafficked by the MMLS3 laterally and longitudinally. The tests were carried out indoors and were designed such that the SIM sensor could be tested under well defined traffic like conditions. Tests focused on variation of Tyre inflation pressure, speed, temperature, lateral position of the wheel and angle with respect to direction of travel. Each parameter was tested while keeping all other controllable variables identical.

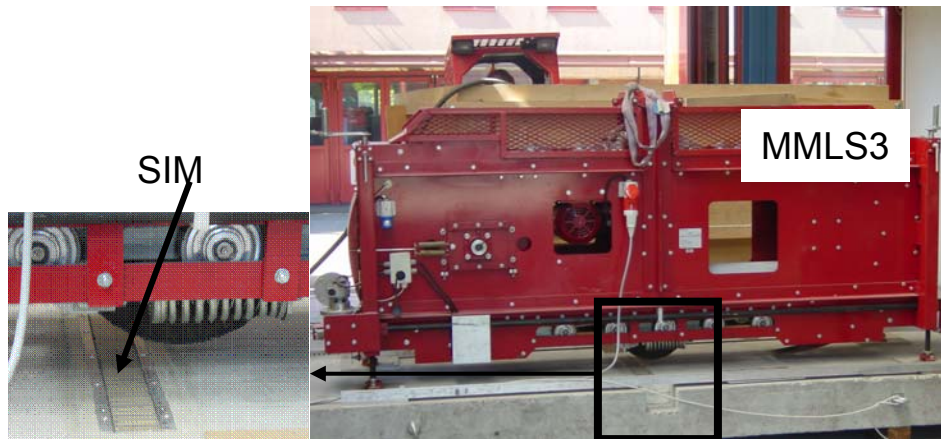


Figure 6. 9: The SIM sensor embedded in a concrete slab and trafficked using the MMLS3

A total of 30 combinations of the parameters were tested. Each experiment was run so that a minimum of 12 passes were made, giving a minimum of three Tyre-pavement contact footprints from each of the four MMLS3 Tyres for each experiment. For each set of comparable experiments, a sample force distribution was extracted from the recorded data. For consistency, this was chosen to be the third event extracted from the data file whenever that event was not anomalous. The threshold of detection was set at 30 N to assure a robust signal to noise ratio. Various parameters were tested as described in detail below:

Variation of Tyre Inflation Pressure

Keeping the speed constant at 9 km/h and the wheel load at 2100 N, the Tyre inflation pressure was varied manually from 2 bar (ca 203 kPa, representing a flat Tyre) to 6 bar (ca 608 kPa, the maximum setting of the MMLS3). Figure 6. 11 shows the 3-D representation of the wheel contact load using the same Tyre at different pressures. It was shown in previous research that a significant difference in the shape of the load distribution under the Tyre can be seen. Correctly inflated and over-inflated Tyres produce an “n-shape” and under-inflated Tyres produce an “m-shaped” contact load/stress distribution (De Beer 1999, 2006). The laboratory results shown in Figure corroborate these findings in that a significant difference in load (and the resulting stress) distribution under the Tyre can be seen for over- and under-inflated Tyres. The 3D representation of contact load distribution from two differently inflated, but otherwise identical Tyres shows this clearly. Furthermore the maximum force registered by a channel for the 2 bar Tyre was 864 N and the 6 bar Tyre was 1200 N indicating a higher contact force for the higher inflation pressure. Summary of sample of the results shown in Figure shows an m-shaped distribution in the case of every under inflated Tyre and one case of a normally inflated Tyre travelling at low speed. Keeping all other controllable parameters identical the standard deviation shown in Table 1 varies between 47 N to 77 N for calculated wheel load inflated at 2 bar and 80 N to 81 N for

calculated wheel load inflated at 6 bar. Indicating a smaller spread of the data at 6 bar. Figure shows an overview of all calculated wheel loads at 2 bar and 6 bar. The difference between the average calculated value from the measured wheel load was 19% and 7% at 6 bar and 2 bar respectively.

Velocity Variation

The influence of velocity of the moving Tyre was investigated using the velocity range of the MMLS3. The force distribution was obtained for 6 bar (608 kPa) Tyres at 1.125 km/h, 4.5 km/h and 9 km/h (maximum setting of the MMLS3) keeping the wheel load constant at 2100N. A sample of the contact forces and summary of the results in Figure 6. 10 show that in the range investigated, variations in velocity do not influence the results of the SIM sensor significantly. The only notable change is the time for which the sensor recorded stresses (latch time) seen in Figure 6. 10. The latch time is dependant on the channel activated and is defined as the maximum time the sensor was recording data from the wheel. This effect can also be observed in the slower runs at the start and end of each test, recorded while the MMLS3 was accelerating or decelerating. While this sensor is not appropriate for static measurements (as shown in Table 6.1), speeds as low as 1.125 km/h produce wheel loads comparable to the desired value.

Temperature Variation

The surrounding temperature was varied using a continuous hot air flow on top of the concrete pavement surface for 2 to 4 hours allowing for the SIM sensor to heat up to a similar temperature to the surrounding air. Thereafter the MMLS3 trafficked the SIM sensor at a constant speed of one of 1.125 km/h, 4.5 km/h and 9 km/h. The quartz element is reported to have a temperature sensitivity of 0.02 %/°K (Kistler Catalogue). Looking at comparable single passes and in Figure 6. 10 for example at 9km/h and 20°C the wheel load of 2516 N (SD = 81 N) was calculated while with 9km/h and 40°C a wheel load of 2479 N (SD = 62 N) was calculated. From Figure 6. 10 where a summary of all passes is presented it is clear that the mean of all data from the two temperatures tested are nearly identical indicating negligible effect of temperature on the results of the SIM sensor.

Table 6. 1: Calculated Wheel Load

Wheel Load (N)	Tyre Press. (bar)	Speed (km/h)	Position ^a (L/M/R)	Temp (°C)	Angle ^b (°)	Shape ^c	Max. Force ^d (N)	Latch Time ^d (ms)	Calculated Wheel Load ^{d,e} (N)	Standard Deviation ^f (N)
2100	2	1.125	M	20	90	m	820	494	2162	47.82
2100	2	4.5	M	20	90	m	816	122	2204	61.91
2100	2	9	M	20	90	m	852	83	2232	77.88
2100	6	1.125	M	20	90	n	1200	443	2535	80.49
2100	6	4.5	M	20	90	n	1219	107	2537	72.57
2100	6	9	M	20	90	n	1234	76	2516	81.34
2100	6	1.125	M	40	90	n	1217	437	2479	80.69
2100	6	4.5	M	40	90	n	1222	109	2504	72.62
2100	6	9	M	40	90	n	1208	74	2479	62.99
2100	6	1.125	M	20	45	n	1298	643	2449	71.12
2100	6	1.125	L	20	90	n	1147	492	2374	84.86
2100	6	4.5	L	20	90	n	1145	105	2489	72.78
2100	6	9	L	20	90	n	1156	66	2472	100.62
2100	6	1.125	R	20	90	m	421	200	748	116.19
2100	6	4.5	R	20	90	n	1190	112	2480	99.13
2100	6	9	R	20	90	n	1176	103	2489	107.10

^aLateral position of MMLS3; L=Left, M=Middle, R=Right

^bAngle of MMLS3 with respect to the SIM sensor

^cShape of the pressure distribution m=double bulge, n=Single bulge

^dFrom the third recorded footprint of each experiment

^eCalculated From Equation [2]

^fRoot mean square (RMS) deviation of three events from the wheel load

Variation of Lateral Position of the Wheels

In order to investigate the effect of lateral position of the passing wheel on the Tyre/pavement contact loads, the MMLS3 was moved laterally to three positions; the left (L = channels 2 to 7), middle (M = channels 15 to 20) and right (R = channels 26 to 31) of the sensor. Figure 6. 10 shows a sample of the contact load distribution and Table 6.1 shows the summary of the calculated wheel loads from all tests. Looking at comparable values of calculated wheel load for the three positions R, M, L at 9 km/h and 20°C, 2489 N (standard deviation (SD) = 107 N), 2516 N (SD = 81 N) and 2472 (SD = 101 N) are obtained respectively, indicating that the sensor produced similar results regardless of the lateral wheel position along the SIM sensor. Figure 6. 10 shows that although the mean of the calculated wheel load in all three positions is ca 2500 N, the standard deviation of the calculated loads resulting from the left and right positions is slightly higher indicating a larger dispersion.

Variation of Angle of the Sensor with Respect to Direction on Travel

Although large angles with respect to direction of travel and the SIM sensor are not expected routinely in situ, this parameter was checked in the laboratory experiments. The MMLS3 was positioned at 90° and 45° angle to the SIM sensor. The sample output shown for 1.125 km/h shows this produced the expected result of an increased latch time of 643 s which can be seen graphically in Figure 6. 10. The mean calculated wheel load shown in Table 2 is 2449 N (SD = 71 N).

Repeatability of Results

In order to ensure accuracy and consistency of results, a minimum of twelve tests were run for each combination of pressure, speed, temperature, position and angle. This corresponds to three tests with each wheel of the MMLS3. In general, the results showed good repeatability. Table 6.1 shows that with the exception of one outlier, the calculated wheel loads range from 2163 N to 2537 N with a standard deviation of 48 N to 107 N indicating good agreement with measured wheel load of 2100 N.

The Contact Pressure Distribution

The non-uniform contact pressure distribution follows from the non uniform force distribution using [2], i.e. the recorded force divided by the area of one sensor element as discussed earlier. The response from the sensor shown in examples of Figure 6. 10 and Figure 6. 1 represent the shape of the stress distribution well.

The Calculated Wheel Load

The wheel loads from all the comparable experimental data available have been calculated using [3] and shown in Table 6.1. The mean values are also calculated and marked. It can be seen that these calculated wheel loads are close to the actual wheel load and show little variation with temperature, speed or position across all the tests performed indicating these variables to be negligible. This method of calculating the wheel load gave results with an average of 2432 N (as compared to the actual value of 2100 kN) and had a standard deviation of 17 N.

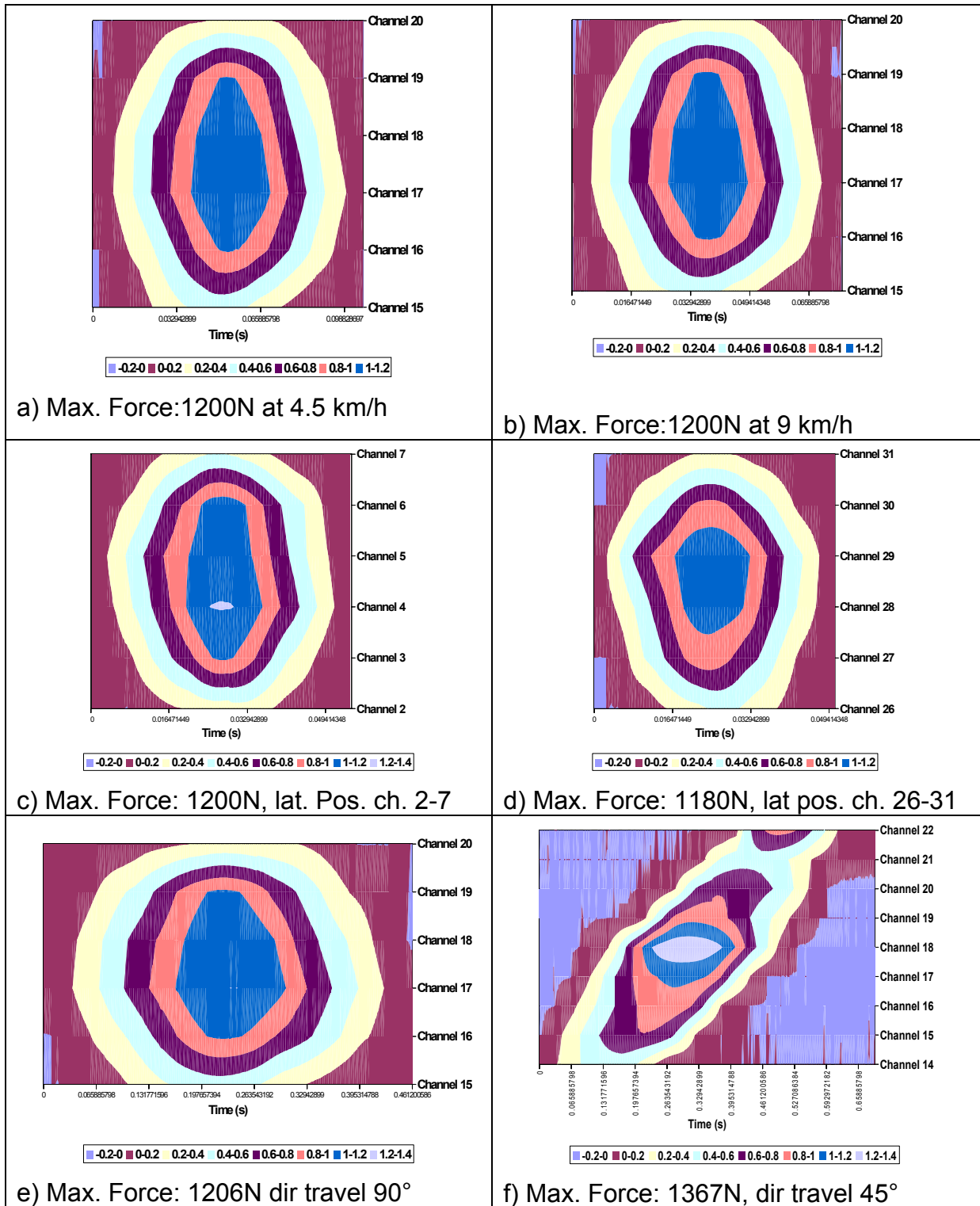
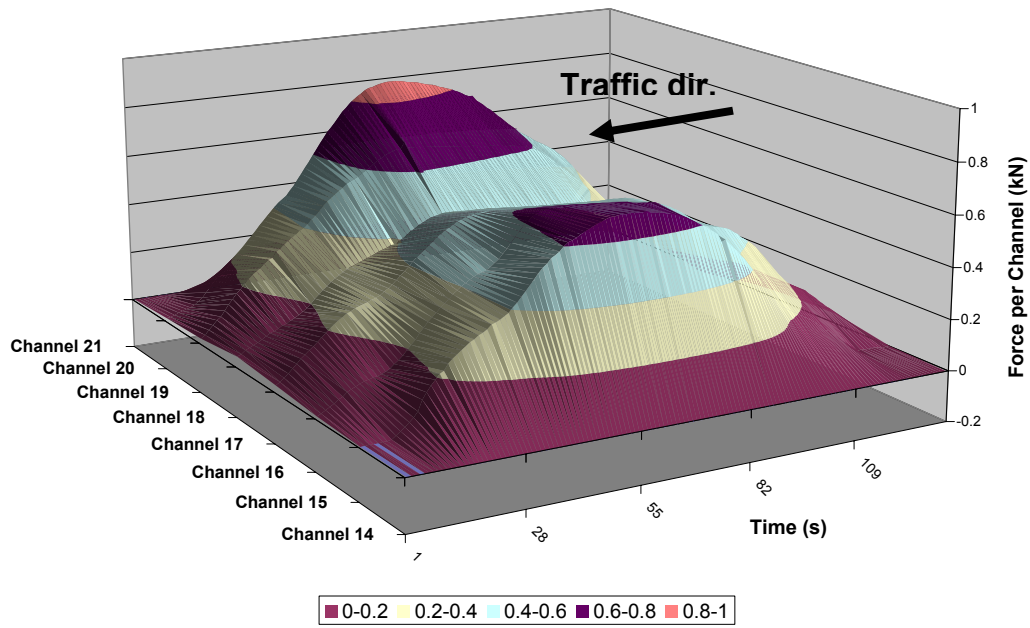
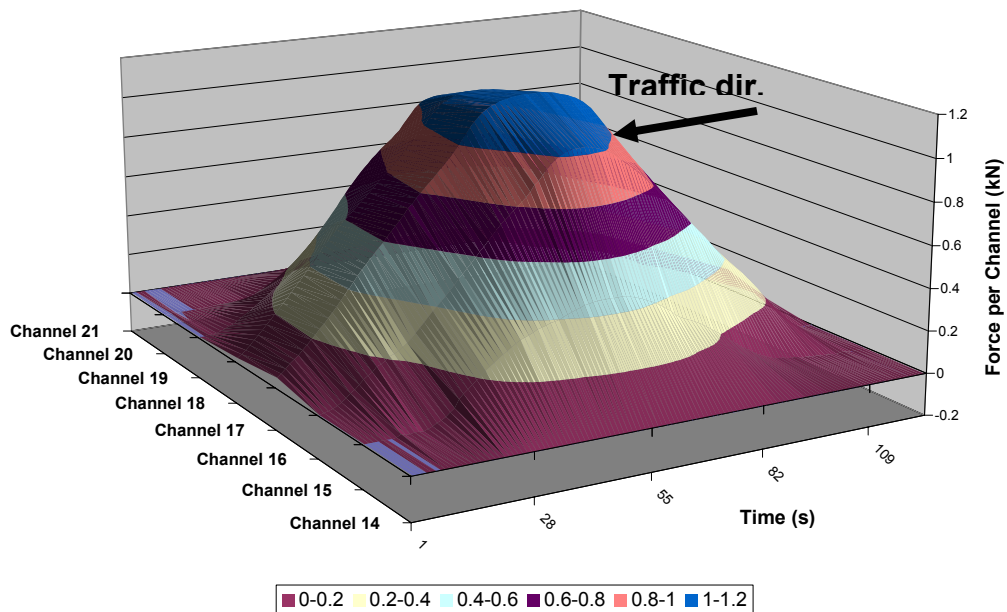


Figure 6. 10: Example “footprints” from the MMLS3



a) $P_{Tyre} = 2 \text{ bar}$, $F_{z\text{tot}} = 2.1 \text{ kN}$, $u_x = 9\text{km/h}$



b) $P_{Tyre} = 6 \text{ bar}$, $F_{z\text{tot}} = 2.1 \text{ kN}$, $u_x = 9\text{km/h}$

Figure 6. 11: 3D representation of force distributions in the footprints of MMLS3 Tyres at 2 bar with »m« shape distribution (top) and 6 bar »n« shape distribution (bottom), traffic direction is perpendicular to the channels

Using Equation 6.4 the inflation pressure was calculated from the contact load distribution. The best results obtained indicate an estimate of 4.56 bar when the measured inflation pressure was 2 bar (SD=0.39 bar) and 5.49 bar for measured

inflation pressure of 6 bar (SD= 0.36). The results so far indicate that the Tyre inflation pressure calculated from the contact loads is not in close agreement with measured values. This may be due to the construction of the Tyres, Equation 6.4 makes some simplifying assumptions about the pressure distribution which may not be accurate for modern Tyres. The one-third scale of the MMLS3 may also contribute to the inaccuracy—increasing the percentage error due to partial lateral contact.

Conclusions of the laboratory experiments and outlook

From the laboratory experiments the following is concluded:

- Variations in speed, temperature, lateral position have had no significant effect on the force distribution obtained by the SIM sensor.
- Variations of angle (tested on a limited basis) have a significant effect on the contact-force distribution measured by the SIM sensor, however the calculated wheel load remains similar.
- Pressure or force distribution under the Tyre is not uniform and can be readily visualized.
- SIM sensor allows the identification of over or under inflated Tyres by inspection of the shape of the stress distribution.
- Tyre inflation pressure calculated from the contact loads is not in close agreement with measured values.
- The MMLS3 has proven to be a useful tool for the laboratory assessment of this new sensor.

The laboratory results show that the SIM sensor promises to become an effective investigative tool as Tyre force distributions can be measured in real time with a high spatial resolution and frequency at highway velocities. However as the ultimate goal for a sensor such as this SIM sensor is in situ performance, it is important to consider the following:

- Road roughness and evenness is an important factor in the sense that it excites the dynamic behaviour in trucks and manifests itself into higher axle loads and can reduce duration of load application. Both these factors are minimal in the controlled laboratory environment in this investigation and as can be seen in the results.
- Formal criteria governing whether the Tyre response shape is “n” or “m” should be established.
- Long term in situ performance of the SIM sensor and changes due to traffic and climate should be investigated.

6.4. Field Installation of the SIM

Concrete Element for Field installation of Modulas

Field installation of all sensors was performed overnight under limited visibility and time restraints. As a result it was decided to produce a concrete element that would hold the Modulas in a tight steel bed. This allows for quality control and precision for the installation of this important sensor as well as the possibility for its removal for repair or inspection purposes. The concrete element 1600mm*700mm designed by the concrete lab at Empa is shown in Figure 6. 12. Detail description of the reinforcement and type of concrete can be found in Moser (Empa report No. 203 894.135).



Figure 6. 12: Reinforcement and steel frame of the concrete element (left) and the modulas installed in the concrete element (right)

6.5. “Dummy” Replacement for Modulas

As this was the first time the Modulas sensor was to be installed on the highway, the durability of the sensor under motorway loading conditions was unknown. As a result two replacement pieces measuring 144 cm*1144 cm*65 cm were prepared in order to allow replacement of the sensors in an emergency. The chosen material for this Dummy was polyacetal POM-C. This material was chosen due to its high stiffness and dimensional stability as well as minimal humidity absorption and ease of machining. Table 6. 2 lists the relevant properties of this material. POM-C is a flammable material

but it is resistant to petroleum, gasoline and diesel. Figure Y shows the dummy replacement installed in the concrete element.

Table 6. 2: Specification of the Modulas “Dummy” element

Property	Value	Unit
Density	1.42	g/cm ³
Tensile strength	70	N/mm ²
Compressive strength	30	N/mm ²
Flexural strength	115	N/mm ²
Elastic Modulas	3000	N/mm ²
Friction coefficient (dry)	0.15-0.32	
Operating temp	-40 to 100	°C
Linear coef of expansion	1.2*10 ⁻⁴	K



Figure 6. 13: Modulas replacement “Dummy” placed in the concrete element

6.6. Sample Output

An important advantage of the SIM sensor is its ability to identify unevenly inflated Tyres and single or dual Tyres. Figure 6. 14 top shows the load distribution of unevenly inflated dual Tyres. In this extreme case one tyre is effectively carrying the load that was meant for dual Tyres. Figure 6. 14 bottom shows the distribution on dual tyres from a calibration pass made with known vehicles.

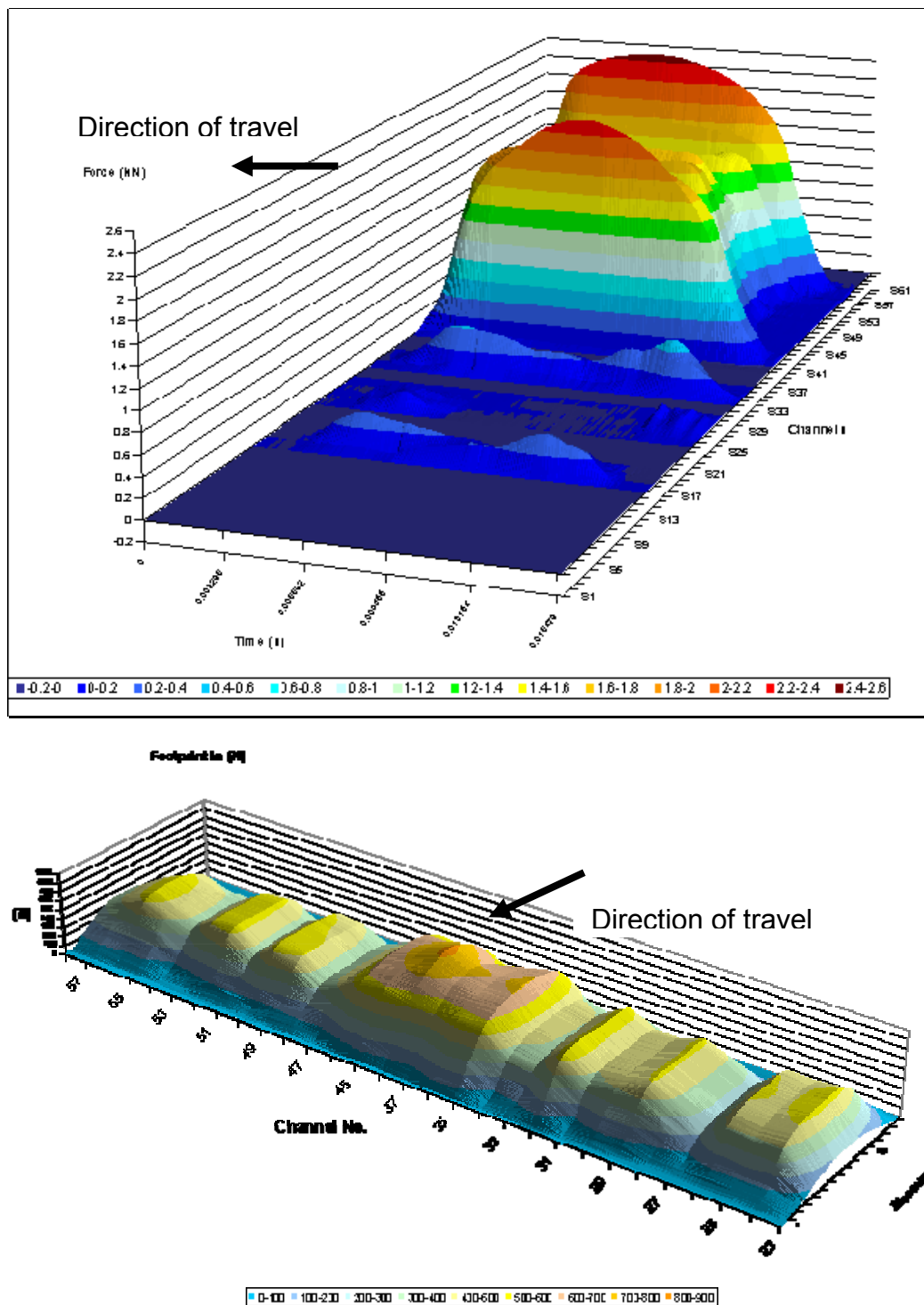


Figure 6. 14: An example of load distribution of unevenly inflated dual Tyres (top) and a closely-spaced dual Tyre (bottom)

6.7. Statistical Analysis of the Road Data

A large amount of data has been collected from the Modulas sensor installed in the A1 motorway. These data have been used to verify the Modulas sensor and the theory presented above on a large dataset as well as to obtain “footprints” from tyres in the

field.

It is known that the WIM system currently installed at the footprint monitoring site is able to predict static axle loads from dynamic passes with a maximum error of about $\pm 10\%$ (chapter 5). By making the assumption that the loads on these axles are mostly balanced or nearly balanced (i.e. wheel load = $\frac{1}{2}$ axle load) this dataset was used to verify the wheel load calculation (Equation 2).

Equation 2 was calculated for all the matched WIM/Modulas events in September 2006. Figure 6. 15 shows the results of this, along with a fit line generated using a robust MM regression algorithm. It can be seen that there is a clear correlation in the data and that the slope is not far off 1:1. It is equally clear that there are a large number of outliers. The reason for these outliers is not yet known but could be attributed to any of the following factors:

- a defect in the mathematical model.
- errors in matching.
- the combined errors in the WIM and the balanced load assumption.
- some combination of the above.

Further analysis of these results is illustrated in Figure 6. 16 which shows an area of $\pm 20\%$ either side of the regression line, and highlights the events that fall within this boundary. It has been calculated that approximately 76% of the events recorded during the four matched days in September gave calculated wheel loads within $\pm 20\%$ of the recorded WIM measurement.

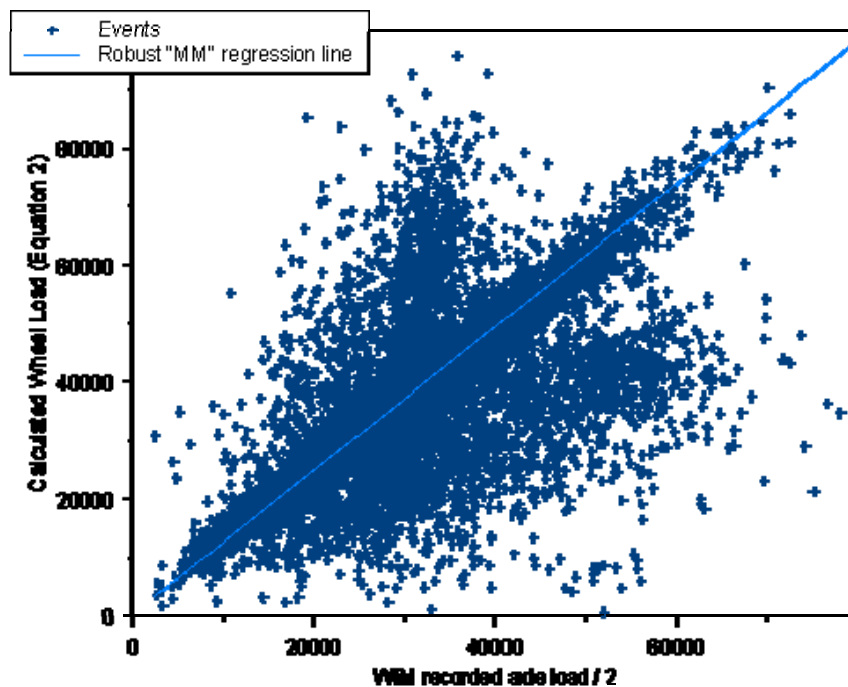


Figure 6. 15: Plot of wheel loads on the A1 (Sept. '06) as measured by the WIM

system and as calculated from the Modulas data.

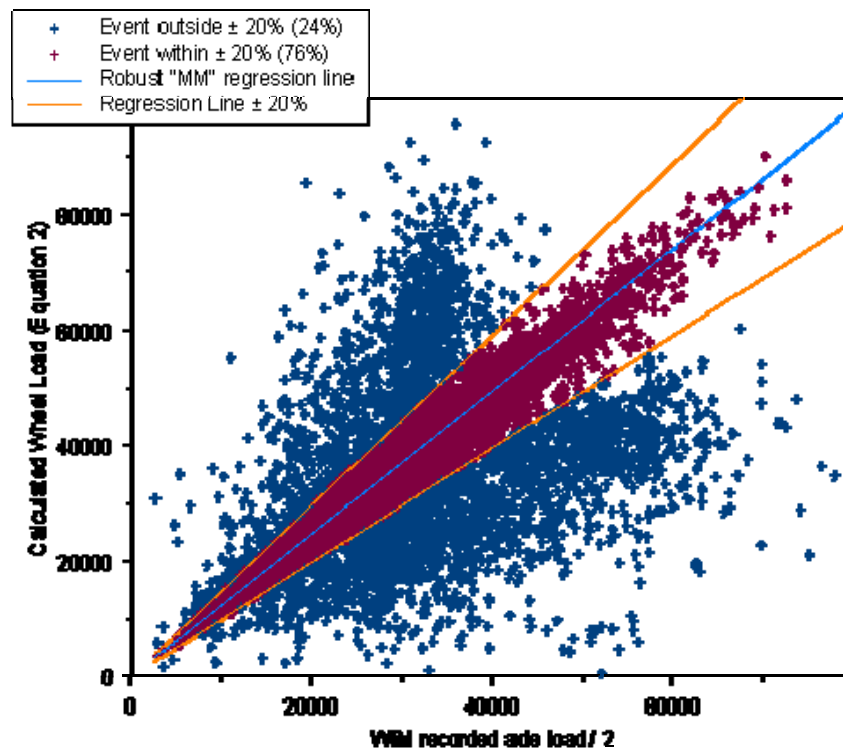


Figure 6. 16: Plot of wheel loads on the A1 (Sept. '06) as measured by the WIM system and as calculated from the Modulas data with 20% boundaries

There are clear secondary correlations in the data presented in Figure 6. 15 and Figure 6. 16. One possible explanation for this is in the matching algorithm. As the matching procedure always takes the first match within the time interval, it is possible for it to match to the wrong axle of a particular vehicle: It is possible that the 'upper' correlation may be double Tyres being matched to single Tyre WIM events and that the 'lower' correlation is single Tyres which have been matched to double Tyre WIM events. This is partially borne out by the fact that the events in the upper correlation tend to have significantly more active channels than those in the lower (Figure 6. 17). While this is, to some extent, expected (as heavier Tyres will have more active channels) we would expect to see a greater proportion of wider Tyres in the lower correlations (from unladen vehicles, etc.). In other words, if the distribution of Tyre widths against load was entirely random, we would expect to see a much higher proportion in the lower correlation and much lower proportion in the upper correlation than we actually do.

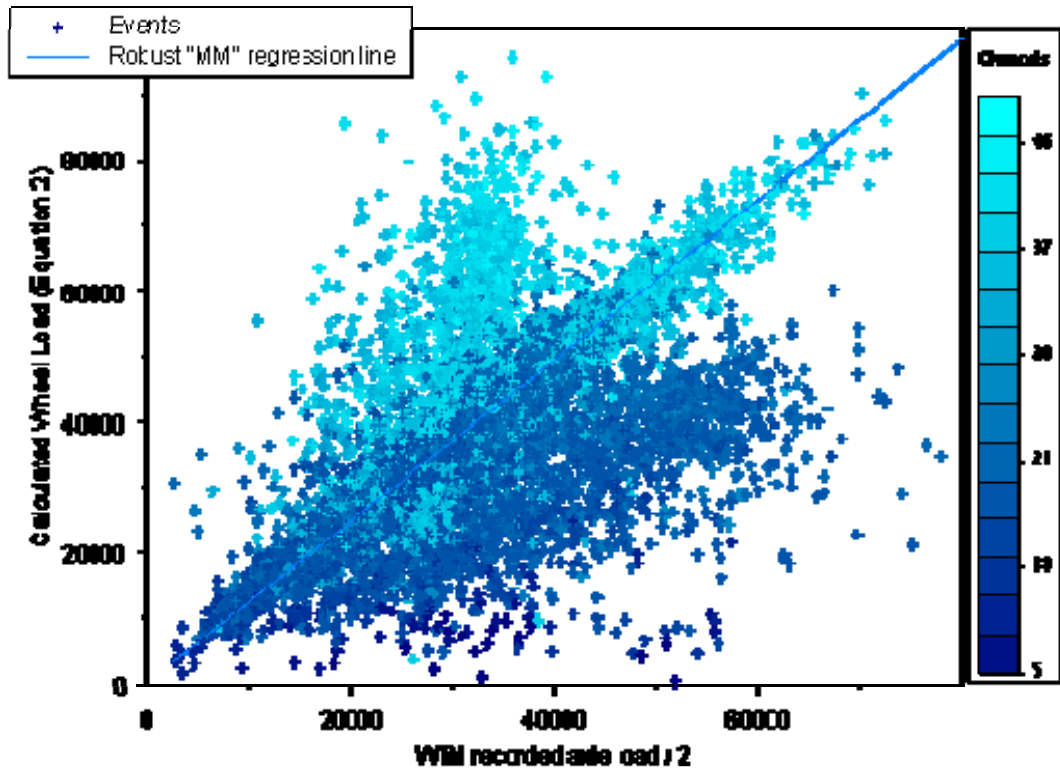


Figure 6. 17: Plot of wheel loads on the A1 (Sept. '06) as measured by the WIM system and as calculated from the Modulas data with events colour coded by number of active channels

6.8. State of the Modulas Sensor End of 2006

The 64 channels of the Modulas sensor were functioning properly until Spring 2006 where some channels started to malfunction. By the end of 2006 the 6 channels shown in Figure 6. 18 were registering signals that were not considered valid in comparison with previous data and in comparison to the neighbour channels. A thorough investigation of the causes of failure in cooperation with the manufacturer Kistler is planned for Spring 2007 within the framework of a follow up project.

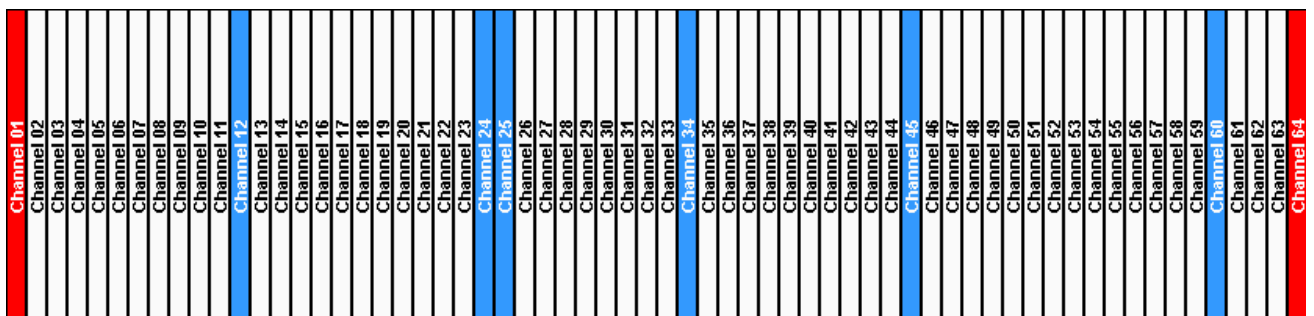


Figure 6. 18: By of end of 2006 the channels shown in blue were malfunctioning

Figure 6. 19 gives an indication of the percentage of events in 2005 where a channel was active. Channel one is towards the centre of the lane and channel 64 towards the hard shoulder showing that the majority of the passes lean towards the hard shoulder. This is due to the fact that the FMS is located after a curve and the vehicles tend to drive towards the hard shoulder. Comparing Figure 6. 18 with Figure 6. 19 shows that the most active channels were not necessarily the ones that failed.

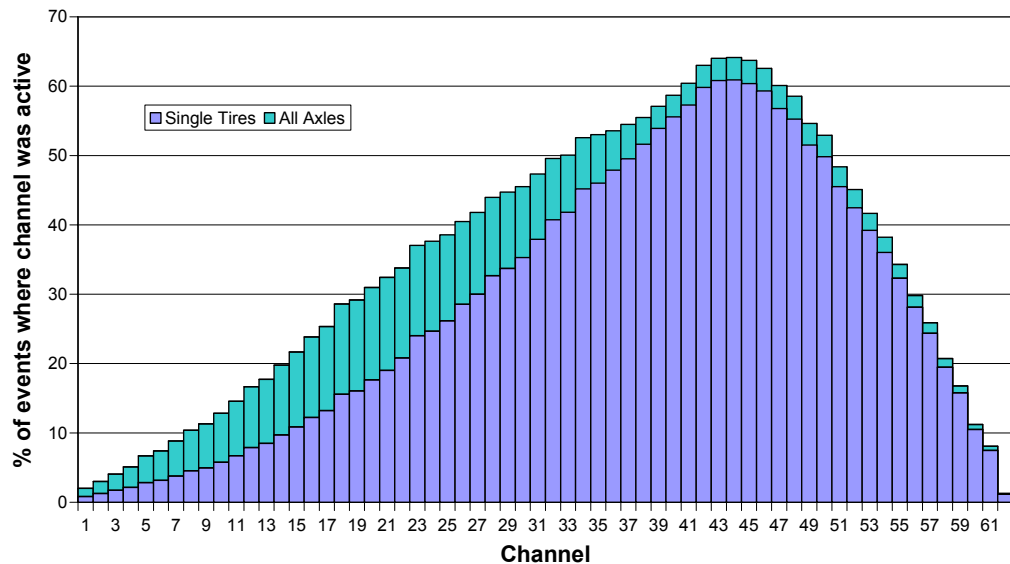


Figure 6. 19: Channel Activity on the Modulas Sensor for all events in 2005

6.9. Conclusions and Further Work

The two methods which have been proposed for the analysis of the SIM data both have certain advantages and limitations which are summarized in Table 6. 3.

Table 6. 3: Advantages and disadvantages of the different stress distribution calculation methods

Method	Advantages	Drawbacks
The P_z / p_z method	Direct use of the recorded data. No errors introduced by post-processing. No data from other sources needed.	The effective averaging out and smoothing of the peaks could, on some occasions, provide an unconservative estimate.
The F_z / σ_z method	Closer to what is physically happening on the pavement. More detailed stress distribution.	Errors propagate through the distribution. Requires vehicles of a known velocity (and is therefore dependant on the accuracy of velocity measurements)

The results from the Modulas appear largely insensitive to temperature, angle and speed.

From a visual inspection of the recorded stress distributions, Tyres which are over/under-inflated, Tyres which are faster/slower than normal and Tyres crossing the sensor at a reasonable angle can be clearly identified. None of these parameters appear to have a significant effect on the wheel load as calculated with equation 4 (except velocity, which is accounted for).

Stress distributions can be determined to be from over/under-inflated Tyres by examination of the shape of the stress distribution and whether it has one peak ('n'-shaped) or two peaks ('m'-shaped). Further work should be undertaken to create a formal classification, which could allow the extent to which a distribution is "n" or "m"-shaped to be quantified. An attempt could be made to relate this to the ratio of load to Tyre pressure.

Applying equation 4 to a sample of the road data shows a clear correlation between the recorded weights and the weights calculated from the Modulas data. This can only be used as a rough guide, however. The recorded data has the errors inherent in the WIM as well as the error involved in calculating wheel load as half the axle load. It is also subject to the accuracy of the matching algorithm.

7. DEFORMATION MONITORING

(Authors :Peter Andereg, Rolf Brönnimann, Rico Muff)

7.1. Sensor Description

The displacement measurement is based on a commercially available magnetostrictive sensor. The sensor consists of a tube enclosing, a magnetostrictive rod and a head with electronic devices. The material of the the rod is a special metallic alloy. An electrical impulse induces an acoustic pulse in the magnetostrictive rod at places where the rod is magnetized. The pulse travels along the rod and its time of arrival is recorded. Knowing the velocity of sound in the rod, the position of the magnetization can be calculated. Small permanent magnets are sufficient to generate the acoustic pulses without contact. Therefore the sensing system can be enclosed hermetically and it contains no moving parts. Several magnets can be moved along the rod and their position can be measured simultaneously. The delay time is measured. The dependence on the temperature T has to be known for accurate results. Figure 7. 1 shows the layout of the sensor within the payment, the measuring principle and the response of the magnestriuctive sensor. Magnet M3 represents the fix point at -640 mm, 'Ref.' is the reference point in the sensor head.

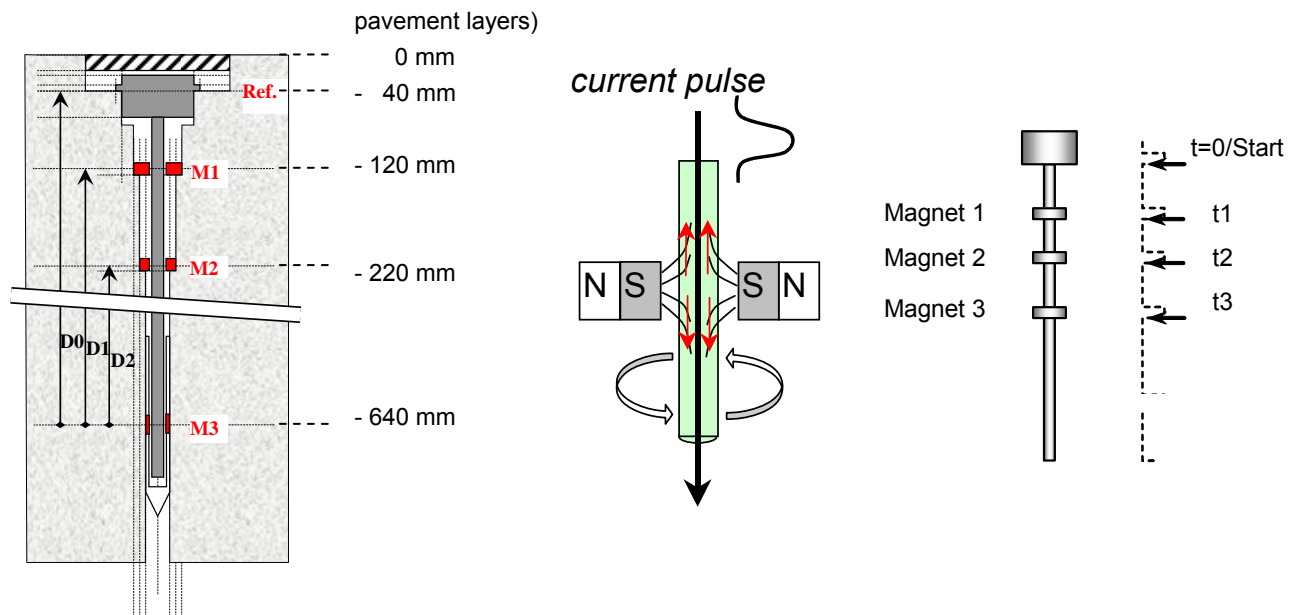


Figure 7. 1: Layout and principle of the installed sensors with the position of the magnets M1 ... M3

To calculate the position x of a magnet as a function of time t a linear function is used:

$$x = v(T) \cdot t + \alpha(T) \quad \text{Resolution: } t = 122 \text{ ps therefore } x = 0.4 \text{ } \mu\text{m}$$

The influence of the temperature T is included in the velocity of sound $v(T)$ and the offset $\alpha(T)$. The approximated velocity of sound is 3000 m/s. The exact value will be delivered with each sensor or can be found by a calibration.

On the A1-monitoring site three sensors were installed each measuring three positions within the pavement (Figure 4. 1). The three sensors are identified as sensor 1 to sensor 3 with sensor 1 located closest to the shoulder and sensor 3 closest to the centre of the slow lane and sensor 2 in between.

7.2. Sample of Measurement Results

The focus in the pavement deformation measurements is twofold. On the one hand the direct deformation from a passing vehicle is measured and on the other hand the long-term effects, i.e. the plastic deformation of the pavement layers. To know more about the development of these effects single truck passages were recorded. Figure 7. 2 gives an example of the measured vertical dynamic deformation within the pavement layers. The distance between the sensors in the driving axis is 1 m. Taking the sensor distances into account a two axle truck crossed with a speed of about 80 km/h over sensor 2 affecting sensor 1 first. Calculated from the two short negative peaks (sensor 2) the axle distance is about 4.2 m.

The measured dynamic deformations are much smaller, than the long term effects we are looking for. Despite these small effects, the weekly 20'000 trucks with an average load of 10t cause plastic long-term deterioration within the pavement layers. Long-term monitoring over five years on the previous established test site nearby (Lenzhard) shows very small plastic deformations in this kind of pavement. A standard deviation of less than 0.1 mm for the long-term measurements is obtained [Anderegg, 2002, Raab 2005].

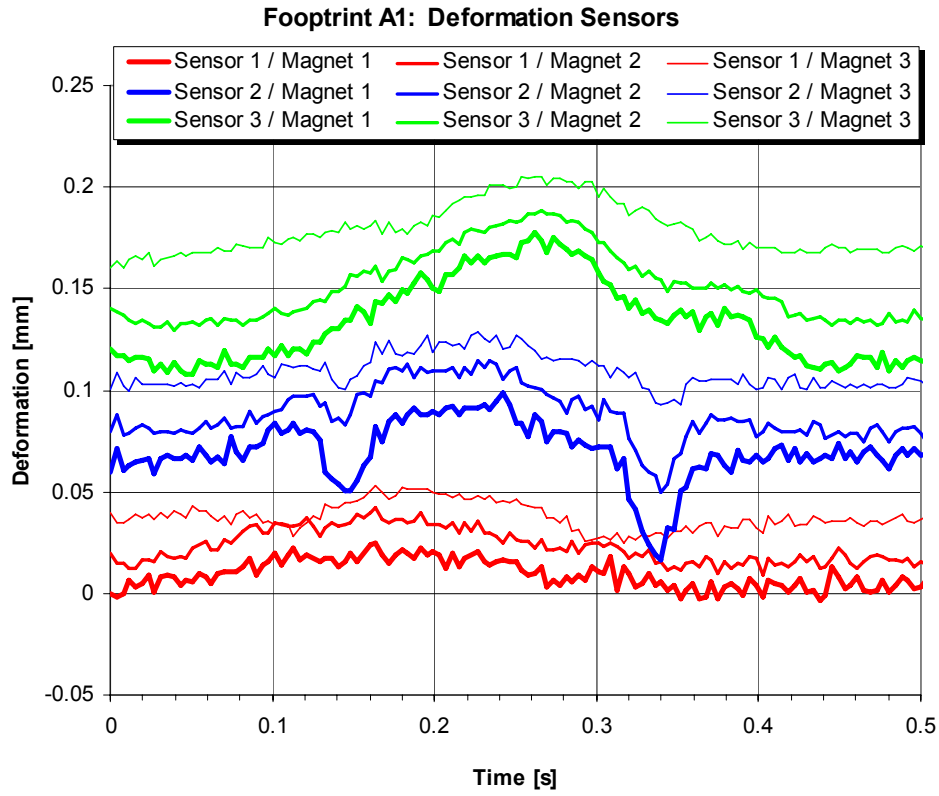


Figure 7. 2: Sample of deformations within the pavement most likely from a two axle vehicle passing over sensor 2

8. TEMPERATURE MONITORING

(Author: Gerald Morgan)

8.1. Sensors' Description

A large number of temperature sensors have been installed at the footprint site. The primary sources for temperature data consist of the cluster of sensors adjacent to the Modulas. This consists of six sensors at three depths—two at each inter-layer interface—and this is therefore the temperature data that was used for finite element modelling (chapter 17). The positions of these sensors can be seen in Figure 8. 1. It should be noted that the three inter-layer regions at which the temperatures are recorded are not the same three regions where the deflections are recorded. In addition to these several other sensors also include temperature monitoring: The Balluff deflection sensors each record their internal temperature as do several components of the DAQ system. While these temperatures are useful for the monitoring and maintenance of the equipment, they have not been used in any analytical procedures as they are affected by the heat generated by the electronic systems of the sensors and DAQ system.



Figure 8. 1: Photograph from installation of temperature sensors showing their location in the pavement

8.2. Sample Output

Figure 8. 2 shows a sample of temperature measurements from May 2005 until October 2006. It is shown that the surface layer temperature (4 cm deep) varied from -3 °C to 46 °C. The medium layer (12 cm deep) varied from -2 °C to 40 °C and the deep layer (22 cm deep) varied from -1°C to 36 °C.

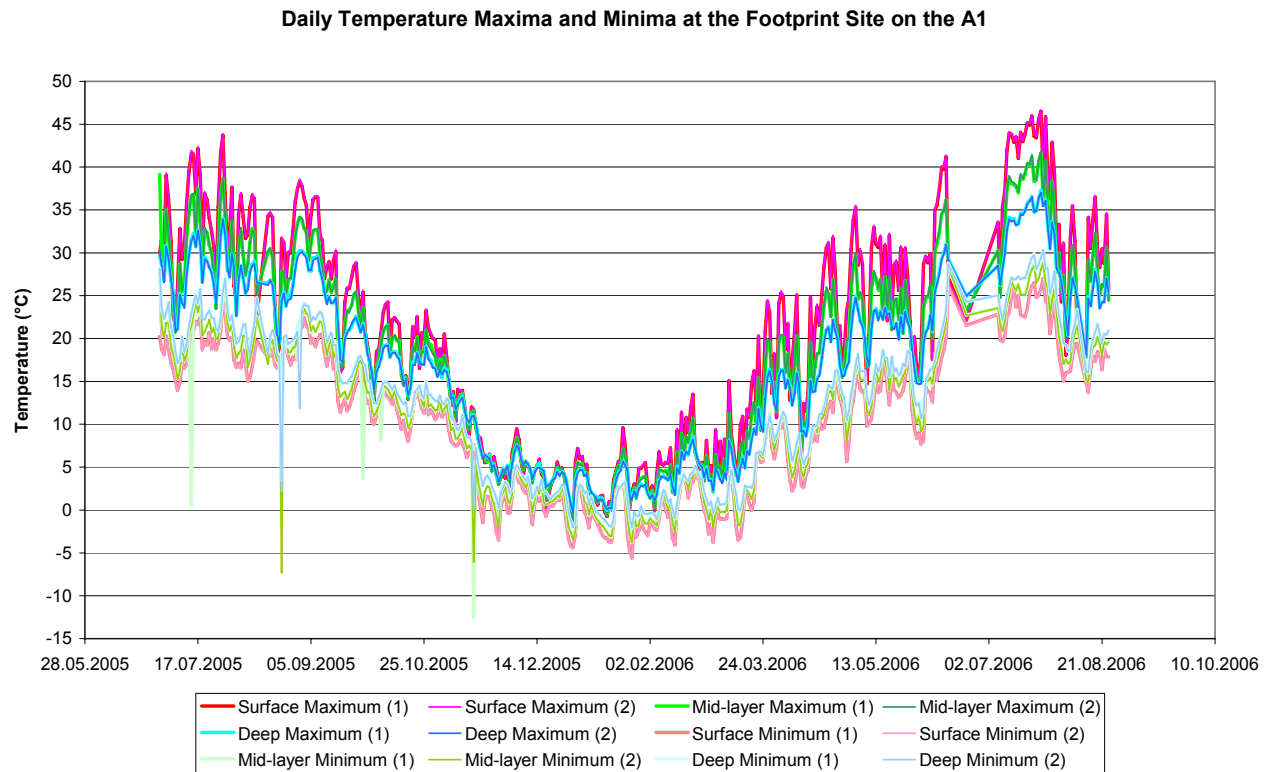


Figure 8. 2: Figure Sample of temperature variation at three layers of the pavement at the FMS: Surface = 4 cm deep, Mid-layer = 12 cm deep and Deep = 22 cm deep from both sets of sensors

9. HUMIDITY MONITORING

(Author: Roman Mastrangelo)

9.1. Sensors Description

The sensor consists of a heat resistant fibreglass cloth with woven, mutually isolated electrical conductors. The electric signal which is being analyzed is the change in the conductance of the sensor.

This sensor-reel was cast-in using a porous primer to ensure that the sensor is not being sealed by hot applied joint sealant during installation.

Three such sensor-strips (A, B and D), each 2m long, are placed at different depths, corresponding to each layer. Sensor A is at a depth of 5cm, B is at a depth of 12cm and sensor D is at a depth of 22cm.

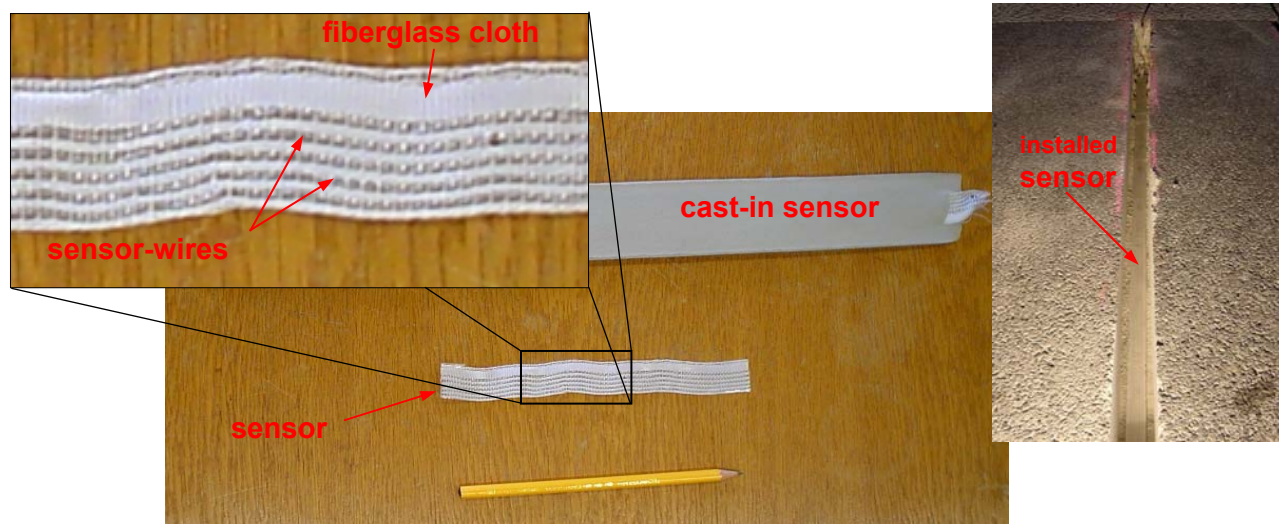


Figure 9. 1: Humidity sensors

9.2. Sample Output

The data in the following diagram were acquired just after installation. Sensor A (in a depth of 5cm) was the only one that became wet during installation. The others stayed dry. After about two or three days, sensor A became also dry.

The threshold value between dry and moist and between moist and wet is not an exact value. It has been determined in the laboratory using a test to clarify the signal. In principle with this kind of sensor it is only possible to detect dry (no signal) and wet (short circuit) state.

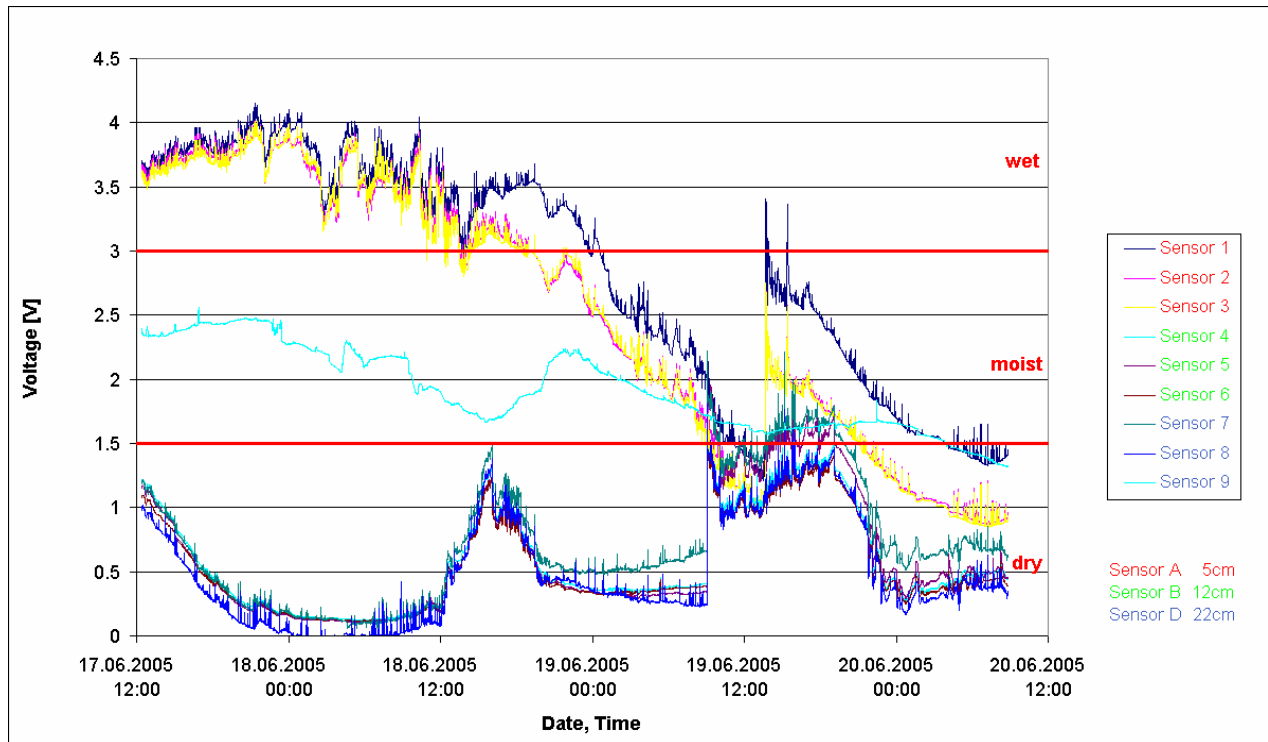


Figure 9. 2: example of humidity monitoring at the FMS

Up to now, the data acquisition works properly but it seems that the pavement is dense and no moisture can reach the sensors yet. That's the reason why a few days after the installation the signal of each sensors was around 0 V and it is still at this level. Hence, there is good reason to assume that in the vicinity of the sensor no water damage to the pavement takes place.

10. ACOUSTIC MONITORING

(Author: Kurt Heutschi)

Introduction

Within the concept of footprint it is desired to get acoustical information of each single vehicle passing a monitoring station. Such a measurement will be performed with a microphone at a certain distance at the border of the road or rail. The more distant the source is, the lower the acoustical signal. For point sources the geometrical spreading A_{geo} , which is the main factor influencing sound attenuation at short distances, has the form

$$A_{geo} = -20 \log(d/d_0) \text{ [dB]}$$

Where d is the distance from source to receiver in meters and d_0 is the reference 1 m. From eq. 8.1 follows that each doubling of distance leads to a reduction of 6 dB corresponding to a bisection of sound pressure amplitude. Best results of a single vehicle measurement can be expected if the moment in time is evaluated for which the vehicle is closest to the microphone. Nevertheless it has to be reckoned that there is unwanted sound at the microphone coming from other vehicles. So the main difficulty in acoustical monitoring of single vehicles is the question of how to handle the disturbing influence of neighbour vehicles.

10.1. Preliminary Measurements on A2 in Reiden

Location

The Swiss Agency for the Environment, Forests and Landscape (SAEFL/BAFU) maintains a permanent road traffic noise monitoring station at highway A2 in Reiden, in Canton Luzern (coordinates: 639'560/232'160, see Figure 10. 1 and Figure 10. 2). The road has four lanes and an extra emergency lane on both sides. The allowed maximum speed is 120 km/h for passenger cars and 80 km/h for trucks. The microphone geometry is based on the ISO 11819-1 standard where two microphones are installed for both directions. In this case the distance and height of the microphone had to be slightly adjusted to avoid shielding from the guard rail. With a resolution of 30 minutes the average sound pressure is evaluated routinely as A-level and in third octave bands. Furthermore traffic is counted where each single vehicle is detected by two induction loops.

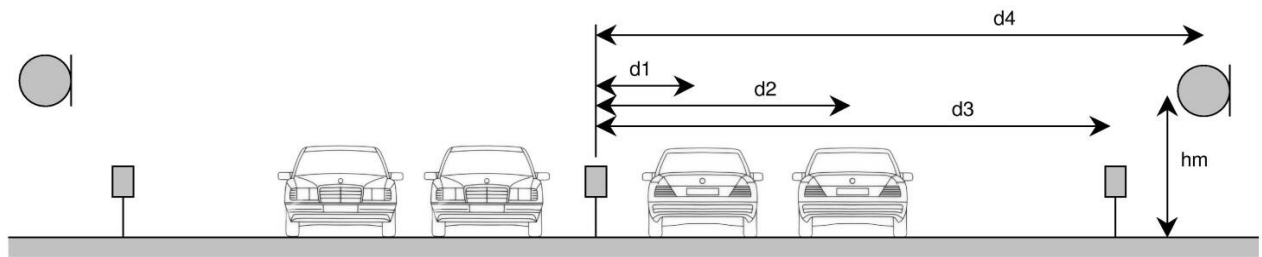


Figure 10. 1: Cross sectional view of the measurement location Reiden with $d1 = 2.55$ m, $d2 = 6.2$ m, $d3 = 10.9$ m, $d4 = 12.7$ m and microphone height $hm = 3.5$ m



Figure 10. 2: Measurement location Reiden. The microphone is protected with a grid basket

For the purpose of a preliminary test measurement for footprint we were allowed to equip the station with an additional sound level analyzer (Norsonic 121, EMPA no. 1) and to use the data from the traffic counter. The analyzer was programmed to record the A, Fast-weighted sound level with a resolution of 100 ms. The microphone used was the one measuring the two traffic lanes heading south. The measurement started on December 04, 2003 and ended January 07, 2004.

Evaluations

The measurements in Reiden delivered a traffic list of all pass-by events with information about

- event time
- traffic lane on which the vehicle passed the measurement site
- category of the vehicle according to the SWISS10 scheme
- speed of the vehicle

Based on the traffic list those events were selected where a truck (categories 8, 9 and 10) passed the microphone on lane 1 (standard lane). Then the sound level time history was inspected to evaluate the maximum level. Based on ISO 11819-1 two criteria were applied to decide whether or not a measurement was valid:

6 dB down rule: The 6 dB down rule is a pure acoustical criterion. It can't be applied directly on a high resolution level-time history as there are always statistical level fluctuations due to the random character of the noise source. Therefore an uncertainty of 0.5 dB(A) was introduced to examine a monotonic 6 dB decrease to both sides of the maximum value (in the future and in the past).

Freedom of disturbing vehicles: The 6 dB down criterion alone does not guarantee a reliable measurement. It is e.g. possible that a disturbing vehicle overtakes the target vehicle just the moment the target vehicle is passing the microphone. The corresponding level-time history would yield a well pronounced maximum with a descent before and afterwards. For that reason a supplementary criterion based on the traffic event list was investigated. There is some elbowroom on how strict such a criterion should be formulated. Under the assumption that the disturbing vehicle emits equal sound power as the wanted vehicle a free time frame of +/- 1 second seems appropriate to assure no interference.

It can be assumed that the percentage of vehicles that can be assigned to a valid measurement value depends on traffic density. Hence for each pass-by event the number of vehicles per hour was evaluated. This figure was determined by counting all vehicles (including passenger cars) travelling on the two lanes in the observed direction. Figure 10. 3 shows the results for the measurements in Reiden.

To estimate the rigorousness of the two validity criteria, the number of valid vehicles was evaluated by applying the two criteria separately. From Figure 10. 3 and Figure 10. 4 it

can be seen, that the +/- 1 sec time frame is clearly the more rigorous criterion compared to the 6 dB down rule. To get a reasonably high portion of valid events the +/- 1 sec time frame has to be dropped with the consequence of a somewhat higher uncertainty.

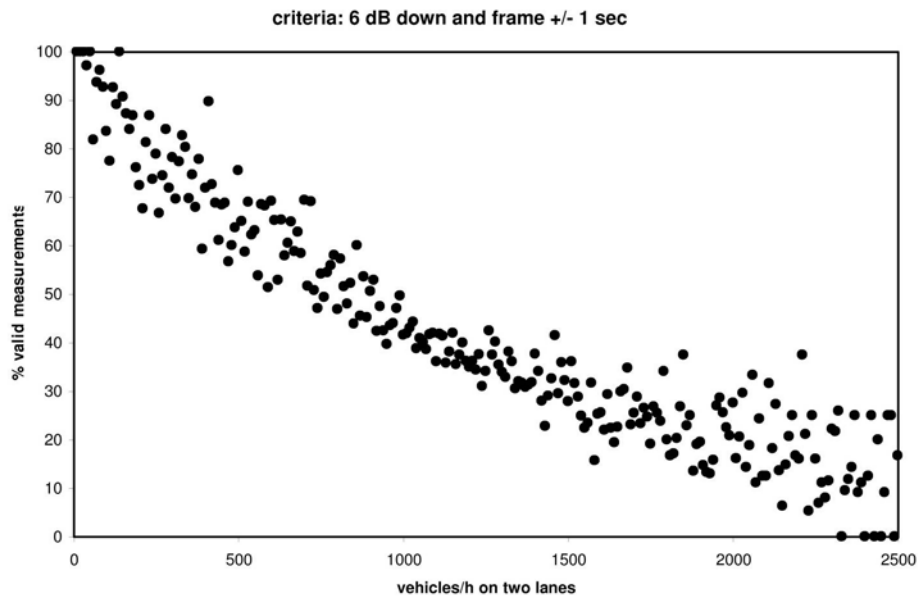


Figure 10. 3: Percentage of valid single truck measurements at station Reiden as a function of number of total vehicles (for intervals of 10 vehicles/h) on the two lanes heading south. The applied criteria are the above mentioned 6 dB down rule and a time frame of +/- 1 sec without any other vehicle on the two lanes south

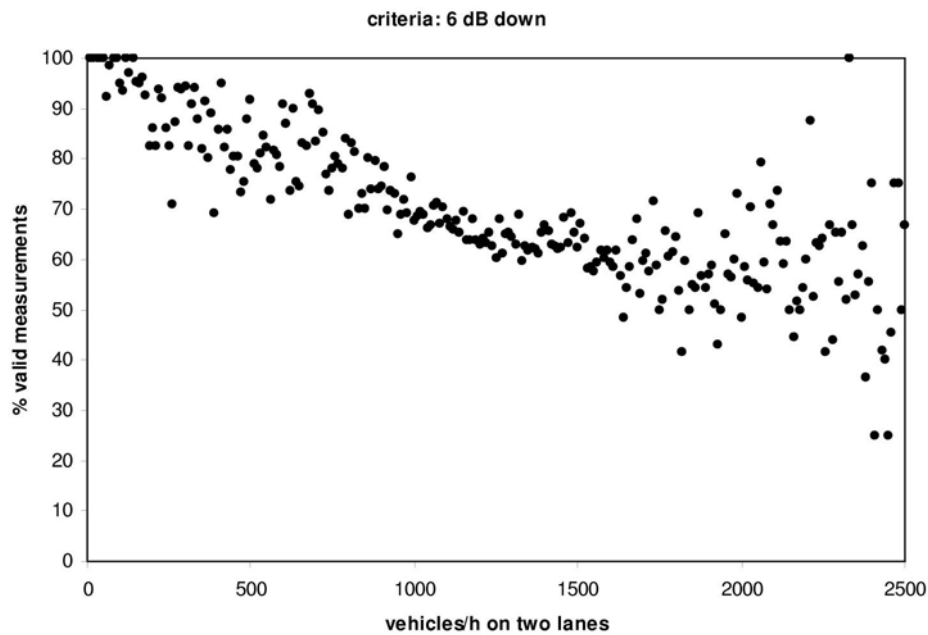


Figure 10. 4: Percentage of valid single truck measurements at station Reiden as a function of number of total vehicles (for intervals of 10 vehicles/h) on the two lanes heading south. The applied criterion is the above mentioned 6 dB down rule

Conclusions

The preliminary measurements lead to the following conclusions:

- The *6 dB down* criterion alone effects that the percentage of valid measurements of heavy vehicles is about 80% for 500 vehicles/hour on the two lanes heading in one direction and about 60% for 2000 vehicles/hour.
- The above mentioned *+/- 1 second free window* criterion is too restrictive. It can't be used to get a reasonable percentage of valid single events. In addition the increase of uncertainty can't be estimated precisely.

10.2. Strategies to Increase the Number of Valid Road Traffic Noise Events

To further increase the numbers of valid measurements the following strategies are possible:

- Elimination of disturbing vehicles
- Reduction of the influence of disturbing vehicles

- Mathematical compensation for the influence of disturbing vehicles

Elimination of disturbing vehicles

Disturbing vehicles may travel on the standard lane (where trucks are measured) or on the overtaking lane. Hence the amount of disturbing vehicles could be reduced by a separation of the two lanes. This measure can be implemented probably only in rare cases.

The probability that a vehicle on the overtaking lane disturbs the measurement could be reduced by introducing a second microphone some 50 m away. If the measurement at the first microphone is not valid there is a chance that the measurement at the second microphone is o.k. Regarding the possible improvement it remains an open question if the cost of the introduction of a second microphone chain is justified.

Reduction of the influence of disturbing vehicles

A decrease of the microphone distance reduces the disturbing effect of neighbour vehicles, as the distance ratios wanted / unwanted vehicles are more pronounced. By reducing the measuring distance, the level time history of a passing vehicle will no longer show one clear maximum with falling edges on both sides. On the contrary a single passage will show several maximums as a consequence of the distributed sources found on a vehicle. For shorter distances than 7.5 m the maximum pass-by level is no longer a suitable descriptor of the sound emission. Alternatively an energy based measure could be used as for example the value of the integral over the relevant part of the level time history. One disadvantage of such a descriptor is that it can not be compared directly to the maximum values according to the ISO standard. With a suitable sound propagation model it might be possible to recalculate one value into the other.

Another possibility to reduce the disturbing effect of neighbour vehicles is to use microphones with a pronounced directivity. The sensitivity of such microphones depends on the angle of incidence of the sound wave. By pointing to the target vehicle the contribution of neighbour vehicles which are located to the side is partially suppressed. The difficulty with such microphones is the calibration. Indeed for high quality measurements the only possibility is to use an intensity probe. The directivity follows a cosine law that is to say a source under 45° is suppressed by 3 dB. Even more extreme directivities could be achieved by using microphone arrays, however at the cost of very

high hardware and software effort.

Mathematical compensation for the influence of disturbing vehicles

At least from a theoretical point of view it is possible to compensate for the disturbing effect of neighbour vehicles. However there are two main difficulties:

Firstly the emitted sound power of the unwanted vehicles has to be estimated. This could be done by using an additional microphone which might be located at a different position. Of course there is no guarantee that the measurement of the unwanted vehicles can be performed without any interference of other vehicles. Another approach is to estimate the sound power from knowledge of the vehicle type and speed. Of course there remains an uncertainty as a result of individual variations (see Figure 10. 5).

The second difficulty is the estimation of the sound propagation attenuation from the disturbing vehicle to the microphone at the moment the wanted vehicle is measured. With today's propagation models it is possible to calculate the effect of geometrical spreading, air absorption and ground effect. What causes problems is the possible shielding by the wanted vehicle. This effect can hardly be accounted for.

Figure 10. 5 shows pass-by measurements of passenger cars at different locations with comparable standard pavement. From such measurements the standard deviation of the uncertainty in sound power level can be estimated to about 1.7 dB. What helps is the fact that trucks are usually noisier than cars. Assuming a vehicle speed of 120 km/h for cars and 80 km/h for trucks, the sound power level of trucks is about 4 dB higher. While measuring the truck, the cars are further away from the microphone. Typically one can assume that the cars that have to be compensated for show about 5 dB lower microphone levels. Figure 10. 6 shows the cumulative frequency distribution for the error in estimating the sound power of trucks. It was assumed that the sound produced by single vehicles follow a Gaussian distribution with a standard deviation of 1.7 dB and an energetic mean value of -5 dB relative to the amount produced by the truck. As can be seen from the figure there is an over estimation by more than 1.2 dB in 5% of all cases and an underestimation by more than -0.7 dB in 5% of all measurements. In 90% of all cases the error of the estimated sound power level of a truck is within the limits of +1.2/-0.7 dB.

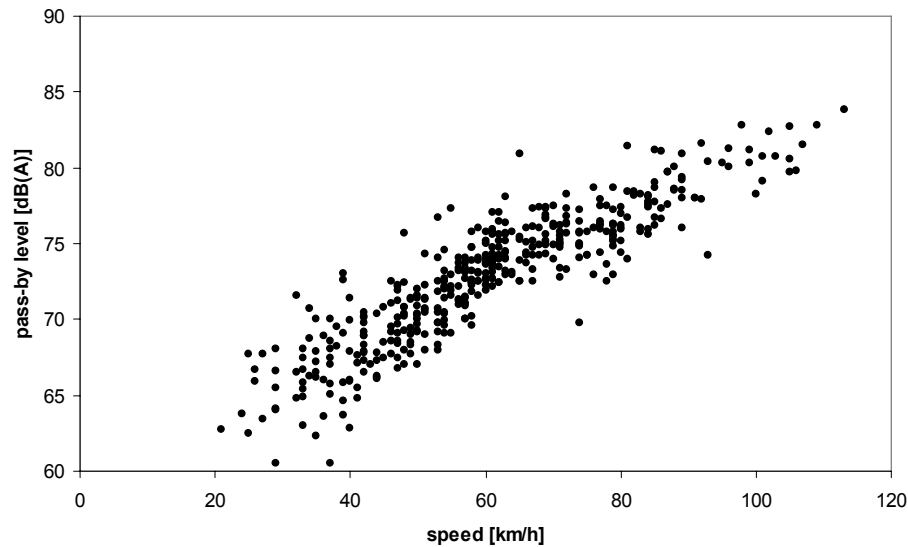


Figure 10. 5: Single pass-by measurements of passenger cars. The maximum pass-by level is shown as a function of vehicle speed

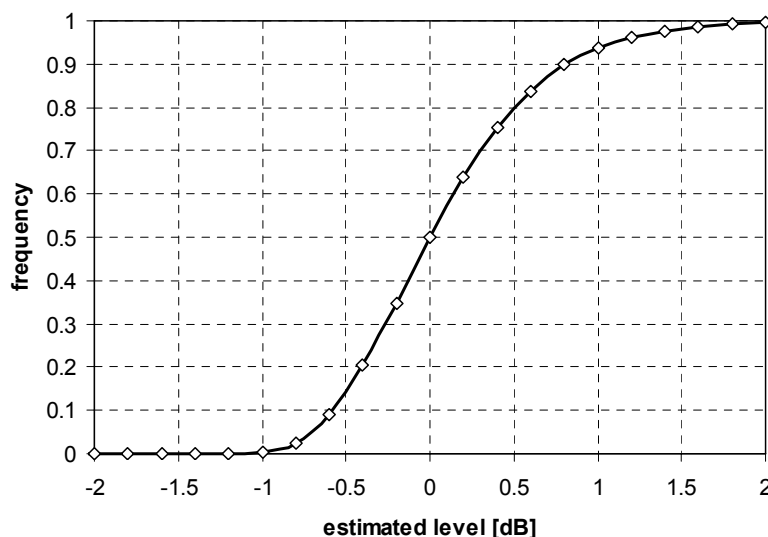


Figure 10. 6: Cumulative frequency distribution of the error in estimating the sound power level of a truck by compensating for the disturbing effect of a car with a level 5 dB below that of the truck

Basis for the above mentioned procedure to compensate for the effect of the contribution of passenger cars is the knowledge of the average sound power emitted as a function of speed. This relationship is not universal as it depends on the type of road surface and possibly on the car fleet. For that reason this relationship has to be established individually for each measurement location. From time to time the relationship has to be reviewed in order to follow possible changes in the conditions (e.g. the aging process of road surfaces).

One problem in compensating for the effect of passenger cars is the possible shielding effect by the truck as mentioned above. In cases where the passenger car is on the overtaking lane and at the same height as the truck while passing the microphone, the contribution of the passenger car is strongly reduced by the shielding of the truck. This effect can hardly be accounted for as the remaining level depends on the geometry of the truck. This information is usually not available. It is proposed to ignore this possible shielding effect which results in a possible overestimation of the passenger car contribution. This would lead to an underestimation of the sound power level of the truck which is o.k. in the sense 'innocent until proven guilty'.

From the above proposed strategies to increase the number of valid measurements a simplified mathematical compensation was chosen and implemented at the A1 footprint station in Lenzburg. As described in detail in the next section the contribution of a disturbing vehicle is estimated from the level time history alone.

10.3. Measurements on A1 near Lenzburg (FMS)

Location

The noise measurement instrument was integrated in the fully equipped *footprint* station on the highway A1 near Lenzburg (Figure 10. 7). Besides noise, acceleration and deformation were measured as well as the contact pressure distribution of Tyres (MODULAS) and the weigh in motion of vehicles (WIM). In cooperation with other European project partners measurement guidelines have been developed and used for noise measurements [Mayer et al 2007]. The road has four lanes and an extra emergency lane on both sides. The allowed maximum speed is 120 km/h for passenger cars and 80 km/h for trucks. The microphone was installed on the northern side of the highway for the evaluation of vehicles heading to the west (direction Bern). The measurement setup was based on the ISO 11819-1 standard. To avoid shielding by the guard rail, the microphone height was increased to 3 m above road level. Microphone signals were evaluated by a sound level analyzer Norsonic 121, Empa No. 1. The analyzer was programmed to record the A, Fast-weighted sound level with a resolution of 100 ms.



Figure 10. 7: Measurement location Lenzburg showing the microphone position 3 m above road level

Evaluations

Based on an event list (pass-by of heavy vehicles, categories 8 and 9) delivered by the WIM system the sound level recordings from September 3 to September 28th, 2005 were examined for detectable peaks. As mentioned above, possible interference with neighbour vehicles was checked by the observation of the level decrease before and after the peak. The *6 dB down* criterion requires that the level drops for at least 6 dB on both sides of the peak. To overcome the problem of stochastic level fluctuations the level decrease was tracked with an uncertainty of 0.5 dB. Under these assumptions the *6 dB down* criterion was fulfilled in about 50% of all events. A relaxation to 5 or 4 dB down would increase the amount of valid events significantly (Figure 10. 8) but at the price of systematic overestimation of the single event levels.

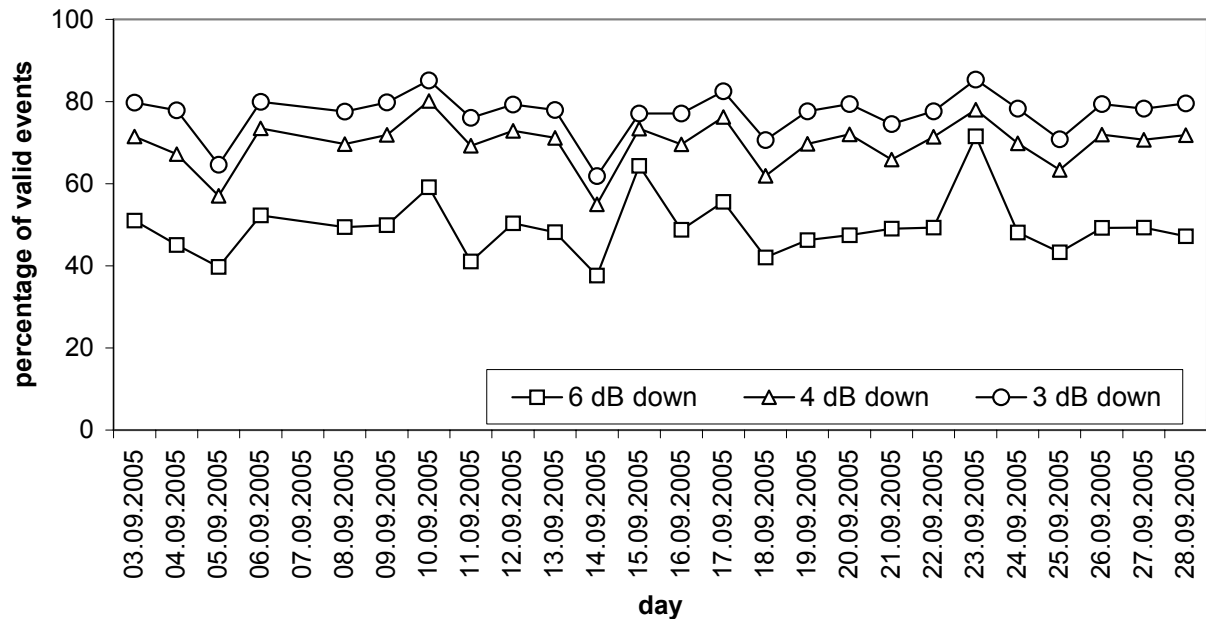


Figure 10. 8: Evaluation of the percentage of events that fulfilled a 6, 5 or 4 dB down criterion.

Correction for interference with disturbing noise

As mentioned above the main problem in evaluating the maximum pass-by level of a single vehicle is the interference with noise from neighbour vehicles. This leads to a systematic overestimation of the maximum level of the considered vehicle. If detailed information about all vehicles on each lane is available, it is in principle possible to estimate the sound powers and from that the effect on the microphone signal. Here a much simpler and more robust strategy is demonstrated that needs knowledge of the level time history only (in addition to the event time for the target vehicle).

Figure 10. 9 shows a pass-by event with an interference of the wanted vehicle and a disturbing vehicle. The microphone measures the total sound pressure level. As can be seen, the true maximum level of the wanted vehicle is a little lower than the maximum of the total microphone level. This is indicated by a violation of the 6 dB down criterion. The task is to estimate and compensate for the contribution of the disturbing vehicle to the total sound pressure at the time when the maximum of the total sound pressure is reached.

To do so the level of the disturbing vehicle is extrapolated along a straight line. This line is defined by two points. The first point is determined by searching the minimum next to the maximum. The second point is found 0.5 s back in time. The line through these two

points clearly overestimates the level of the disturbing vehicle at the moment the maximum of the target vehicle occurs. It was found that the level of the first point has to be lowered by 1 dB to yield more precise estimates. However this correction still ensures that the contribution of the disturbing vehicle is overestimated. The maximum level of the target vehicle is then calculated by subtracting the contribution of the disturbing vehicle from the total sound pressure level. By this procedure the resulting maximum values tend to underestimate the true values.

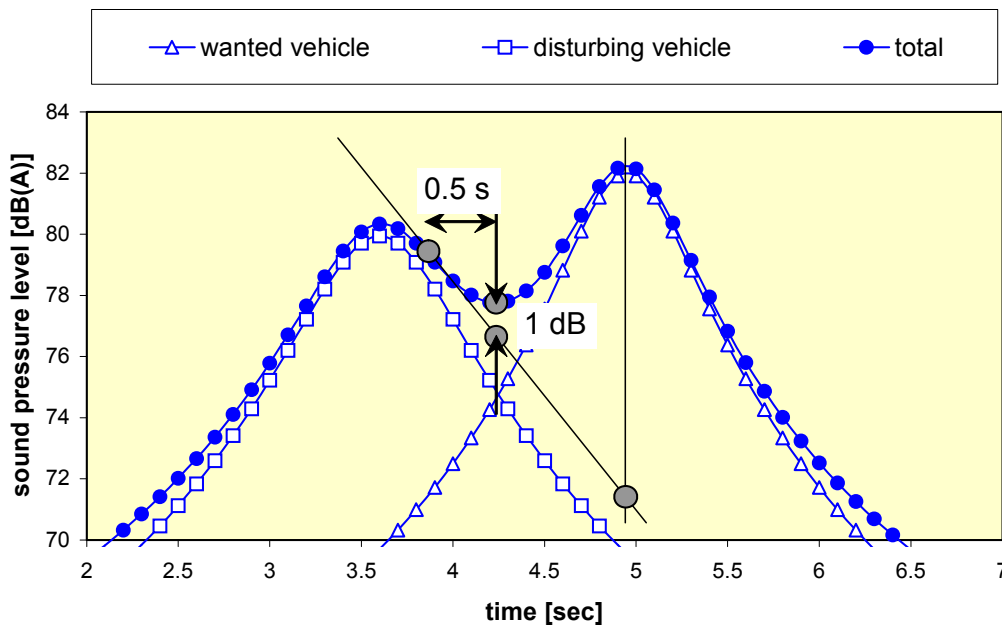


Figure 10. 9: Strategy to compensate for the interfering effect of a disturbing vehicle, shown for simulated level time curves (see text). Note that only the total sound pressure can be observed by the microphone

Figure 10. 10 shows a statistical analysis of the corrections applied for the measurements in Lenzburg for heavy vehicles (Swiss10 categories 8, 9, 10). The total number of vehicles evaluated was 47'000. For more than 90% of the vehicles the correction was below 3 dB.

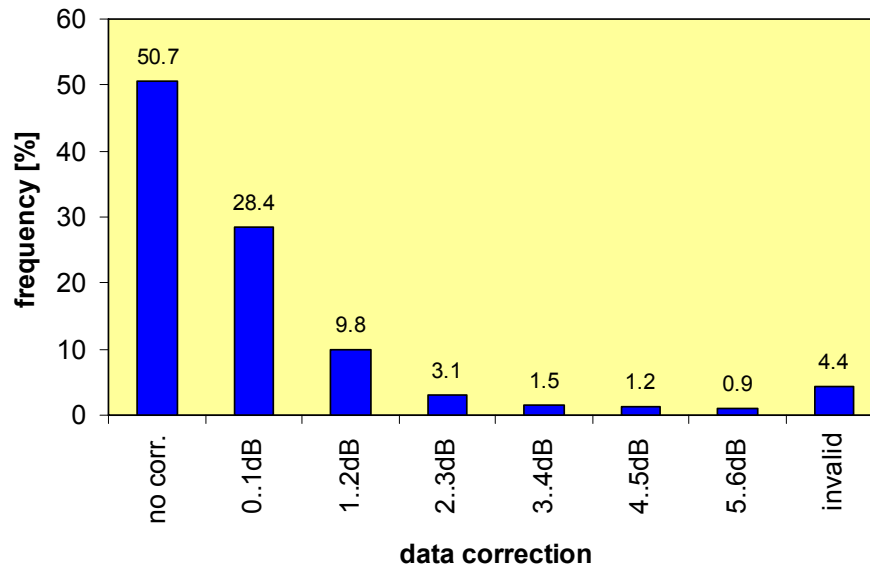


Figure 10. 10: Statistics of corrections applied to the measured max values in the Lenzburg measurements. 50% of the data fulfilled the 6 dB down criterion and needed no correction. 28.4% of the data were corrected for 0 to 1 dB, etc.

Results

Figure 10. 11 to Figure 10. 16 show the evaluated maximum levels for vehicles of Swiss10 categories 5 to 10. Table 10. 1 gives the corresponding median values and standard deviations.

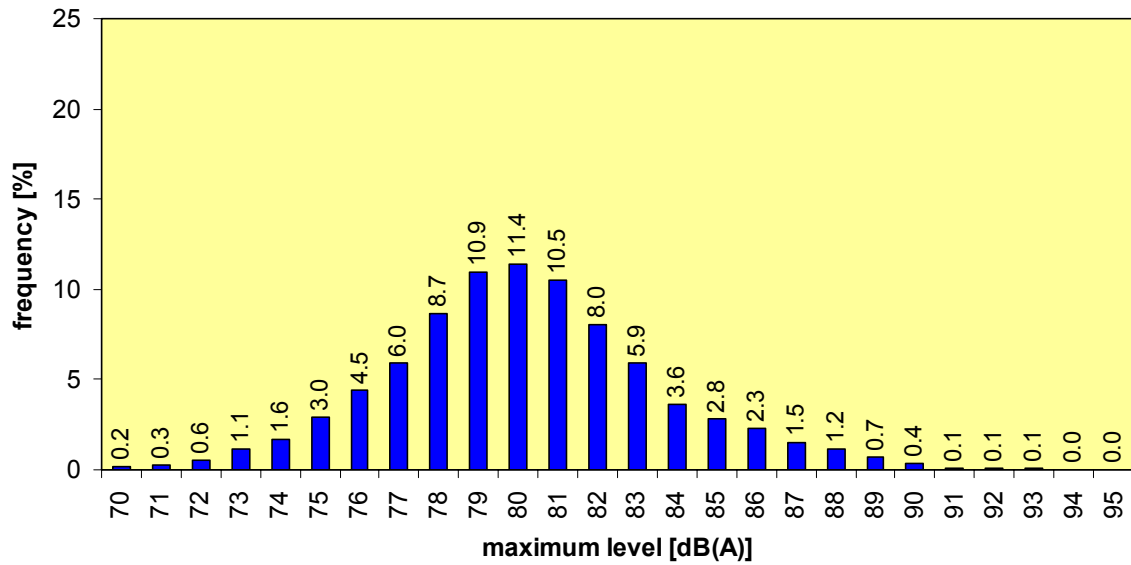


Figure 10. 11: Statistical distribution of the evaluated maximum levels of category 5 vehicles, delivery pick ups (Lieferwagen) at Lenzburg

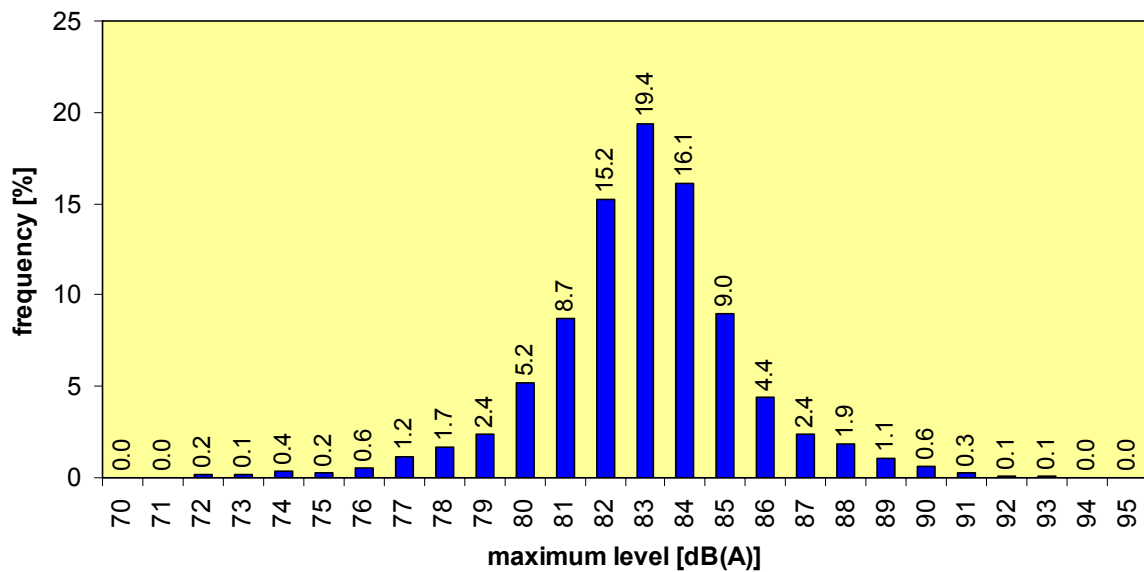


Figure 10. 12: Statistical distribution of the evaluated maximum levels of category 6 vehicles, delivery pick ups with trailer (Lieferwagen mit Anhänger) at Lenzburg

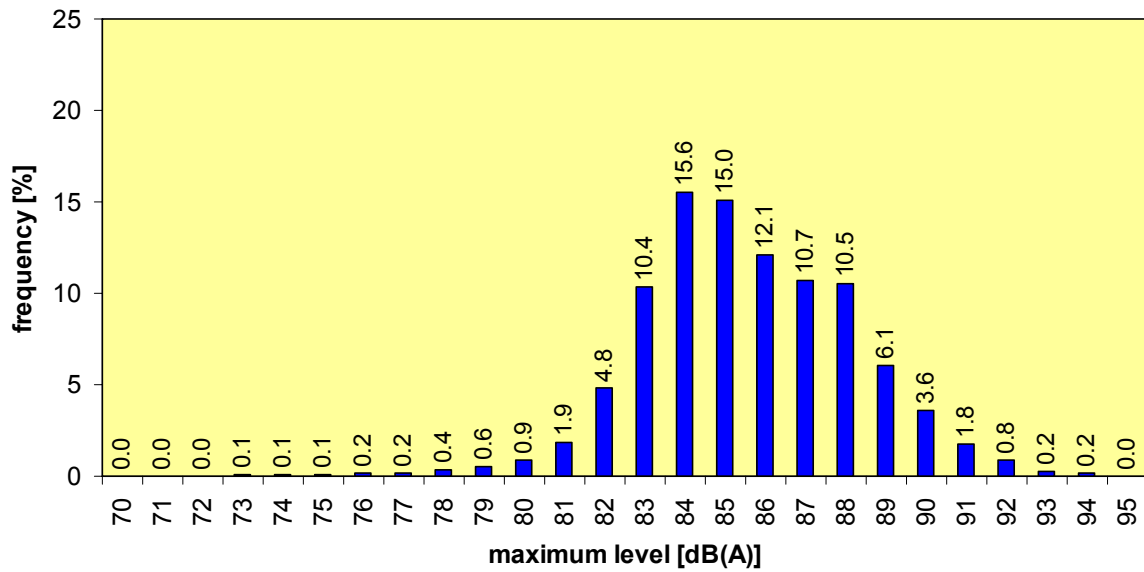


Figure 10. 13: Statistics of the evaluated maximum levels of category 7 vehicles, articulated delivery truck with semi-trailer (Lieferwagen mit Auflieger) at Lenzburg

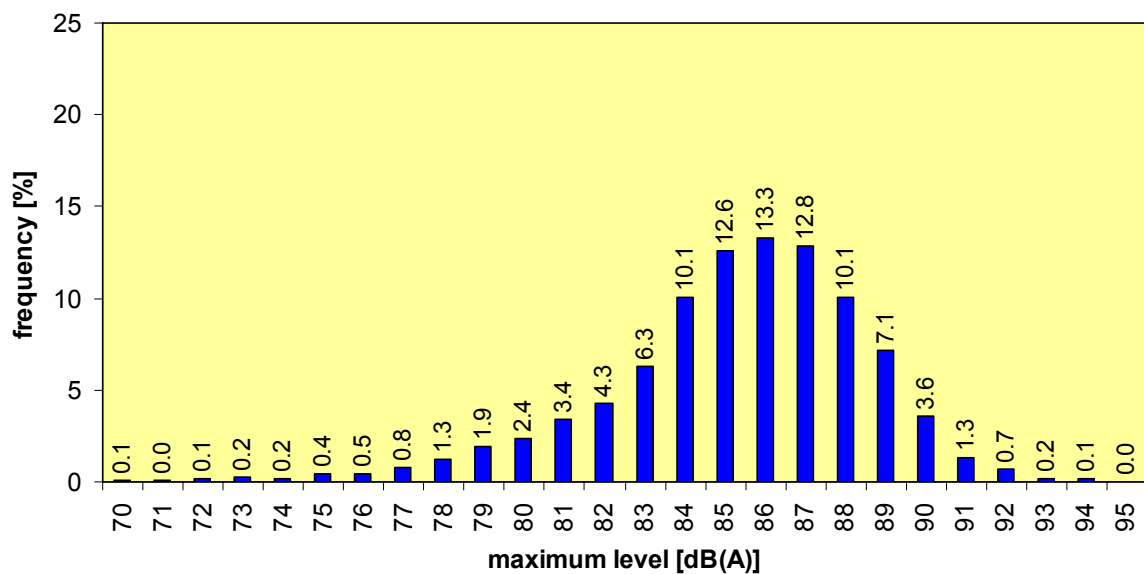


Figure 10. 14: Statistics of the evaluated maximum levels of category 8 vehicles, freight truck (Lastwagen) at Lenzburg

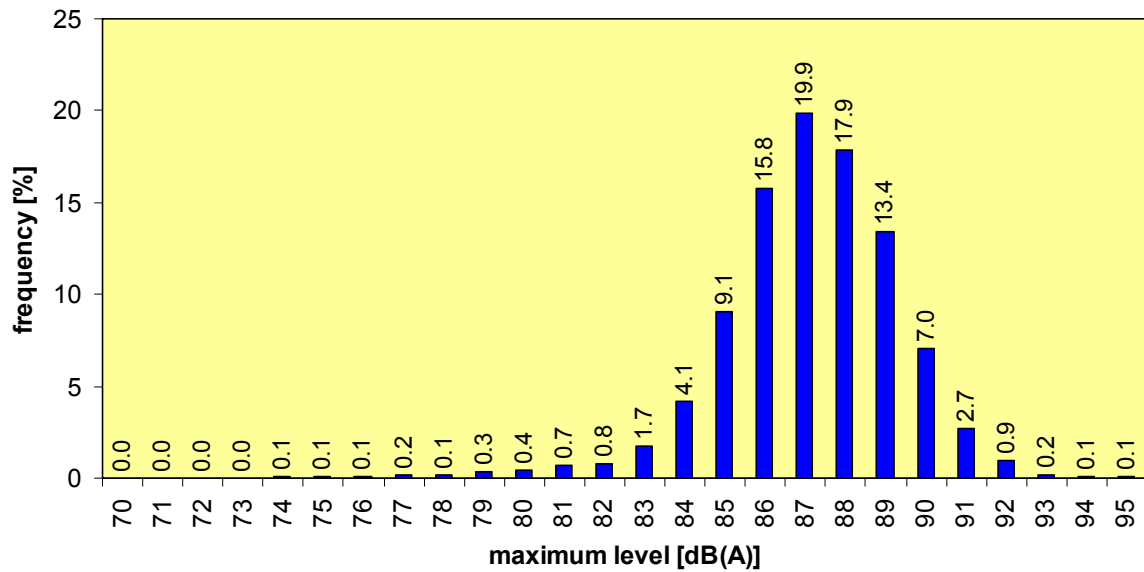


Figure 10. 15: Statistics of the evaluated maximum levels of category 9 vehicles, freight trucks with trailers (Lastenzug) at Lenzburg

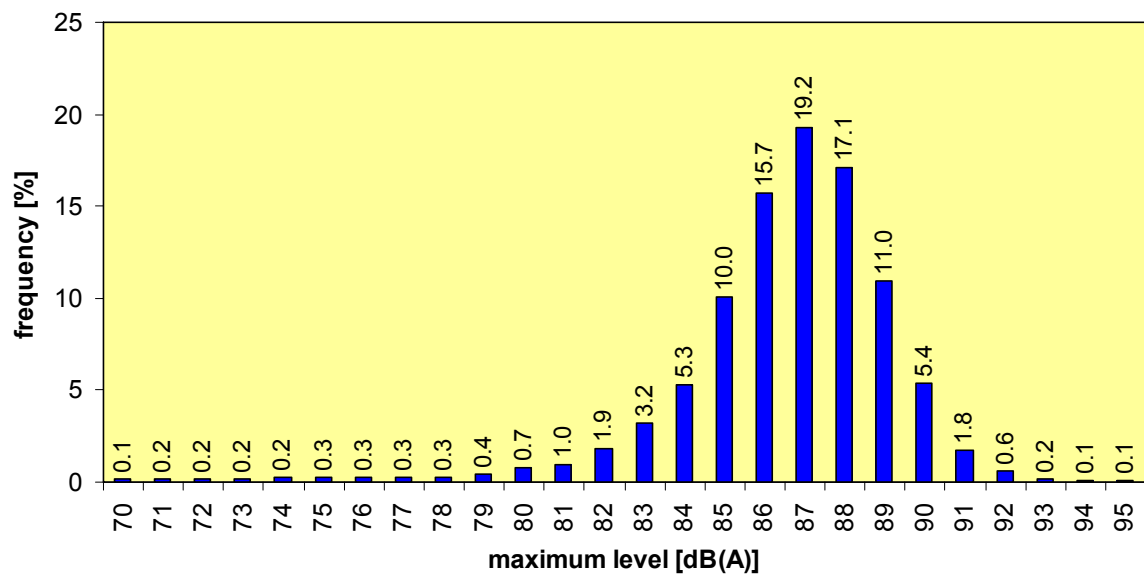


Figure 10. 16: Statistics of the evaluated maximum levels of category 10 vehicles, articulated freight truck with semi-trailer (Sattelzug) at Lenzburg

Table 10. 1: Median and standard deviations of the statistics of maximum pass-by levels and of vehicle speed for each vehicle class

vehicle class	median max. level [dB(A)]	stdev. max. level [dB(A)]	median vehicle speed [km/h]
cat 5	83.4	3.0	105
cat 6	84.0	2.7	88
cat 7	86.2	2.7	88
cat 8	86.3	2.8	88
cat 9	87.9	2.4	87
cat 10	87.5	2.5	87

Strategies for calibration

The measured sound level attributed to a single vehicle can not be interpreted on an absolute scale as there is a significant effect of the type of road surface on the emission of a vehicle. A vehicle should not be punished for a noisy road surface. For that reason an adaptive calibration procedure has to be included. For example a classification scheme could be based on the deviations of the single event value relative to a mean value for that site. This mean value could be adapted continuously to take into account factors such as temperature, surface condition etc. that influence Tyre noise.

10.4. Conclusions

The acoustical footprint of a vehicle passing by can be determined by evaluating the maximum sound pressure level received at a microphone in a distance of 7.5 m from the traffic lane. The validity of the measurement is checked by the *6 dB-down* criterion. If this criterion is not fulfilled the interference stemming from neighbour vehicles is estimated and compensated for based on the level time history. A maximum correction of 6 dB(A) is allowed. If a higher correction is deemed necessary from the calculations, the measurement is categorized as invalid. Current data from the Footprint Monitoring Site indicate that this procedure led to an increase of the percentage of pass-by events that could be evaluated successfully in the order of 95%. This result is for roads with dense traffic and an improvement can be expected for traffic that is less dense. The measurement uncertainty is estimated to 1 dB in the sense of a standard deviation.

11. VIBRATION MONITORING

(Author:Martin Arraigada)

One of the objectives of Footprint is to assess the impact of vehicles on the environment and characterise them in terms of their environmental friendliness. One parameter considered is the ground borne vibration produced by individual vehicles, as they may affect persons and buildings standing near the traffic corridors.

This chapter describes the vibration monitoring system incorporated in the Footprint monitoring site, at the A1 motorway near Lenzburg. It explains how to analyze and evaluate the vibration data and presents the result of a two months measuring period.

11.1. Basics of Ground Born Vibration

Introduction

Traffic vibrations are caused by dynamic Tyre forces on the pavement surface. These dynamic forces are generated by the rolling of the vehicle Tyres over the pavement's irregular surface and by the bouncing of the different parts of the vehicle itself. They comprise an average static value plus an oscillating dynamic component (Figure 11. 1). These forces, applied on the surface of the road, generate successive stress waves in the pavement structure and the supporting soil. Pavement and soil act as a transmission path of the waves, which travel and dissipate with the distance. The propagation of the stress waves through the ground is in the form of body waves (compression and shear waves) and in the form of surface or Rayleigh waves (Figure 11. 2). Wave stresses can be partly reflected on the bedrock and eventually can reach the foundations of adjacent buildings causing nuisance to people living or working inside. These are the receivers of the vibration.

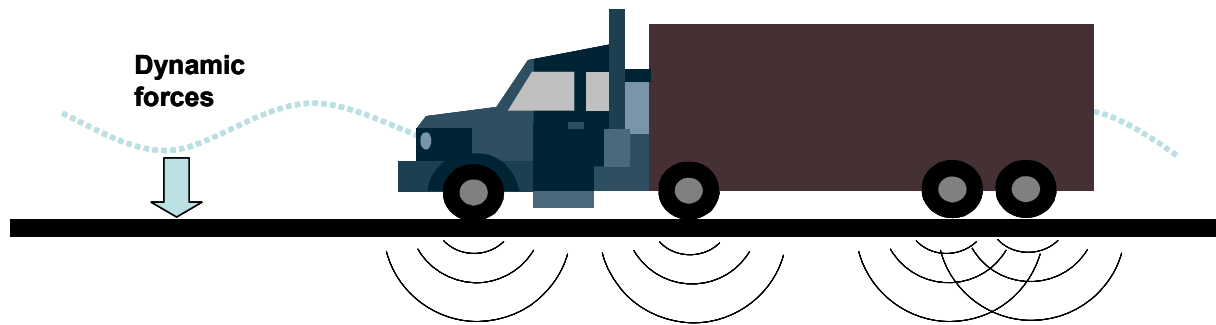


Figure 11. 1: Vehicle as source of vibration of different frequencies

The amount of energy transmitted into the structure is strongly dependent on the induced impact forces. These are a function of the characteristics of the vehicle (gross vehicle weight, axle load, speed, type of suspension, etc.) and also depend on the roughness of the road surface as well as the presence of potholes, pavement joints, etc). This energy propagates and dissipates in the structure, sub structure and sub-grade. The characteristics of the propagation are strongly influenced by factors such as type of soil and its compaction, humidity condition, temperature, where and how the sensor is installed, topography, etc. When considering the buildings near the source of vibration, factors like the coupling of the building foundations with the ground, shape and mass of the building also influence the characteristics of the vibration. Therefore, vibration is highly dependent on the measurement location and conditions. Figure 11. 2 illustrates how the amount of vibration measured in 5 different locations (points 1 to 5) provide different results ($V_1(t)$ to $V_5(t)$) as a result of the decay and distortion of the vibration waves in the distance.

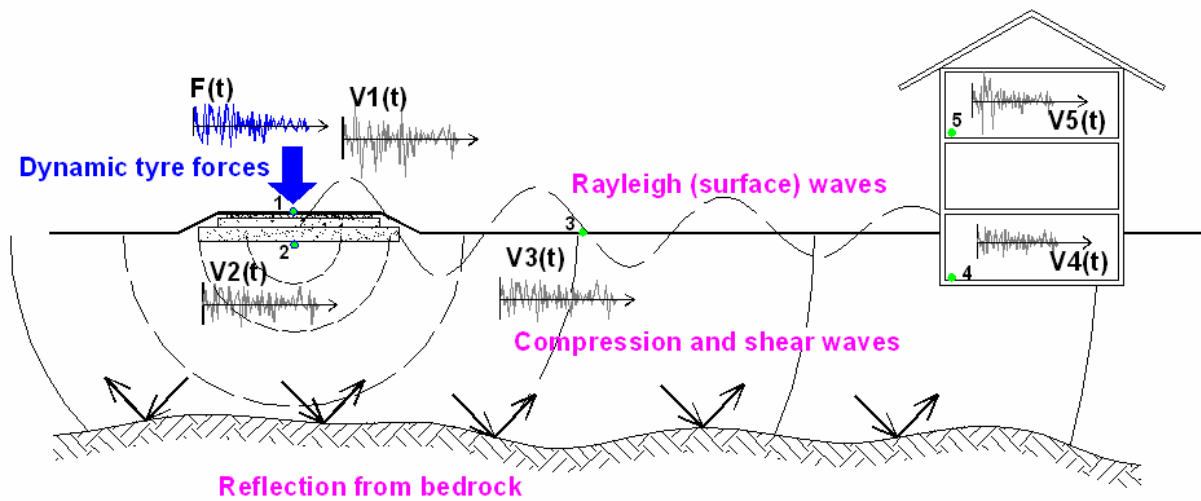


Figure 11. 2: Propagation of the vibration in form of different waves

The effects of all the factors that influence vibration are interdependent, and it is difficult to find simple relationships between them. For example, (Al-Hunaidi 2000) affirms that vibration amplitude is more sensitive to vehicle speed if the road is rough. Furthermore, effect of suspension system also depends on vehicle speed and road roughness. For low speed and smooth road conditions, the effect of the type of suspension system is not significant. But for high speeds and rough roads, the type of suspension system becomes important and air suspension systems produce more vibration than leaf steel spring suspension systems. However, according to (Hajek, Blaney et al. 2005), trucks equipped with steel (leaf-spring) suspension can produce higher dynamic loads compared to vehicles equipped with air suspensions. On the other hand, it is known that temporal changes in the soil acting as transmission path may affect vibration levels, and measurements made during a certain period of the year may not be comparable to those done during other seasons of the year. Other reports (Hendriks 1996) and (Hanson, Saurenman et al. 1995), make a description of the factors that influence levels of ground borne vibration and characterize the vibration dependency on the gross vehicle weight, vehicle speed, soil type, bedrock depth and building characteristics among others. Though, there is no exact knowledge about the contribution of each factor.

11.2. Quantifying Vibration

Vibration is an oscillatory motion of an element inside a medium with no net movement.

The number of times a complete motion cycle takes place in one time period is called frequency and is usually measured in cycles per second (Hz). The amplitude of the motion can be measured in terms of displacement, velocity or acceleration during a certain period of time. Usually, any one of these three magnitudes is used as an indicator of the severity of the vibration. The most common way, is to present them in terms of amplitude or frequency descriptors like:

- peak-to-peak value*: indicates the difference between the maximum and minimum values of a signal during a certain period of time
- peak value* is the maximum instantaneous negative or positive value of a signal during the measurement period. It is widespread to use the peak of the vibration velocity, called Particle Peak Velocity (PPV) in mm/s
- root mean square (RMS)*: is the average of the squared amplitude of the signal in a certain period of time (RMS velocity) in mm/s²
- Fourier, power, octave and one-third octave spectra*: they are techniques to present the frequency content of a signal

It is usual to characterize vibration events by identifying their peak. This method is simple and gives a reference value of the vibration intensity. Studies have shown that peak particle velocity in the vertical direction correlates best with damage and complaints (Hendriks 1996). Furthermore, for a frequency range between 1Hz to 80Hz damage levels in terms of velocity tend to be independent of frequency. The same is true for complaint levels within a range of 8 – 80Hz. In addition, (Siskind, Stagg et al. 1980) found that horizontal peak particle velocity measured on the ground outside of a structure correlated well with cosmetic structural damage. Although other descriptors of the ground motion were considered in that work, PPV was chosen for its effectiveness and simplicity.

The root-mean-square (RMS) is used to describe the “smoothed” vibration amplitude (Hanson, Saurenman et al. 1995). It is more representative of the time history of the signal and therefore appropriate for evaluating human response, as it takes some time for humans to feel vibration. The RMS values obtained from continue vibration records depend on the time period used for its calculation.

Sometimes, it is also necessary to estimate the frequency content of vibration as different frequencies can affect the response of humans, building and processes differently. Tools for estimating the frequency spectrum of a signal is the Fourier Transform or other techniques based on Fourier Transform like Power Spectra, octave spectra, Short Time Fourier Transform or Wavelet analysis.

Vibration levels and frequency

Typical vibration produced by traffic has, according to Norm ISO 2631-2, a frequency range of 1Hz to 80Hz and is composed of continuous and transient excitation depending

on the amount of traffic. (Al-Hunaidi, Rainer et al. 1993), broaden this range and suggest that traffic induced vibrations typically have a frequency range of 4 to 80Hz, sometimes up to 125Hz, and amplitudes are in the range of $0,005\text{m}^2/\text{s}$ to $2\text{m}^2/\text{s}$ for acceleration and $0,05\text{mms}$ to $25\text{mm}/\text{s}$ for velocity. The same author (Al-Hunaidi 2000), limits the most probable frequencies to a range from 5 to 25 Hz. According to (Hajek, Blaney et al. 2005), highway traffic induced ground vibration is a forced, non-resonant, vibration with the dominant frequency between 10 and 15 Hz and can be perceptible only in extreme circumstances, where a heavy truck circulates over a highly rough road. Even in those cases, the peak vertical velocity at foundations of buildings separated 2.9 m from a severe pavement surface irregularity did not exceed 1.0 mm/s

Vibration measuring system

A vibration measuring system usually consists of three parts:

- *Vibration transducer (accelerometers or velocity sensor)*
- *Signal conditioning (amplifiers, filters, analogue to digital converters)*
- *Recorder (analogue or digital, PC based)*

Transducers produce a voltage output that is proportional either to velocity (geophones) or to acceleration (accelerometers).

Vibration transducers

Velocity sensors

Their work is usually based on exciting a moving coil system which through magnetic induction produces a voltage proportional to velocity. The most common types are electromagnetic and piezoelectric:

- *Electromagnetic velocity sensors (geophones)* – they use the principle of magnetic induction, with a permanent magnet and a fixed geometry coil, such that the induced (output) voltage is directly proportional to the magnet's velocity relative to the coil.
- *Piezo-velocity transducers (PVTs)* – they are piezoelectric accelerometers with an internal circuit which produces a velocity signal.

Other types of velocity sensors like *cable extension-based* or *optical and microwave* velocity sensors are described elsewhere.

Typical characteristics of the Geophones are their large size and heavy mass. They measure relatively low frequency ranges (1 to 200Hz).

Accelerometers

Accelerometers use the mass of an element to convert force into acceleration in accordance with Newton's second law. The classification of the different kinds of accelerometers depends on the physical characteristic used in their work principle. Basically, they are divided in two groups: deflection type and force balance accelerometers.

— *Deflection type* - they employ mechanical spring restoring forces. They are in turn, classified considering the sort of system they use:

- *Piezo-electric* - piezoelectric effect of quartz or ceramic crystals to generate an electrical output proportional to an applied force
- *Piezoresistive (Strain Gauge)* - alter resistance in response to stress
- *Capacitive* – gives an electrical output proportional to the gap between two plates or electrodes that change under acceleration.

For these type of accelerometers, the bigger the mass they use, the grater the sensitivity and the lower the frequency response. High sensing range transducers typically have high natural frequency.

— *Force-balance or servo accelerometers* – instead of mechanical restoring forces, uses servo electromagnetic restoring forces. The deflection signal is used as a feedback in a servo system that moves the inertia mass back to the equilibrium position (close-loop). They offer high sensitivity and low frequency response, even with small masses.

For traffic induced vibration, the most suitable and widely used transducers are Geophones and Force Balance accelerometers. Table 11. 1 gives a qualitative comparison between both sensors.

Table 11. 1: Main characteristics of geophones and accelerometers

	Geophone	Force-balance accelerometer
Size	Large	Miniature - Small
Mass	Heavy	Light
Frequency range	1-5Hz to 100-1500Hz	0 to 5Khz
Resolution	High	High
Construction	Extremely rugged	Rugged
Cost	Low	High

Signal conditioning

Signal conditioning is needed to enhance the signal of the transducer. Usually, it is necessary to amplify the output voltage of the vibration transducer, to bring it over the

noise level and to clean the vibration signal of undesired noise outside the frequency range of interest. Typically, it is recommended to have an amplifier with different gain levels and before the digitalization of the analogue signal an anti-aliasing filter will avoid errors due to aliasing effect. Other high pass or low pass filters can be added in order to improve the signal to noise ratio, but their design must be carefully studied as they might produce undesired changes in the amplitude and phase of the signal.

Recorder

Nowadays, data recording is mainly done in digital format using portable PC systems.

Measuring location, direction and transducer mounting

Figure 11. 3 shows a typical attenuation curve of the vibration amplitude with distance to the source, normalized to 5m as found by Hendriks (1996). However, it is only valid for a specific site under certain conditions (for example, soil parameter α in the formula of the same figure, tries to account for the influence of the type of soil) and different measuring locations will give different vibration values of the same vibration source. The location of the vibration transducers should be selected so that the vibration levels reflect the purpose of the measurement. For example, if a vibration analysis is done due to complains of people living in buildings neighboring to a traffic corridor, measurements should be carried out at a location inside the building where the vibration is supposed to be the strongest.

The direction of the measurement also depends on the element that wants to be monitored: the vibration of a wall or a window should be done perpendicular to the element direction. For free field measurements (the sensor is coupled directly to the ground) a complete description of the vibration is obtained by measuring in three directions. However, for simplicity, only vertical direction can be monitored as it gives usually the biggest amplitude.

Figure 1. Typical Normalized Distance Attenuation Ratio Curve of Earthborne Surface Vibrations (Reference Distance, $D_0 = 5$ m)

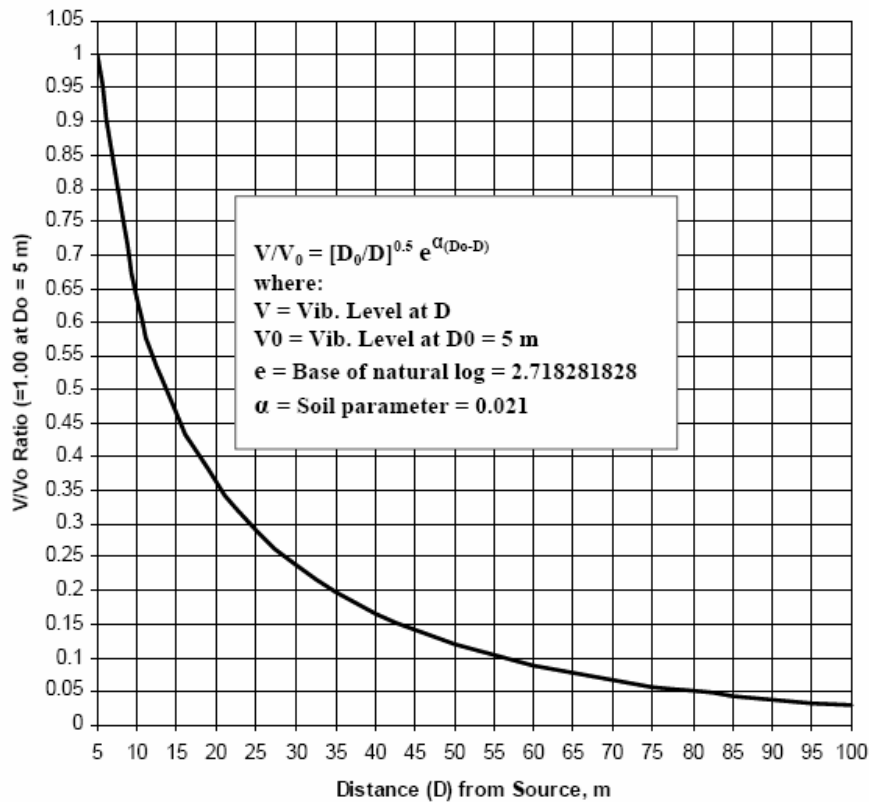


Figure 11. 3: Typical attenuation curve of the vibration amplitude (Hendriks 1996)

There is no standard method for mounting transducers; instead there are a variety of methods. In any case, these methods are generally designed to minimize errors within a frequency range of interest (Al-Hunaidi and Rainer 1990). The main condition is that the system should be stiff and light so that the resonance frequency of the mounting system is large compared to the frequency range of the vibration.

For measuring the vibration on buildings or rigid structures, the transducer can be fastened using a metal cube or directly with double adhesive tape or wax. In case of better coupling or permanent installation, a plate can be screwed to the element and the sensor can be in turn screwed to the plate.

For free field measurements where the sensor has to be coupled to the ground, the methods can be classified into the following categories (Al-Hunaidi and Rainer 1990):

- Surface plate mounting: the sensor is attached to a plate that simply rest on the ground surface. The plate can be also embedded in a mortar base in the ground or connected to the ground with welded fine rods that are driven into the soil.
- Stake mounting: the transducer is attached to one end of a steel or aluminium stake that is driven into the ground. The length of the stake can range between

150mm to 500mm and the sensor can be screwed to a welded plate on the free end of the stake.

- Embedded box mounting: Transducers are buried into the ground. For protection, they can be put into a box. The size of the box should be selected so as to minimize the difference of the average density of the box plus sensor system and the density of the ground.
- Compensation method: this is a complicated system where vertical inertial effects of surface mountings are compensated through an auxiliary vibrator that acts to maintain the zero dynamic contact pressure between the vibration system and the ground.

Several research projects tested the mounting methods described above. In general, the resonance frequencies of the mounting systems calculated for different types of soils were higher than the traffic generated frequency. (Krohn 1984) found that resonance frequencies of different systems ranged from 100Hz to 500Hz, depending on the type of soil and other physical characteristics of the mounting system. For example, loose soils decrease the resonance frequency of the system while longer spikes provide a better coupling and higher resonance frequencies in the vertical direction. Al-Hunaidi and Rainer (1990) arrived to similar results when testing loose sand and a mixture of clay and sand and proved that results using stake mounting tends to be more independent of the type of soil than the rest of the mounting types. As a result the stake mounting method was chosen for the FMS.

Calibration and control

The control of the proper functioning of the chain of measuring instruments shall be done approximately every 4 months or every time the data doesn't show reasonable results. This can be done statically, using the gravitational field of the earth. At the same time, the mounting should be checked visually to detect any problem in the connection to the ground. For example, after a heavy rain, a good coupling with the ground may be lost due to the compaction of the surrounding soil. A more complete control of the installation can be done using an impact hammer, by calculating the frequency response function of the mounting. The calibration of the individual instruments of the system should be done every two years or less, according to the manufacturer's specifications.

Criteria for the assessment of vibration severity levels



To avoid potential problems due to human discomfort or building damage, there are various guidelines that establish maximum values to be measured at the receiver location. These reference levels of “acceptable vibration” are usually established in terms of Particle Peak Velocity (PPV) or acceleration and sometimes the frequency content of the signal is also considered. In addition, either the type of activity of the disturbed person or the type of building that is affected is taken into account.

For example, researchers of the UK Transport Research Laboratory (TRRL) developed guidelines to assess traffic induced vibration based on a substantial number of tests. The proposed values are presented in Table 11. 2.

Table 11. 2: Reaction of people and damage to buildings according to TRRL (Whiffen A. C. 1971)

PPV ^[a] (mm/s)	Human Reaction	Effect on Buildings ^[c]
0 – 0.15	Imperceptible	Unlikely to cause damage of any type
0.15 – 0.3 ^[b]	Threshold of perception	Unlikely to cause damage of any type
2.0	Vibrations perceptible	Recommended upper level to which ruins and ancient monuments should be subjected
2.5	Continuous exposure to vibrations begins to annoy ^[d]	Virtually no risk of “architectural” damage to normal buildings
5	Vibrations annoying to people in buildings	Threshold for risk of “architectural” damage in houses with plastered walls and ceilings
10 – 15	Continuous vibrations unpleasant and unacceptable	Would cause “architectural” and possibly minor structural damage

^[a] Peak Particle Velocity in the vertical direction. For human reaction, the value applies at the point at which the person is situated. For buildings, the value refers to the ground motion (but without an allowance for the amplifying effect of structural components). It is assumed that the frequency of vibration is in the 5 to 20 Hz range

^[b] This level applies to a continuous sinusoidal vibration. However, truck induced vibration is of shorter duration (about 2 to 3 seconds) and thus higher levels appear to be applicable

^[c] The criteria for buildings recognize that the building damage will result from a fatigue failure over a long period of time (not from a one-time event)

^[d] Vibration levels causing annoyance may be lower for occurrences during night time and for occurrences that are very frequent

The US Department of Transportation proposed their vibration limits, based on more than 20 years of experience. The values, expressed as rms vibration, are shown in Table 11. 3.

Table 11. 3: Ground Borne Vibration limits according to US DOT (ANSI S3.29-1983)

Land Use Category	Ground-Borne Vibration
-------------------	------------------------



	Impact Levels (mm/s, rms)	
	Frequent Events ^a	Infrequent Events ^b
Category 1: Buildings where low ambient vibration is essential for interior operations	0.05 ^c	0.05 ^c
Category 2: Residences and buildings where people normally sleep	0.10	0.25
Category 3: Institutional land uses with primarily daytime use	0.14	0.36

[a] “Frequent events” are defined as more than 70 vibrations events per day. An event is considered to be a passing train or a rapid system

[b] “Infrequent events” are defined as fewer than 70 vibrations events per day.

[c] This criterion limit is based on levels that are acceptable for most moderately sensitive equipment such as optical microscopes. Vibration sensitive manufacturing or research will require detailed evaluation to define the acceptable vibration levels.

Several standards provide values of human and building response to vibration. A list of standards can be found in next section.

Normative references

There are no specific standards about traffic induced ground borne vibration. Instead, there are guidelines prepared by different institutions based on their own experience. There are as well standards about vibration in general and how it affects the human body. The most significant guidelines used to write this chapter are:

US Department of Transportation, Federal Transit Administration. Transit noise and Vibration Impact Assessment, Report DOT-T-95-16, April 1995

California Department of Transportation, CALTRANS. Transportation Related Earthborne Vibrations, Technical Advisory, Vibration TAV – 02 – 01 –R9601

These guidelines and other papers (see 5.1.10 References) are partially based on norms for the evaluation and control of all kind of human produced vibration that may cause discomfort to people, malfunctioning of sensitive equipment or damage to buildings. Some of the norms are:

ISO 2631-1:1997 Mechanical vibration and shock -- Evaluation of human exposure to whole-body vibration -- Part 1: General requirements

ISO 2631-2:2003 Mechanical vibration and shock -- Evaluation of human exposure to whole-body vibration -- Part 2: Vibration in buildings (1 Hz to 80 Hz)

ANSI S3.29-1983 (ASA 48-1983), “American National Standard: Guide to Evaluation of

Human Exposure to Vibrations in Buildings”, Acoustic Society of America

SN 640 312a: 2005 “Erschütterungen - Erschütterungseinwirkungen auf Bauwerke“, Swiss Standard

DIN 4150/2 1999-02 “Structural vibration - Effects of vibration on structures”, German Standard

BS 6472 (BSI 1992) “Evaluation of human exposure to vibrations in buildings (1 to 80Hz)”, British Standard

BS 7385 (BSI 1993) “Evaluation and measurement for vibration in buildings. Part 2: Guide to damage levels from ground borne vibration”, British Standard

11.3. Vibration Measurements at the Footprint Monitoring Site

The objective of performing vibration measurements is to evaluate vibration levels produced by road traffic and to determine what types of vehicles (identified using the information registered by the Weigh in Motion (WIM) sensor) are the most disturbing ones. This part of the chapter describes the vibration measuring system used at the Footprint monitoring station and presents some results. In cooperation with other European project partners measurement guidelines have been developed [Mayer et al 2007].

In addition to ground borne vibrations measured outside the road acceleration was also monitored with an accelerometer installed 4 cm below the pavement surface [Arrigada et al 2007]. These measurements were used as an alternative method to the deformation measurements to measure the elastic deflection of the road. The results have been used for the validation of the model (chapter 17) and are compared to the deformation measurements (chapter 7).

Description of the equipment and measuring position

The vibration measuring system consists basically of an electromagnetic velocity sensor positioned outside the road. The sensor is connected to the data acquisition system of the monitoring site where the measured signal is amplified and low-pass filtered (anti-aliasing filter). The data is eventually recorded and sent for storage and evaluation purposes via FTP connection.

Sensor and installation

The appropriate transducer type should be selected according to the frequency and vibration amplitude ranges of interest, that, for traffic vibration, are between 1Hz to 80Hz with a resolution of 0,001mm/s. Either geophones or force balance accelerometers can be used. Geophones were selected for vibration monitoring at the Footprint station

because of their good sensitivity, robustness and economy. Furthermore, traffic vibration guidelines define the vibration in terms of particle velocity, as it seems to be related to human sensitivity and building damage independent of the frequency content. Another reason to choose a velocity sensor rather than an accelerometer is that in this case the size of the sensor is not a problem as vibration is measured outside the road and a large sensor size does not cause an installation problem. Therefore a velocity sensor model 2003+ from the company SYSCOM was chosen to monitor vibration. The “desired” specifications for Footprint vibration transducers and the characteristics of the sensor installed in the A1 monitoring site are summarized in Table 11. 4.

Table 11. 4: Desired specifications and specification of the vibration sensors in the A1 Footprint site

	Desired Specifications	SYSCOM Velocity sensor model 2003+
Type	Velocity sensor	Velocity sensor with linearised frequency response and built-in amplification
Principle	Electromagnetic	Active, electronically linearised geophone with internal amplifier
Output	Velocity	Velocity
Directions	Vertical	Horizontal x Horizontal y Vertical z
Frequency range	1 – 80Hz	1-350 Hz
Dynamic range	100dB (0,001 to 100mm/s)	> 130dB (0.0001 to 100 mm/s)
Sensitivity	High (more than 1V/cm/s)	1.95 V/cm/s
Location	7.5m from the middle of the low speed lane	7.5m from the middle of the low speed lane
Installation	buried in the ground / surface plate mounting / stake mounting	stake mounting

The sensor was mounted using a metal stake with cruciform section that has a welded plate in one end. First, the stake was driven into the ground and the transducer was then screwed to the plate. This system provides good coupling with the ground in the vertical direction and high resonant frequency in comparison to the frequency of interest.

Measuring location

In principle, for the determination of the induced vibration of every single passing vehicle it is necessary to measure as close to the source as possible to minimize the influence of the transmission path. One possibility is to measure directly under each Tyre. But the main drawback is that the relative transversal position of the vehicles on the road (and therefore the distance of the Tyres to the sensor) changes for every vehicle. This gives sensible different vibration levels, depending on the position of the vehicle. It would be necessary as well, to measure at different points in the Tyres paths, as the dynamic Tyre forces are spatially randomly distributed along the way. Even though under those conditions, the influence of the road roughness and the rigidity of the pavement can not be neglected and will affect the vibration levels. This means that under no circumstances it is possible to make vibration independent of the road and soil conditions. Other sources of vibration, classified as environmental vibration, can also affect in some grade the measurements. However it is difficult to identify and filter out its influence.

On the Footprint site the vibration sensor was installed outside the road. This location has various advantages in comparison to an installation closer to the source:

- It is situated outside the road, in a position which is comparable to a building or person located as a receiver of the vibration.
- It is close enough to the source to minimize the wave drop-off but enough distant to measure every truck as a bulk source of vibration, and not the vibration of individual Tyres.
- The distance between the sensor and the vehicles passing in the slow lane (source) is large in comparison to the variation in position of the vehicles within the lane. This means that the decay of the vibration is approximately similar for every vehicle, allowing comparisons between them.
- The influence of the transmission path characteristics is on the average equal for all vehicles. Therefore it is possible to make a comparison between different vehicles.
- The distance to disturbing vehicles passing in the opposite lane is big enough to reduce their perturbing effects
- Thanks to the alignment with the WIM sensor it is supposed that the maximum vibration registered by the sensors will occur simultaneously with the WIM detection. That means that both time stamps should be similar.

The distance adopted for vibration measurements was 7,5m away of the centre of the slow lane (Figure 11. 4). This value is the distance that the ISO norm recommends for noise measurements.

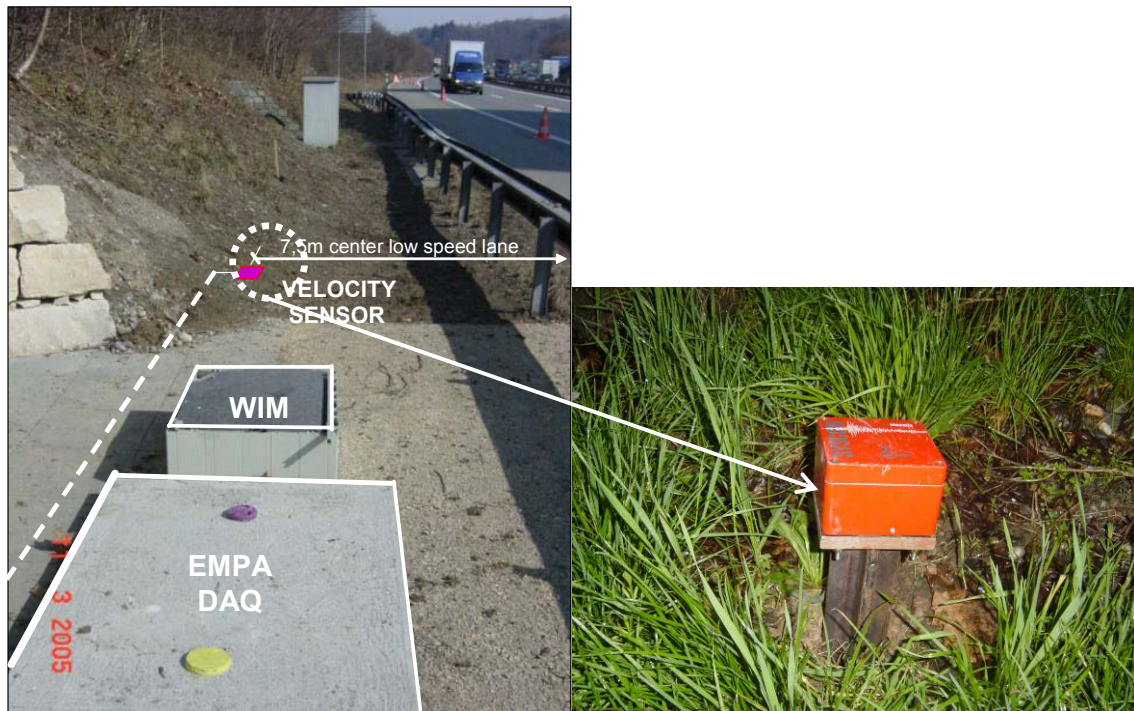


Figure 11. 4: Location and mounting of the velocity sensor at the Footprint site, A1 highway.

Measurement procedure

Vibration as well as WIM data are monitored continuously. The voltage signal obtained from the sensor is passed through an anti-aliasing filter and digitalized at 2048 samples per second, although 512 samples per second are enough not to miss any peaks. The system is programmed to sequentially compare 1s vibration data (in three directions) to a threshold value that, after trial and error, was set to 0.005 mm/s (1mV). When the vibration level is higher than the threshold, the 1s data is recorded as binary file. Each file is named and identified with its event time (time stamp) and contains three columns corresponding to each measuring direction. The daily vibration files as well as WIM daily files are sent via modem and stored in a PC at Empa for later processing.

Data processing

The evaluation of the vibration levels and the identification of vehicles are based on the analysis of vibration and WIM data. Vibration levels are estimated calculating the Particle Peak Velocity (PPV) in the vertical direction, which means that from every file the maximum negative or positive value is obtained. At the same time, WIM delivers information about vehicle class (in accordance to Swiss standards), speed, gross vehicle weight, axle load, and lane. PPV and WIM information are related through their time stamps.

Vibration monitoring started mid August 2005 and continues measuring since then. In this report, sample results obtained from 24th August until 24th October 2005 are

presented.

Valid measurements

Valid measurements are those vibration measurements where the vehicles that produce them can be identified from WIM measurements with high level of confidence. In order to spot the time correlation between the vibration files and the WIM data, time stamps are plotted together and contrasted. Figure 11. 5 represents the comparison of time stamps during one day, shown as lines (WIM time stamps are red lines and vibration time stamps are blue lines). From the plots, it was found that, although vibration and WIM were monitored continuously, some of the data could not be used because either one or both systems were not working during a certain period. This was due to technical problems, mostly of clock synchronization that was solved later.

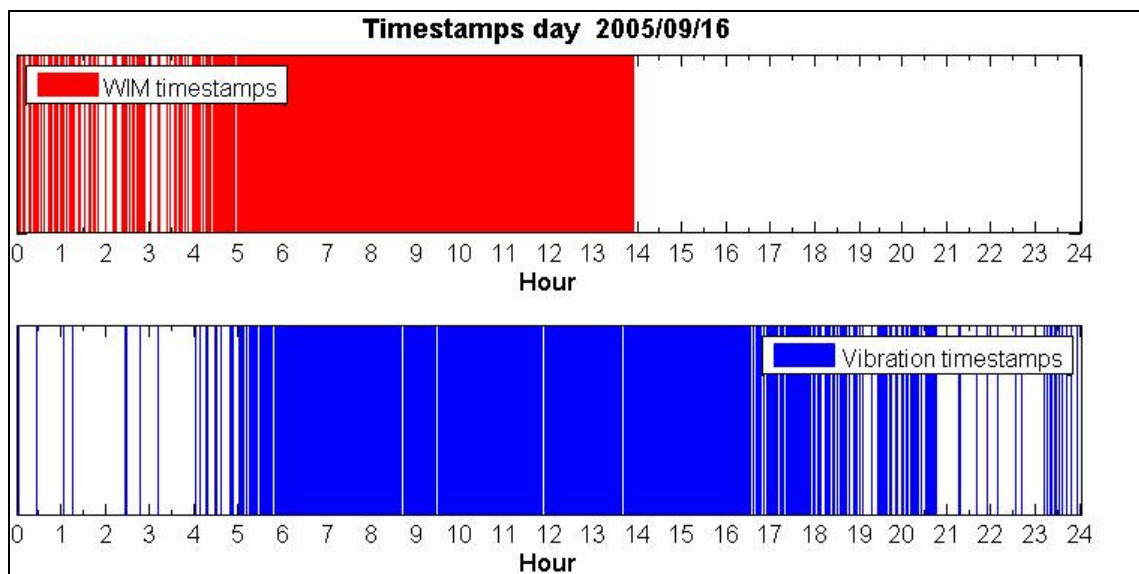


Figure 11. 5: Comparison of the vibration and WIM time stamps during a day

As previously stated, the identification of a PPV through WIM data is done through their time stamps. The strategy is to compare both time stamps supposing that the calculated PPV is induced by the vehicle with the same WIM time stamp. But closer analysis of the time stamp plots show that some corrections of the data are needed. First, many vibration events are separated into different files containing each 1s long measurements. Under the assumption that the same vehicle produces all the vibration recorded in successive files, the files with consecutive time stamps must be merged under a single file and the PPV must be calculated from these merged files. Second, it was found that there is a variable gap between the time stamp of the vibration files and the WIM files. This gap might be due to factors like a mismatch of the computer clocks of the WIM and vibration systems or the occurrence of the maximum vibration at a distant location of the sensor. Usually, time stamps of WIM are 1s to 3s in advanced to those of

vibration (Figure 11. 6). Therefore, in order to identify a vibration measurement, it is necessary to look for WIM time stamps in a time frame of 0 to 3 seconds before the vibration time stamp.

Other conditions to define a valid measurement are:

- If there is more than one WIM time stamp within a 4s time frame the vibration measurement is discarded, as it is the result of the contribution of more than one vehicle. This condition tends to accept only those measurements of individual vehicles, eliminating the disturbing influence of simultaneous vehicles passing together.
- The vehicle that produces the vibration must be circulating in the slow lane. With this condition we assume that all vehicles pass relatively at the same distance from the sensor.

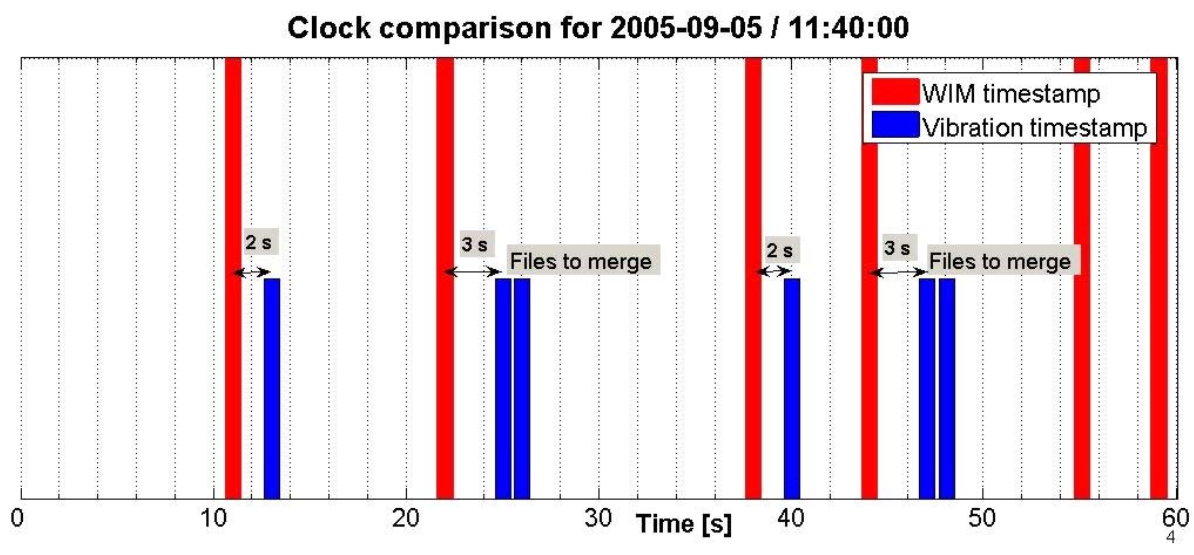


Figure 11. 6: Detailed comparison of the vibration and WIM time stamps

Analysis of the results

Figure 11.7 shows a typical vibration signal measured at the Footprint monitoring site. On the left side of the figure is the time stamp of the vibration file and the computed PPV. In the square on the right part of the figure, the time stamp of WIM and the identification of the vehicle regarding their speed, number of axes, total load and lane are shown.

The information of the vehicle and the measured PPV for every day and every month is stored in tables. From a total of 165443 vehicles registered by WIM from August 2005 to October 2005, there are 26866 that were considered valid passes following the

guidelines enumerated in Chapter. Figure 11. 8 shows a Histogram of PPV for the valid measurements. Although the PPV values range from 0.008 mm/s to 1.6mm/s, there are only sparse measurements beyond 0.11mm/s, clearly outliers. These outliers were identified by visual inspection of the time series and a frequency analysis using the Fast Fourier Transorm (FFT). Considering the vibration time history shape and its frequency content, it was concluded that the outliers are probably errors due to noise in the electronics vibration system of unknown origin. To clean the measurements from invalid measurements, the results are filtered taking as valid those less to 0.15mm/s. The histogram of PPVs presents a peak at 0.03mm/s, taken into account a class interval of 0.002mm/s. In order to have a feeling about the order of magnitude of the vibration levels measured at this site using the system described above, the recorded vibration levels are compared to those reference levels presented in Table 11. 2. The simple contrast reveals that vibration would represent no environmental threat and measured values are far below the threshold of human perception.

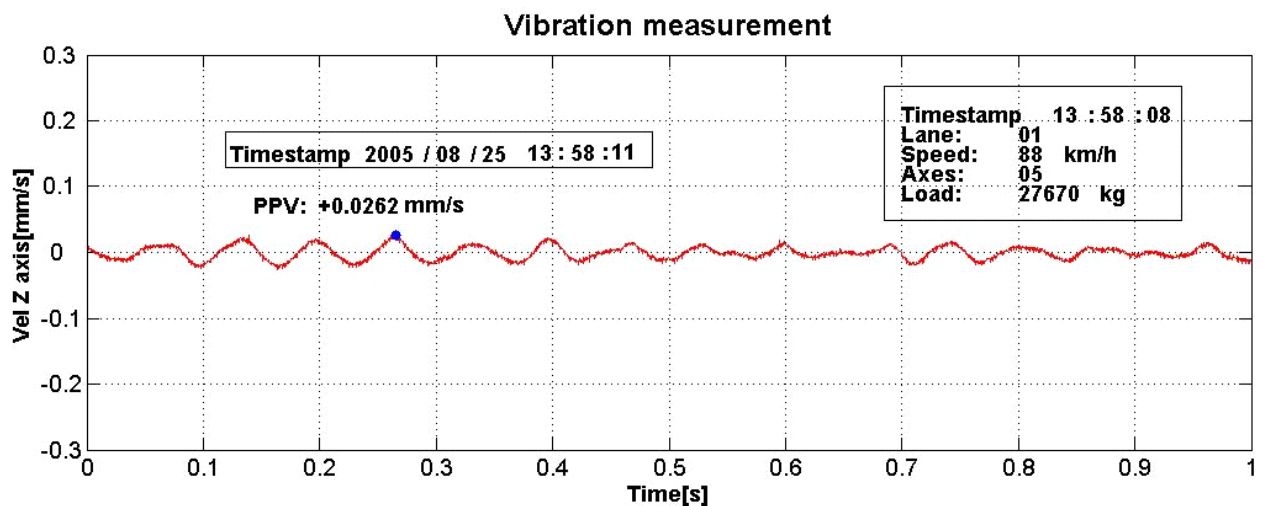


Figure 11. 7: Typical vibration signal produced by a passing by vehicle

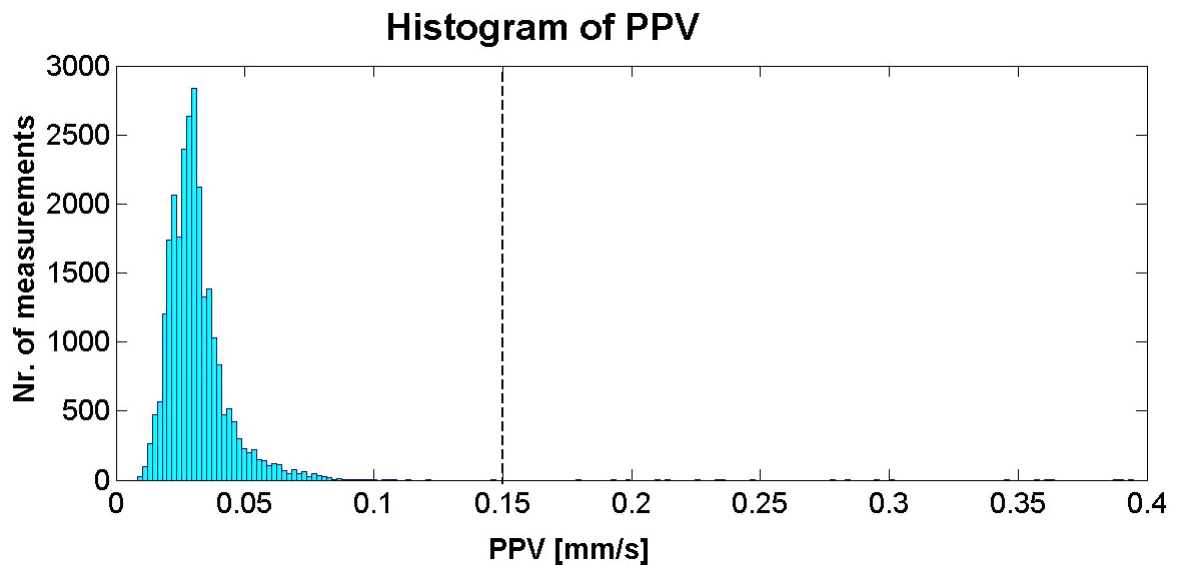


Figure 11. 8: Histogram of PPV obtained during two month measuring campaign

Influence of vehicle class in the levels of vibration

The distribution of the traffic according to Swiss 10 classification (Table 5. 2, Figure 11. 9), reveal a predominant presence of Class 8, 9 and 10 vehicles representing around 87% of the valid measurements. Buses (Class 1) represent 5% of the total valid measurements while delivery trucks (Class 5 to 7) sum together 8%. Classes 2 to 4 are not considered in this analysis, as they correspond to motorcycles and cars.

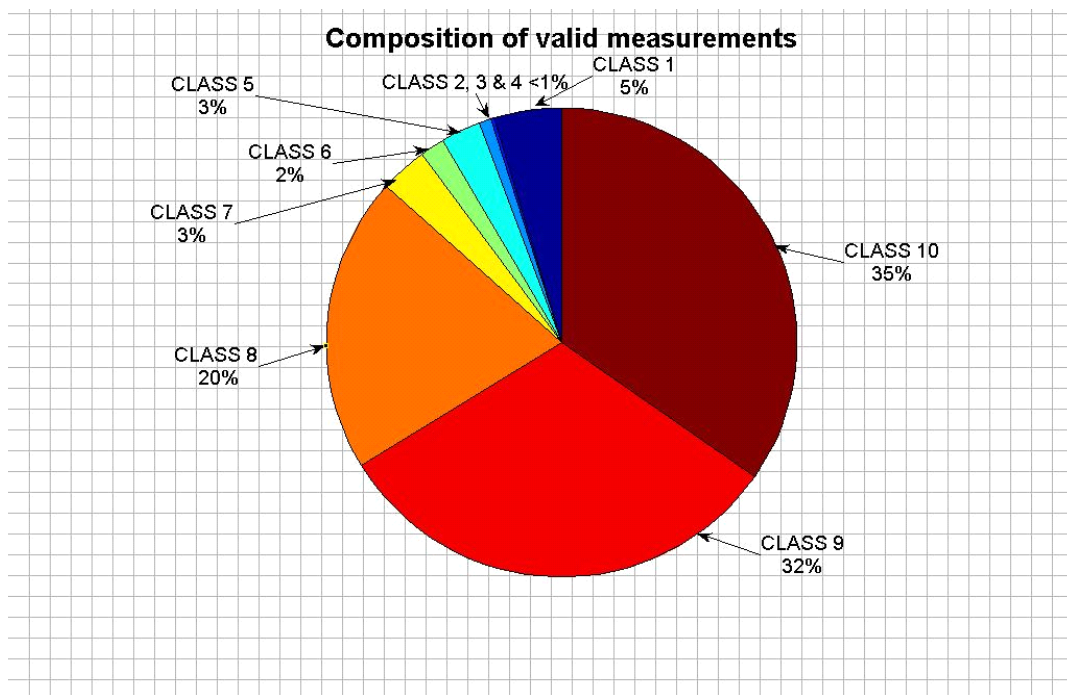


Figure 11. 9: Vehicle class composition of valid measurements

The left part of Figure 11. 10 presents the speed and gross vehicle weight (GVW) distribution (Intensity maps) of the valid measurements corresponding to Classes 1 and 5 to 10. The right part shows the distribution of PPV for each class. Data from vehicle classes 1, 5, 6 and 7 show that vehicles have a non uniform speed and load distribution, while vehicles of class 8 to 10 usually circulate with similar speeds and continuous GVW distribution. The PPV distribution doesn't show a clear tendency depending on vehicle class.

Figure 11. 11 shows an box and whisker plot of the PPV for each vehicle class. A box and whisker plot shows the median and lower and upper quartile values of the distribution. The whiskers are lines extending from each end of the box to show the extent of the rest of the data. Outliers are data with values beyond the ends of the whiskers. From this figure it is difficult to identify any clear correlation between vehicle classification and PPV. Figure 11. 12 summarize the PPV levels depending on vehicle class. The information about speeds and GVW is also included.

From the analysis of Figure 11. 10 to Figure 11. 12, the influence of GVW and speed of the vehicle seems to play an important role on the vibration levels, independently of the vehicle class, as discussed in the next section.

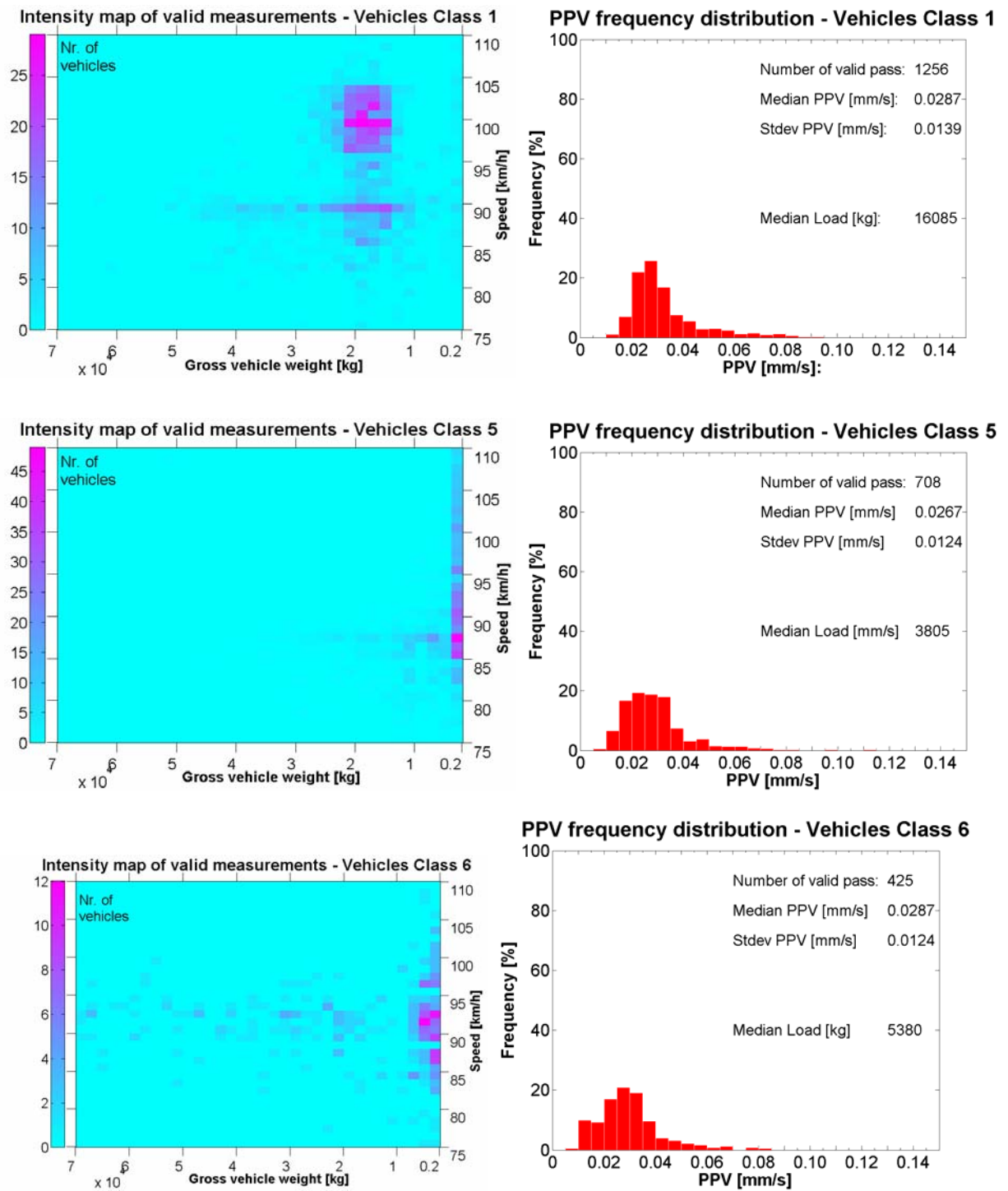


Figure 11. 10: Intensity map of GWW and vehicle speed for vehicle class. Frequency distribution of PPV produced by each class during the two months measuring campaign.

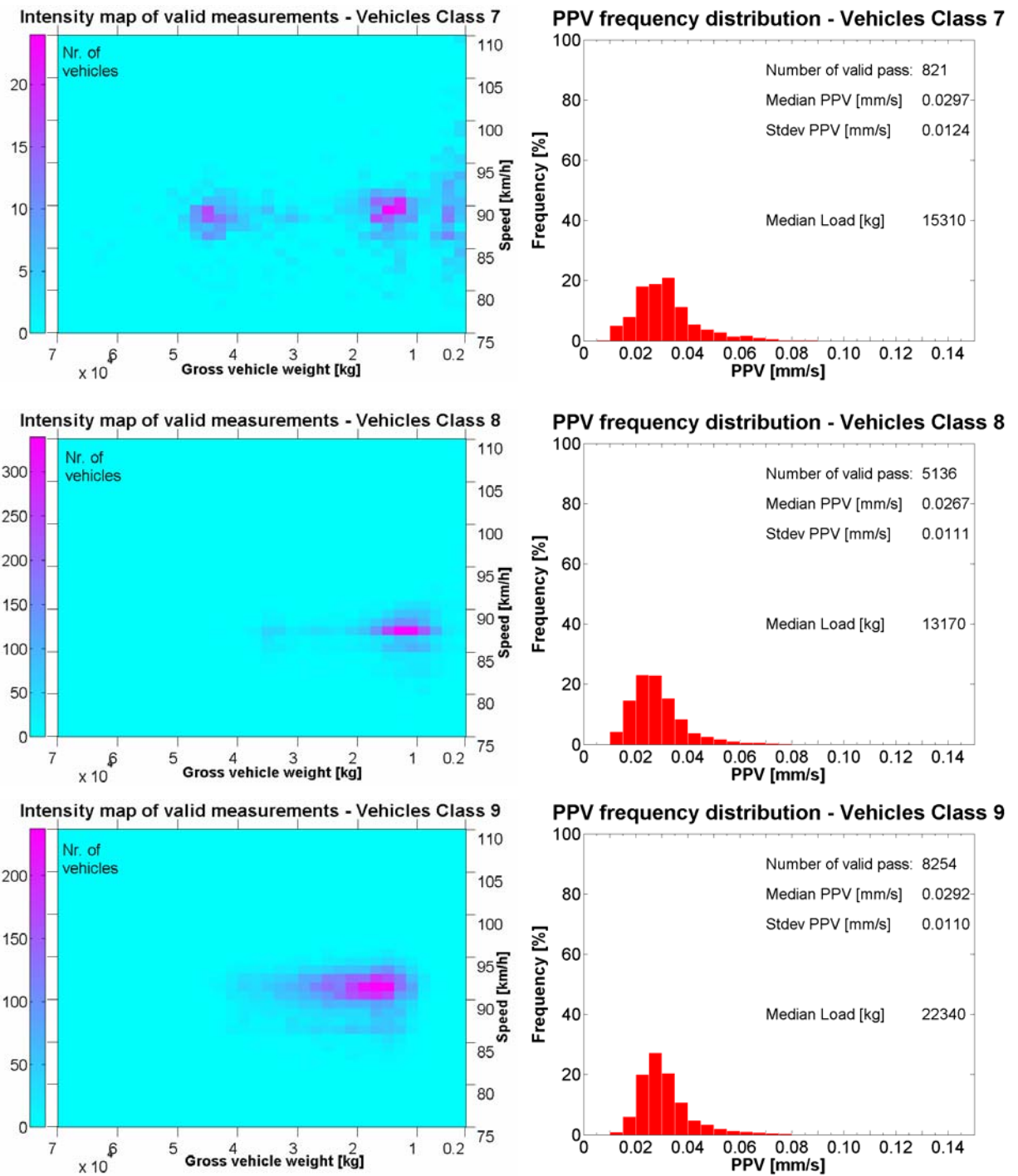


Figure 11.10: (cont.)

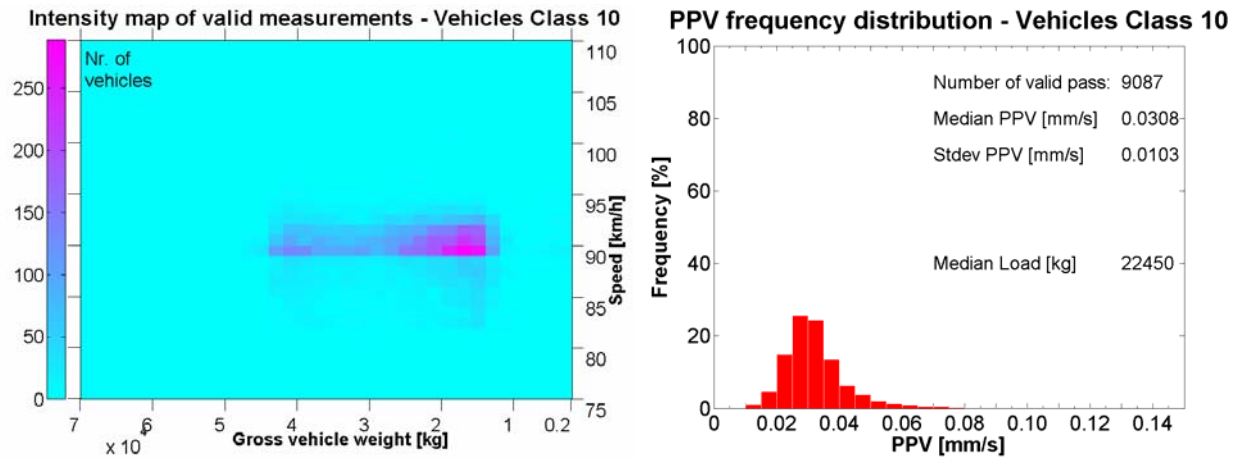


Figure 11.10: (cont.)

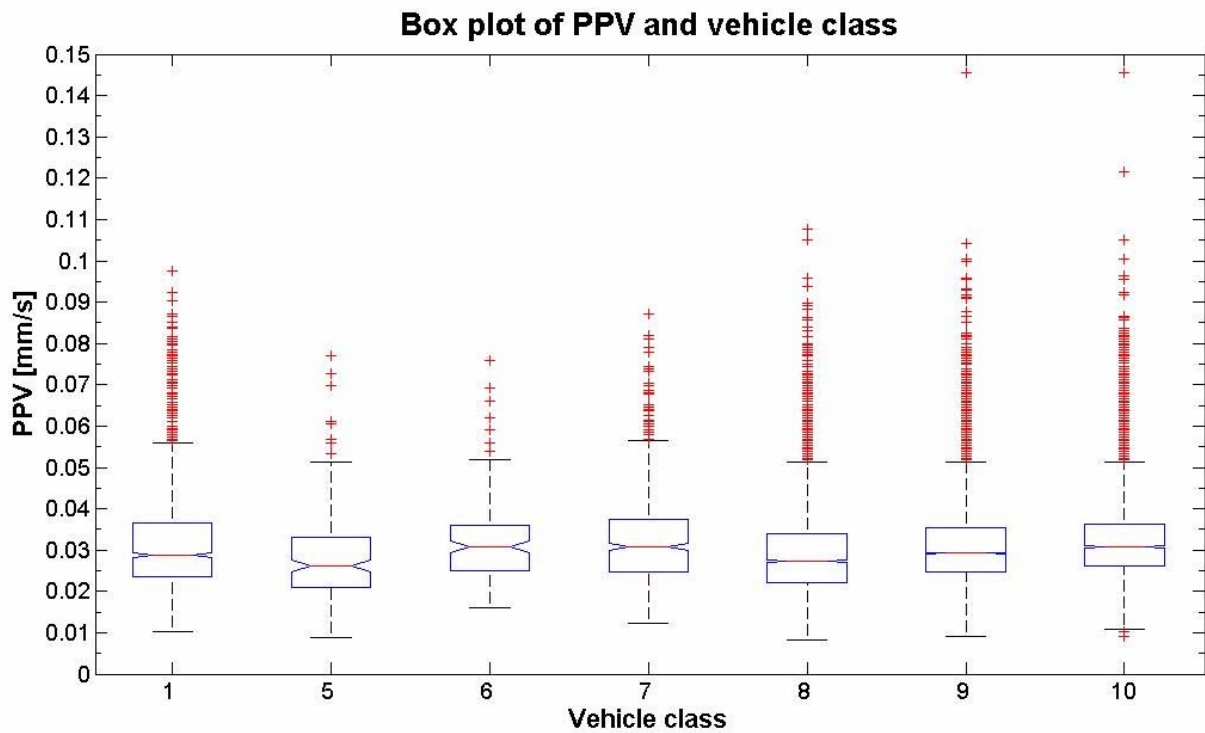


Figure 11. 11: Box plot of PPV during the two months measuring campaign

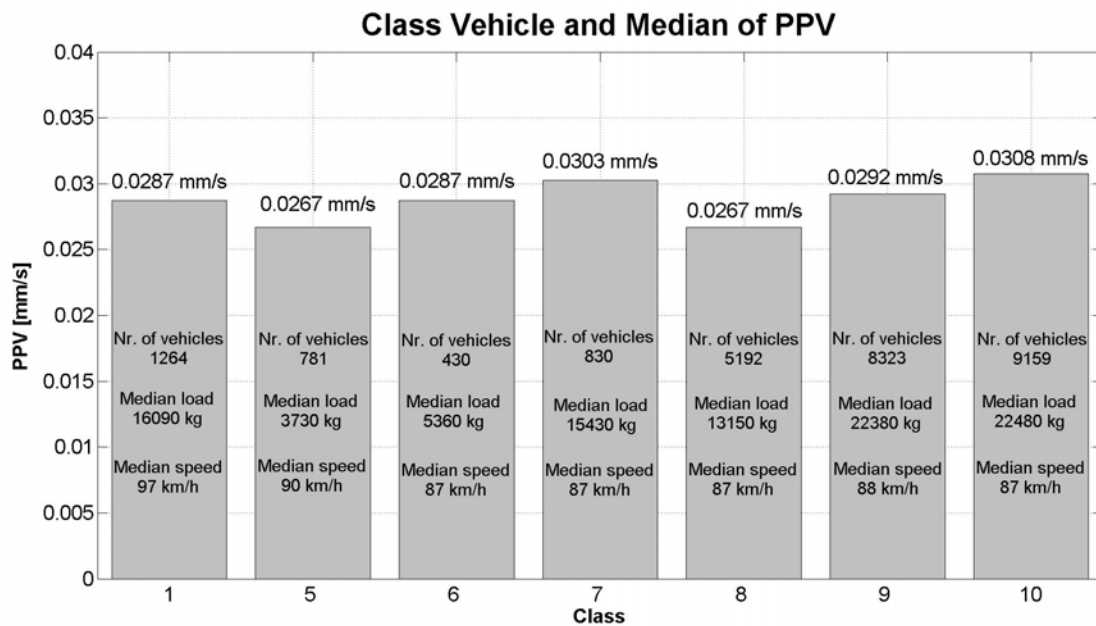


Figure 11. 12: Summary of PPV levels of each vehicle class

Influence of gross vehicle weight (GVW) and speed in vibration levels

The graph in Figure 11. 13 gives information about the distribution of gross vehicle weight and speed for all vehicle classes. There is a peak with the most frequent gross vehicle weight and speed at around 16000kg and 86km/h. There is another band between 3000kg and 4000kg that has speed ranging from 70km/h to 110km/h. There is an area of most frequent speed and load that can be defined between 81km/h and 90km/h and between 3000kg to 45000kg.

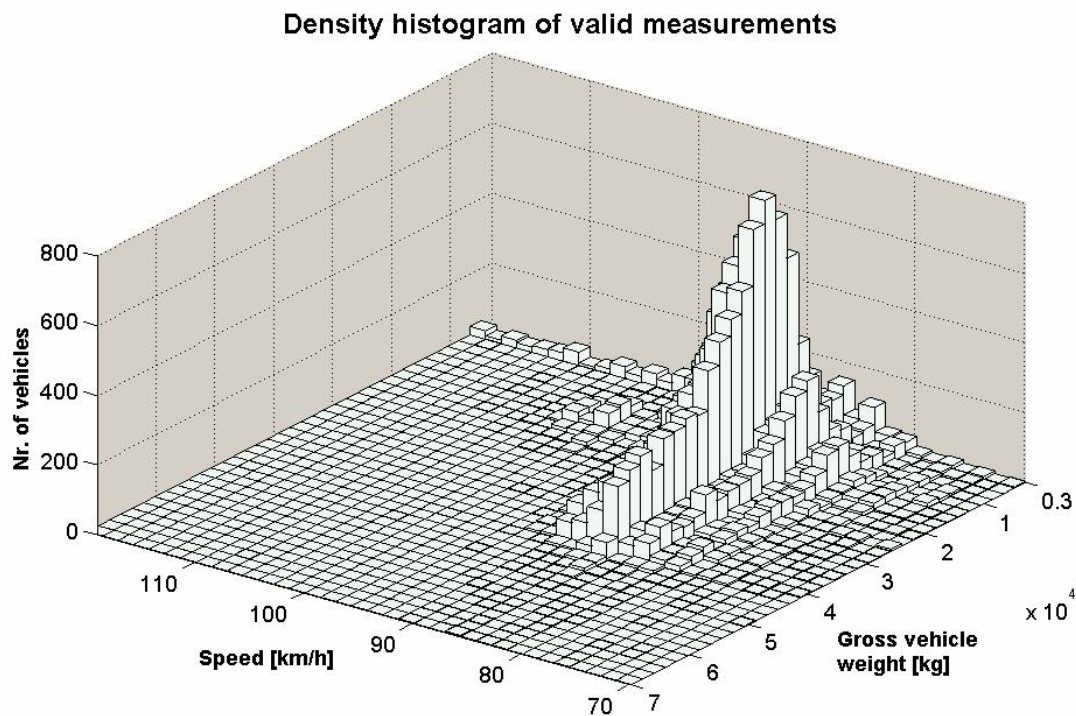


Figure 11. 13: GVW and speed distribution of vehicles during the two months measuring campaign

Analysis of the vibration levels in this region between 80km/h to 95km/h and 3000kg to 50000kg in steps of 5km/h and 5000kg respectively is depicted in Figure 11. 14. The stair shaped form of the 3D plot reveals a steady grow of vibration levels with grow of the gross vehicle weight, with exception of the “light” vehicles between 3000kg and 5000kg. 51% of the vehicles with gross weight between that ranges belong to Class 5, while 65% of the vehicles between 5000kg and 10000kg correspond to Class 8. Among different speed levels there is no significant difference although that PPV levels appear to increase with vehicle speed.

Median of PPV in intervals of speed and load - Aug/Sep/Oct 2005

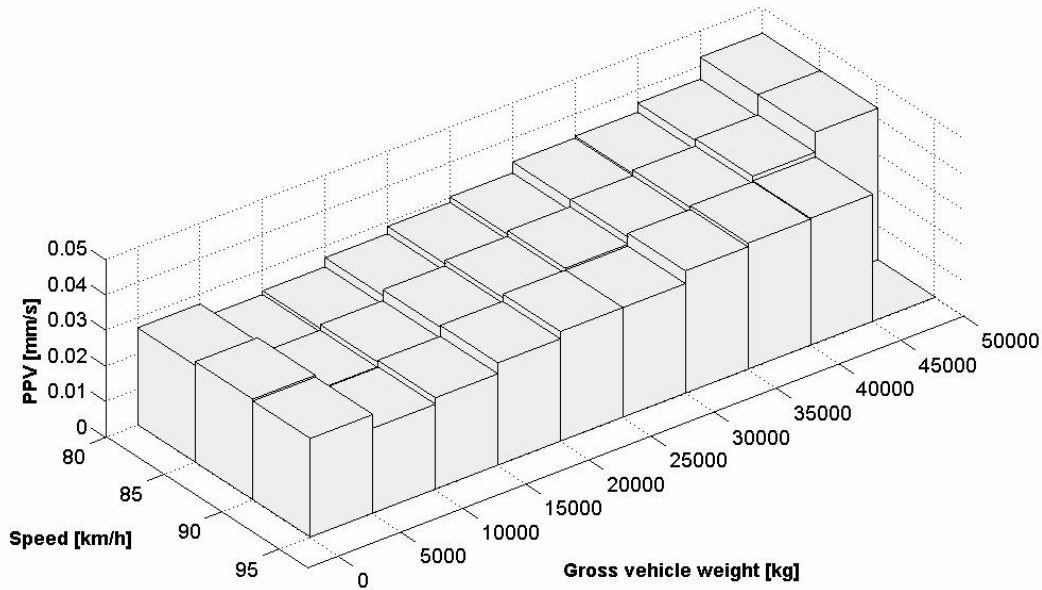


Figure 11. 14: correlation between PPV to GVW and vehicle speed

Figure 11. 15 shows the PPV and the GVW for all the valid measurements. The line represents a linear approximation using minimum squares. It confirms the growing tendency of PPV with GVW.

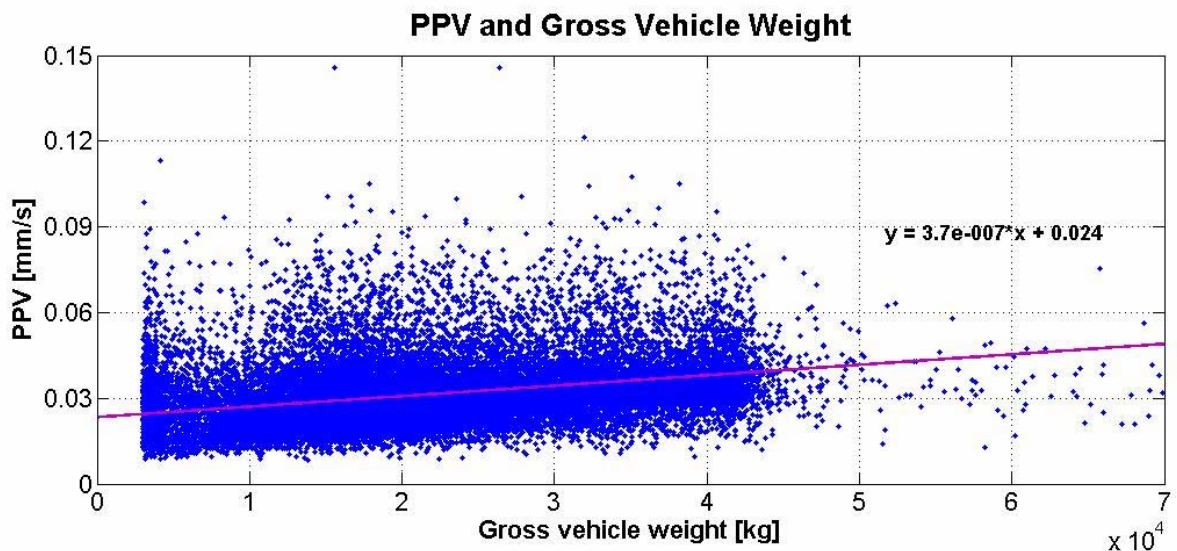


Figure 11. 15: PPV correlation to GVW

11.4. Conclusions and Outlook

The vibration levels of individual vehicles were measured using a geophone installed on the ground, 7.5m from the centre of the slow lane. The identification of the passing vehicles was done using WIM data and the vibration levels were assessed calculating the PPV. Valid measurements were selected by comparing the time stamps of the vibration and WIM measurements, and rejecting those vibration measurements that matched more than one WIM measurement in a time window of 4 seconds. A brief analysis of the vibration levels depending on vehicle class, gross vehicle weight, vehicle speed and maximal axle load was presented.

The vibration levels obtained during this two months measuring campaign are not absolute as they depend on variables such as the road roughness, soil type, environmental conditions, etc. It is possible to make comparisons between vibrations produced by vehicles at this site as long as measurements are taken under the same conditions. Nevertheless, a simple comparison to reference values shows that the measured vibration is low compared to the human perception threshold.

In order to improve future vibration measurement sites and to be able to compare vibration measurements made at other locations, it might be helpful to obtain more information or standardize the physical characteristics of the site where the measurements are carried out, i.e. measuring roughness, soil characteristics, etc. Vibration models could be constructed and correction factors between measuring sites can be used to compare results.

12. AIR POLLUTANTS

12.1. Background

Any consideration of the environmental footprint of vehicles is incomplete without taking into account air pollutants produced by the vehicles. Although the production of such pollutants is not debatable, the in-situ measurements per vehicle as such are not a simple task. Road traffic is the main source of air pollutants in Switzerland [Hueglin et al 2006]. Various monitoring sites throughout Switzerland measure emission source of air pollutants. Emission factors are widely used to describe road traffic emissions. They are defined as emitted mass of air pollutants per travelled distance and vehicle [Hueglin et al 2006]. A thorough examination of this topic is beyond the scope of this project however some examples follow.

Long term air quality measurements are performed at several road sites of the Swiss national air pollution monitor network (NABEL). Gaseous and particulate pollutants are monitored on a routine basis. These sites measure NO_x , NO, NO_2 , CO and SO_2 . One important site is near Haerkingen. This site is next to a four lane motorway located at a busy intersection of two major transit axes through Switzerland, the north-south and east-west. Comparing the emission factors of the above listed pollutants from 1992 to 2004 shows a general reduction as shown by Hueglin et al (2006).

Particulate matter with an aerodynamic diameter smaller than $10 \mu\text{m}$ (PM10) is an indicator for health effect due to fine particles in ambient air. Although the amount produced by rail vehicles is smaller than that produced by road traffic, they are not negligible. On the rail side PM10 emissions are due to abrasive mass loss of wheels, brakes and tracks. PM10 emissions from rail traffic monitored for example by Gehrig et al (2006) show that the railway induced contribution to ambient PM10 decreased rapidly with increasing distance from the tracks. For example at 120 m they dropped to 25% of values at 10 m. Figure 12. 1 shows a comparison of different sources of PM10 (Gehrig, 2007).

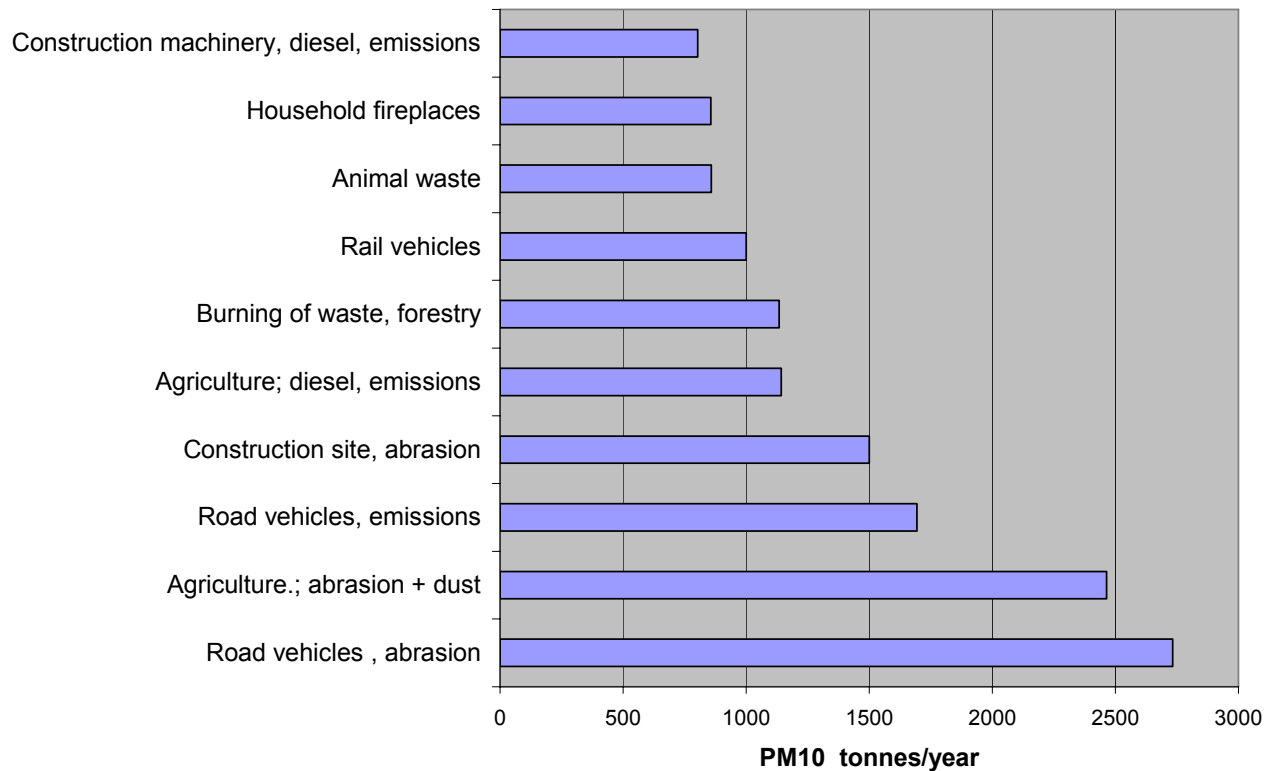


Figure 12. 1: PM10 emissions ba category (Gehrig, 2007)

12.2. Measurement of Gaseous Emissions of Individual Road Vehicles

(Author: Patrik Soltic)

EU Emission limits for Heavy Duty Vehicle (HDV), engines were introduced in 1992 (Euro 1). These limits were successively tightened in, 1995 (Euro 2), 2000 (Euro 3), 2005 (Euro 4) and 2008 (Euro 5). For the type approval of HDV engines, their emissions are measured under exactly defined ambient conditions with a reference fuel on engine test benches and they are limited in a work-specific manner (emission mass per unit engine work). For engines without exhaust gas treatment, the engine is operated in a number of steady state conditions in the so-called ECE R49 cycle (up to Euro 2) or in the ESC (European Steady-state Cycle). Engines with exhaust gas treatment (e.g. particle trap or selective catalytic reduction systems as they will be introduced with Euro 4), are tested additionally in the dynamic ETC (European Transient Cycle), i.e. varying engine speed and torque over time. The following table shows the limits.

Table 12. 1: Description of the Euro emission ratings

			CO limit	HC limit	NOx limit	Particle limit
Legislation	Introduction	Test Cycle	[g/kWh]	[g/kWh]	[g/kWh]	[g/kWh]
Euro 1	1992	ECE R 49	4.5	1.1	8.0	0.36
Euro 2	1995	ESC (+ETC)	4.0	1.1	7.0	0.15
Euro 3	2000	ESC (+ETC)	2.1	0.66	5.0	0.10
Euro 4	2005	ESC (+ETC)	1.5	0.46	3.5	0.02
Euro 5	2008	ESC (+ETC)	1.5	0.46	2.0	0.02

Gaseous and particle emissions of vehicles driving on the road depend on a combination of factors including, climate, driving pattern, road type, vehicle model, engine state and fuel. The result is that it is not possible to estimate directly the emissions of a vehicle in a certain driving situation from its known type approval emission data. The direct measurement of gaseous emissions of individual road vehicles at one single engine operating state in the framework of a Footprint Monitoring Site does not accurately reflect the actual emissions.

Ideally, the average emission factors [g/km] for different classes of HVD (Bodies, emission classes Euro 1, 2, 3, ...) should be found. In addition, driving pattern, road gradient and loading (empty vehicle ... maximum allowed mass) should be taken into account.

To estimate realistic emission factors (i.e. regulated emissions in g/km for Particle Matter, NO_x, HC and CO) for different engine technologies, different classes of vehicles (rigid truck, truck-trailer, urban bus, coach, garbage truck, etc.), different loading and in different driving profiles, several research programs exist.

The European ARTEMIS emission model could provide data for this purpose. ARTEMIS is a EU FP5 project with 37 partners developing a real-world emission model for different transportation modes which will be finished in 2005.

Within a German-Austrian-Swiss (D.A.CH) cooperation, the "Handbook of Emission Factors for Road Transport" has been developed and is updated continuously with new technologies (<http://www.hbefa.net>). This data base contains thousands of emission factors that are based on systematic emission measurements in several European laboratories. The experimental determination of heavy duty engine emissions in a laboratory is a very costly task (approx. 100'000 CHF per engine) so that such an international cooperation is needed to gain enough data in a statistical sense. From the



Swiss side, the project is supported by FOEN Air Pollution Control and NIR Division. In the framework of the FMS, using a method of vehicle identification such as a camera, it is possible to identify the HDV-Euro limit of individual vehicles using the vehicle registration (license plate). Road gradient is also known at each FMS. Vehicle load could be determined using the WIM data. However driving pattern is an unknown factor. The best available technique would be to select the emission factors of that vehicle class for a defined driving pattern from the "Handbook of Emission Factors for Road Transport" data base.

13. DATA ACQUISITION

(Authors: Peter Anderegg, Rolf Brönnimann, Rico Muff)

Introduction

The sensor outputs for measuring parameters like axle and wheel load, pavement deformation, vibration, noise, temperature and humidity need to be recorded and synchronized. Analogue and digital signals with quite different dynamics and sample rates can be processed using commercially available electronic devices. They range from quasi static signals like temperature and humidity to the highly dynamic signals of wheel load distribution, requiring a sample rate of 8192 Hz to obtain reliable data at speeds up to 100 km/h. To gain readout speed, load measurement data were stored in binary form and analyzed offline. This provides a higher flexibility for the analysis and independence of the measurement system. Figure 13. 1 gives an overview of the data acquisition system for the Swiss Footprint station on the motorway A1.

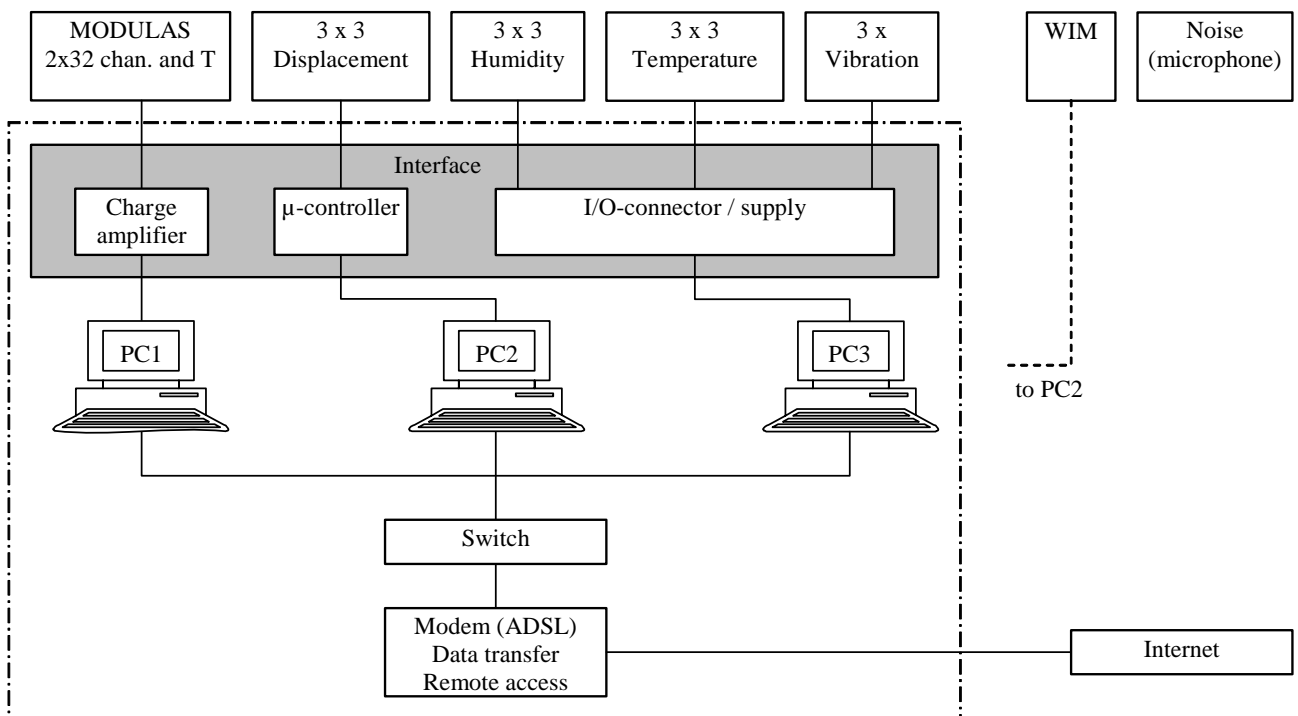


Figure 13. 1: Overview of the Data Acquisition System on the Swiss Motorway

WIM data

The Weigh in Motion (WIM) sensors and data acquisition system logs all trucks above a certain weight (here above 3.5 tons). Axle load, total weight, number of vehicles and

axles as well as the speed are recorded. The average 3700 recorded truck passages on a workday generate a file of about 800 KB. The WIM data are the master data to select single passages. All the other data will be searched by time stamp according to this selected passage.

Vibration data

The vibration data require a sample frequency of 512 Hz. A threshold value provides the possibility to reduce the amount of data. Hence, only valid vibration data from a passage will be saved. This threshold after trial and error has been set currently at 0.005 mm/s (1mV).

Noise data

The noise data are only measured temporarily and will not be acquired with this acquisition system (see chapter 10) at this time. However the data acquisition system can be adjusted to include noise acquisition.

Pavement deformation data

The magnetostrictive sensors which measure the deformations within the pavement layers record with 250-300 Hz. This is sufficient for speeds up to 100 km/h. Dynamic data are saved by detecting an event from the standard deviation of the signal change. A mean value for all 9 channels (magnets) is stored every minute in a daily file.

Temperature and humidity data

To find a correlation to the main data like load, deformation, vibration and noise, temperature and humidity are necessary auxiliary data. These data are recorded with a much lower frequency: one measuring point per minute for the temperature and one measuring point every 4 seconds for the humidity. While humidity is recorded within three layers of the pavement, temperature is recorded within the pavement, within the deformation sensors as well as within the data acquisition box in order to monitor the temperature of the electronic equipment.

Tyre pressure (MODULAS)

The MODULAS-system measures the load distribution under the Tyre by means of 64 piezo electric sensors. In a first step, raw data are stored every 0.5 seconds in a binary

file of 1 MB size (= 4096 points x 64 channels x 4 Byte). In a second step these data are reduced. A limit value currently set at 1000 N defines the minimal force in a channel for a detection of a vehicle passage. If in a file the signals of all 64 channels are below this limit, the raw data will be deleted immediately. After a detection of a passage, a second limit value defines the noise level. All values below this limit will be deleted in order to reduce the measurement points to the relevant data of the vehicle passage. The size of this reduced array depends on the speed and the Tyre size. The reduced data will then be saved with the exact time stamp name as a binary file, together with a text file containing the information of the active channels. The raw data will then be deleted. Figure 13. 2 gives an impression of the reduction process. In the shown example the data have been reduced from 4096 measuring points an a file size of 1024 KB to 70 points which leads to a file size of 17 KB.

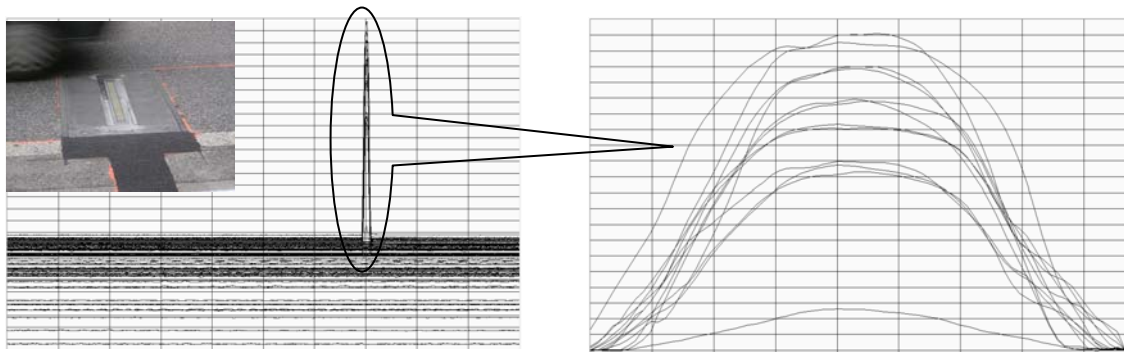


Figure 13. 2: Data reduction in this passage by a factor of approximately 60

Figure 13. 3 shows the used reference two-axle truck for testing the system. In Figure 13. 4 the footprints of one single front Tyre and one double rear Tyre during a passage with 50 km/h are shown.



Figure 13. 3: Reference truck with total weight of 14.5 t

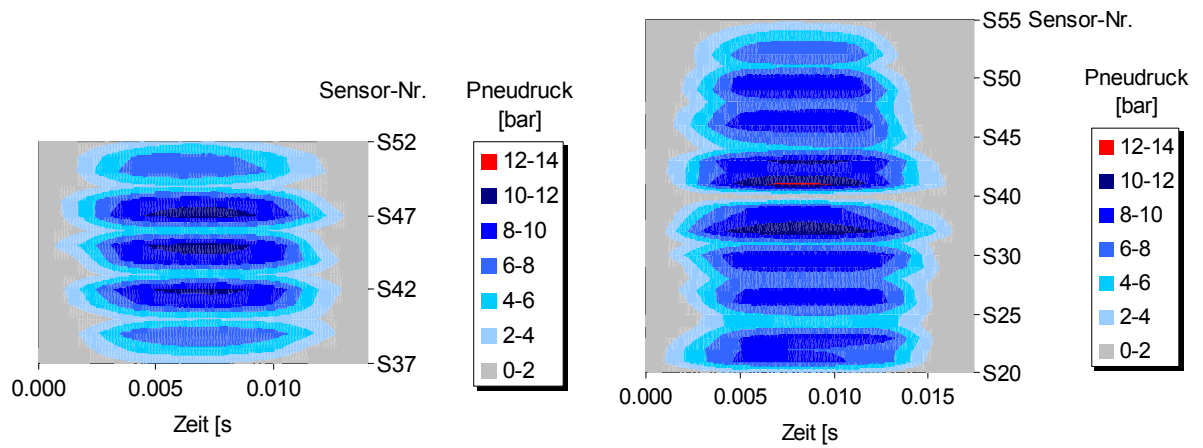


Figure 13. 4: Distribution of Tyre contact pressure in the single front Tyre (left) and the double rear Tyre (right)

14. THRESHOLDS FOR ENVIRONMENTALLY FRIENDLY VEHICLES

Based on in-situ monitoring and available literature various thresholds for environmental friendly vehicles based on dynamic load, ground borne vibration and noise are under discussion among the European partners in the project. As of November 2006 the following thresholds have been suggested:

Vibration

Threshold suggested is based on Table 11. 2 and can be summarized as:

- 0.15-0.3 mm/s Human perception
- 5 mm/s Architectural damage

Noise

Determining an environmentally friendly noise level is a complicated task as it is not only the vehicle that produces the noise but also the infrastructure. As such two methods are under discussion:

- It is suggested to set thresholds for an FMS based on noise emission distribution of that site; defining the upper 20% as environmentally unfriendly, Lower 20% as environmentally friendly. This method allows for the vehicles not to be penalized for noisy infrastructure.
- The use the same threshold as for rail for example 86 dB(A) which is technically achievable for rail (BAFU)

In Switzerland there is an emission limit for retrofitted coaches (84 dB(A)) and retrofitted freight wagons (86 dB(A)). 80.2 dB(A) for one type of retrofitted coaches has also been reached. For new coaches and freight wagons the limits of the TSI are used. For new freight wagons with k-blocks measurements from BAFU showed values from 75 to 82 dB(A) on a very smooth track. The measurements at Swiss monitoring sites with smooth tracks showed that for 25-30% of whole passenger trains (loco included) values of 78 and below were reached (Attinger, 2006).

Axle Load

In Switzerland 11 categories of allowable axle loads are defined ranging from a minimum of 10 t to maximum of 27 t on groups of axles (Table 2. 1). This wide range is based on axle configuration, axle distance and type of suspension. Vehicles with axle loads under 10 t are not required to pay a fee in several European countries and are considered pavement friendly.

- < 10t environmentally friendly

Tyre Pressure

It has been shown that higher tire pressures can be damaging to the pavement. There is evidence to indicate that an empty truck with high inflation pressure [770 kPa (110 psi)] will induce as much fatigue damage to the pavement as a fully laden truck that is operating at low [350 kPa (50psi)] tire inflation pressure [Owende et al 2001]. The current suggestion for an environmentally friendly tire pressure is:

- < 750 kPa (7.4 bar)

Gaseous emissions

			CO limit	HC limit	NOx limit	Particle limit
Legislation	Introduction	Test Cycle	[g/kWh]	[g/kWh]	[g/kWh]	[g/kWh]
Euro 1	1992	ECE R 49	4.5	1.1	8.0	0.36
Euro 2	1995	ESC (+ETC)	4.0	1.1	7.0	0.15
Euro 3	2000	ESC (+ETC)	2.1	0.66	5.0	0.10
Euro 4	2005	ESC (+ETC)	1.5	0.46	3.5	0.02
Euro 5	2008	ESC (+ETC)	1.5	0.46	2.0	0.02

Politically, Euro VI emission levels are in discussion now. They will be introduced around 2011-2012 limiting particle and NO_x emission so strictly, that all available exhaust gas treatment technologies will be needed (exhaust gas recirculation, particle trap, SCR).

15. SAMPLE DATA OF WIM, NOISE, VIBRATION FROM SEPTEMBER 2005

(Authors: Lily Poulikakos, Kurt Heutschi, Martin Arraigada)

Measurement methodology and analysis techniques for WIM, noise and vibration monitoring were discussed in chapters 5, 10 and 11 respectively. In order to define environmentally friendly, vehicles in this chapter a sample of WIM, noise and vibration data for a selected group of vehicles with the highest impact during September 2005 are presented and discussed. Detail data are shown in Appendix V.

In Switzerland the maximum allowable Gross Vehicle Weight (GVW) is 40t (Table 2. 1). Figure 15. 1 presents the maximum GVW per day of all trucks passed at the FMS each day. It can be seen that every day the limit of 40 t has been surpassed. This is possible as overweight vehicles are allowed under special circumstances with permits. The heaviest vehicles recorded in September 2005 passed by on the 8th, 13th, and 19th with GVW of 90.06 t, 91.16 t and 90.55 t respectively. Keeping in mind the goals of the project, a closer look at the subject large vehicles revealed that for example the vehicle on the 8th was a 9 axle, class 8 truck with maximum axle load of 13.42 t. The vehicle on the 19th was a 6 axle, class 10 and axle load of 16.33 t. Figure 15. 2 shows the maximum axle loads per day for the same period. Maximum axle loads range from 12.48 t to a maximum for the month of 20.14 t. This latter maximum for the month was for a class 7 truck with four axles and a GVW of 45.45 t which is considerably lower than the maximums seen for GVW. In considering what vehicles contribute most to pavement damage it is important to take into account maximum axle loads. Therefore the axle load data is matched with the SIM data and is fed into the FE pavement model in order to determine the effect on the pavement as shown in chapter 17.

The Federal Roads Office, FEDRO/ASTRA, has a set of allowable axle loads that can be found on www.admin.ch/ch/d/sr/741_11/a67.html and are summarized in Table 2. 1. 11 categories of allowable axle loads are defined ranging from a minimum of 10 t to maximum of 27 t for group of axles. This wide range is based on axle configuration, axle distance and type of suspension.

In the framework of Footprint, the result of various axle loads on the pavement have been analysed using the matched SIM data (chapter 6). That is the effect of axle configuration, axle distance and suspension is already an integral part of the footprint registered by the SIM in-situ. According to the project guidelines it is important to present the effect of single vehicles regardless of frequency of occurrence. I.e. the 90 t vehicle should pay a higher road access charge even if it comes once through Switzerland. A sample of the SIM results analysed using the vehicle infrastructure interaction model is presented in the following chapter.

An overview of the ground borne vibration measurements measured 7.5 m outside the slow lane is presented in Figure 15. 3. The maximum per day ranges between 0.0464

mm/s to 0.1137 mm/s for this period. As discussed in detail in chapter 11, the threshold of human perception, although very subjective, starts at 0.15 mm/s. Measurements so far at this monitoring site, including the September 2005 monitoring, indicate that all measurements are below values for human perception. It is therefore concluded that with current soil and traffic conditions, ground borne vibrations are not an environmental nuisance at this site. Monitoring will be continued and the development of ground borne vibrations at this site will be reported.

Figure 15. 4 shows an overview of the noisiest vehicles per day during this period. The highest noise emissions per vehicle per day range from 90.8 dB(A) to 97.4 dB(A). The latter from a four axle truck with GVW of 36 t and highest axle load of 11 t. The values shown in Figure 15. 4 have not been normalised for 80 kph and they are the actual measured values. It is difficult to identify the noisiest vehicles in absolute terms as the site and weather conditions play a role in the noise emissions. In addition, noise is more of a nuisance at night than during the day.

Summary and Observations:

1. WIM data are not complete. In September 2005 data from the 1st, 2nd, and 7th are missing.
2. Peak noise, vibration, WIM and axle load are not simultaneous. I.e. various vehicles are responsible for the various peaks, that is various vehicles are environmentally unfriendly in different ways.
3. Maximum valid noise recorded per day was always by vehicle classes 8 or 9.
4. Maximum WIM is by vehicle with Swiss 10 classification 10, 8.
5. Maximum axle load and gross vehicle weight was by Swiss 10 vehicle classes 10, 9, 8, 7, 4
6. On Saturdays and Sundays considerably less vehicles over 30 t were recorded at the site
7. In no cases in September, were the noisy vehicles the heaviest ones.
8. Example of night noise emissions: On 21.09.2005 the noisiest vehicle arrived at 4:49am with 93.3dB(A).
9. In most cases the maximum axle load is carried by axle number 2.

It is clear from analysis of the data that the heavy vehicles are not necessarily the ones with the highest axle loads causing the most damage to the pavement nor are they the noisiest or the ones causing the most vibrations. It is imperative that each vehicle is assessed separately for the various parameters that it causes. Environmental friendliness criteria is under discussion and has to be established as summarized in chapter 14.



The following obstacles were observed in the acquisition of this set of data. Suggestions for improving the future data acquisition have been made in chapters 5, 10, 11.

1. Valid noise data for all passes
2. Time stamp for various sensors are different and difficult to automatically go through various data, vibration for example
3. Vibration data in x and y directions have some electrical disturbance. z direction was displayed

This chapter went through the exercise of identifying vehicles with the highest impact using WIM, noise and vibration data. The next step was to match the WIM data with the SIM data and use the recorded contact stress distribution in the FE model to determine the effect of the wheel load on the pavement in terms of stresses and strains produced in the pavement. These topics are addressed in chapters 6 and 17.

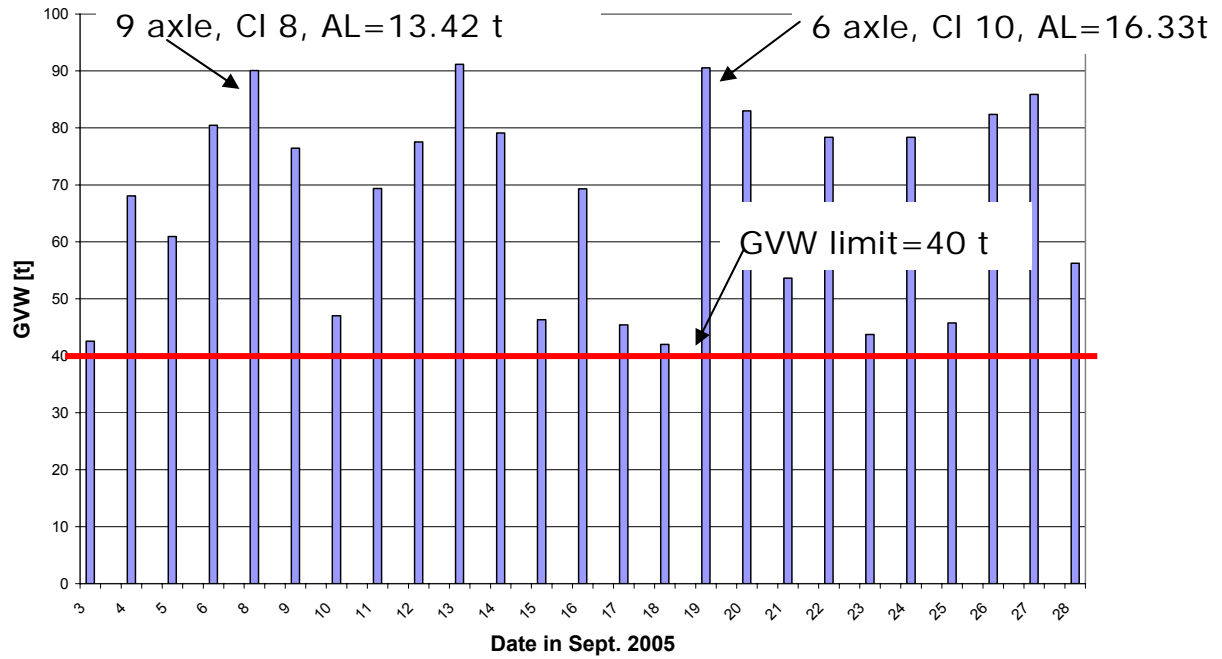


Figure 15. 1: Maximum Gross Vehicle Weight (GVW) per day. CI=vehicle Swiss 10 class, AL=axle load

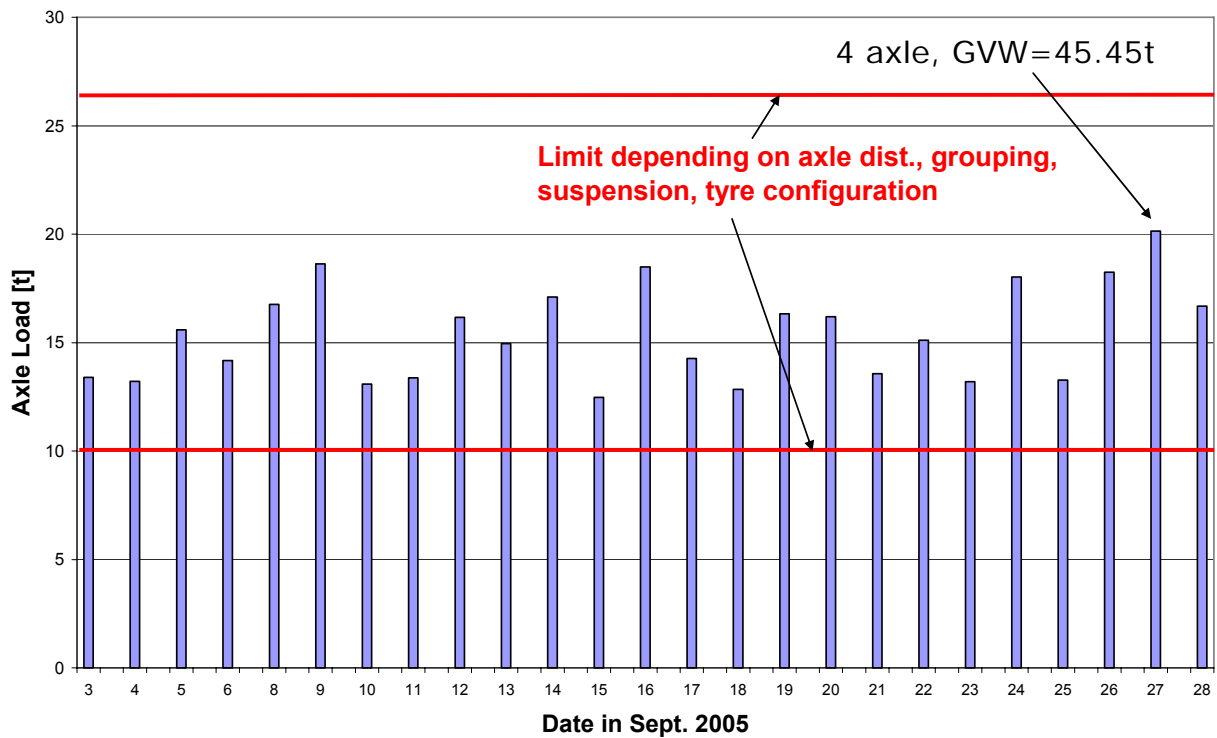


Figure 15. 2: Maximum Axle load per day. CI=vehicle Swiss 10 class, AL=axle load

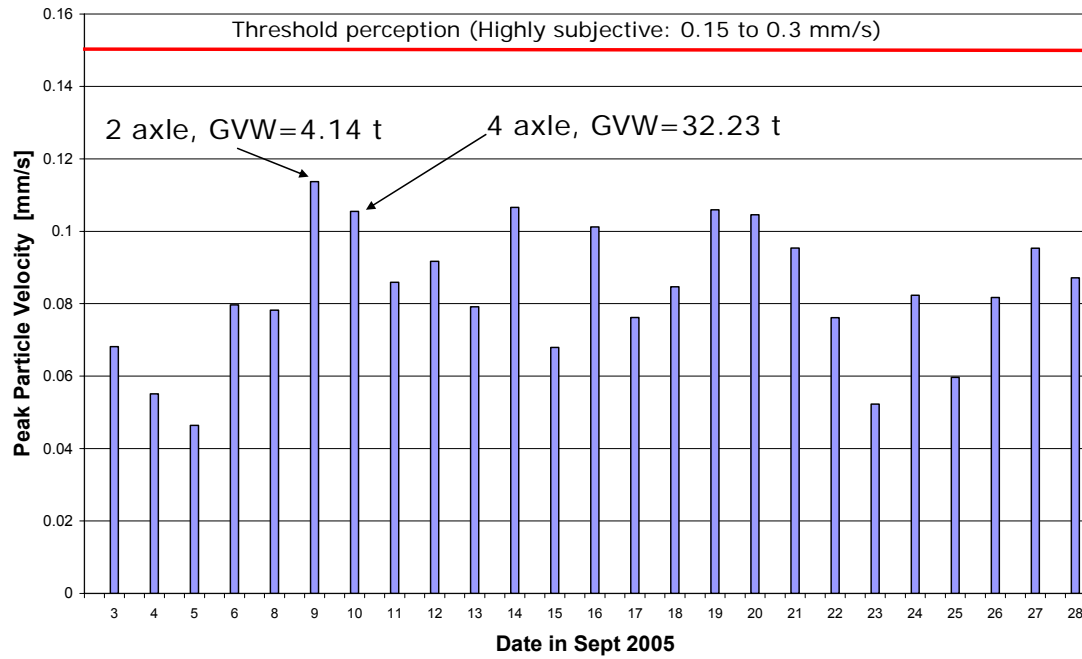


Figure 15. 3: Maximum vibration per day for a single vehicle presented as peak particle velocity (PPV)

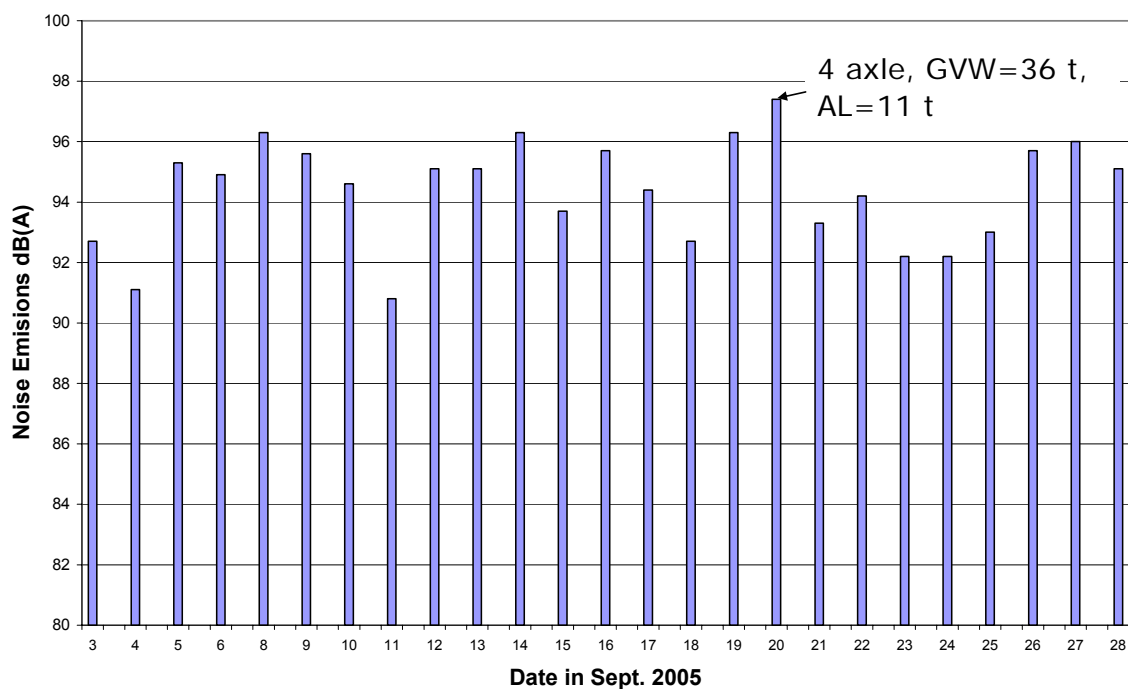


Figure 15. 4: Maximum noise emission per day for a single vehicle

16. SAMPLE DATA FROM OTHER FOOTPRINT MONITORING SITES

16.1. Rail FMS in Austria [Kalidova, M. (2006)]

The rail FMS in Austria is located 16.4 km north of Vienna and complies with TSI requirements [2005]. During a pass-by a number of different signals are recorded as shown in Figure 16. 1. Axle signals are merged with noise and vibration levels. This exercise allows to relate emission data with train and wheel positions as shown in a sample of data in Figure 16. 2

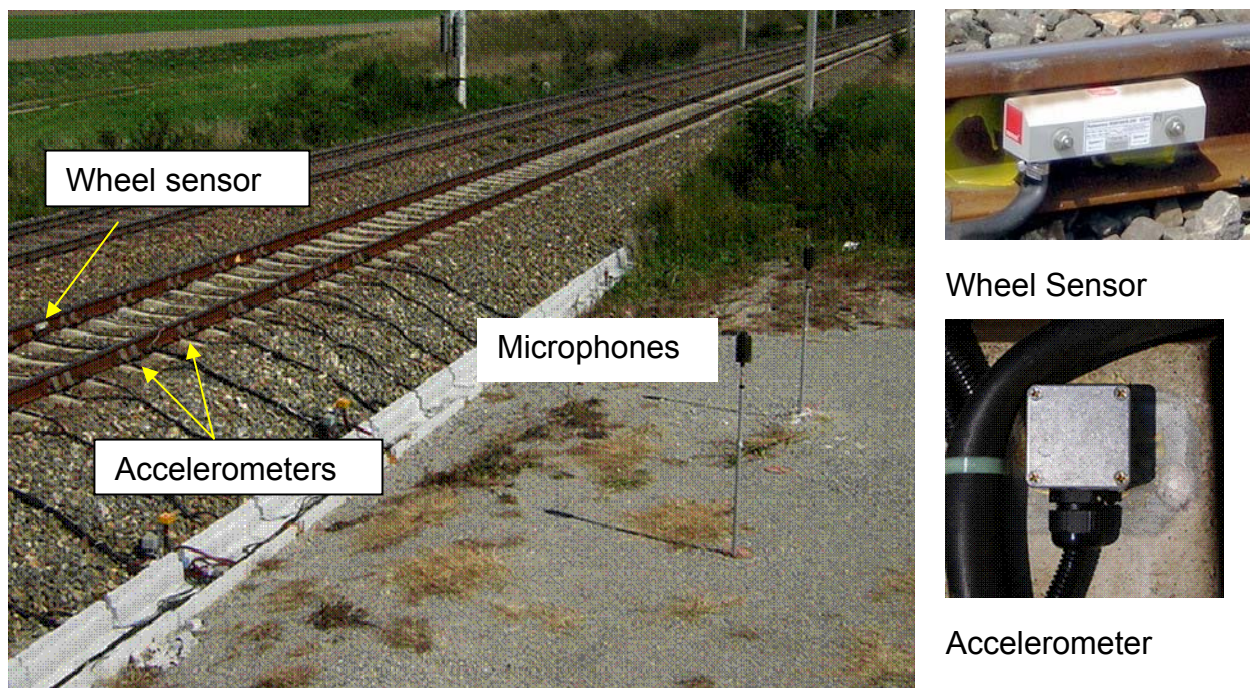


Figure 16. 1: Nordbahn, track 2 @ km 14.6 north of Vienna

The FMS allows the identification of noisy vehicles or wheels and appropriate maintenance and rehabilitation of the affected rail vehicles.

Figure 16. 3 shows a sample of the results where the yellow triangles represent "ordinary" freight trains with cast iron brakes. They start with about 92 dB(A) at 80 km/h and have a speed dependency of about $23 \cdot \lg \cdot v$ (v =velocity). The green dots represent the TSI-noise test train equipped with k-bloc brakes. Although one axle had a small wheel flat (that increases level) the train is 9 dB(A) less noisy at 80 km/h with a higher speed dependency of $27 \cdot \lg \cdot v$. The TSI-noise limit for this wagon category would be 85 dB(A) at 80 km/h. To this end, a noise emission of 80 - 85 dB(A) depending of the vehicle category is average or state of the art. Environmentally friendly rolling stock can be defined as everything in the range of 76 - 79 dB(A).

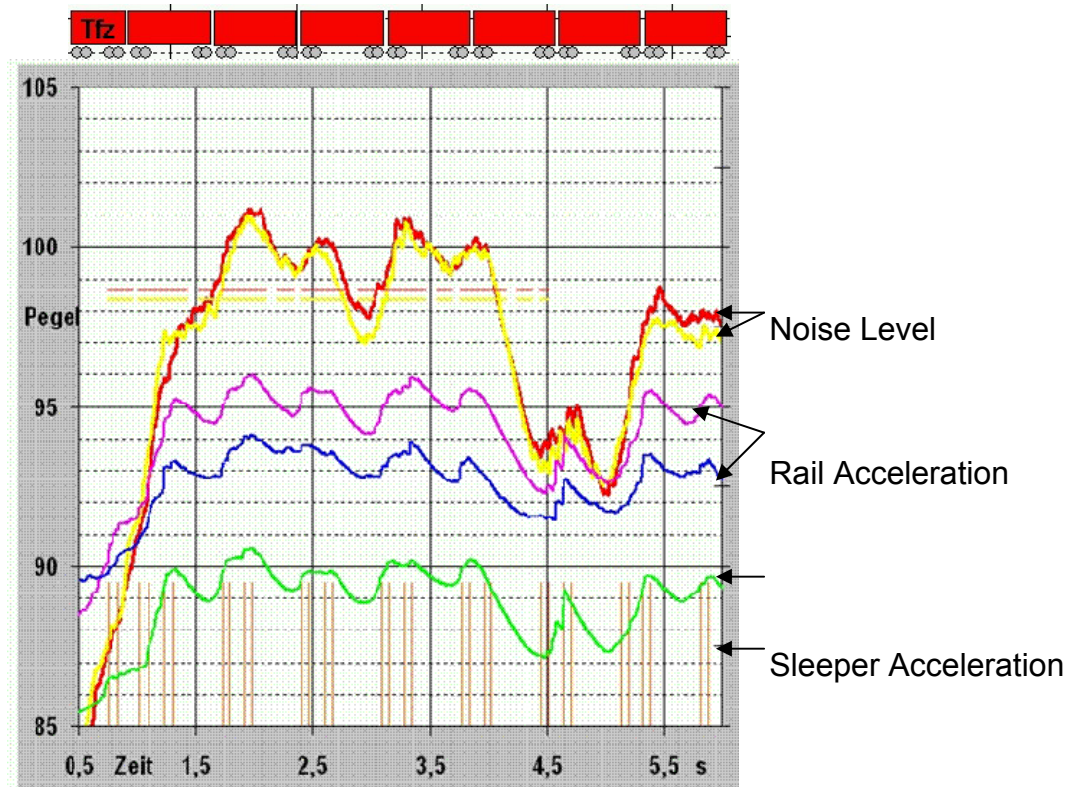


Figure 16. 2: Figure Sample of data from FMS Austria from the Acramos data acquisition system (Courtesy psiA-Consult GmbH)

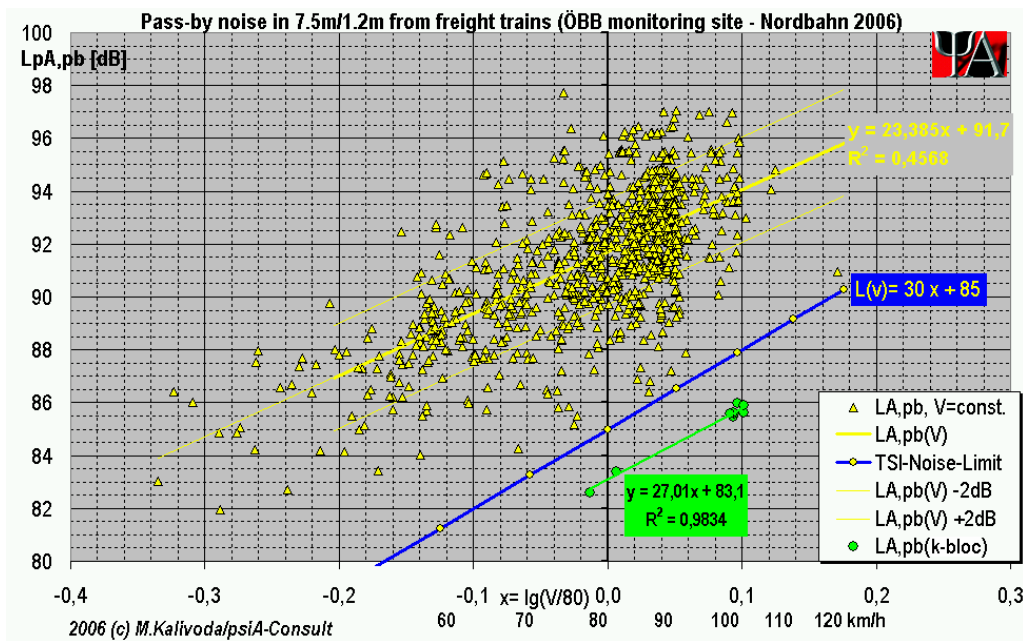


Figure 16. 3: Figure Sample of data from FMS Austria from the Acramos data acquisition system (Courtesy psiA-Consult GmbH)

16.2. Road FMS in the UK [Lees, A. (2006)]

There are currently 3 road FMS in the UK (Status 2007). Two sites are under

construction and should be operational by spring 2007. An urban site on A374 Plymouth, England with 64 kph speed limit and a rural location on the A9 in Tomatin Scotland with 97 kph speed limit. The first one in operation since October 31st, 2006, and the one current results are from is located on A303 Trunk road in Somerset, a dual carriage way. Although in a rural setting it has an average daily flow of 20,268 vehicles with 10% Heavy Goods Vehicles (HGV). The site is on a major east-west route linking London with the south west. This site is originally a WIM station which was updated to a FMS by adding microphone, vibration sensors and weather instrumentation. Initial vibration signals corroborated the findings of the Swiss FMS (chapter 11) and were below thresholds for perception and therefore vibration monitoring was not continued on a regular basis. Figure 16. 4 shows the average noise level for three categories cars, 5 axle artics and 6 axle artics. The average noise level for a category is defined by the sum of the noise levels for that category divided by the number of vehicles in that category. As a 10 dB(A) increase is an indication of doubling of noise. The results indicate that the emissions are significant by vehicle type indicating that the 6 axle artics being the noisiest followed by the 5 axle artics.

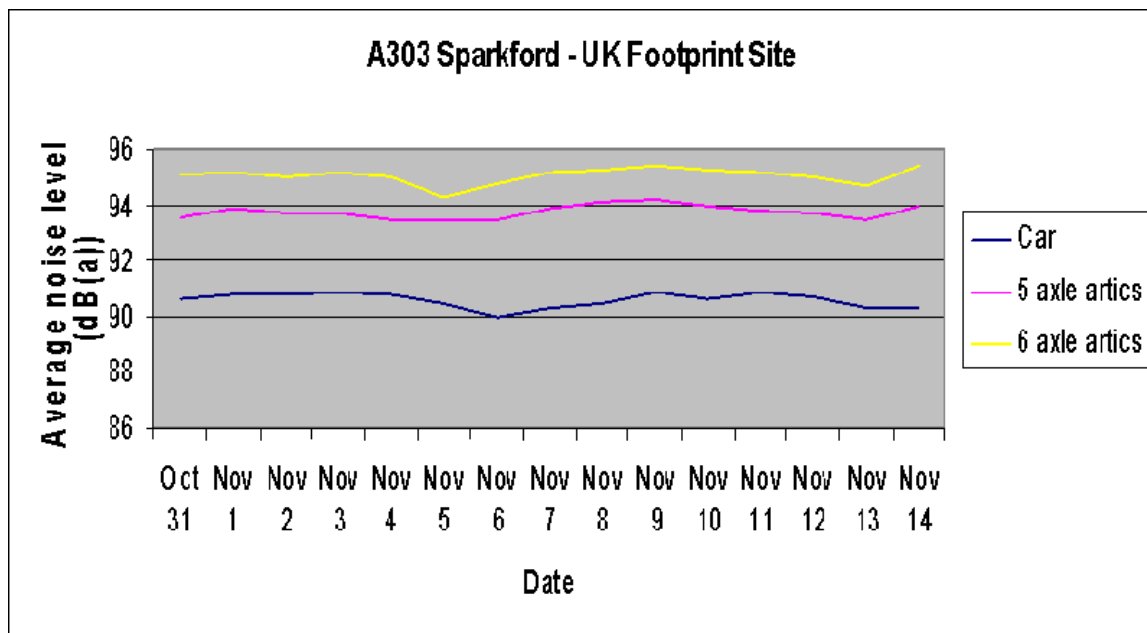


Figure 16. 4: Average noise level dB(A) from the FMS in the UK in November 2006 (Courtesy Department of Transport UK)

Figure 16. 5 shows the hourly traffic volume versus the average noise level. Although noise level drops with a decrease in traffic volume, it is clear that noise at night will become a greater nuisance than that during the day. This initial set of data shows that traffic levels at night are relatively low compared with the rest of the day but the average noise level being generated is as high if not higher than that during the rest of the day. In

terms of HGV's as a proportion of total traffic within the hour, during the quieter hours, up to 50% of the traffic is HGV.

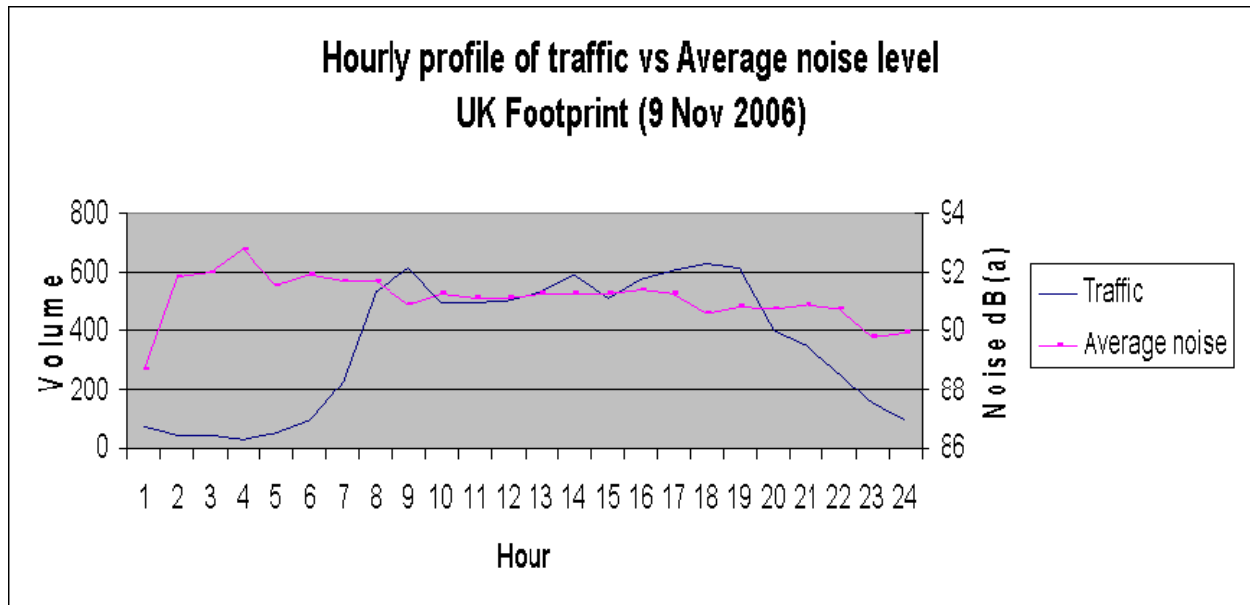


Figure 16. 5: Traffic vs. average noise level (Courtesy UK Department of Transportation)

Figure 16. 6 shows the heaviest vehicles and heaviest axles per day in November 2006. The allowable GVW in the UK is 40 t and it can be seen that this limit is surpassed every day. The allowable axle load without any special provisions on axle spacing and configuration is 10 t.

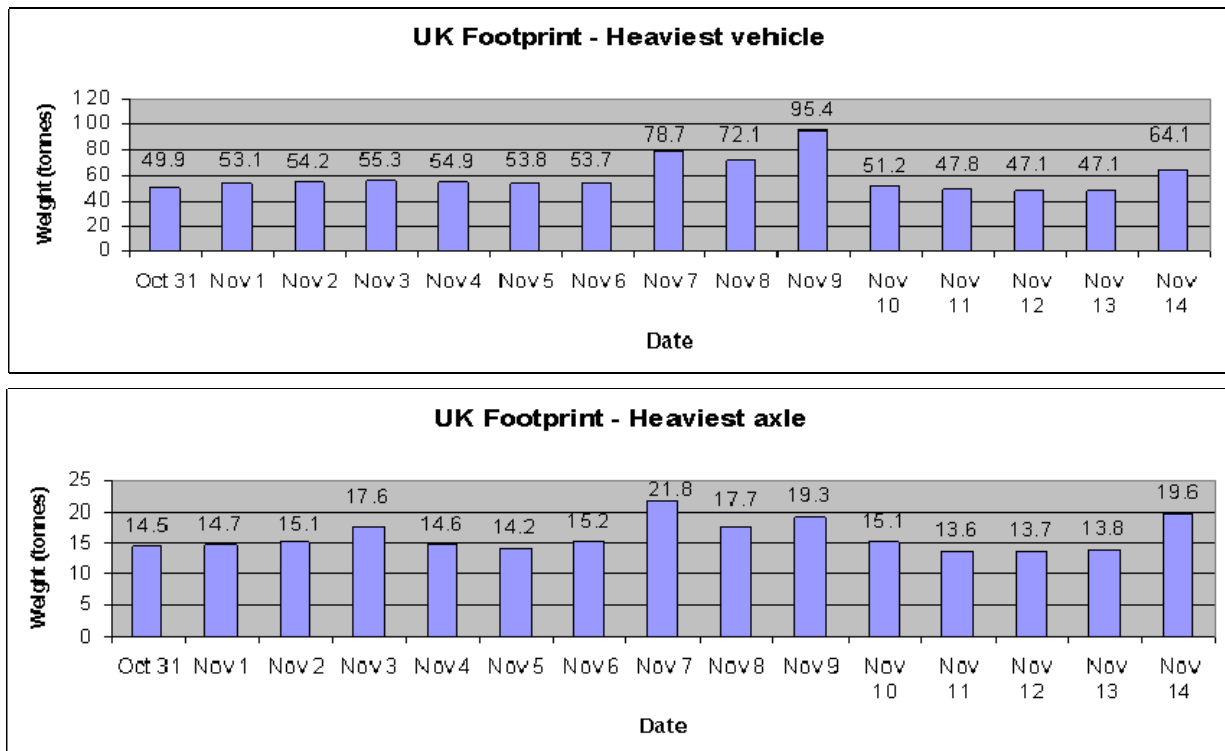


Figure 16. 6: heaviest vehicles and heaviest axles per day in November 2006 (Courtesy UK Department of Transportation)

The noise level of 6 axle articulated trailers was presented versus the GVW to investigate if there was any correlation between the weight of a vehicle and the noise generated (Figure 16. 7). This example indicates no correlation between weight and noise. In this case the noise level being generated by a 6 axle artic is consistent regardless of its weight. However a definite correlation was observed between noise level and speed as shown in Figure 16. 8.

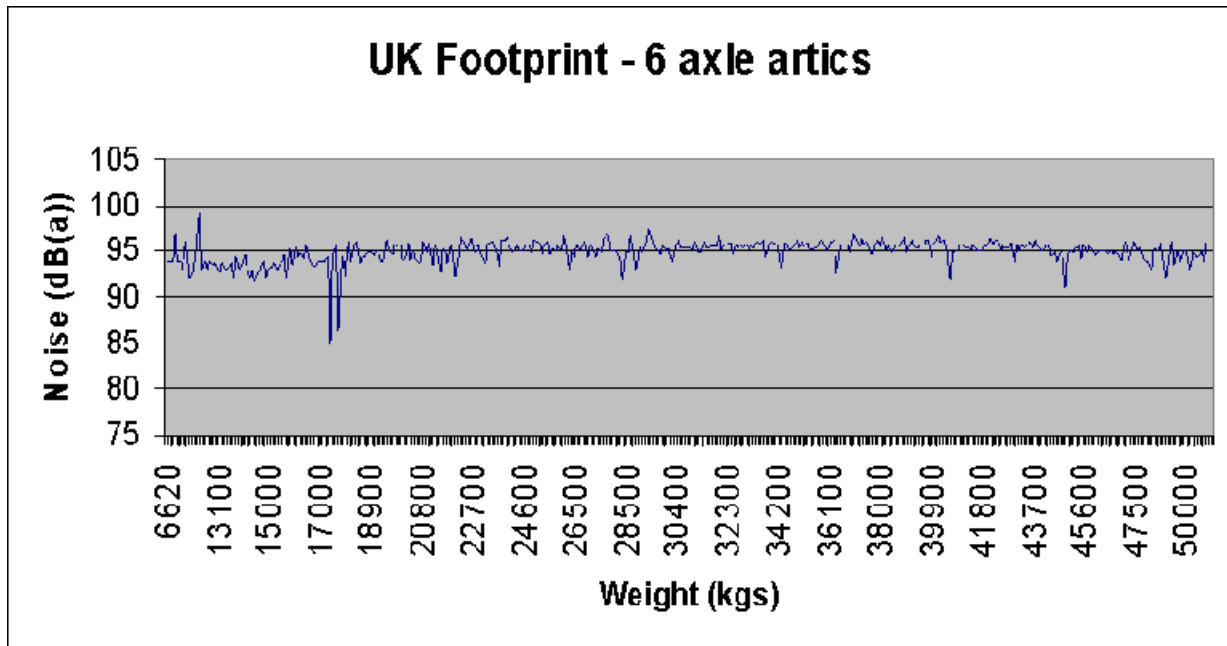


Figure 16. 7: Noise level produced by 6 axle artics vs. GVW

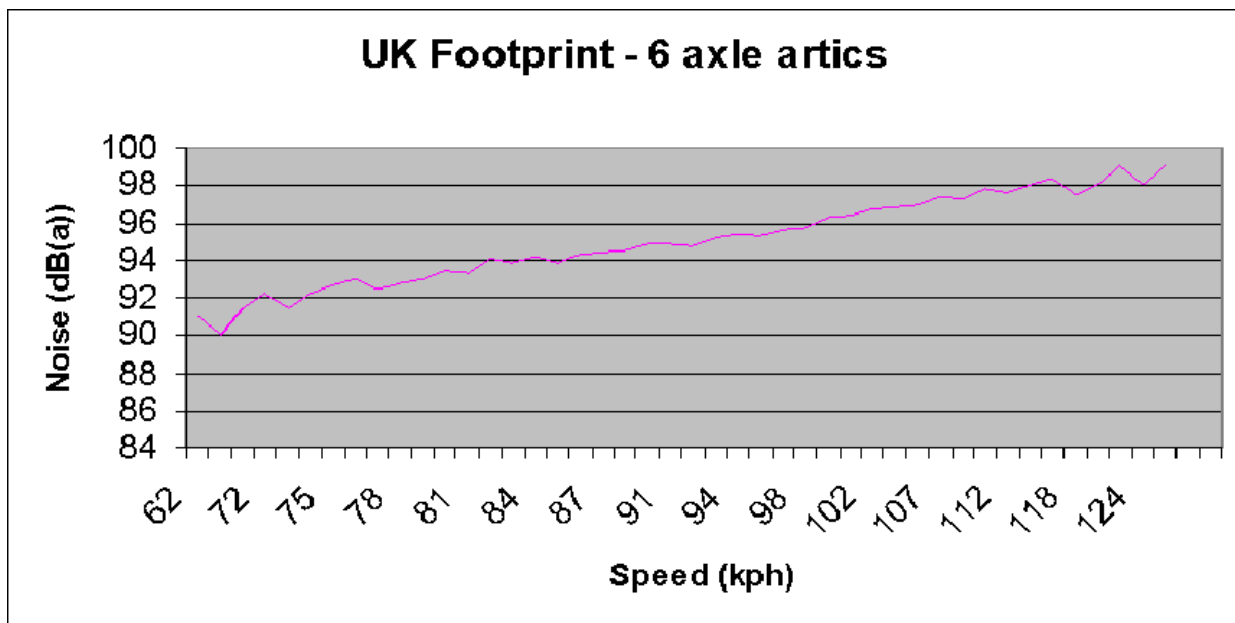


Figure 16. 8: Noise level produced by 6 axle artics vs. speed

17. VISCOELASTIC FE PAVEMENT MODEL

(Author: Gerald Morgan, Martin Arraigada, Kirill Sokolov)

17.1. Creation of the Finite Element Model

Objectives

The key objectives for the finite element modelling work are to determine what relationships exist between the wheel load, speed, contact pressure distribution and the stresses and strains in the pavement.

The basis of the model

The finite element model used in this project was based around the commercial, ABAQUS code which was extended by Man Ho Lam (2005), using the Python API. The plug-in consists of an interface accessible through the ABAQUS/CAE environment where the user can enter the data of the geometry, temperature, loads, speed, etc to simulate and evaluate the effect of a passing truck on the pavement. It also comprises a material and load library. Initially two models were developed: a so-called static model and a dynamic model. Both use the ABAQUS/Explicit solver with reduced integration, eight-noded elements. Due to the high (motorway) speeds of the vehicles to be modelled, it was decided that the dynamic model would be more appropriate and the static model was abandoned. However, a new static model for viscous materials was later proposed using ABAQUS/Standard in order to evaluate the static deformation data.

Key Model Features

Overview

The model that was used for validation and testing is shown in Figure 17. 1. It has the following key features:

- A temperature dependent elastic model and a viscoelastic material model according to the materials for each bituminous road layer. The latter enhanced the material model with respect to different loading frequencies depending on the vehicle speed.
- Material master curves and shift factors calculated and incorporated into the viscoelastic model, using the WLF equation [1]. This allowed the model to take into account the change in material properties of the road due to temperature.
- Symmetry boundaries in vertical and horizontal direction on the four 'in-road' sides with the base pinned at every node.
- Two ruts with a 1.8m internal separation (unless the axle width of the vehicle was known).

- Final model dimensions of 4,50 x 5,00 x 1.975 m and 30 x (28 + 2 x active channels) x 20 elements. The elements under the ruts were sized to match the SIM channel sensors, providing as close a match to reality as possible.

17.2. Material Properties

The material properties of the asphalts in the A1 were determined in a series of tests using the CoAxial Shear Test (CAST). The CAST is a mechanical pavement test method used at EMPA [Junker, 1993, Sokolov 2005]. The subgrade material properties were estimated with a light drop weight tester during the installation of the SIM sensor.

The viscoelastic properties and temperature dependency of each material were deduced from the CAST results., which present the complex elastic moduli and phase angle of the material as a function of the frequency and the temperature. This was done by using Prony series approximation [Abaqus Documentation] from a set of CAST data at 20°C.

The parameters g_i , G_0 and τ_i were deduced from the following equations:

$$G'(\omega) = G_0 \left(1 - \sum_{i=0}^N g_i \right) + G_0 \sum_{i=1}^N \frac{g_i \tau_i^2 \omega^2}{1 + \tau_i^2 \omega^2} \quad [17.1]$$

$$G''(\omega) = G_0 \sum_{i=1}^N \frac{g_i \tau_i \omega}{1 + \tau_i^2 \omega^2} \quad [17.2]$$

where $G'(\omega)$ and $G''(\omega)$ are the storage and loss modulus respectively and ω the angular frequency. N is the number of terms used to approximate the results.

The results were extrapolated from 20°C (reference temperature) to any temperature by calculating the parameters C_1 and C_2 of the WLF shift function, according to the following equation:

$$-\log(\alpha_\theta) = \frac{C_1(\theta - \theta_0)}{C_2 + (\theta - \theta_0)} \quad [17.3]$$

Where α_θ is the shift function and θ and θ_0 are the temperature and the reference temperature, respectively.

Values of the Prony and the WLF parameters are given in Table 17. 1.

For modelling, the asphalt layers were numbered from 0 to 3, where 3 is at the surface and 0 is just above the subgrade.

Table 17. 1: Viscoelastic data used in the finite element model.

Prony series parameters					
	Layer 3	Layer 2	Layer 1	Layer 0	Subgrade
G_0	2560	3590	3413	2336	130 ⁽¹⁾
g_1	0.415	0.271	0.263	0.404	
τ_1	2.25	4.11	6.30	1.89	
g_2	0.231	0.186	0.196	0.150	
τ_2	10.36	28.76	47.88	43.60	
g_3	0.194	0.363	0.260	0.262	
τ_3	58.21	315.55	400.78	599.16	
g_4	0.159	-	-	-	
τ_4	10034	-	-	-	
	-	-	-	-	
	-	-	-	-	

(1) This is the measured subgrade modulus. This parameter was later used for calibration as the measurement was considered to be unreliable. The value used in the final model was 260 MPa.

WLF parameters					
C_1	14987	14987	14994	14987	-
C_2	110000	110000	109999	110000	-

Loading

The model was loaded by applying the p_z (see chapter 6) pressure distributions to the small cells in the wheel paths. It can be seen from Figure 17. 1 that each cell in the ruts corresponds to one channel of the SIM sensor. For each surface rut cell, a load curve was calculated which closely followed the p_z distribution for that channel while keeping the number of points to a minimum. By applying a time shift to the load curves based on the cell's x co-ordinate and the velocity, u_x , of the vehicle, it was possible to simulate a rolling Tyre (chapter 6).

Geometry

The depth of each of the model layers was taken as an approximate average value of the layer thicknesses of the cores used to determine the material properties. The average of the exact measurements from the sample cores was not taken so as to better reflect the entire road surface, which would have been designed using round numbers. The final modelled mesh and layer thicknesses are shown in Figure 17. 1.

The depth of the subgrade was assumed. A value of 1.65 m was chosen so that the

model could retain a reasonably grid while modelling as much depth of subgrade as possible. It is desirable to give a relatively large depth to the modelled subgrade in order to reduce the effects of the boundaries on the critical areas of the model.

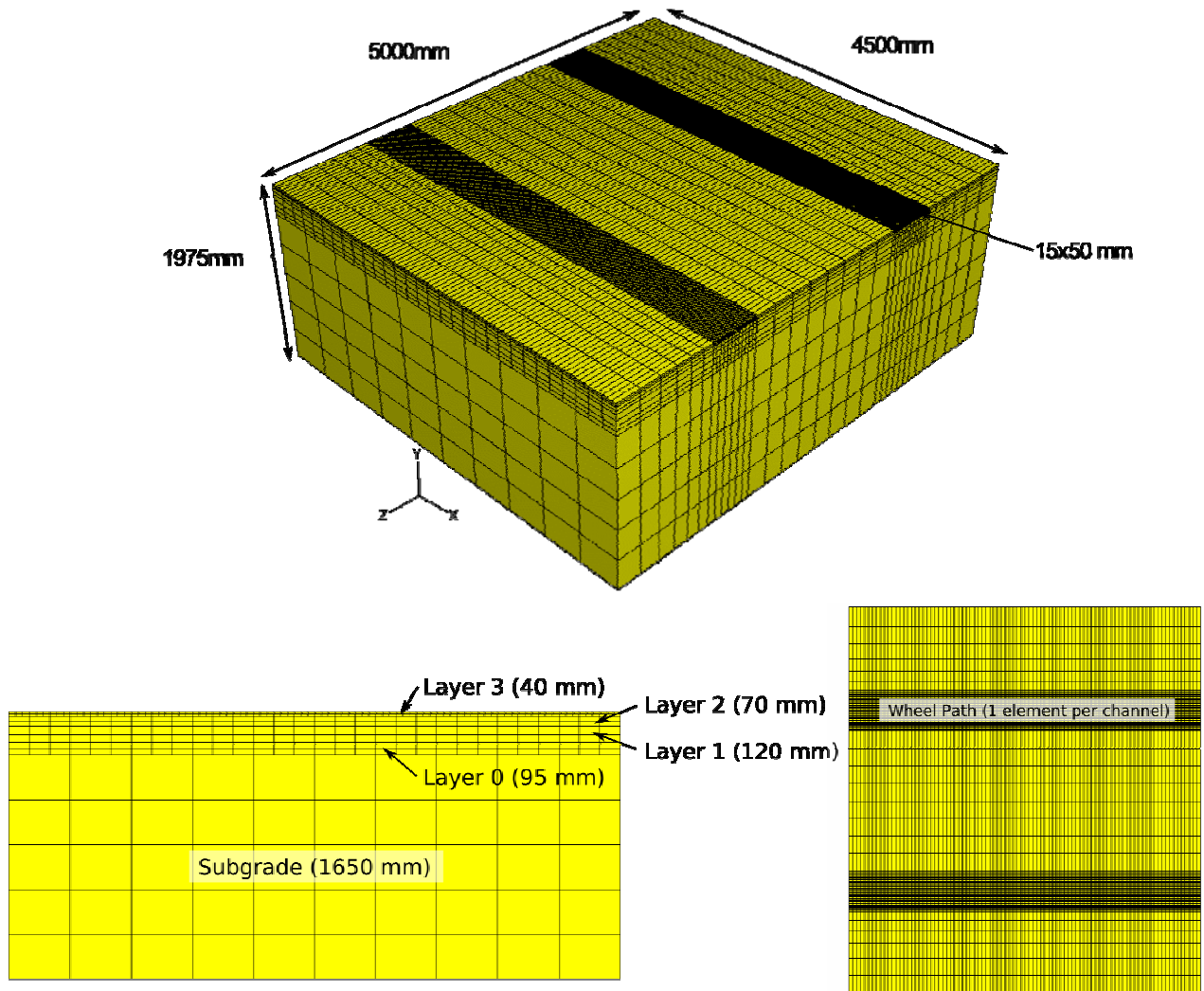


Figure 17. 1: The finite element model, showing the geometry and mesh

17.3. Validation of the Finite Element Model

Events chosen for validation

The finite element model was validated using the temporary acceleration sensors installed at the footprint site. On the night of 30th June 2005 two vehicles of known weights and configurations were used to test the acceleration sensors installed in the road. Using this recorded sensor data, the road deflections were calculated using a double-integration procedure [Arraigada et al 2007]. The two vehicles that were used for this calibration were designated 6102 and 6103 and are shown in Figure 17. 2 and Appendix IV.



Figure 17. 2: Vehicles used in the finite element model validation with the lengths and wheel loads shown

Due to the location of the acceleration sensors, the Tyre contact pressure distribution was, in some cases, only partially captured by the SIM sensor (a portion of the outer Tyre did not cross the sensor). This portion of the distribution was reconstructed based on the parts of the distribution that were available, similar distributions that had previously been recorded, and the measured value of the total wheel load.

Validation procedure

Accelerations and deflections were output from the model at approximately 255 Hz for a single point under the wheel imprint. This point was chosen to be as close as possible to the estimated location of the acceleration sensor under the Tyre. The exact location is not known as the precise alignment of the Tyre on the sensor during the calibration event was dependant on the skill of the driver. The frequency of recording was chosen to match that of the acceleration sensor tests as closely as possible.

The model results were then compared to the data recorded by (and calculated from)

the acceleration sensors. The unknown parameters in the model were adjusted until the model results were comparable to those from the field. A complete list of model runs for validation, with the parameters that were varied, is provided in Morgan (2006). This report also documents a continuous process by which the model was improved and brought closer to reality. During the course of these runs, several errors and inaccuracies were discovered in the original model.

Wherever possible, field data were used in the model. The footprint site's temperature sensors were consulted, and the correct pavement temperature (28°C) used for all runs (except where stated). Two models were run for each 'run number'. One with vehicle 6102 at 50 km/h and one with vehicle 6103 at 70 km/h. Three sets of recorded data existed for each of these conditions: passes 19-21 and passes 22-24, respectively.

Results of the validation

Comparative plots of the modelled acceleration and deflection and the recorded acceleration and calculated deflection are shown in Figure 17. 3. As can be seen from the plots, measured and simulated deflections present a good agreement in amplitude and shape, mostly for the data set of vehicle 6102.

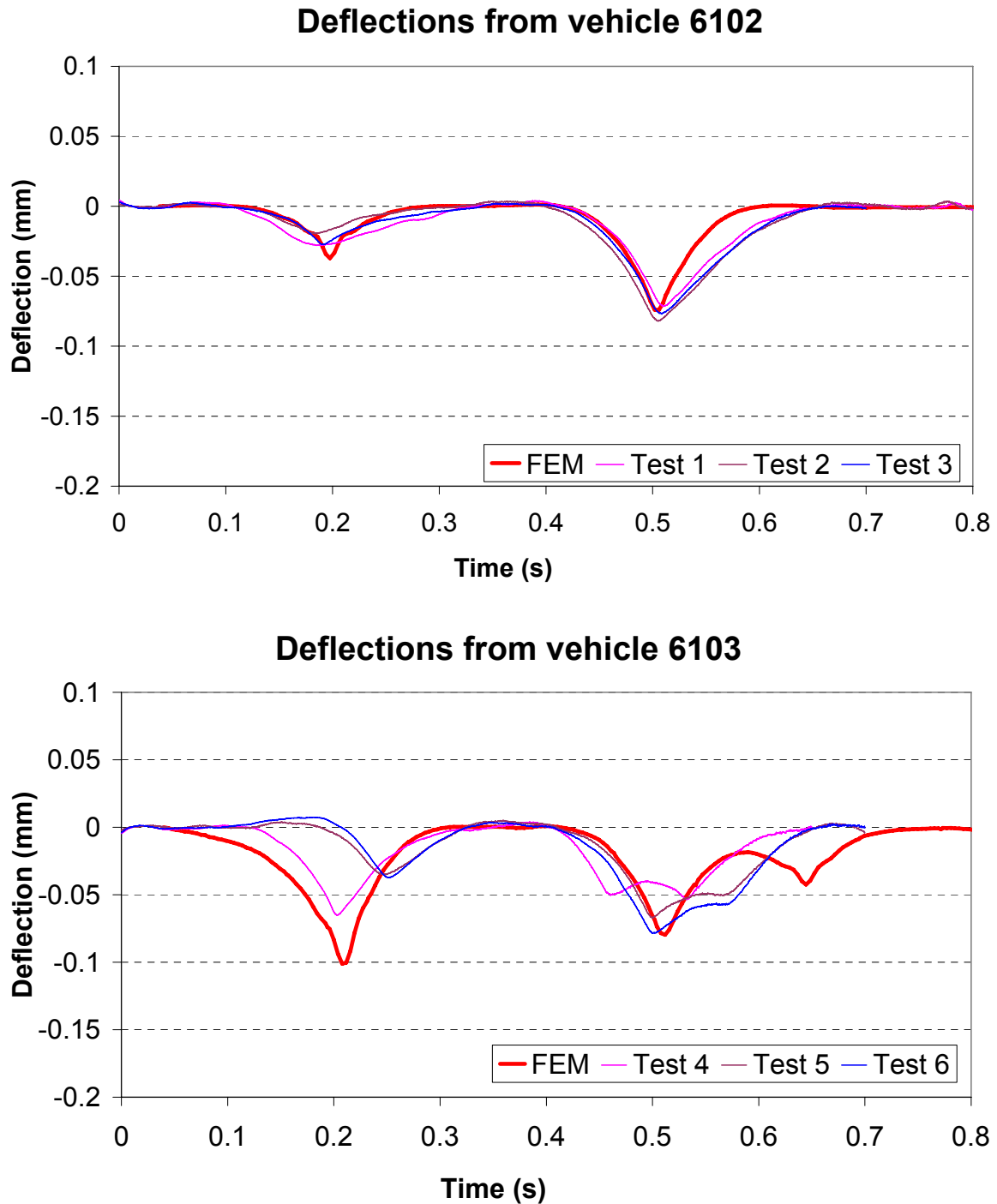


Figure 17. 3: Comparative plots of the finite element model results (run 021) and the measured data

It was decided to adjust the model for the best fit with vehicle 6102, as it was deemed to be the most trustworthy set of measured results. This is because more of the stress distribution was recorded by the SIM sensor for 6102. Additionally, a comparison of the deflection plots in Figure 17. 3 with the known wheel loads in Figure 17. 2 shows that the

peak values are much more in proportion with the loads for vehicle 6102.

The value of Young's modulus for the subgrade which resulted from the calibration was 260 MPa.

Other validations

The night of the 5th of September 2006, the road was closed again to check the functioning of the sensors, especially the deflection sensors (Balluff) and SIM sensor (Modulas). New tests, planned in the same way and using the same trucks described above were carried out. Additionally, some static test were done. During these tests the trucks were positioned with their rear Tyres on the deflection sensors for more than 10 min, while the deflection was continuously measured. Figure 17. 4 shows the measured deflection compared to the calculated FE deflection. All deflections are not absolute, but relative to the instrument base situated 40mm under the road surface as shown in the figures. Hence, each measurement corresponds to the difference between the deflection of each point (M1, M2 or M3) and the deflection of the pavement at the sensor base.

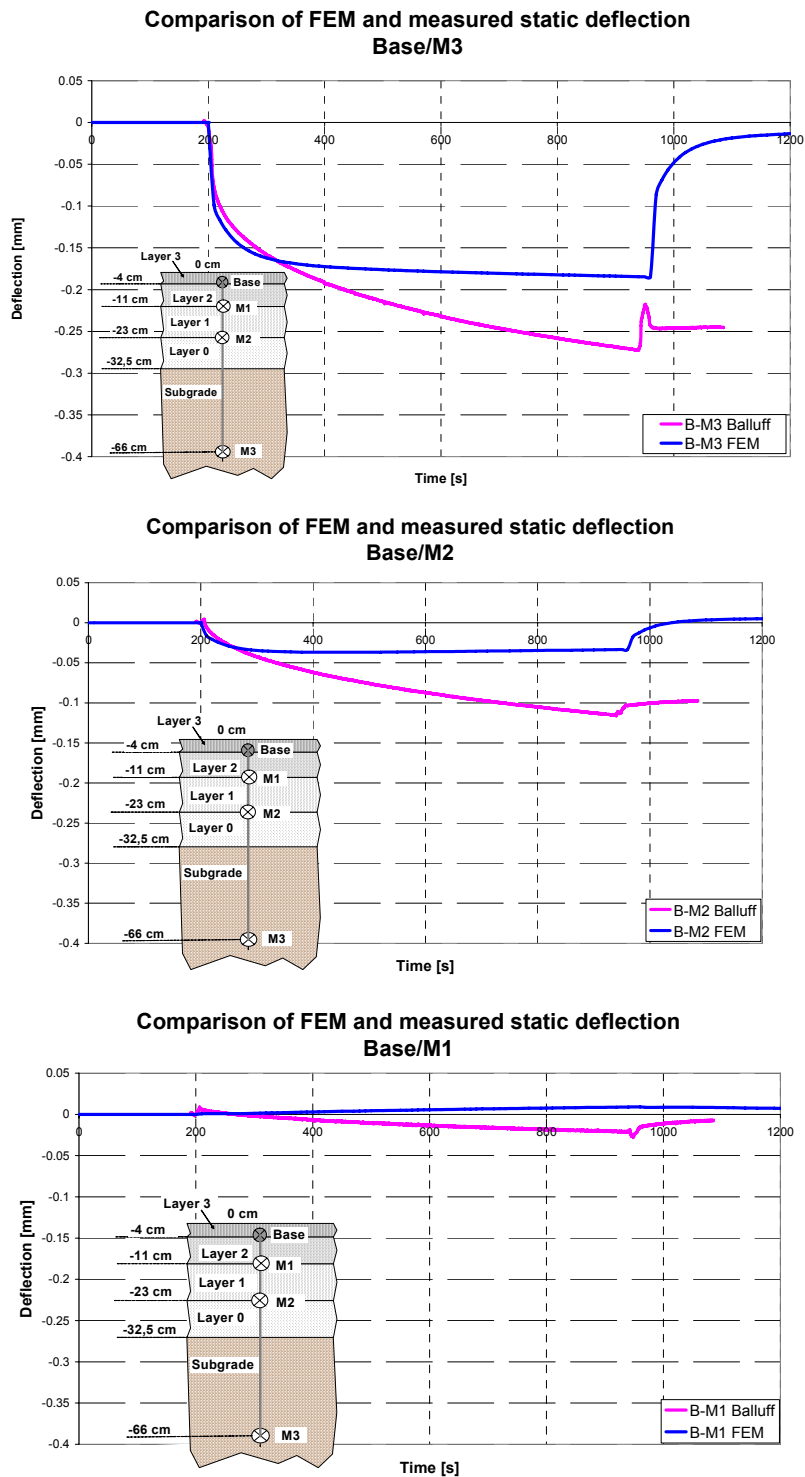


Figure 17. 4: Comparative plots of the finite element model static deflection and the measured data.

Similarly, “deflection maps” of the dynamic tests at 50km/h were constructed using the results of the three deflection sensors installed at the Footprint site. These maps show the relative deflection of the road between the sensors’ bases and the M3 point during a

truck pass-by. Similar maps were constructed from the model results by subtracting the simulated deflection of the model nodes that are in the same position as the Base from the M3 point of the sensor. Figure 17. 5 shows both calculated and measured deflection maps.

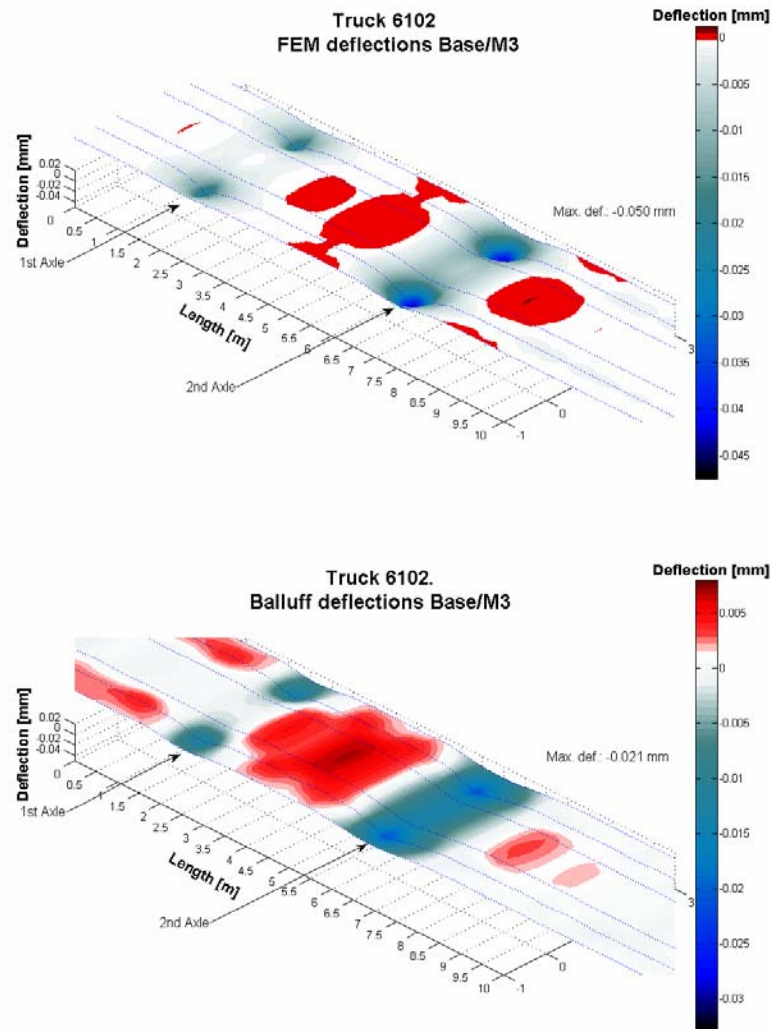


Figure 17. 5: Comparative deflection maps constructed from simulated and measured deflection.

Further work

It is clear that the model does not produce an exact match as there are some inaccuracies when analyzing the deflections of different points within the pavement structure. For example, Balluff data shows that there is a upward deflection of the layers under the vehicle, between the wheels (shown in red in Figure 17. 5). Although the model shows the same effect, the order of magnitude of this effect is 10 times smaller. Further work could be done to improve the validation procedure itself. For example,

further directly measured deflection data could be collected from the road. If some reliably matched data from WIM, SIM and Balluff could be recorded, this would allow the validation of the model using directly measured data, rather than deflection data calculated through the accelerations and resulting double integration procedures.

Recording such data may prove to be a tricky task, however. There will be an increased difficulty in matching three sets of data together reliably and this will be compounded by the fact that shortly before this period, some SIM channels had begun to behave erratically, reducing the number of reliable SIM events.

17.4. Modelling the Road Data

All the events presented here correspond to an early phase of the modelling which was validated using the acceleration measurements from June 2005 (Morgan 2006). For all the following runs, which present a limited number of real events, the material properties of the model were entirely linear elastic, although the elastic modulus varied with temperature. The length of the model was limited to 1.5 m when a sufficiently fine mesh was used for the subgrade and the asphalt layers under the surface layer. The subgrade considered in this case, was modelled with 1 m thickness. It is planned to re-run all the events with the improved validated model. However, due to the fact that the model is still under continuous development, it was only possible to include the following results on this report.

Selection of events

Events for modelling were selected from the matched WIM/SIM data in September 2005. It is notable that none of the very high recorded wheel loads were matched—the peak recorded wheel load that was matched was 83.8 kN. It is not known whether the matching algorithm or some other effect is responsible for the lack of high, matching wheel loads. It is possible that such loads are simply too rare to expect a match. It is also possible that many of the higher wheel loads were anomalies in the WIM data.

The events were chosen in such a way that the effects due to the variation of any single parameter could be isolated wherever possible. A complete list of the modelled load cases with their key parameters is given in Table 17. 2. Most loads were taken from the September 2005 dataset, but in order to ensure that they were representative, some load-cases were taken from May 2006. These events have the advantage of having associated measured deflection data which may be compared with the model results. However, the SIM sensor in May 2006 was in a poor state of repair and some channels were behaving erratically—the reason why only a few events have been used.

To date, no attempt has been made to model more than one event from the road in a single model run, with the exception of the validation events. All of the runs presented below correspond to single SIM events. There is no reason, other than that of available resources, why multiple Tyres, representing entire vehicles or convoys from the road, could not be modelled.

Table 17. 2: List of the events which have been used in the finite element model

Run No	WIM ID	Wheel Load (N)	Speed (m/s)	Temperature (°C)	Category ⁽¹⁾
52	56054	50521.5	25.00	27.41733	m
53	56054	50521.5	25.00	27.41733	n
54	45882	50619.6	25.00	24.17817	n
55	45882	50619.6	25.00	24.17817	n
56	22951	50227.2	25.00	20.46683	n
58	42803	50619.6	25.00	24.306	nn
59	62489	50619.6	20.83	28.81467	nn
62	49016	71858.25	23.61	24.18133	n
63	62797	76419.9	23.88	28.69317	n
64	52079	72495.9	24.44	24.8145	nn
66	35054	72446.85	22.22	20.8135	n
67	35054	72446.85	22.22	20.8135	mm
70	48971	83875.5	21.66	24.51367	mm
101	3495	73918.35	24.44	15.7145	nn

(1) The category was determined by a visual inspection of the pressure distribution. n is for single 'n'-shaped Tyres, mm is for dual 'm'-shaped Tyres etc.

Comparison of Selected Results

Comparison at 5 tonnes

Stresses

The results files produced by each model run are very large and it is clearly not possible to present the complete sets of results here.

The plots of model stresses and strains shown below are from a cross-section underneath the Tyre. The cross-section is taken half-way along the model and is facing in the positive x direction. The model time at which the cross-sections were taken varies from run to run because the modelled wheels took varying amounts of time to cross the model domain. The times at which the cross-sections were chosen were always half way through the modelled loading time. The tables show the highest maximum principal

stresses and strains in tension and compression which occurred during each model run.

A selection of 'baseline' cases were selected from the model runs, along with a few runs which used distributions which were interesting for other reasons. The following model runs were selected:

- 52 A ~5 t single 'm'-shaped distribution at 90 km/h and 27 °C.
- 54 A ~5 t single 'n'-shaped distribution at 90 km/h and 24 °C.
- 58 A ~5 t double 'n'-shaped distribution at 90 km/h and 24 °C.
- 59 A ~5 t double 'n'-shaped distribution at 75 km/h and 28 °C.

These four runs have been chosen as a representative sample of the wheel loads on the borderline of environmental friendliness as defined by the Swiss authorities: vehicles with axles under 10 tonnes do not have to pay road access charges for the use of Swiss roads.

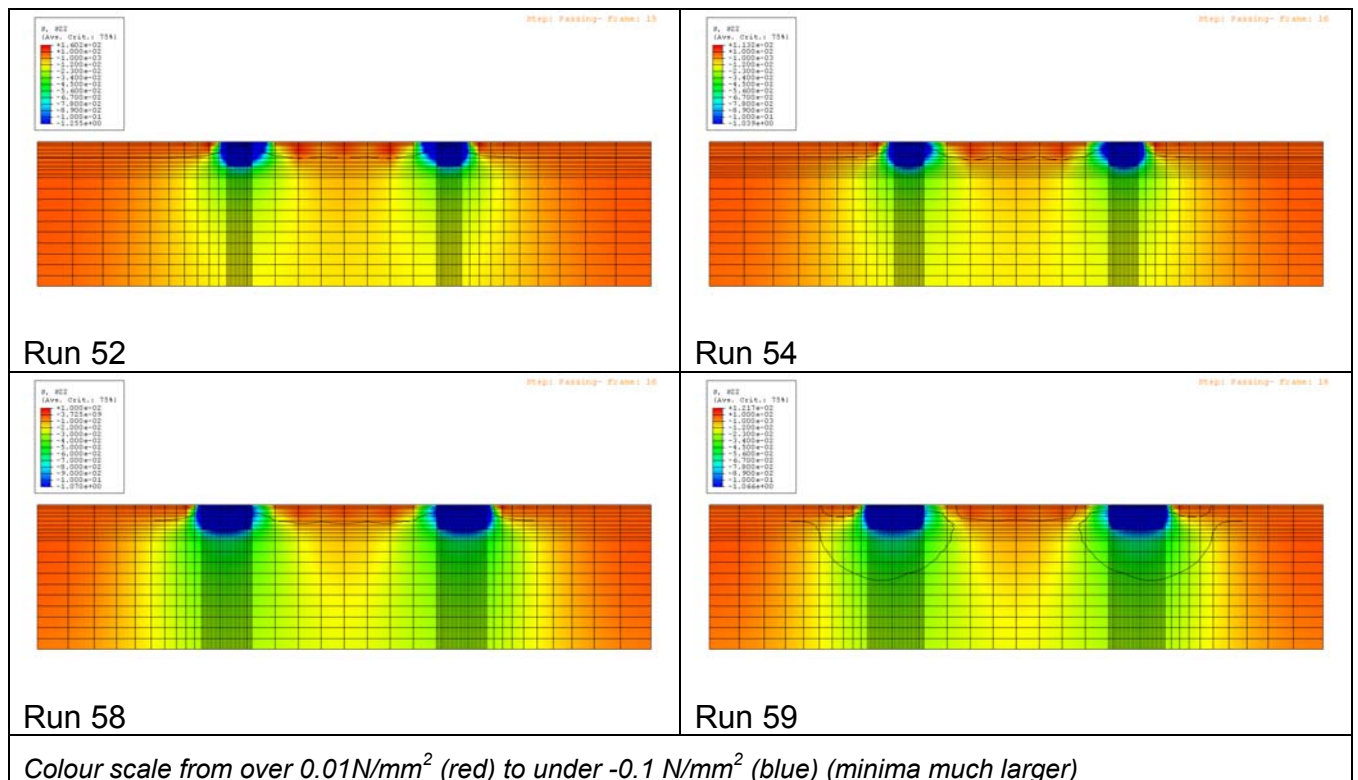


Figure 17. 6: Vertical stress distributions in a cross-section of the pavement under the Tyre (5 t)

Table 17. 3: Maximum principal stresses from the FEM (5 t)

Run Number	Maximum Principal Compressive Stress in Subgrade (N/mm ²)	Maximum Principal Compressive Stress in Asphalt (N/mm ²)	Maximum Principal Tensile Stress in Asphalt (N/mm ²)
52	0.06462	1.4107	0.47647
54	0.06532	1.2733	0.47653
58	0.09015	1.2311	0.52970
59	0.10453	1.2723	0.70784

It can be seen from Table 17.3 and Figure 17. 6 that the dual Tyres (58 and 59) produce higher maximum principal tensile stresses in the asphalt layers, whereas the single Tyres produce higher vertical tensile stresses in the asphalt.

The ‘m’-shaped distribution clearly produces higher compressive stresses in the asphalt layers. It can also be seen that the stress bulb for the ‘m’-shaped run 52 extends well beyond the width of the Tyre (The width of the Tyre is equivalent to the width of the dense mesh). It is not certain whether this extension of the stress bulb can be attributed to the shape of the distribution, as it can also be seen with some ‘n’-shaped distributions. However, it is more common on the ‘m’-shaped distributions than the ‘n’-shaped distributions. It should be noted that few conclusions may be drawn from the size or shape of this extension as it will be heavily influenced by the comparatively coarse mesh in this region, making these parameters insufficiently accurate.

Strains

Table 17. 4: Maximum principal strains from the FEM (5 t)

Run Number	Maximum Principal Compressive Strain in Subgrade (μ ϵ)	Maximum Principal Compressive Strain in Asphalt (μ ϵ)	Maximum Principal Tensile Strain in Subgrade (μ ϵ)	Maximum Principal Tensile Strain in Asphalt (μ ϵ)
52	534	548	200	249
54	531	332	196	203
58	720	352	253	251
59	865	562	316	320

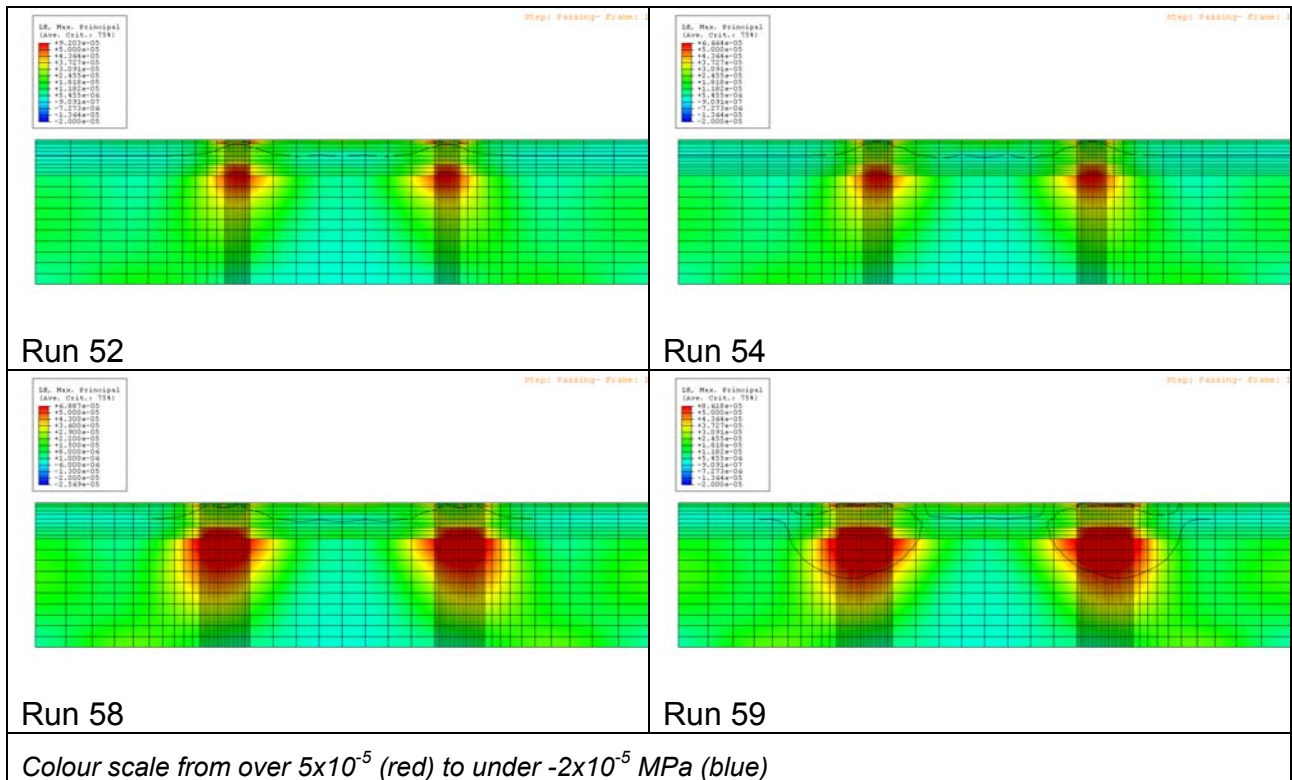


Figure 17. 7: Maximum principal log(strain) distributions in a cross section of the pavement under the Tyre (5 t)

It is difficult to see any clear difference in Figure 17. 7 and Table 17. 4 between the cross-sections of the ‘m’ and the ‘n’-shaped Tyre. It can be seen, however, that the ‘m’-shaped Tyre produces a much greater maximum principal compressive strain and also a greater vertical tensile strain. It should be noted that similar increases also occur with run 59 and so no conclusions can be drawn at this time, as the possibility exists that this increased strain may be related to the temperature differences in the models.

Figure 17. 7 also shows that a much greater volume is strained by the passage of a dual Tyre compared to a single Tyre, and higher peak compressive and tensile strains accompany this.

The otherwise broadly similar distributions of runs 58 and 59 suggest that slower Tyres produce greater strains in the pavement than faster Tyres.

Some heavier wheels

Three runs were selected from among those with higher wheel loads.

- 62 A 7.2 t single ‘n’-shaped distribution at 85 km/h and 24°C.
- 70 An 8.4 t dual ‘m’-shaped distribution at 78 km/h and 25°C.
- 101 A 7.4 t dual ‘n’-shaped distribution at 88 km/h and 16°C from May 2006.

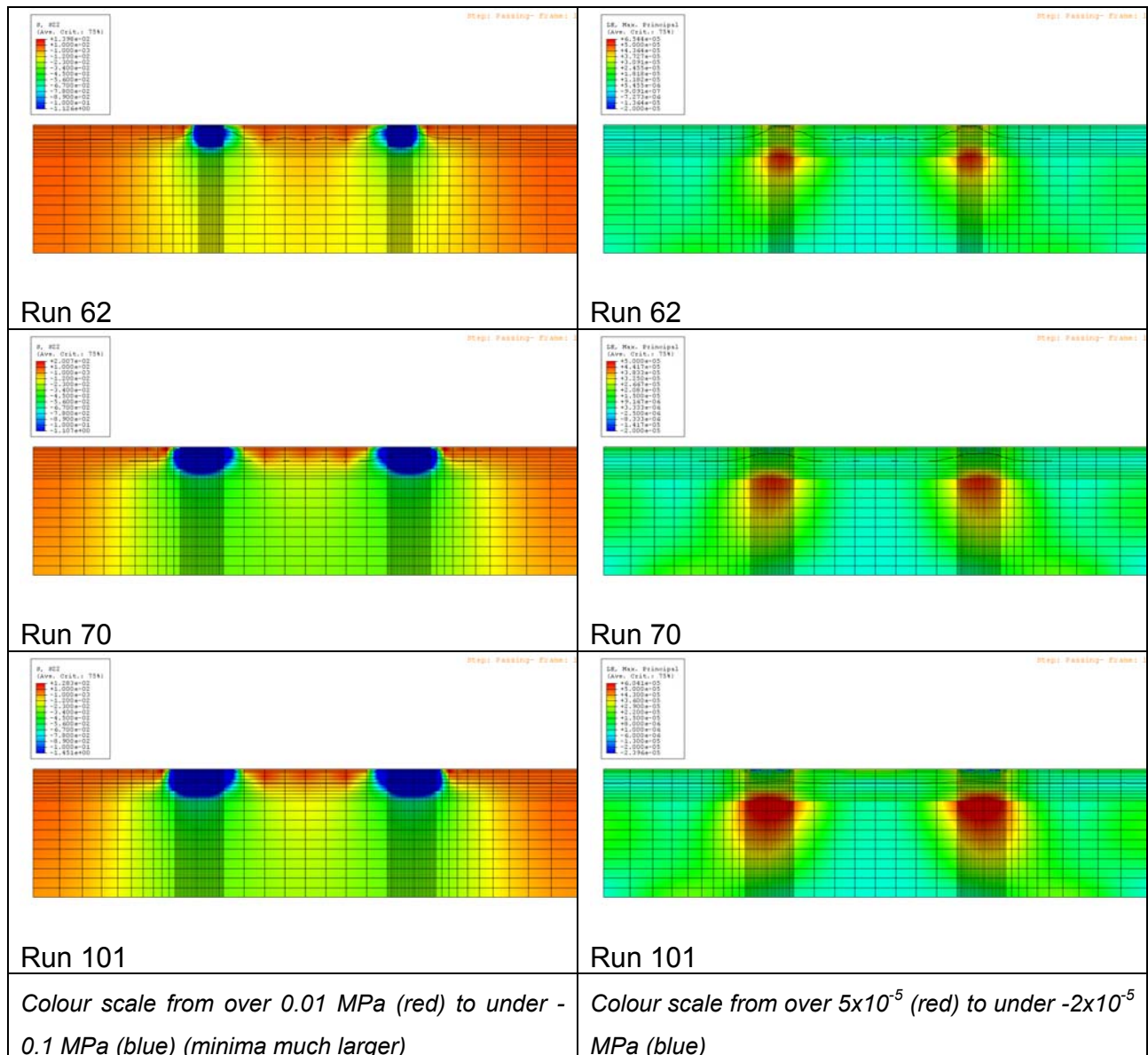


Figure 17. 8: Vertical stress (left) and maximum principal log(strain) (right) distributions in a cross section of the pavement under the Tyre (>7 t)

The results for these three runs are illustrated in Figure 17. 8 , Table 17. 5 and Table 17. 6. It can be clearly seen that the general trend in these results is for increasing stresses and strains with increasing wheel load. It is interesting, however, that while the stresses and strains have increased, the difference between the peak stresses and strains of the 5 t wheels and these, heavier wheels is not as great as might be expected.

Table 17. 5: Maximum principal stresses from the FEM (>7 t)

Run	Maximum Principal	Maximum Principal	Maximum Principal
-----	-------------------	-------------------	-------------------

Number	Compressive Stress in Subgrade (N/mm ²)	Compressive Stress in Asphalt (N/mm ²)	Tensile Stress in Asphalt (N/mm ²)
62	0.06689	1.3790	0.47988
70	0.08185	1.8505	1.03402
101	0.09517	1.7289	0.86051

Table 17. 6: Maximum principal strains from the FEM (>7 t)

Run Number	Maximum Principal Compressive Strain in Subgrade ($\mu\epsilon$)	Maximum Principal Compressive Strain in Asphalt ($\mu\epsilon$)	Maximum Principal Tensile Strain in Subgrade ($\mu\epsilon$)	Maximum Principal Tensile Strain in Layers ($\mu\epsilon$)
62	548	332	198	207
70	592	216	184	175
101	734	311	239	235

It should be noted that several modelled peak strains are significantly less than comparable runs with only 5 tonne loads.

Some anomalous results

Runs 66 and 67 form an interesting pair of results for several reasons. They are two different SIM events which have matched to the same axle but, more interestingly, run 67 contains a second distribution which is believed to represent a double Tyre combination with one Tyre flat or punctured.

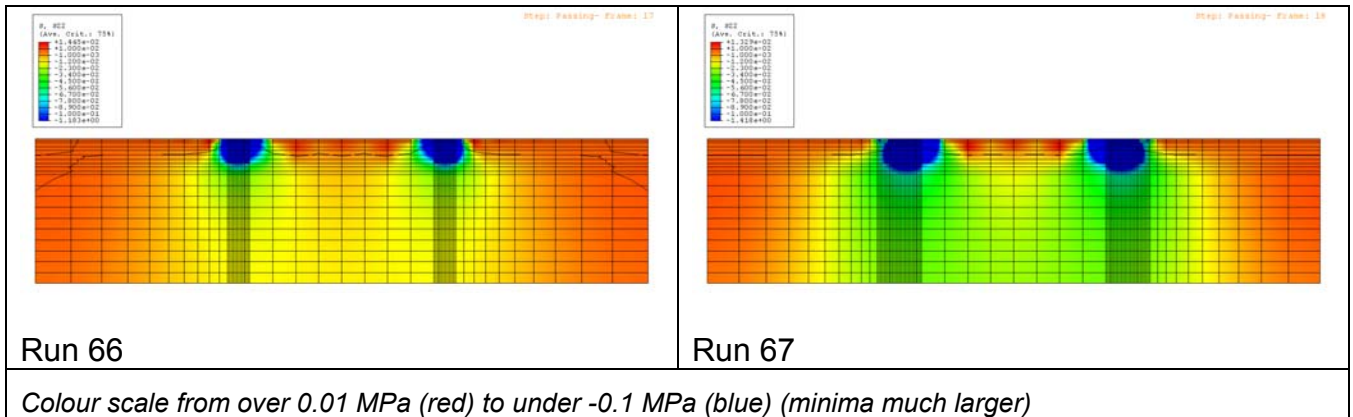


Figure 17. 9: Vertical stress distributions in a cross section under the Tyre (anomalies)

Table 17. 7: Maximum principal stresses from the FEM (anomalies)

Run Number	Maximum Principal Compressive Stress in Subgrade (N/mm ²)	Maximum Principal Compressive Stress in Asphalt (N/mm ²)	Maximum Principal Tensile Stress in Asphalt (N/mm ²)
66	0.05266	1.3029	0.39107
67	0.10444	1.6067	0.72383

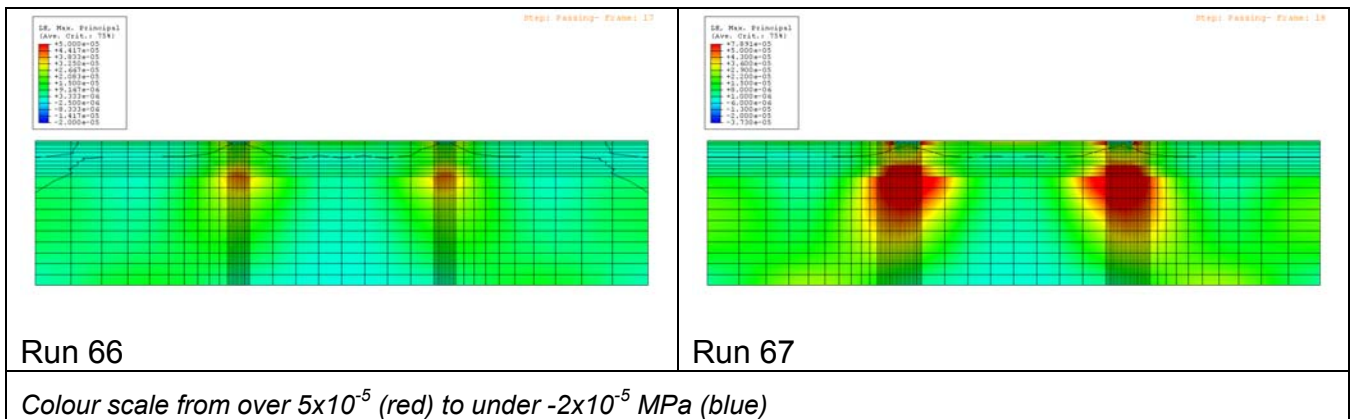


Figure 17. 10: Maximum principal log(strain) distributions in a cross section of the pavement under the Tyre (anomalies)

Table 17. 8: Maximum principal strains from the FEM (anomalies)

Run Number	Maximum Principal Compressive Strain in Subgrade ($\mu\epsilon$)	Maximum Principal Compressive Strain in Asphalt ($\mu\epsilon$)	Maximum Principal Tensile Strain in Subgrade ($\mu\epsilon$)	Maximum Principal Tensile Strain in Asphalt ($\mu\epsilon$)
66	417	256	157	166
67	819	375	292	299

It can clearly be seen that run 67 is more onerous than run 66 and, by comparing these results with the 'baseline' cases, we can probably assume that it is run 67 which correctly matches the wheel load of 72.5 kN recorded by the WIM. Looking at the 3D plot of the pressure distribution in Figure, we can see that while the footprint is of double width, one Tyre is taking almost all of the load, the other being severely under-inflated.

Comparing run 67 with a complete dual-Tyre distribution with a similar loading (run 101) reveals that run 67 produces higher tensile and compressive strains. The temperature difference between these two runs should be noted, however.

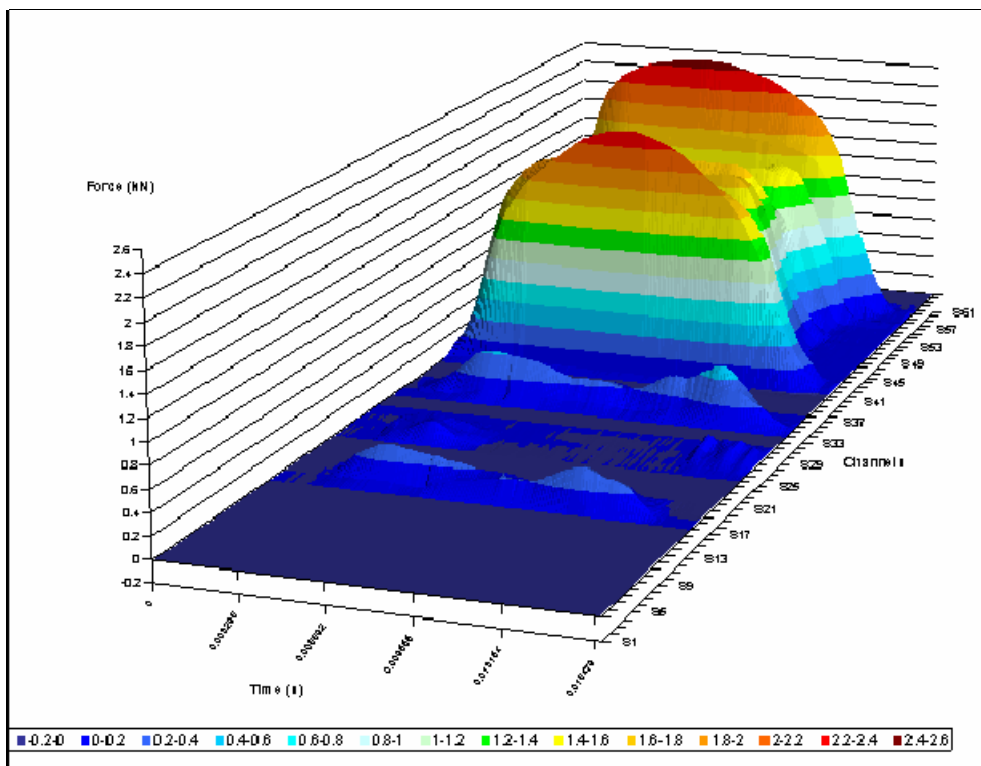


Figure 17. 11: Pz force distribution under a dual 'm'-shaped Tyre with very uneven inflation (run 67)

17.5. Potential Improvements to the Finite Element Model

While it is thought that the model in its current state is giving relatively accurate and dependable results, there are many ways in which it could still be improved, either by increasing its efficiency or by changing its parameters to better reflect the real world. Some of the areas where scope for improvement has been identified have been outlined below.

Model loading

The loading of the model currently uses the p_z pressure distribution as defined in chapter 6. Given the large x dimension of the elements, this seems to be a sensible choice. While it would be instructive to do a sensitivity analysis on the use of the σ_z distribution as this would not only give more information as to the performance and sensitivity of the model, such an analysis would require significantly more time and computational resources than are available at this time.

Material properties

Another aspect of the material properties which could be improved is the data associated with the subgrade. The subgrade modulus was obtained through a test using a light drop weight tester. However, it is suspected that the subgrade sample (which is of a clayey nature) was disturbed prior to this test (for example, due to the water used during the installation of the SIM sensor) and does not accurately reflect the in-situ conditions. The results are therefore suspect and therefore the subgrade stiffness was used as a calibration parameter.

Further work could usefully be done to investigate whether the calibrated value of the subgrade modulus is a close approximation to the real material.

Model geometry

As with the material properties, while our knowledge of the layers' geometry is good, the geometry of the subgrade is unknown. No sensitivity analysis has yet been performed on the subgrade depth or grid density. It is probable that the model could be made more efficient without significant loss of accuracy by refining the subgrade mesh.

Model temperatures

All of the modelled data from real events has, so far, excluded temperature gradients from the pavement from consideration. This decision was made, in part, on the strength of an early sensitivity analysis into variable temperatures which yielded little effect on the overall deflections (Table run 001). Since this sensitivity analysis was undertaken, however, major revisions have been made to the model, and it would be useful, in the light of these changes, to repeat this test.

In order to do this accurately, an event with a very significant temperature gradient, for which matched WIM/SIM/Balluff results are available should be found. Such data are not yet available, however, and further analysis of the model's sensitivity to temperature should be postponed until this is rectified.

17.6. Conclusions and Suggestions for Further Study

The finite element model described in this chapter has been shown to be a useful tool for the quantification of the stresses and strains induced due to loaded Tyres trafficking a multi-layered pavement.

Using the outputs from the SIM, WIM and temperature sensors, in combination with a good understanding of the pavement construction, the effects on the pavement can be modeled to a reasonable degree of accuracy.

From the results presented here we can say with certainty that the distribution of the contact stresses under a Tyre has a very significant effect on the type, magnitude and distribution of the stresses and strains in the pavement. These stresses and strains can be related to pavement wear and performance.

It is clear that there are a large number of parameters which affect the stresses and strains in the pavement other than the contact stress distribution and wheel load

The results presented here can be used to suggest several areas of further study. The following hypotheses are at least partially supported by the results and could be investigated in more detail using this model:

- Vehicles produce deformations and strains which are inversely proportional to their speed when all other factors are removed from consideration. i.e. faster vehicles strain the pavement less.
- 'm'-shaped distributions produce larger deformations and strains than 'n'-shaped distributions. i.e. an overloaded vehicle with a given load causes greater strain in the pavement than an under loaded vehicle with the same load.

Both of these hypotheses would require some procedure to be created that could objectively determine whether a distribution was 'm' or 'n'-shaped. Preferably, the procedure could produce a value which could be taken as the degree to which the vehicle was overloaded.

There is some evidence in literature [Addis et al 2001] that, super-single Tyres cause



more road damage than dual Tyre configurations with equivalent loading. While this has not been tested in this study, the model developed here could be used to investigate this claim.

It is clear from this study that it is very difficult to draw accurate conclusions about the stresses and strains (and hence damage) to the pavement based upon any one of the easily measurable parameters in isolation. This supports the conclusion that the use of combined monitoring sites such as the Footprint Measuring Station is currently the best way to measure the total environmental impact of road vehicles in a moving traffic stream.

18. COST MODELING

(Authors: Philipp Jordi, Cornelia Petz)

The transport sector is the fastest growing economic sector in the last years and thus it bears a large portion of the economic process. The road and rail transport generate various benefits for the population and the economy; in addition, they create costs for the user and the public funds. The transport financing grew historically and differently for private and public transport. The means of transport of each traffic mode are self-financed. The infrastructures are paid to a large extent from public funds with tied yields (oil tax, vignette, motor vehicle taxes) and taxes. Public traffic is operated by the transportation enterprises. These finance themselves from their yields and contributions of the public funds ordered in common economical achievements (public service). Additionally the incomes from road charging are reinvested into the traffic sector. A share of these revenues are to cover investment costs for infrastructure and public transport. But there is no complete cost recovery and so the additional uncovered costs debit public funds.

The theme of this chapter is the source, the composition and the distribution of the costs of land transport sector. The project partners in the cost modelling work group, produced a report originating from the lack of previous research linking physical effects to road and rail infrastructure charging, including economic factors such as cost recovery profile / horizon [Peter Doran et al], here after referred to as “the work group study”. The report considers how costs are defined and then attributed to vehicles using measures of damage/demand to the infrastructure. The question of detail (by vehicle, by route, by causing factor) is balanced against practicality, transparency and features that promote easy use and understanding of any tariff including price signals and incentives. Also described are the external costs to society due to environmental impact, congestion and accidents. These costs are often more difficult to define, but including them in charges can produce lower emissions, or incentives for travelling at off peak times. A review of road and rail charging schemes in a number of countries is included, as well as a brief appreciation of how other models of transport deal with charging. Based on data concerning the external costs of transport and the measured emissions, the project team determined the emission costs per vehicle. The data of this report is based on the UNITE project (UNification of accounts and marginal costs for Transport Efficiency, <http://www.its.leeds.ac.uk/projects/unite/>). UNITE is a part of the European Union’s Fifth RTD Framework Programme (1998-2002) in the thematic programme Competitive and Sustainable Growth.

In addition, a comprehensive cost analysis report by the federal offices for spatial development and statistics (ARE) and by the federal office for environment (BAFU) in

Switzerland makes it possible for the first time to have a total view of the costs and use of the land transport and its financing on national level hereafter referred to as “ the Swiss study”(ARE, BAFU 2006). This study was handled by INFRAS, a Swiss research and consulting company.

A recent study in Switzerland [Sutter and Rapp et al 2006] shows that road pricing is an instrument of the market economy which can influence traffic demand as well as contribute to generating transport revenues. The research project analyses the possible implementation scenarios for Switzerland. For this purpose, first the experiences from foreign countries are examined and the individual model parameters are discussed systematically. Then the possible application schemes in Switzerland are sketched and broadly evaluated using four illustrative case studies. The project is focused on road user charges and prepares the ground for further in-depth studies on regional and national level.

This chapter provides a comparison of the two approaches in cost modelling listed above in order to gain more insight into the cost of transport. Generally, both studies have similar approaches and measurement methods of determining the external costs of transport. Below, various costs and approaches by the two reports are discussed.

18.1. Structure of Costs

Both studies assume a similar cost structure. In large part the costs of transport are used for acquisition, operation and maintenance of vehicles and rolling stock. These costs are the operating costs. Further costs are due to the building and maintenance of the infrastructure, the so called infrastructure costs.

These costs are internal costs of transport. They are measurable and therefore are recovered by fuel tax, vignette and motor vehicle taxes, for instance. But in addition, there exist external costs. These external costs arise from damages caused by transport and cannot be reliably calculated because it is very difficult to quantify them in relation to individual polluter. The measurement of the various parameters causing damage to road and environment is an important part of this project. In the following table the structure of costs and the composition of the external costs is shown in Table 18. 1:

Table 18. 1: Overview of cost structure in both studies

Work group report	Swiss studies
operating costs	operating costs
costs of infrastructure	costs of infrastructure
environmental costs	costs for environment
noise emissions, air pollution climate changes others	noise air pollution climate changes nature and landscape others
costs of accidents	costs for accidents and safety
	property damages accident follow-up costs medical treatment insurance police courts
congestion costs	

The cost grading in these two approaches is very similar. There are operating and infrastructure costs. Added there are the external costs for environment, accidents and safety. The work group report does not divide costs of accidents and lists additional costs of congestion.

18.2. External Costs of Transport

Table 18. 1 shows the cost structure of different modes of land transport in Switzerland. It is clear to recognize that the costs for operating and infrastructure are the main part of the whole costs; only 4 to 14 % of costs are external costs. Freight transport on road causes a particularly high portion of external costs. Comparatively, public transport on road causes a low portion of external costs. But the cost covering should not be the main aim rather to reduce the environmental damages and to enhance a sustainable transport system.

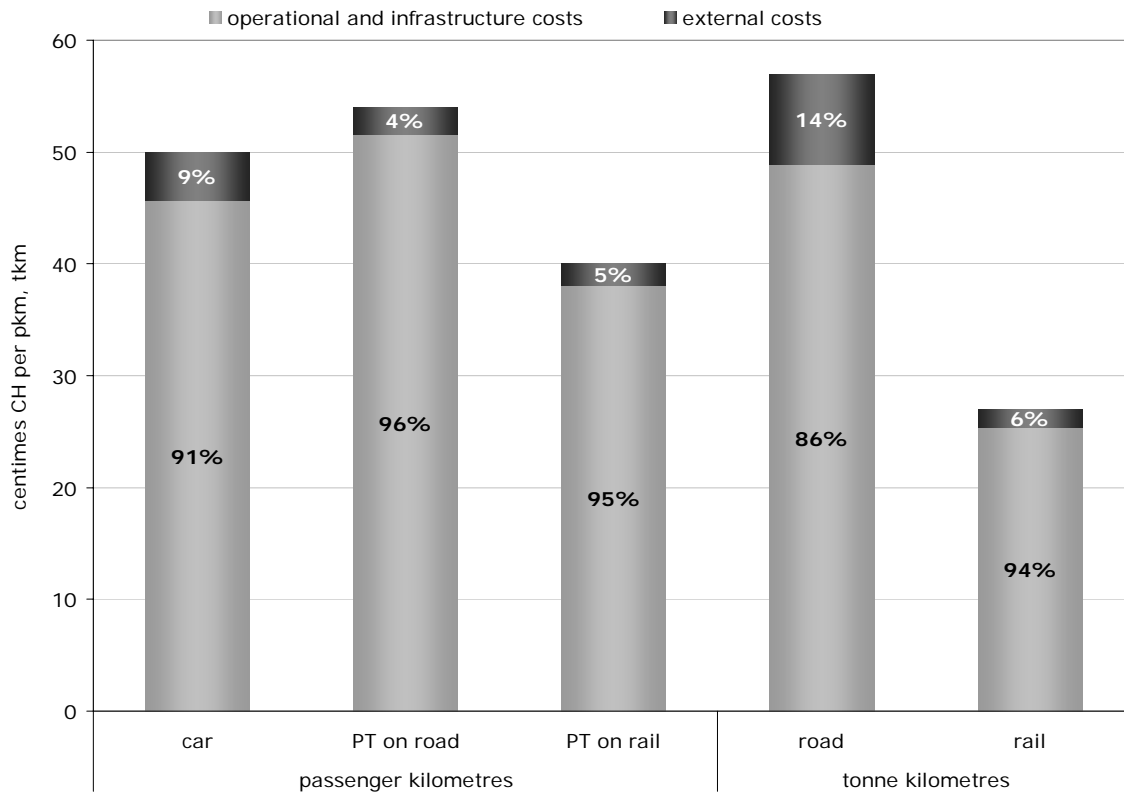


Figure 18. 1: Cost structure of the land transport sector in Switzerland in 2003 where pkm=person km and tkm=tonne km [Swiss Fed Statistical Office, ARE]

These external costs of transport should be considered more closely. The main challenges are to determine how to allocate these costs to the polluter and how to convert the damage caused by the emissions and pollutions in terms of costs. These allocated costs are intended to clarify to the causer, which damage proceeds from it and urge him to use more modern methods and technologies in order to avoid these costs and preserve the environment.

Noise

Noise is a significant nuisance and it impacts human health, nature and wildlife. Additional noise also decreases property prices. Railway noise is generally considered less annoying than road noise, so a 5 db(A) increase in level was allowed. The work group report predicts noise costs for the UK in 2005 (UNITE) as follows:

- passenger rail transport: 119 million €
- freight rail transport: 25 million €

The level of noise emanating from a road is regulated by the EU Directive 92/97/EEC. Private cars are not allowed to create more than 74 dB(A) and HGVs no more than 80 dB(A) at 7.5 m from the source. So it seems very easy to measure noise levels. But noise depends also on the road surface, type of tyres, speed of traffic, proportion of HGV's, weather and the presence of noise barriers. And these other problems or

influences are dependent on the respective situation. So, for instance, a fluttering canvas cover can cause high levels of noise and in connection with higher speed of traffic and stormy weather. So it is nearly impossible to determine real values of noise. But there is an approach from the University of Karlsruhe which tries to identify noise costs for different traffic situations.

MARGINAL NOISE COSTS FOR ROAD TRAFFIC IN DIFFERENT TRAFFIC SITUATIONS SCENARIOS ALREADY USED FOR THE INFRAS/IWW 2000 STUDY												
Scenarios			Marginal costs per vehicle kilometre					Marginal costs per pass. / tonne kilometre				
			Euro / 1000 vkm					Euro / 1000 pkm			Euro / 1000 tkm	
Area	Time	Traffic	Car	MC	Bus	LDV	HDV	Car	MC	Bus	LDV	HDV
Rural	Day	Thin	0.14	0.28	0.69	0.69	1.27	0.07	0.25	0.05	2.30	0.24
		Dense	0.06	0.13	0.32	0.32	0.58	0.03	0.11	0.02	1.05	0.11
	Night	Thin	0.25	0.50	1.26	1.26	2.31	0.13	0.45	0.08	4.19	0.44
		Dense	0.12	0.23	0.58	0.58	1.06	0.06	0.21	0.04	1.92	0.20
Sub-urban	Day	Thin	1.19	2.39	5.97	5.97	10.99	0.63	2.13	0.40	19.91	2.07
		Dense	0.43	0.86	2.14	2.14	3.94	0.23	0.77	0.14	7.14	0.74
	Night	Thin	2.18	4.35	10.88	10.88	20.01	1.14	3.88	0.73	36.26	3.78
		Dense	0.78	1.56	3.90	3.90	7.18	0.41	1.39	0.26	13.01	1.35
Urban	Day	Thin	18.49	36.98	92.45	92.45	170.11	13.21	33.02	4.62	308.18	32.10
		Dense	7.63	15.25	38.13	38.13	70.16	5.45	13.62	1.91	127.11	13.24
	Night	Thin	33.68	67.35	168.38	168.38	309.82	24.05	60.14	8.42	561.26	58.46
		Dense	13.89	27.78	69.45	69.45	127.79	9.92	24.80	3.47	231.50	24.11

Figure 18. 2: Noise costs for different traffic situations (UNITE)

In this approach the surrounding area, the daytime and the intensity of traffic is considered, but important influences like the conditions of the track and tyres, weather and speed of traffic are disregarded.

Additionally there are costs for loss of house rents, cost of health problems and medical treatment and immaterial costs for destroying natural habitats through noise.

Emissions and air pollution

Emissions can affect the health of local residents and damage nearby buildings and crops. Emissions from rail transport include those from burning diesel fuel and indirectly through electricity generation. The main emissions produced by burning fuel are:

- Carbon dioxide, CO₂
- Particulates less than 10mm in a diameter; PM₁₀
- Nitrogen oxides, NO_x

- Carbon Monoxide, CO
- Sulphur dioxide, SO₂
- Volatile organic compounds, VOCs

Rail environmental costs for air pollution for the UK 2005 (UNITE) are:

Passenger rail transport: 362 million €

Freight rail transport: 58 million €

The composition and quantity of exhaust emission from road transport depends on the type of fuel (diesel, petrol, alternative fuel), emissions category, vehicle weight or load on the engine and the average speed.

Air pollution costs were calculated by UNITE by emission estimation, dispersion and chemical conversion modelling, calculation of physical impacts and monetary valuation of these impacts. Costs included were from damage to building through acid rain, reduced crops yields and public health costs. Classification of vehicles by their type and age is a beginning of identifying main causers of pollution. But similar to noise there are additional factors which cannot be calculated because they are changing from situation to situation.

The Swiss study includes extensive calculations to identify the costs for human health, for damages of materials and buildings and the loss of crops and agricultural production.

Climate changes

The direct consequence of emissions and air pollution are the costs for climate changes. Because of emissions there is a change of local climate and a worldwide climate change too.

Climate change cost values were obtained by assigning costs to each tonne of carbon dioxide emitted. These costs were related to the average EU cost to meet the Kyoto agreement (20 €).

The approach of external costs of climate changes is based on avoidance and damage costs. Figure 18. 3 shows the connection between costs, damages, reduction of emissions and the global temperature.

The vertical representation shows that the higher the damage or the risk for the people the higher the costs of avoidance will be.

The horizontal representation shows that the reduction of atmospheric CO₂ and the increasing in global temperatures work opposite. That means, the lower the share of CO₂ in the atmosphere the less the global warming.

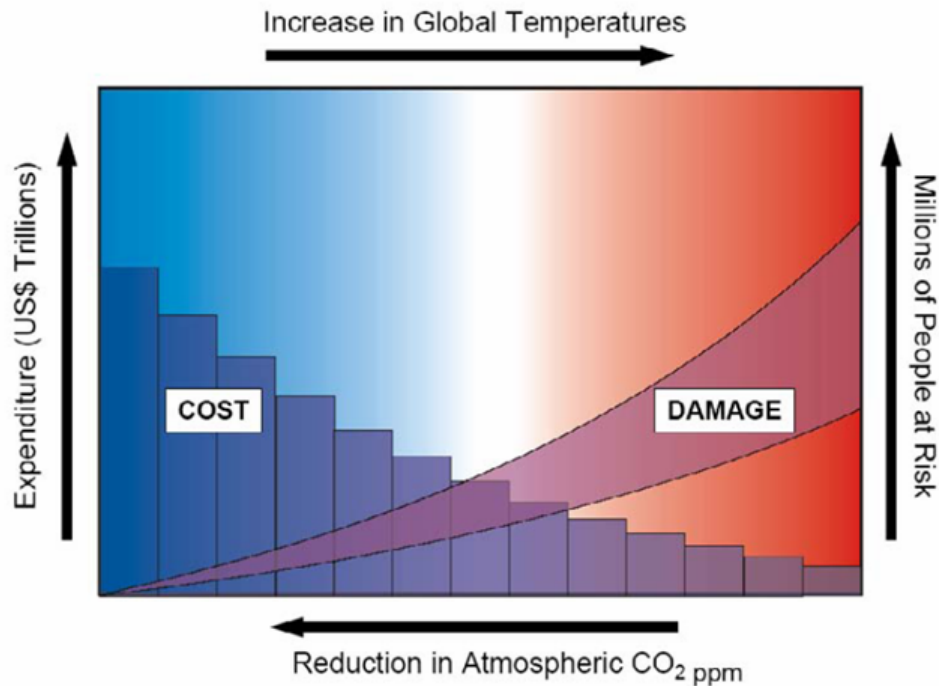


Figure 18. 3: schematic diagram of costs of climate changes (UNFCCC (<http://unfccc.int/>))

Nature and landscape

In addition to air pollution, the transport sector is also responsible for pollution of soil and water. This can be from fuel or oil leakages, de-icing agents and spillages. Road traffic is one of the largest sources of zinc, polynuclear aromatic hydrocarbons and lead. These pollutants are washed into nearby rivers and streams when precipitation occurs. The main contributors to road runoff pollution are combustion processes, the wear and tear of vehicles, roads and highway structures, winter maintenance and leaking of oil and fuel.

The costs caused by those different damage sources cannot be reliably calculated because it is very difficult to quantify them in relation to the individual polluter. And also the damages on nature and wildlife through barriers to species movement, habitat losses and fragmentation, severance of areas, incidental mortality on road and rail and artificial lightning cannot be reliably allocated..

Other external costs

The costs for congestion and for accidents are also very important costs of transport. But in the content of this report these costs are of less interest. Thus, there is only a short description.

Costs of congestion

These costs have an impact on human health and nature and wildlife because they are caused by additional fuel consumption, emissions and noise. The effects of the damages are described in the earlier chapters. But, additionally, there are also damages on the economic welfare because of time losses (higher travel times, less timetable slots) and higher vehicle operation time. Time (peak or non-peak), location (urban or rural) and type of vehicle are important factors. Costs arising from an inefficient use of the existing infrastructure and the evaluation are defined according to economic welfare theory. Costs are determined in terms of lost hours and vehicle, operational costs such as fuel consumption, value of time for a person-hour and per tonne of freight related to a country's GDP per capita.

Costs of accidents (accident follow-up costs)

Costs of accidents can be separated in direct costs for medical treatment and non-productive time and indirect costs, the accident follow-up costs.

A monetary estimation of resulting diseases and deaths is possible but not for physical and mental hurt (e.g. grief, fear) and loss of customers and/or turnover by delayed deliveries.

18.3. Summary

In Doran et al (2006) there is a comparison of the external costs of transport between Switzerland and the EU17 states. For the EU17 states the data are not so specific like the Swiss data. It is to be recognized that in the European comparison, Switzerland has lower costs per pkm / tkm as the other countries.

In Switzerland the passenger vehicles causes altogether external costs of approx. 2.7 Cents/pkm. The external health and accident costs as well as the climatic costs dominate. On the public road, passenger transport the health costs are relevant. In the rail transport sector however the noise costs as well as the costs within the costs of nature and landscape (cutting effects) dominate.

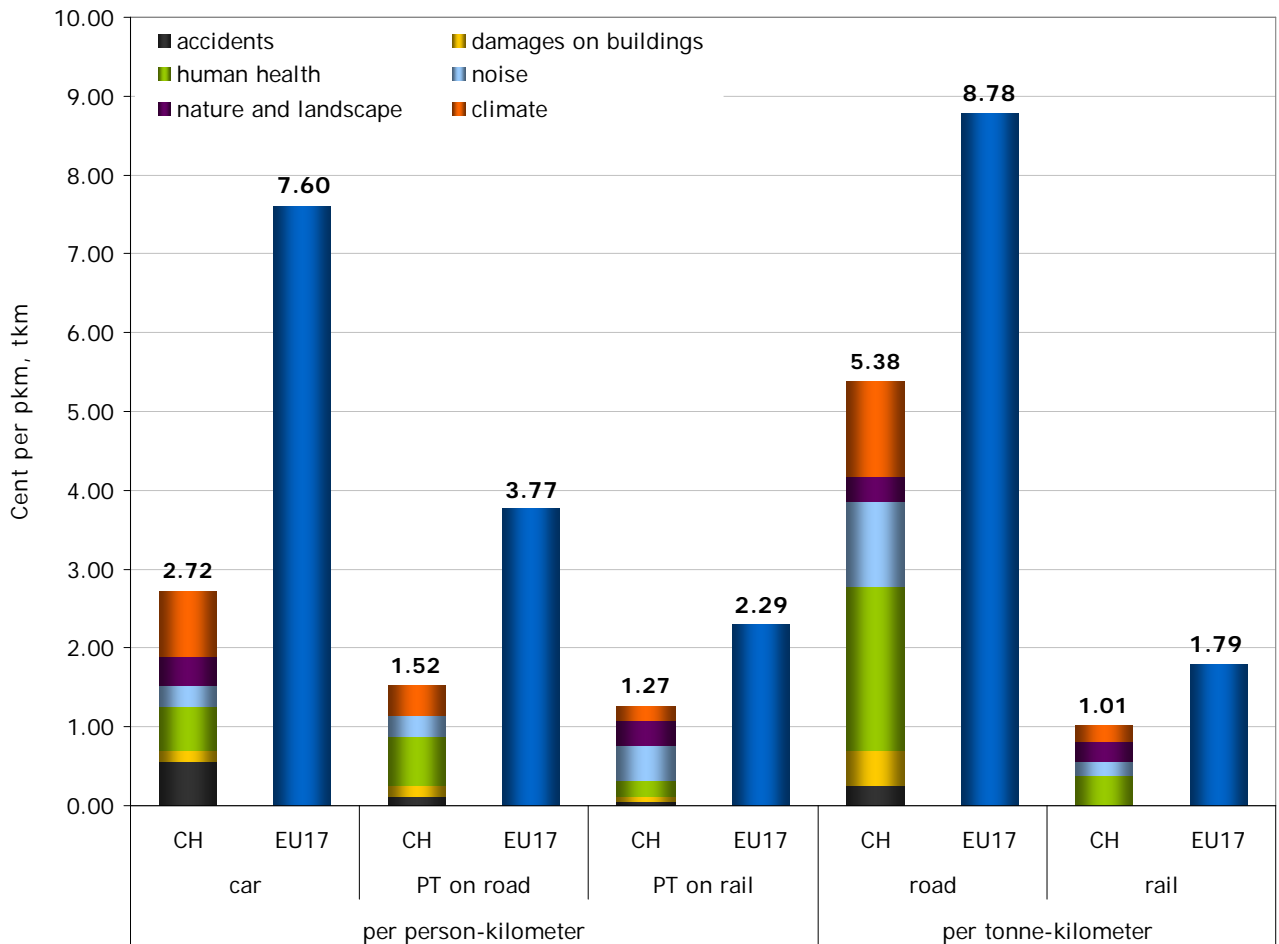


Figure 18. 4: External costs of transport in comparison between CH and the EU17 where PT=public transport (Doran et al 2005)

18.4. Different Charging Regimes in Europe

In this chapter some rail and road charging schemes of European countries are shortly described. (Doran et al 2005)

United Kingdom

Because of increasing difference between the costs and charges of rail transport a review of the rail network charging scheme is planned. This review includes incentives for transport operators to increase efficiency. But this will be delayed until April 2009. The existing charging system takes into account axle load, vehicle speed, unsprung mass and a vehicle type factor.

The planned launch date of the UK road charging scheme is in 2007/2008. Then, foreign lorries over 3.5 tonnes have to pay for using the infrastructure. The charge will be dependent on:

- weight

- distance travelled
- possibly type of road
- emissions category
- time of day.

National lorries would reclaim fuel duty, so would not be charged more than they are at present.

Germany

The German railway charging covers the operating costs but not the cost for renewing the network. Operators are charged per track-km depending on line category.

German lorry charging scheme was launched in 2005. The reasons are the contribution of lorries to infrastructure damage, fairer competition and reducing emissions. Charged are lorries over 12 tonnes. The important facts are kilometres on motorways, number of axles and emissions category.

Switzerland

The objective of charging the road transport was to encourage the use of rail to transport freight. Lorries over 3.5 tonnes have to pay for km over all roads, weight and emission category. Decreasing traffic volumes and distance driven by lorries were the results.

France

The French railway is heavily subsidised by the government. The infrastructure charges do not cover the maintenance of the track. The track charge is composed of a three part tariff:

- right of access charge covered by the operating company
- reservation charge
- operating charge
- the charging system takes account of the user's ability to pay i.e. charging more for more profitable routes.

Finland and Sweden

Finland and Sweden charge for environmental and accidental costs. They have non differentiation on the basis of vehicle characteristics. In Sweden the diesel charge is

0.036€ per litre for old passenger and freight vehicles and 0.018€ per litre for newer ones. The accident charge is 0.118 per train km for passenger transport and 0.059 per train km for freight transport.

In Finland, a supplementary charge for freight transport 0.19€ per tonne is levied.

Netherlands

Infrastructure charging was introduced in 2000 and 15% of costs were included and in 2005 100% of costs were included. The following types of charges are levied:

- variable charge per train-km
- charge per station stop to passenger trains

18.5. Conclusions

In this chapter the approaches regarding cost modelling in Switzerland (ARE; BAFU 2006) and the United Kingdom (Doran et al 2005) are compared and discussed.

The costs of transport were calculated depending upon the two studies with emphasis on the basis of accident statistics, pollutants and noise emissions as well as by means of aerial photo interpretation. With most modern technology the damage to environment and nature like forest dieback or melting glaciers and polar caps can be made visible. On the basis of these realisations, measuring methods and complicated calculations, the portion of external costs which are produced by transport are charged and allocated into costs. But where a direct collection of the costs is not possible, there is another approach. According to welfare theory, damages represent welfare losses for individuals. The evaluation of these external costs is only possible on the basis of the willingness-to-pay or willingness-to-accept approach that is based on individual preferences. And so all calculations are based on values and acceptance. But the actual external transport costs are clearly underestimated with the assigned methods. An improvement of potentials for evaluation schemes and a development of a basis with complete representation of the environmental costs of all transport modes are necessary. There is an urgent need for a weighting of all factors and an EU wide consensus on the method of calculating. Transparency, fairness and acceptance as important conditions ought to be considered.

The collected data are not to serve as additional taxation. They are to promote an environment-friendly and sustainable transport system.

19. POLICY OPTIONS

(Authors: Irène Schlachter, Philipp Jordi, Lily Poulikakos)

Various policy options are under discussion with other European partners in the project. The following is a summary extracted from project documentations [Doran et al, 2005, Mayer et al, 2007] and discussions.

The goal of the current project is in cooperation with other European partners and incorporating the results of measurements from the monitoring sites as well as modelling to identify policy options which are cost effective to reduce interaction at source and make direct comparison between road and rail transport modes. An important part is the identification of environmentally friendly vehicles and infrastructure and to produce European labels to identify vehicles and infrastructures as such.

Goal oriented policy options can aid in encouraging particular behaviour in transportation. For example to encourage a mode of transport, reduce contribution of lorries to infrastructure damage, encourage fairer competition and reduce emissions (air pollutants, noise, vibration). It can for example promote a more environmentally friendly transport as is the aim of the current project. To this end, allocation of costs induced by transport can be used through charging schemes. However as shown by Doran et al (2005) and in chapter 18 this is a complicated task. Once costs are identified, other important factors to be considered are ease of recovery of certain costs and ease of implementation. In general it is shown [Doran et al 2005] from consultation with industry and users that there is a clear preference for simplicity of charging regimes, even at the expense of greater accuracy. Furthermore, it is shown that in addition to simplicity, the charging regime has to be economic and practical to implement. In other words the charging scheme should not be more costly than the recovered costs.

The current charging schemes in Europe are inconsistent between the various modes of transport and between the various countries as shown in Chapter 18 and by Doran et al (2005). In Switzerland the current road charging scheme provides an example where distance travelled and pollution (only air pollutants, noise is missing) produced by the vehicle is used [Krebs, 2004]. However this is one of the few cases where costs are partially allocated to the users as external costs missing. Although as the title suggests this is a fair and efficient charging scheme but the methodology is not exactly advanced in identifying the actual costs preventing a 'true' bottom up allocation of effects of vehicles on infrastructure and environment.

Ultimately the goal is to try to influence behaviour in order to reduce environmental impact. User behaviour can be influenced for example by setting standards with rewards and penalties and feed measurements back to operators. A further example is that for environmentally friendly suspension a 6 axle truck could be allowed to carry 44 t instead of the 40t.

The project at the European level is still on going. Therefore no final results or consensus as such is available (status Jan 2007). However intermediate results can be summarized as follows [Doran et al, 2005]:

Although most European countries have charging regimes for rail and some have charging for road there is great diversity in how transport costs is calculated, which costs are passed onto the user and the method of charging. In order to harmonise infrastructure charging across Europe a consensus needs to be reached on these and allocation frameworks established. The decisions on what costs to charge for and how they are calculated need to be based on evidence and be transparent to the users.

There are common goals throughout Europe:

- Reducing congestion;
- Fair competition between countries and transport modes;
- Obtaining revenue to improve transport infrastructure;
- Incentivising more environmentally friendly (air pollutants, noise) transport.
- The fundamental principle of infrastructure charging is that the charge for using infrastructure must cover not only infrastructure costs, but also external costs, that is, costs connected with accidents, air pollution, noise and congestion.

[WHITE PAPER European Communities, 2001]

It has been concluded by many that **differential charging** can help achieve these goals. However in order to calculate costs fairly and accurately, details of the impact transport has on infrastructure, environment, health and society have to be known. These details may not be available either through lack of record keeping or insufficient scientific knowledge. In order to disaggregate costs so that they can be attributed countries will need to collect detailed records of maintenance and renewal expenditure, and costs due to accidents, congestion and pollution. Further research is required on the impact transport has on the wear and tear of infrastructure and on society and the environment. To this end the current operating Footprint Monitoring Sites on the road and rail provide vital data. None the less several examples of cost calculations for the major impacts of transport can be found in the literature. These may form a basis for cost allocation frameworks to be initiated. It should be noted that accuracy may sometimes need to be sacrificed for reasons of practicality and economics, but these decisions and the reasons behind them should be transparent to the users.

As a solution for the future of transport logistics solutions (e.g. combined transport) can be a solution. With all costs allocated transport can be in favour of roads. Furthermore, transport on rail is not possible to all places or does not make sense. It makes sense to combine good transports and have the final distribution as near as possible to the

customer.

The conclusions that can be drawn from this project so far are (status Jan 2007, Doran et al 2005):

- The need for a weighting of all factors (dynamic loading, noise, emissions, etc.) before arriving at a final index of vehicle 'footprints'.
- Lack of base data is a constraint that prevents the use of 'true' bottom up allocation of effects to vehicles and infrastructure. Additional Footprint Monitoring Sites are needed for a broad data base.
- A consensus within the EU needs to be reached on the method of calculating marginal costs and which costs are to be included in charges.
- Charging regimes vary across the EU and **harmonisation** is desirable in order to encourage fair competition between countries and transport modes.
- For acceptance of the charging regimes, **transparency** and **fairness** need to be demonstrated. Implementation must be practical and economic. Also a specific use for the money collected, such as improving infrastructure increases public acceptance.

20. SUMMARY, CONCLUSIONS AND OUTLOOK

This project in cooperation with partners from the European cooperative project, Eureka Logchain Footprint, proposes methods to measure the dynamic impact of heavy vehicles on the environment. To this end the input from the monitoring sites in Europe have been used to propose methods listed below to identify environmentally friendly vehicles. The complete set of “Guidelines for the Specification, Design and Data Analysis of Footprint Measuring Systems for both Road and Rail Vehicles” will be published separately [Mayer, 2007]. The Swiss contribution to the “Guidelines” is attached in the Appendix VI. It was shown that WIM technology alone is an important part but is not sufficient for identifying the effect of vehicles on the environment. When addressing issues such as intermodality, the overall effect of freight vehicles should be considered.

Using the results of weigh in motion (**WIM**) monitoring it was observed that the vast majority of the vehicles recorded on the A1 are considered to have environmentally friendly axle loads in accordance to existing criteria i.e < 10 tonnes.

The study focused on axle loads in excess of 10 tonnes. The number of axles exceeding the 10 tonne limit is less than 6% of the total number of axles recorded by the WIM during the period under investigation.

Maximum axle load, maximum gross vehicle weight (GVW), maximum vibration and maximum noise were recorded and compared. It was shown that the maximum of these parameters do not occur simultaneously; i.e. the noisiest vehicles are not the heaviest and vice versa. In the majority of road HGVs, axle loads on larger vehicles (i.e. high GVW) are within acceptable limits and therefore it was suggested that GVW should not be used as an environmental friendliness (EF) criterion on roads. However it is important for bridges and road design.

Results with the stress in motion (**SIM**) sensor show the sensor being a promising tool for pavement designers. These results also show that a significant difference in contact pressure distribution under the Tyre can be seen for over/under inflated Tyres which should be used in pavement design. Furthermore the axle load alone is not an indication of pavement friendliness rather as shown the load distribution can have a significant effect on the strains produced in the pavement using the finite element model.

The process of matching **data** currently still requires considerable work and time. A way of automating the process further is required if data over longer periods needs to be efficiently matched. An alternative to improving the methods of matching the WIM and Empa clocks might be to ensure that the WIM and Empa data acquisition system use the same clock in future. This would eliminate almost all errors due to matching, which would significantly improve the accuracy and reliability of the data and is being

considered in a follow up project.

From a visual inspection of the recorded stress distributions, Tyres which are over/under-inflated, Tyres which are faster/slower than normal and Tyres crossing the sensor at an angle can be clearly identified. None of these parameters appear to have a significant effect on the wheel load (except velocity, which is accounted for).

Stress distributions can be determined to be from over/under-inflated Tyres by examination of the shape of the contact pressure distribution and whether it has one peak ('n'-shaped) or two peaks ('m'-shaped). Further work should be undertaken to create a formal classification, which could allow the 'n' or 'm'-ness of a distribution to be determined objectively. An attempt could be made to relate this to the ratio of load to Tyre pressure. Static measurements have shown that a high percentage of truck Tyres are either over-pumped or under-pumped. Stress in motion measurements using Modulas have been useful in characterising contact pressure on the pavement however improvements need to be made with regard to resolution and durability of the sensor as well as placement on the pavement.

The **acoustical** footprint of a vehicle passing by can be determined by evaluating the maximum sound pressure level received at a microphone in a distance of 7.5 m from the centre of the traffic lane. The validity of the measurement is checked by the 6 dB-down criterion. If this criterion is not fulfilled the interference stemming from neighbour vehicles is estimated and compensated for based on the level time history. A maximum correction of 6 dB(A) is allowed and If a higher correction was deemed necessary from the calculations, the measurement was categorised as invalid. Current data from the road Footprint Monitoring Site indicates that this procedure led to an increase of the percentage of pass-by events that could be evaluated successfully in the order of 95%. This result is for roads with dense traffic and an improvement can be expected for traffic that is less dense.

Ground borne **vibration** levels obtained during the measuring campaign at the FMS are not absolute as they depend on variables such as the road roughness, soil type, environmental conditions, etc. It is possible to make comparisons between vibrations produced by vehicles at this site as long as measurements are taken under the same conditions. Nevertheless, a simple comparison to reference values show that the measured vibration is low compared to the human perception threshold.

In order to improve future vibration measurement sites and to be able to compare vibration measurements made at other locations, it is helpful to obtain more information and standardise the physical characteristics of the site where the measurements are carried out, i.e. measuring roughness, soil characteristics, etc. Vibration models could be constructed and correction factors between measuring sites can be used to compare results.

Within the European framework of the project environmental friendliness (EF) thresholds have been suggested and are under discussion.

It has been concluded that **differential charging** can help achieve “true” bottom up allocation of effects of vehicles on the infrastructure and environment. However in order to calculate costs fairly and accurately, details of the impact transport has on infrastructure, environment, health and society have to be known. In order to disaggregate costs so that they can be attributed, countries will need to collect detailed records of maintenance and renewal expenditure, and costs due to accidents, congestion and pollution. Further research is required on the impact transport has on the wear and tear of infrastructure and on society and the environment. To this end the current operating Footprint Monitoring Sites on the road and rail provide vital data. None the less several examples of cost calculations for the major impacts of transport can be found in the literature. These may form a basis for cost allocation frameworks to be initiated. It should be noted that accuracy may sometimes need to be sacrificed for reasons of practicality and economics, but these decisions and the reasons behind them should be transparent to the users.

21. ACKNOWLEDGEMENTS

This project has been possible by the financial support of the Swiss Commission for Technology and Innovation (CTI), Swiss Federal Roads Authority (FEDRO/ ASTRA), Swiss Federal Office for the Environment (FOEN/ BAFU) and Empa and material support of Kistler Instruments AG, Switzerland and SIKA AG, Switzerland. The authors would like to thank Rayner Mayer, Eureka Logchain Footprint's project coordinator and Peter Richner of Empa for their continuous support and encouragement. Roger Siegrist, Partic Jegge, Mario Rubin and Roland Aellen of ASTRA, Robert Attinger of BAV for providing important information and support for the project. Additionally Simon Kuentzel, Hans Kienast, Markus Erb, Stephan Meier, Willy Knecht and Roland Takacs, are thanked for their contributions during installation of the sensors and laboratory experiments. For the German and French translations we thank Michèle Koehli and Jean-Pierre Emery. The project has been enriched by our continuous interaction with our European colleagues and we thank them for their contributions.

22. REFERENCES

- ABAQUS Documentation: Version 6.5; ABAQUS Inc. (2004)
- Addis, R et al.: COST 334(2001): Effects of Wide Single Tyres and Dual Tyres; EC. Brussels
- Al-Hunaidi, M. O. (2000). "Traffic vibrations in buildings." Construction Technology Update.
- Al-Hunaidi, M. O. and J. H. Rainer (1990). Evaluation of Measurement Limits of Transducer Mountings in the Ground, National Research Council Canada, Institute for Research in Construction.
- Al-Hunaidi, M. O., J. H. Rainer, et al. (1993). "PC-Based measurement and analysis of traffic vibrations."
- Anderegg, P., Brönnimann, R., Raab, C., Partl, M.N. (2002). „Long Term Monitoring of Pavement Deformations on an Expressway“, Proceedings of the 3rd International Measurements Conference, IMEKU, Celle, Germany, 23-27.
- ARE, BAFU (2006). „Externe Kosten des Strassen- und Schienenverkehrs 2000“, Bundesamt für Raumentwicklung (ARE), Bundesamt für Umwelt (BAFU), Bern, 2006
- Arraigada, M.; Partl M. N.; Angelone S. M. (2007): Determination of Road Deflections from Traffic Induced Accelerations; International Journal of Road Materials and Pavement Design (in press)
- Attinger, R. (2006). Private correspondence.
- Bukowiecki, N., Gehrig, R., Hill, M., Lienemann, P., Zwicky, C., Buchmann, B., Weingartner, E. and Baltensperger, U. (2006). Iron, manganese and copper emitted by cargo and passenger trains in Zürich (Switzerland): Size-segregated mass concentrations in ambient air. Atmospheric Environment (in press).
- Bukowiecki, N., Hill, M., Gehrig, R., Zwicky, C. N., Lienemann, P., Hegedus, F., Falkenberg, G., Weingartner, E. and Baltensperger, U. (2005). Trace metals in ambient air: Hourly size-segregated mass concentrations determined by Synchrotron-XRF. Environ. Sci. Technol. 39(15): 5754-5762.
- COST 323 (1999), European Specification on Weigh-in-Motion of Road Vehicles, EUCO-COST/323/8/99, LCPC, Paris, August, 66 pp.
- De Beer, M. (2006). "Reconsideration of tyre-pavement input parameters for the structural design of flexible pavements" Proc. 10th International Conference on Asphalt Pavements, Quebec, Canada.

De Beer, M., Kannemeyer, L., Fischer, C. (1999). "Towards improved mechanistic design of thin asphalt layer surfaces based on actual tyre/pavement contact stress-in-motion (SIM) data in South Africa, 7th Conference on asphalt pavements for Southern Africa, CAPSA '99.

De Beer, M., Kannemeyer, L., Fischer, C., (1999) Towards improved mechanistic design of thin asphalt layer surfaces based on actual tyre/pavement contact stress-in-motion (SIM) data in South Africa, 7th Conference on asphalt pavements for Southern Africa, CAPSA '99.

Doran, P, Ramda, V. draft report of cost modelling sub-group to footprint partners "The Attribution of Infrastructure Costs to Vehicles",2005.

Doupal, E., Gysi, M. (2002a). "Measurement of Dynamic Wheel Load Distributions, Proceedings of NATMEC - ICWIM-3 Congress, Orlando, FL, USA.

E. Doupal, M. Gysi Measurement of Dynamic Wheel Load Distributions, Proceedings of NATMEC 2002 - ICWIM-3 Congress, Orlando, FL, USA May 13-15,2002.

E. Doupal, R. Calderara, R. Jagau Measuring of Dynamic Wheel Loads, 9th International Conference on Asphalt Pavements, Copenhagen, Denmark, August 2002.

E. Doupal, R. Calderara, R. Jagau, (2002b). "Measuring of Dynamic Wheel Loads", 9th Internat. Conference on Asphalt Pavements, Copenhagen, Denmark.

EN ISO 11819-1 (1997): Acoustics - Measurement of the influence of road surfaces on traffic noise - Part 1: Statistical Pass-By method.

Epps, A. L., Ahmed, T., Little, D., Mikhail, M. Y., Hugo, F. (2001a). "Performance Assessment with the MMLS3 at the WesTrack", Journal of the Association of Asphalt Paving Technologists, AAPT Vol 70.

Epps, A.L., Ahmed, T., Little, D.C. and Hugo, F. (2001b). "Performance prediction with the MMLS3 at WesTrack". Report Number 2134-1. Texas Transportation Institute. The Texas A & M University.

Epps, A.L., Hugo, F., Walubita, L.F. and Bangera, N. (2001c). "Comparing Pavement Response and Rutting Performance for Full-Scale and One-Third Scale Accelerated Pavement Testing". 80th Annual Meeting of the Transportation Research Board, 7-11 January, Washington, D.C.

European cooperative project ARTEMIS on emission models

European cooperative project Eureka Logchain Footprint, homepage, www.Eureka.be, Project Number E!2486.

European Cooperative Project OECD IR 6 DEVINE, Dynamic interaction between vehicles and infrastructure experiment. 26-Oct-1998.

European Noise Directive (END); 2002/49/EC, <http://www.imagine-project.org/bestanden/2002-49-EC.pdf>

Eurovignette Directive for Taxation of heavy goods vehicles, Directive 1999/62/EC of the European Parliament and of the Council of 17 June 1999 on the charging of heavy goods vehicles for the use of certain infrastructures.

Externe Kosten des Strassen- und Schienenverkehrs 2000, Bundesamt für Raumentwicklung (ARE), Bundesamt für Umwelt (BAFU), Bern, 2006

Ford, T. L., and Yap, P. "Truck Tire/Pavement Interface". Technical Papers Vol. II, XXIII FISITA Congress, Torino, Italy, 1990.

Gehrig, R., Comparison of various sources of PM10. Information compiled from Federal office for the environment (BAFU) data. 2007.

Gehrig, R., Hill, M., Lienemann, P., Zwicky, C., Bukowiecki, N., Weingartner, E., Baltensperger, U. and Buchmann, B. (2006). Contribution of railway traffic to local PM10 concentrations in Switzerland. Atmos-pheric Environment (submitted for publication).

Gubler, R., Küntzel, S., Partl, M.N., Comparison of Rutting Behavior on Test Sections and Circular Test Track Using a Model Mobile Load Simulator. 1st Int. Symp. on Design and Construction of Long Lasting Asphalt. ISAP, Auburn 7-9Juni 2004.

Hajek, J. J., Blaney, C. T., et al. (2005). Highway Traffic Induced Vibrations. Transportation Research Record. Washington, DC, National Academy Press; 1998.

Hanson, C., H. Saurenman, et al. (1995). Transit Noise and Vibration Impact Assessment, Final Report. Prepared by Harris Miller Miller & Hanson, Inc. for the US Department of Transportation, Federal Transit Administration, DOT-T-95-16, April 1995.

Hendriks, R. (1996). Transportation Related Earthborne Vibrations (Caltrans Experiences).

Home page of the European cooperative projects Eureka, [www. Eureka.be](http://www.Eureka.be), Project Number E!2486.

<http://www.aren.admin.ch/aren/de/verkehr/monatsinfo/>

<http://www.kistler.com>

http://www.umweltschweiz.ch/buwal/de/fachgebiete/fg_ubeobacht/rubrik3/mfm

Hueglin, C., Buchmann, B. and Weber, R. O. (2006). Long-term observation of real-world road traffic emission factors on a motorway in Switzerland. *Atmos. Environ.* 40(20): 3696-3709.

Hugo F. and Epps Martin F (2004). "Significant Findings from the Full-Scale Accelerated Pavement Testing. Synthesis 325", Transportation Research Board, National Research Council, Washington DC.

Hugo, F., (2000). "Rutting Performance of Dustrol Rehabilitation under TxMLS Trafficking with Increasing Tire Pressure", Texas DOT, Report No. 1814-4.

INFRAS (2004). University of Karlsruhe, "External costs of Transport", INFRAS / IWW, October 2004.

Junker, J. P.; Fritz, H. W.; Partl, M. N. (1993): „Bestimmung mechanischer Materialkennwerte an bituminösen Baustoffen“; Eidgenössisches Verkehrs und Energiewirtschaftsdepartement, Bundesamt für Strassen (ASTRA), Report no. 270

Kalidova, M. (2006). Presentation at the Eureka Logchain Footprint Project meeting, Brussels November.

Kim S.M., Hugo F. and Roeset J.M. (1998). "Small-Scale Accelerated Pavement Testing", *Journal of Transportation Engineering*, ASCE, Vol. 124, No.2, pp. 117-122.

Kim, O., Bell, C.A., and Wilson, J.E., (1989). "Effect of Increased Truck Tire Pressure on Asphalt Concrete Pavements." *J. Trans. Engrg.*, ASCE, 115(4), 329-350.

Kistler Catalogue, "Measurement of Wheel Load Distribution with MODULAS Sensor Type 9197" 53.609e-08.00.

Krebs, P. "Fair and Efficient", The distance related Heavy Vehicle Fee (HVF), www.bbl.admin.ch/bundespublikationen, Form 812.004.1.e. Also available in German and French.

Krohn, C. E. (1984). " Geophone Ground Coupling." *Geophysics* publ. by the Society of Exploration Geophysicists.

Lam, Man Ho (2005): Finite Element Modelling of Vehicle-Road Interaction with ABAQUS and Python; EMPA Internship Report

Lees, A. (2006). "UK participation in Eureka Logchain Footprint Σ! 2486 November 2006", presentation, Statistics Roads,DfT, UK.

Machemehl, R.B., Wang, F., Prozzi, J.A. (2005). "Analytical Study of Effects of Truck Tire Pressure on Pavements Using Measured Tire-Pavement Contact Stress Data", *Proc. Transportation Research Board Annual Meeting*.

Mastrangelo, R. (2005) WIM-Vergleichsmessung, Anlage Schafisheim, Bericht Nr. 437369/07, Datum 18./19. Oktober 2005.

Mastrangelo, R. (2006), WIM-Vergleichsmessung, Anlage Schafisheim, Bericht-Nr. 441165/05, Datum 12./13. Juli 2006.

Mayer, R., Poulikakos, L., Heutschi, K., Anderegg, P., Arraigada, M., Van der Brink, J., Lees, A., Partl, M. (2007). "Guidelines for the specification, design and data analysis of Footprint measuring systems to characterise the environmental footprint of vehicles" (in print)

MLS Test Systems (2002). MMLS3 Traffic Simulator Operator's Manual, MLS Test Systems, April.*

Moor, A.H.K. (2003). Footprint Rail measurement System Specifications of the Fiber optic based Measurements Station for train Weight and Dynamic Axle Load, Document Nr. 51661D003b Baas Engineering.

Morgan, G.C. (2006). "Investigating the effects of the Contact Pressure Distribution of heavily Loaded tires using the Modulas Sensor Array". Internship Report.

Moser, K. (2005) Design of concrete element for in situ installation of the Modulas sensor. Empa report No. 203 894.135

Ohry, B. (2005) "Swiss Heavy Vehicles Fee LSVA Policy, Technology, Effects" Presentation at Eureka Logchain Footprint project meeting, Brussels.

Owende, M.O., Hartman, A. M., Ward, S.M., Gilchrist, M.D., O'Mahony, M.J. (2001). "Minimizing Distress on flexible pavements using variable tire pressure". J. Trans. Engrg., ASCE.

Partl, M.N., Hean, S. and Poulikakos, L. (2002). "Asphaltic Plug Joint Characterization and Performance Evaluation". Proc. Ninth International Conference on Asphalt Pavements Copenhagen.

Poulikakos, L., Heutschi, K., Anderegg, P., Calderara, R., Doupal, E., Siegrist, R., Partl M.N (2005). "Determination of the Environmental Footprint of Freight Vehicles", Proc. 4th Int. Conference on Weigh-in-Motion ICWIM4, Taipei, Taiwan.

Raab, C., Partl, M. N., (2005), Monitoring Traffic Loads and Pavement Deformations on a Swiss Motorway, Paper submitted for 4th International Conference on Weigh-in-Motion ICWIM4, Taipei, Taiwan. 20-22 February.

Raab, C., Partl, M.N., Jenkins, K., Hugo, F. (2005). "Determination of Rutting and Water Susceptibility of Selected Pavement Materials using MMLS3". Proc. 7th Int. Conference on the Bearing Capacity of Roads, Railways and Airfields, BCRA'05,



Trondheim.

REORIENT Further Info: www.reorient.org.uk

Rix, G. J. "Civil Engineering Vibrations." from http://courses.ce.gatech.edu/200202/CEE6442A/Course_Notes/Vibration%20Criteria.pdf.

Siskind, D. E., M. S. Stagg, et al. (1980). Structure Response and Damage Produced by Ground Vibration from Surface Mine Blasting, United States Dept. of the Interior, Bureau of Mines.

Sokolov, K., Gubler, R., Partl, M.N. (2005). "Extended Numerical Modeling and Application of the Coaxial Shear Test for Asphalt Pavements", J. of Materials & Structures Nr 279, pp 515...522.

Sutter, D. , Rapp, M. et al.(2006). Road Pricing Schemes for Motorways and urban areas in Switzerland. SVI 2001/523.

Swiss allowable gross vehicle weights and axle loads: http://www.admin.ch/ch/d/sr/741_11/a67.html

TSI, 2005. Technical Specifications for Interoperability (EC/2005/C5666)

UNFCCC (<http://unfccc.int/>)

University of Leeds, UNITE, <http://www.its.leeds.ac.uk/projects/unite/>


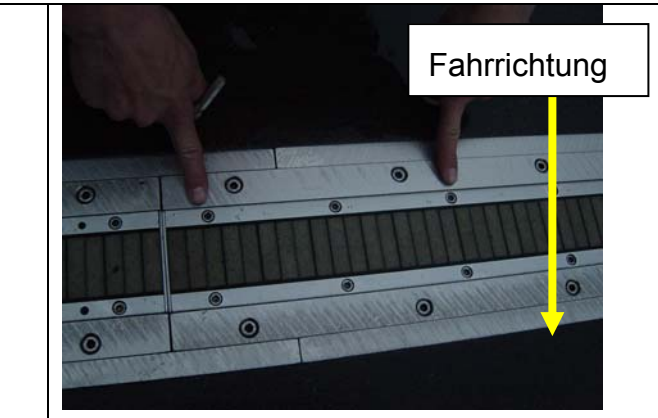


Whiffen A. C., L. D. R. (1971). "A Survey of Traffic Induced Vibrations." Transport and Road Research Laboratory, RRL Report LR418. Crowthorne, Berkshire, England.

Appendix I: Visuelle Beurteilung der Footprint-Messstelle (Visual inspection of the FMS)

Datum, Zeit: 27.04.2006, 20:00-21:00

Anwesend: M. Arraigada, S. Kuentzel, L. Poulikakos

Kurze Zusammenfassung von L. Poulikakos

	
<p>1. Lineas Sensoren: keine Schäden</p>	<p>2. Modulas: Zwei Schrauben wurden befestigt Beton Ausbruch in zwei Positionen ca. 1-2cm</p>
	
<p>3a. Deformationssensoren Klebstoff auf der Oberfläche der zwei Sensoren sind teilweise weg Grosse Fugen- keine Schaden</p>	<p>3b. Deformationssensoren Kleine Fugen sind teilweise los gekommen und damit teile des Asphaltbetons ca. 2cm x7cm Zustand nicht gefährlich aber muss bei Installation der Beschleunigungssensor repariert werden</p>



4. **Feuchtigkeitssensoren:** Fugen In Ordnung



5. **Beschleunigungssensor- Geophone**
keine Schäden - Sensor war mit einen neuen ersetzt



6. **Schacht 1:** Kein Wasser keine Schäden



7. **Schacht 2:** Kein Wasser keine Schäden



8. **Elektroschrank:** Kein Wasser keine Schäden

Appendix II: SANITY TEST MODULAS SENSOREN (6.6.2006)

Author: Emil Doupal

Zwei MODULAS-Sensoren 9197A5 mit zwei 32-Kanal-LV 5151A111 sind seit Juni 2005 auf der Autobahn A1 bei Lenzburg erfolgreich im Betrieb. Sie sind ein wichtiger Bestandteil der Forschungsanlage, welche auch Fahrbahndeformations-, Vibrations-, Temperatur- und Akustiksensoren umfasst.

Mit MODULAS wird 64-kanalig die Kraft- und Druckverteilung unter den rollenden Lastwagenreifen gemessen und mit Daten der obengenannten Sensoren korreliert. Diese Messungen werden auch synchronisiert mit den Verkehrsdaten, welche mit der benachbarten WIM-Anlage des ASTRA (32 Lineas-Sensoren auf 4 Fahrspuren) erfasst werden.

Eine Routine Überprüfung der Footprint Messtelle nach der Winterperiode 2005-06 wurde durch die EMPA Mitarbeiter durchgeführt.

- Optischen Zustand des Modulas und der Belagsübergänge ringsherum photographisch dokumentieren. Dies kann ev. OHNE STRASSENSPERRE bei streifendem Sonnenlicht und Teleobjektiv durchgeführt werden.
- Beobachten der Ebenheit und allfälliger Relativbewegungen.
- So könnten zB. Risse, lose Schrauben oder Vergussteile auch ohne Strassensperre gefunden werden.

Eine Routine Überprüfung der Modulas Sensoren auf Ihre Zuverlässigkeit nach der Winterperiode 2005-06 wurde durchgeführt.

"Sanity test" anhand der Modulas-Resultate-Files. Wie anlässlich der Sitzung bei EMPA vorgeschlagen, bei einer grösseren Anzahl Überfahrten die Einzelkanaldaten wurden summiert, um festzustellen, ob die Empfindlichkeiten aller Modulaskanäle auf einen logischen Durchschnitt kommt, oder ob einzelne Kanäle systematisch tiefere Signale liefern.

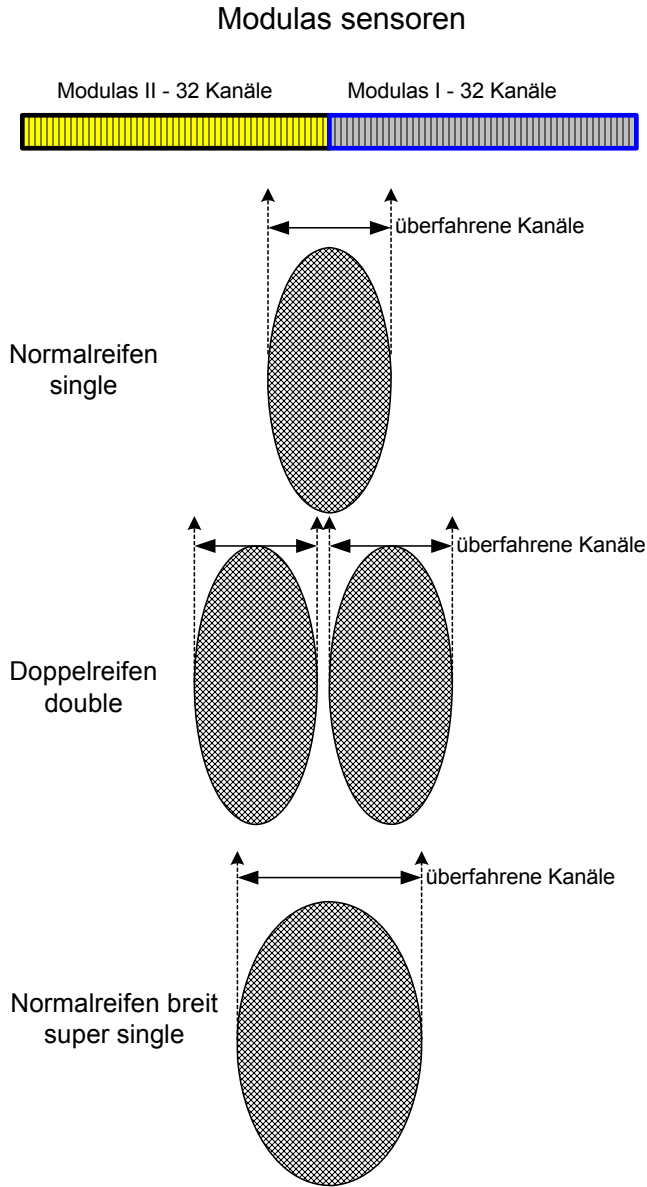
In zweitem Schritt wurden die repräsentativen Messdaten der einzelnen Kanäle untersucht und die Kanalfunktion überprüft, um festzustellen, ob alle 64 Messkanäle die logischen Signale liefern können.

Resultat

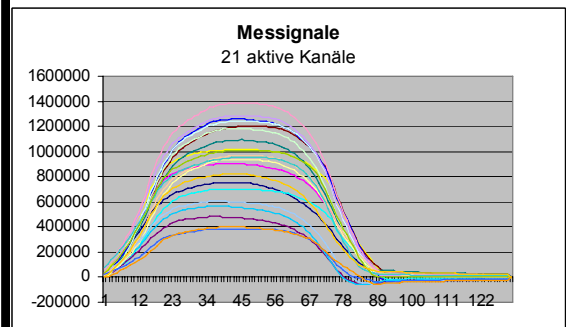
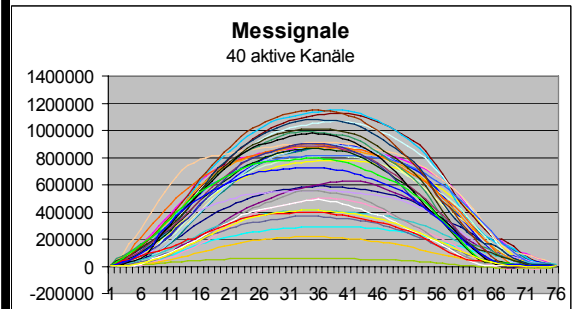
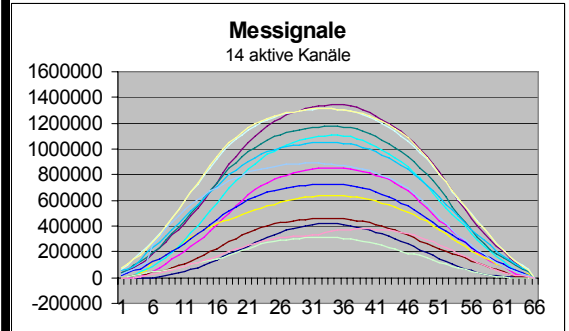
Trotz diesjährigen harten Winterbedingungen mit teilweise sehr tiefen Temperaturen und sehr starkem Einsatz des Salzes für Winterdienst, haben die beiden Modulas Sensoren die Winterperiode gut überstanden.

- Alle 64 Messkanäle der beiden Modulas Sensoren sind aktiv.
- Die Kanäle zeigen keinerlei systematischen Abweichungen der Messdaten an.

Übersicht der typischen Messresultate - Footprint



Beispiele der Messdaten



Zusammenfassung der durchgeführten Arbeiten

- Die Installation der Footprint-Messanlage auf der A1 Schafisheim und die Kalibrierung aller Komponenten sind sehr erfolgreich verlaufen, alle Systeme arbeiten einwandfrei.
- Die vollautomatische Messanlage liefert uns eine enorme Menge von Verkehrsdaten (alle Fahrzeuge mit Gesamtgewicht >3.5t). Diese Daten werden online reduziert und für die weitere Bearbeitung werden nur Messungen mit schweren Lastwagen ausgewählt.
- Empa hat inzwischen ein numerisches Modell zusammengestellt. Randbedingungen wie Geometrie, Materialimplementierung, Parametrisierung, Belastung, Kontakteigenschaften werden in Modell mitberücksichtigt.
- Die Kalibrierfahrten mit den 2 Referenzfahrzeugen bilden eine Basis von experimentellen Resultaten, mit deren Hilfe das numerische Model verifiziert wird. Gleichzeitig wird an der Analyse des Kontakt- respektive Pneudruckes gearbeitet.

Für das Jahr 2006 sind die folgenden Schritte zu überlegen

- Kalibrierung mit weiteren Pneutypen: Super-single und kleine LW-Pneus mit hohem Druck und kleiner Latschfläche
- Verifizierung des numerischen Modells
- Voraussage des mechanischen Verhaltens durch numerische Simulation

Ausblick

- Die gemeinsamen Projektbesprechungen bei Empa (ASTRA, BUVAL, KISTLER, RTS) sind wertvoll für die stets sehr gute Zusammenarbeit des gesamten KTI-Teams.
- Die Präsentation des Footprint Projektes an der Internationalen WIM Konferenz (Taipei, Februar 2005), weckte grosses Interesse bei den Fachleuten aus ganzen Welt.
- Wenn dieses Projekt erfolgreich abgeschlossen wird, können die Resultate eine sehr wichtige Rolle für den Bereich Strassen-Dimensionierung spielen.

Appendix III : Swiss 10 Vehicle Classification

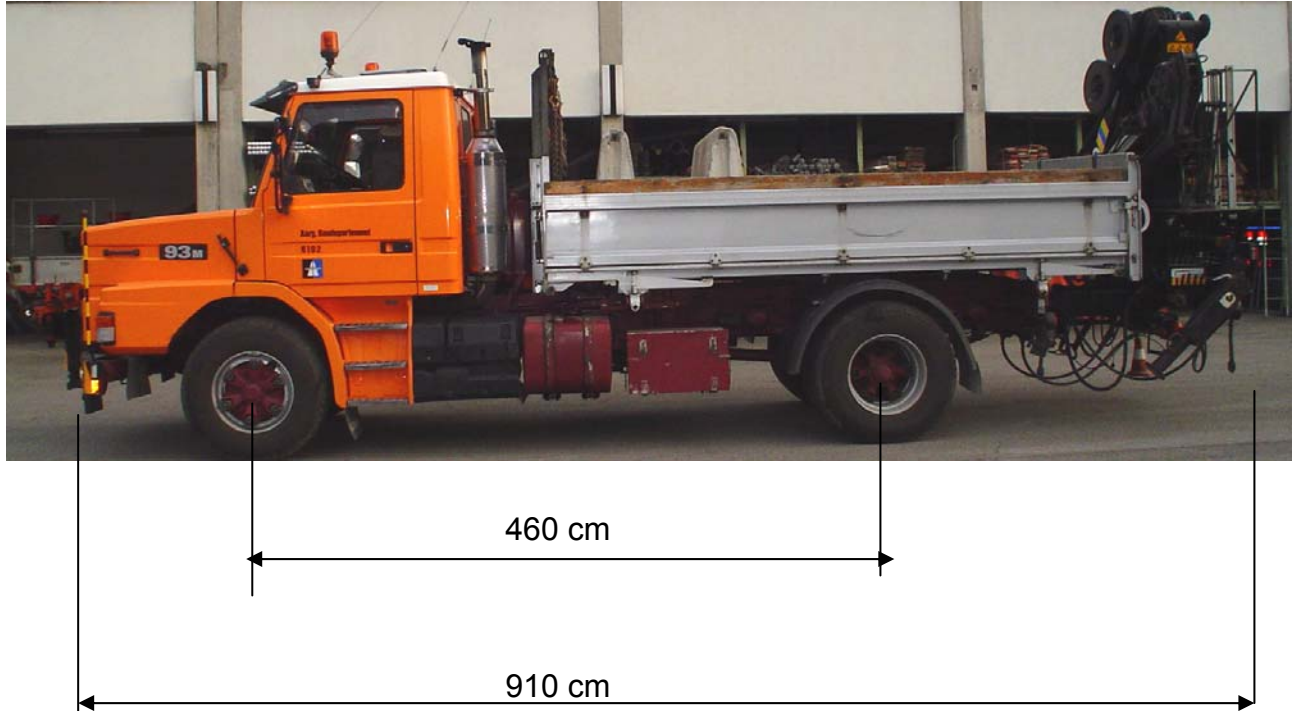
Klassifizierung nach Swiss 10 Schema					
1	Bus		8	Lastwagen	
2	Motorräder		9	Lastenzüge	
3	Personenwagen				
4	Personenwagen + Anhänger				
5	Lieferwagen				
6	Lieferwagen + Anhänger				
7	Lieferwagen + Auflieger		10	Sattelzüge	

Appendix IV : Vehicle Information used for Validation Passes

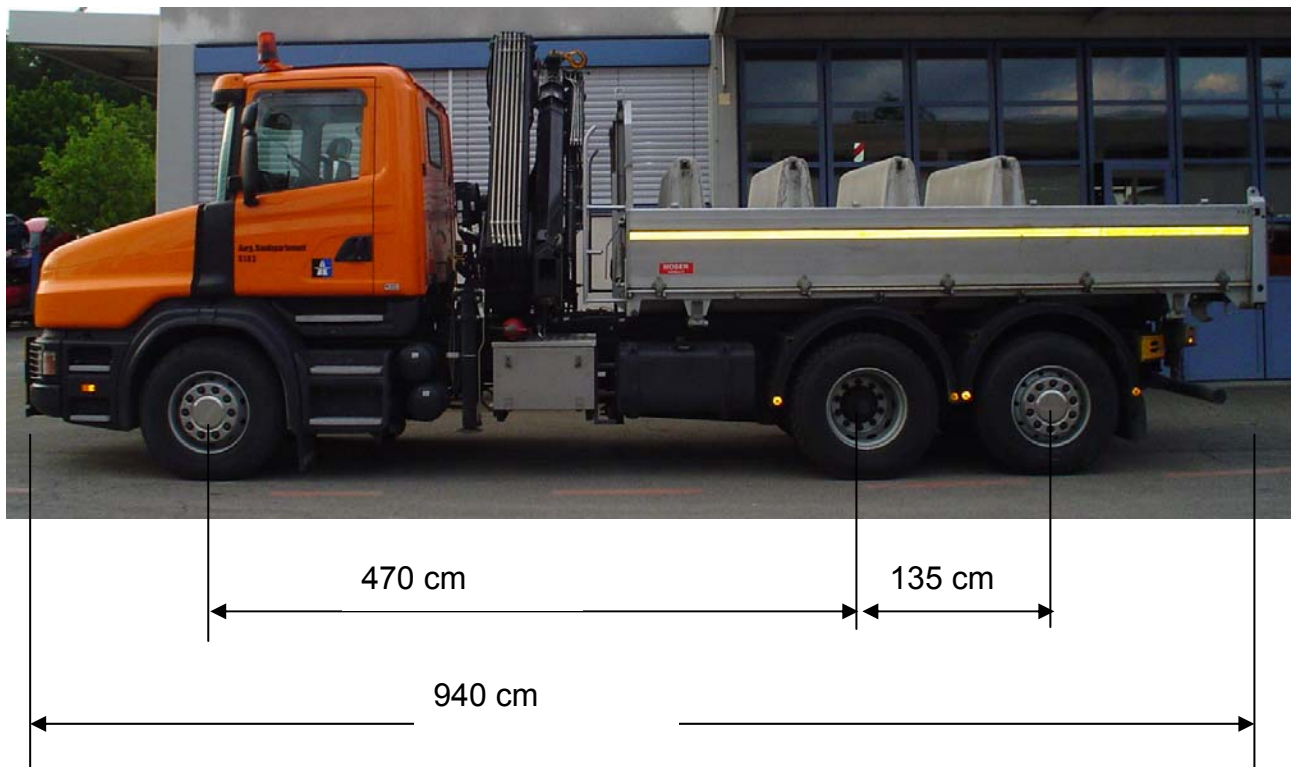
Date: 30.06.2005

Prepared by: Lily Poulikakos

Vehicle 6102



Vehicle 6103





Vehicle 6102								
Total Weight =14550 kg								
	Type	Weight [kg]		Type	Weight [kg]		Type	Weight [kg]
Front Axle	Single tires	4250	Middle Axle	-	-	Rear Axle	Double tires	10300
Tire, Front left	Pirelli AP05 315/80 R 22.5 155/150K	1900		-	-	Tire, Rear Left	Pirelli WT30 12R 22.5 152/148L	4750
Tire, Front Right	Pirelli AP05 315/80 R 22.5 155/150K	2350		-	-	Tire, Rear Right	Pirelli WT30 12R 22.5 152/148L	5550
Vehicle 6103								
Total Weight= 21300 kg								
	Type	Weight [kg]		Type	Weight [kg]		Type	Weight [kg]
Front Axle	Single tires	8050	Middle Axle	Double tires	8400	Rear Axle	Single tires	4850
Tire, Front left	MichelinX XZY 385/65R 22.5	3850	Tire, Middle Left	MichelinX E22.5 Pilote XDY 154/150M	3900	Tire, Rear Left	MichelinX XZY 385/65R 22.5	2300
Tire, Front Right	MichelinX XYZ 385/65R 22.5	4200	Tire, Middle Left	MichelinX E22.5 Pilote XDY 154/150M	4500	Tire, Rear Left	MichelinX XZY 385/65R 22.5	2550



6102 Front single tire



6102 Rear double tires



6103 Front single tire



6103 middle double and back single tires

**Appendix V : Summary Septemper 2005 Data WIM, Noise, Vibration**

Notes: bold indicates maximum for that day
 N1=no valid measurements
 N2=GVW<30t; nc N3=max noise values are not unique, i.e more than one occurance

DDMMYY	Head/Astra Nr	Time			WIM [t]	Max Ax Ld [t]	No axles	Veh Class CH	Noise dB(A)	speed	Vib PPV (mm/s) vertical
		hhmm	s	ms							
03.09.2005	20014	1316	23	50	42.58	10.52		10	N1		0.036
	7298	758	21	300	18.68	6.15		9	92.7		N1
	5578	701	9	90	34.88	13.4		10	N1		0.035
	7463	803	4		15.1	11.14	2	1		102	0.068
04.09.2005	47474	1023	51	60	68.07	10.41		10	N1		0.030
	3707	2115	20		16.11	4.86		8	91.1		0.030
	45493	907	5	0	36.65	13.22		10	N1		0.036
	61460	1733	4		15.4	10.57	2	1		102	0.055
05.09.2005	20033	1026	3	90	60.93	9.32		10	N1		N1
	22546	1143	21	0	20.14	8.06		9	95.3		N1
	19209	959	57	40	38.59	15.59		10	N1		N1
	8162	544	28		15.22	8.36	2	8		81	0.046
06.09.2005	14863	1920	26	30	80.46	11.67		10	N1		0.037
	61330	1153	49		12.09	5.12		9	94.9		N1
	64200	1321	19	70	69.51	14.17		8	N1		0.032
	50293	712	53		16.69	11.13	2	1		98	0.080
08.09.2005	9627	1047	19	40	90.06	13.42		9	8	N1	0.031
	12867	1222	18		12.47	5.57		9	96.3		N1
	13635	1245	53	20	60.17	16.77		4	N1	83	0.038
	7753	951	3		32.06	12.32	4	9		90	0.078
DDMMYY	Head/Astra Nr	Time			WIM [t]	Max Axel L [t]	No axles	Veh Class CH	Noise-A dB(A)	speed	Vib PPV (mm/s) vertical
hhmm	s	ms									
09.09.2005	52407	1132	23	20	76.44	9.89		10	N1		N1
	39314	608	51		34.65	11.57		4	8	95.6	N1
	56347	1316	8	50	31.06	18.63		4	9	N1	N1
	45136	813	0		4.14	2.52	2	5		93	0.114
10.09.2005	19548	706	50	10	47.02	13.09		5	9	N1	0.030
	30840	1202			42.4	9.65		5	9	94.6	0.047
	30020	1144	6		32.23	11.88	4	9		85	0.105
11.09.2005	4835	1454	50	10	69.38	11.97		10	N1		0.034
	19642	2220	46	50	15.6	4.7		4	8	90.8	N1
	4489	1443	48	10	37.09	13.38		5	10	N1	N1
	16364	2002	0		19.21	12.43	2	1		101	0.086
12.09.2005	46534	1615	9	70	77.55	9.12		12	9	N1	0.049
	23536	624	10		28.35	9.78		4	9	95.1	N1
	35112	1050	35	60	43.38	16.16		5	10	N1	0.028
	23'439	1945	34		36.86	11.99	4	10		88	0.092
13.09.2005	7313	1629	43	70	91.16	13.58		10	N1		N1
	2893	1439			19.05	7.17		3	8	95.1	N1
	5482	1547	55	80	40.17	14.96		5	10	N1	N1
	10013	1205	52		36.3	10.67	4			87	0.079
14.09.2005	24217	647	27	50	79.12	10.86		11	10	N1	N1
	32530	939	24		27.68	10.64		4	9	96.3	N1
	48971	1654	22	60	34.06	17.1		4	9	N1	N1
	24428	651	35		3.37	2.04	2	5		114	0.107



DDMMYY	Head/Astra Nr	Time			WIM [t]	Max Ax Ld [t]	No axles	Veh Class CH	Noise-A dBA	speed	Vib PPV (mm/s) vertical
		hhmm	s	ms							
15.09.2005	62468	517	5	40	46.33	10.72	5	10	N1	86	0.035
	62782	544			11.06	6.64	2	8	93.7	88	N1
	62724	540	51	50	40.82	12.48	5	7	N1	83	0.041
	62787	545	18		21.74	5.62	5	9		89	0.068
16.09.2005	54908	1242	15	0	69.32	10.6	9	10	N1	82	N1
	53728	1207	37		11.06	4.46	4	9	95.7	78	N1
	50473	1033	52	0	41.73	18.49	4	7	N1	87	N1
	41834	707	13		19.72	7.42	4	4	9	88	0.101
17.09.2005	29014	1136	34	70	45.41	12.29	5	10	N1	87	0.044
	18152	526	40		21.77	6.83	4	9	94.4	88	N1
	33101	1309	58	0	41.83	14.27	3	8	90.5	73	0.027
	45594	1803	4		17.82	8.6	3	1		103	0.076
18.09.2005	56348	434	5	20	41.98	12.84	5	10	N1	87	N1
	15073	2019	12		14.12	7.31	2	8	92.7	92	0.018
	60925	1034	30		12.51	8.69	2	1		99	0.085
19.09.2005	21221	619	51	0	90.55	16.33	6	10	N1	82	0.0445
	31624	1018			3207	1221	4	8	96.3	85	N1
	35'842	1227	33		33.7	12.16	4	8		88	0.106
20.09.2005	5920	1009	27	50	82.99	12.36	10	10	N1	86	0.028
	2758				3626	1052	4	8	97.4	84	0.031
	9165	1151	1	30	40.87	16.19	4	9	N1	88	0.052
	64'136	725	10		43.88	10.84	5	10		90	0.105
21.09.2005	35523	622	39	40	53.62	8.2	9	9	88.5	87	0.045
	34138	449			9.33	6.22	2	8	93.3	96	N1
	35359	617	32	20	35.32	13.57	4	10	N1	88	0.038
	35'139	609	50		24.25	12.08	3	10		87	0.095
DDMMYY	Head/Astra Nr	Time			WIM [t]	Max Ax Ld [t]	No axles	Veh Class CH	Noise-A dBA	speed	Vib PPV (mm/s) vertical
hhmm	s	ms									
22.09.2005	28497	1259	14	80	78.36	15.05	9	9	90.5	89	0.033
	39178	1708			17.84	6.01	4	9	94.2	89	N1
	38090	1651	3	20	39.72	15.11	4	9	85.8	86	N1
	46'712	1927	48		15.33	9.86	2	1		107	0.076
23.09.2005	52846	513	15	60	43.74	13.2	5	10	N1	87	N1
	52716	450	27		9.52	6.24	2	8	92.2	97	0.028
	52'105	100	6		25.06	9.53	4	9		88	0.052
24.09.2005	25093	830	14	90	78.37	12.29	12	10	N1	79	0.036
	22139	450			15.93	5.75	4	9	92.2	82	0.042
	26281	900	35	60	42.98	18.03	5	9	89	89	0.061
	25'292	835	35		13.2	9.84	2	1		102	0.082
25.09.2005	61000	452	37	50	45.74	13.27	5	9	N1	91	0.033
	4991	13.21			40.9	10.75	5	9	93	88	0.034
	63'181	902	23		13.93	9.4	2	1		99	0.060
26.09.2005	49822	1601	20	20	82.37	11.95	12	9	N1	85	N1
	36009	920			31.65	13.4	4	9	95.7	85	N1
	60741	2000	56	20	48.99	18.25	5	10	N1	230	N1
	46'670	1433	39		3.37	1.71	2	5		115	0.082
27.09.2005	11590	1034	20	30	85.9	14.15	8	9	N1	85	N1
	21104	1511			14.83	5	4	8	96	85	N1
	22974	1558	20	60	45.45	20.14	4	7	N1	90	N1
	7789	842	22		32.69	10.64	5	9		86	0.095
28.09.2005	10529	1724	27	80	56.23	9.7	9	9		88	0.034
	984	1352			34.6	13.02	4	8	95.1	84	N1
	15543	1853	13	60	3175	1668	2	10		212	N1
	573	1342	25		6.61	2.78	3	7		95	0.087

Appendix VI : Swiss Partners' Contribution to Mayer et al [2007] Status March 2007

Road Weigh in Motion (WIM)

Introduction

There is a need to characterise both the static and the dynamic interaction of a vehicle with its infrastructure. These loads can be measured by Weigh-In-Motion or WIM sensors which measure the dynamic forces exerted through the tyre of a moving vehicle and estimate the corresponding static tyre loads. The sensor array used to measure loads can also provide information on –

- gross vehicle mass
- mass per axle
- number and spacing of axles
- vehicle speed
- direction of travel
- lane of operation

The number and spacing of the axles will enable the vehicle type to be classified (Chapter 9). A method of automatic vehicle recognition (Chapter 8) will help to advise operators of vehicles that are over loaded.

This information is also relevant when characterising the noise and vibration impacts (Chapters 4 and 5)

Footprint has adopted portions of the COST 323 and ASTM standards that are relevant to this project.

The topography of the site and layout of the array design form part of the site survey. These are discussed below and in more detail in chapter 6.

Normative References

- COST 323 “Weigh-In-Motion of Road Vehicles” Final Report Appendix 1, European WIM Specifications. Version 3.0, August 1999
- ASTM E 1318-2: Standard Specification for Highway Weigh-In-Motion (WIM) Systems with user Requirements and Test Methods, 2002.

Definition of terms

Accuracy The degree of agreement between a value measured or estimated by a WIM system and an accepted reference value.

Axle Two or more wheel assemblies with centres lying approximately on a common axis oriented transversely to the nominal direction of motion of the vehicle.

Axle load Sum of all the wheel loads of an axle of a vehicle

Calibration Adjustment to a reference level of values

Gross Vehicle Weight The total weight of the vehicle calculated from sum of all Tyre loads of all wheels of the vehicle

High Speed WIM Weighing vehicles in motion in the traffic flow at speeds of 30 to 130km/h

Sensor types and measurement equipment

A wide selection of high speed WIM equipment is commercially available that can deliver the data required in section 2.1 and 2.6 within the accuracy defined in section 2.7. Below two examples of sensors used at the footprint monitoring sites in UK and Switzerland are discussed.

BL piezoelectric sensors made by TDC Systems LTD are used at the UK site. Both lanes are covered with these sensors that are fully encapsulated in resin and do not present a significant intrusion in the road structure.

At the Swiss monitoring site WIM measurements using Lineas sensors made from silicon-dioxide, SiO₂, and manufactured by Kistler are used. Both lanes are covered each containing two rows of three sensors (Figure).

A wheel rolling over the Lineas applies vertical forces to the quartz crystals in the sensor, with virtually no deformation. The piezoelectric quartz discs yield an electrical charge proportional to the forces applied (Figure). The piezoelectric sensitivity is virtually independent of temperature, time and speed. The electric charge signals are converted by a charge amplifier into exactly proportional voltages that can be further processed as required. The accuracy of the measured wheel load is not influenced by Tyre type, Tyre quantity or Tyre pressure. In the case of dual Tyres, the Lineas measures one signal and expresses it as one wheel load, which is equal to the sum of both wheel loads (www.kistler.com).

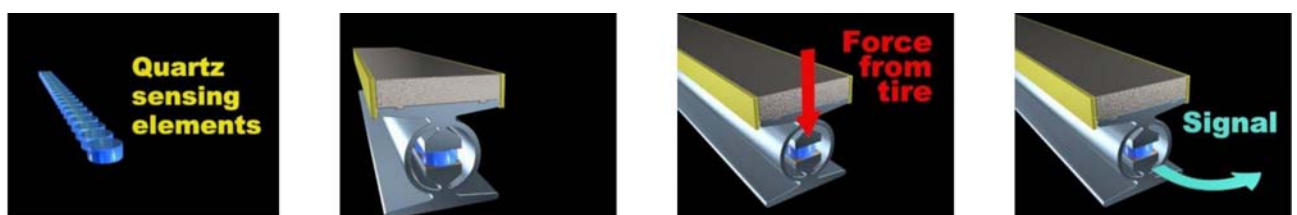


Figure A. 1: Lineas WIM Sensor (courtesy Kistler instrumente AG)

Site safety criteria

In order to assure safety of personnel at site, it should be accessible from off the main highway. Failing this, a site should at least have a safe stopping/parking area adjacent to the site.

Equipment

A Footprint monitoring site requires a high speed WIM system with sensors installed in one or more lanes capable of accommodating highway vehicles moving at speeds of 30 to 130km/h. For each vehicle processed, the system shall produce as a minimum the data shown in Table 2.1.

Table A. 1: Minimum Data needed from a WIM System

1	Wheel load (optional)
2	Axle load
3	Gross Vehicle Weight
4	Speed
5	Centre to centre spacing between
6	axels
7	Vehicle class
8	Lane and direction of travel
	Date and time of passage

Performance requirements

Accuracy

In the normative references listed in section 2.2, the accuracy is referred as the correlation of dynamic loads with the static loads. Footprint aims to evaluate the impact of dynamic impact forces applied by the wheel on the pavement. As such the accuracy concept developed by COST and ASTM should be re-evaluated.

Accuracy of a WIM system under moving loads is defined by a confidence interval of the relative error of a unit (an axle, an axle group or gross vehicle weight), defined by (Ref: COST 323, 1999, ASTM E1318):

$$\delta = 100 \times \frac{W_d - W_s}{W_s}$$

where

δ is the difference in the value of the data produced by the WIM system and the corresponding reference value expressed in%

W_d is the value of the data item measured by the WIM systems

W_s is the corresponding reference value of the same unit

As accurate knowledge of weights by axles or axle groups and gross weights are needed for a Footprint monitoring site, accuracy class as defined in COST 323, (1999) should be specified.

Calibration

WIM sensors typically produce a force-time series that is linearly proportional to the magnitude of the component of dynamic tyre force applied perpendicular to the road surface by the tyres of a moving vehicle. The dynamic tyre force results from a complex interaction among vehicle components, the WIM sensor, the road surface surrounding the sensors, and other factors. Site conditions are different at every WIM site, and every vehicle has unique tyres, suspension, mass, and speed characteristics. Calibration at every site allows compensation for these site specific and vehicle specific influences.

A Footprint monitoring site should be calibrated annually as a minimum using calibration criteria and methods defined by COST 323, 1999 or ASTM 1318-2. The timing of the calibration should consider seasonal and temperature changes.

Specification summary

Measurement parameters

- minimum two rows of high speed WIM sensors installed on the slow lane
- calibration annually as a minimum using calibration criteria and methods defined by COST 323, 1999 or ASTM 1318-2.
- The timing of the calibration should consider seasonal and temperature changes

The following parameters should be reported:

- Wheel load (optional)
- Axle load
- Gross Vehicle Weight
- Speed
- Centre to centre spacing between axles
- Vehicle class
- Lane and direction of travel
- Date and time of passage
- Location

Environmental noise measurements

Introduction

The measurement of noise coming from a passing vehicle depends on the interaction between the vehicle and the infrastructure, the presence of an internal combustion engine within the vehicle, the weather conditions and the presence of other vehicles on adjacent lanes. In addition a fundamental difference between the two modes is the presence of the rubber tyre on a pavement (generally tarmac) and a steel wheel running on a steel track. Also the background noise could be appreciable particularly if the site is located in an urban or semi-urban area.

Footprint has adopted the single vehicle by pass method as set out in the relevant ISO standards which requires only one microphone located at a specified distance from the pavement or track. This method is also specified in the TSI for measuring noise from railway vehicles [14]. This TSI stipulates very narrow limits for both the track alignment and the requirements of the measurement site, and has to be complied with in order to obtain the TSI/CEN certification.

However, Footprint is interested in measuring environmental noise for reasons other than gaining type approval:-

- noise is enhanced if the vehicle has a wheel defect or the suspension is faulty; so this can be used alongside other data to decide if a vehicle is operating in an unsafe condition
- noise restrictions in environmentally sensitive areas such as residential areas at night
- populating the source models used for modelling noise such as those required for meeting the environmental noise directive [13] and for developing subsequent strategic action plans

As with other sensors, it is also possible to use additional microphones for improving accuracy.

The influence of adjacent vehicles in the same lane becomes of greater importance as the distance between vehicles decreases for higher traffic flows. Under such circumstances the measurement rules set out in the standards may no longer apply so a methodology is being developed to characterise vehicles under such conditions. For trains which comprise a set of linked vehicles it is necessary to determine where one vehicle ends and another starts in order to characterise the noise of an individual vehicle.

As the microphone is situated outside of the outer lane (or track) it should be possible to measure the noise signal of a vehicle passing in an adjacent lane by correcting for the

distance of the vehicle from the microphone. These considerations together with the topography of the site all form part of the site survey and layout of the array design. These are discussed further below and also in chapter 6.

Normative References

- ISO 11819-1: Acoustics - Measurement of the influence of road surfaces on traffic noise - Part 1: Statistical Pass-By method, 1997.
- ISO 3095: Railway applications - Acoustics - Measurement of noise emitted by railbound vehicles, 2005.
- IEC 61672: Electroacoustics - Sound level meters, 2002.

Definition of terms

Sound pressure p Fluctuating pressure superimposed on the static pressure by the presence of sound, in Pa

Sound pressure level L_p Level, in decibels, given by $L_p = 10 \log(p/p_0)^2$

where: $p_0 = 20 \mu\text{Pa}$

A-weighted sound pressure level L_{pA} Sound pressure level, obtained by using the frequency weighting A, in decibels

Third-octave filtered sound pressure level $L_{p,n}$ Sound pressure level obtained by using the n-th third octave band-pass filter to limit the frequency range under investigation, in decibels

AF-weighted maximum sound pressure level L_{pAFmax} Maximum value of the A-weighted sound pressure level using time weighting F (Fast), in decibels

A-weighted equivalent continuous sound pressure level $L_{pAeq,T}$ Energetically averaged A-weighted sound pressure level measured for a time interval T, in decibels

A-weighted sound exposure level $L_{A,E}$ A-weighted sound pressure level of a single event measured for a time interval T and normalised to 1 sec, in decibels

Composite whole-day rating level L_{den} Composite rating level to describe a community noise environment by one single number in decibels. It is calculated as weighted energetic mean of daytime, evening and night rating levels. The penalty for night time is usually 10 dB, for evening periods 5 dB. The periods of day, evening and night are defined by national authorities.

L_{night} Rating level for night time periods.

General

Road

Single vehicle road noise measurements should be performed according to the pass-by method described in the standard ISO 11819-1. The standard gives specifications for the measurement equipment, defines the geometry that should be used and describes in

a verbal manner conditions for valid measurements. The acoustic measurements should take place in line with a WIM sensor to identify the vehicle and to deliver a trigger signal.

The measurements are made with vehicles operating at and above the speed limit which could be as high as 180 km/hour.

Rail

Railway noise measurements should be performed according to the method described in ISO 3095. This standard specifies the conditions for obtaining reproducible and comparable measurement results of levels and spectra of noise emitted by all kinds of vehicles operating on rails or other types of fixed track except for track maintenance vehicles in operation.

A new version, ISO 3095:2005, will replace the original 1975 version of this standard. This new version provides a more detailed description of the assessment of the rail decay rate and rail roughness of the test site, and also gives limit spectra for these quantities because they have a large influence on the obtained rolling noise level of the vehicle.

The standard is applicable to type testing and periodic monitoring testing. The results may be used, for example, to characterise the noise emitted by these trains, to compare the noise emission of various vehicles on a particular track section, and to collect basic source data for trains. The test procedures specified in ISO 3095:2005 are of engineering grade (grade 2, with a precision of 2 dB), that is the preferred one for noise declaration purposes, as defined in ISO 12001 (Noise emitted by machinery and equipment -- Rules for the drafting and presentation of a noise test code). The procedures specified for accelerating and decelerating tests are of survey grade.

The measurements are made with vehicles operating at line speed, which could be up to 350 km/hour if operating on high speed track.

Geometry

According to ISO 11819-1 and ISO 3095 the microphone must be located at a distance of 7.5 m from the lane or track of interest. The microphone height should be 1.2 m above the pavement or track. For road the ground surface around the microphone has to be acoustically hard. The area around the microphone must be free of reflecting objects. If a guard rail or any other obstacle that may distort the sound propagation is present, the microphone height has to be increased accordingly and suitably calibrated.

The acoustic measurements should take place in line with a vibration or WIM sensor to identify the vehicle and to deliver a trigger signal

Equipment

The acoustic measurement chain has to fulfil IEC 61672 type 1 specifications and consists of a 12 mm outdoor microphone with omni-directional characteristics with windscreen and a sound level meter or A/D converter as front end to a computer for further signal processing.

The ISO standards only refer to a vehicle passing a single microphone located 7,5m from the centre of the nearest lane or track. For a 2 lane road (or track) one microphone should be positioned on either side of the road. To save space, the microphone can be positioned across the opposite track/lane from that being measured (Figure 4.1).

>> As this may not be possible due to space restrictions, Footprint is evaluating the validity of measuring with only one microphone for traffic passing in either lane

For 4 lanes, it is only possible to position the microphone 7.5 m from the centre of the nearest lane and to correct for any vehicle passing in the outer lane.

For 6 or more lanes, it is only possible to measure with any accuracy the noise emissions from vehicles in the inner two lanes.

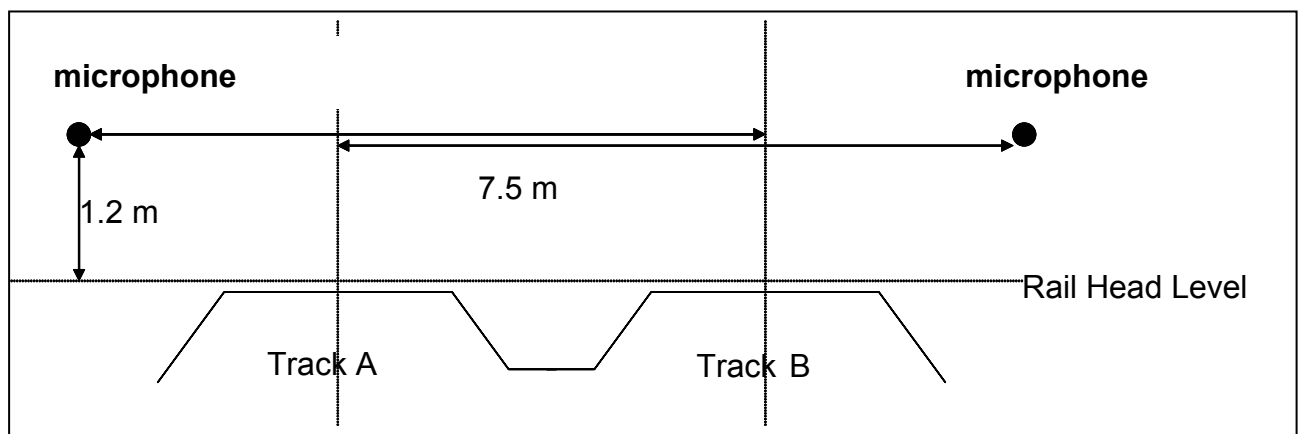


Figure A. 2: Geometry used by to measure noise

Note the spacing between the two tracks can vary from 3.05 to 4.07 m; thus the positions of the microphones are outside the operational limit of the railway. This method complies with ISO 3095 in terms of the distance of the microphone from the centre of the track i.e. 7.5 m. The ISO method does not allow measurement over another track or lane because of the reflections this might induce.

4.7 Specifications of the measurement equipment

The acoustic measurement chain should be able to handle

- a dynamic range from 40 to 110 dB(A)
- a frequency range from 20 Hz to 10 kHz (corresponding to a sampling rate of at least 22 kHz)

A periodic calibration has to assure that any sensitivity drift of the measurement chain can be detected and compensated for. The calibration can be performed by using a calibrator adjacent to the microphone or by evaluating events of known strength.

4.8 Additional, non-acoustic data needed

For the evaluation of the noise parameters the following additional data are needed:

- vehicle type
- vehicle speed
- type, position and speed of adjacent vehicles when the maximum value of the vehicle being measured is reached
- degree of rail roughness (norm in preparation)
- direction of travel

Furthermore the following data should be recorded:

- air temperature and temperature of pavement
- humidity of pavement (road only)

Signal processing

Road

For a single road vehicle the microphone signal is A-weighted and exponentially time averaged with time constant FAST (125 ms). The averaged time history is sampled every 100 ms, delivering a sequence $L_{pA}(k)$. Further processing is based on this sequence $L_{pA}(k)$ only. A vehicle is characterised by the maximum value L_{pAFmax} of $L_{pA}(k)$ during the passage (see Figure 4.2 below).

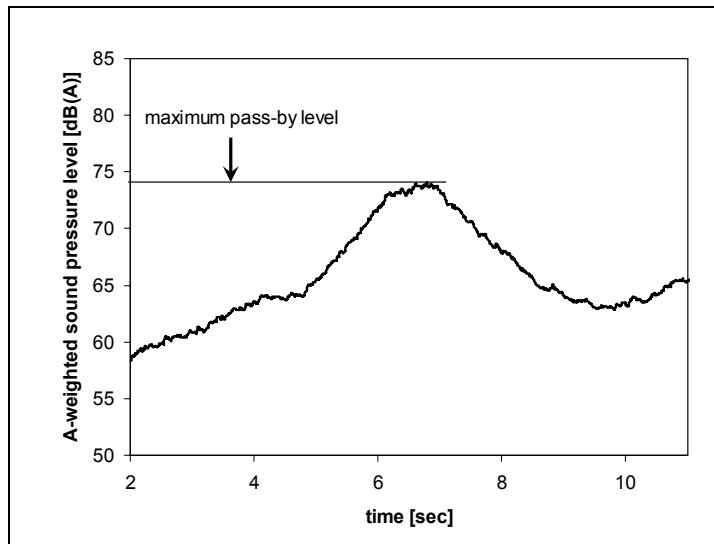


Figure A. 3: Example of the level-time history of a road vehicle pass-by event.

The maximum value of the A-weighted sound pressure level is determined and used to characterise the vehicle noise-footprint.

A measurement can be disturbed by noise sources from the environment or by other vehicles. For that reason it has to be examined for validity using two criteria:

- 6 dB down: the $L_{pA}(k)$ sequence has to drop down monotonically (with a suitable tolerance) to both sides of the maximum value L_{pAFmax} by at least 6 dB(A).
- no disturbance: there is no other noise source that influences the maximum value L_{pAFmax} .

If one or both criteria are not fulfilled, the measurement is not valid in terms of the standard. These criteria will only hold in light traffic flow and so one can only characterise a small proportion of the traffic flow.

>> *So Footprint is considering methodologies which will characterise noise of individual vehicles at higher traffic flows.* Under such conditions L_{pAFmax} found can be regarded as an upper limit of the true value. By use of compensation strategies to deliver an estimate of the distortion by unwanted noise sources the two criteria may be reduced.

For the END directive [13] where the noise emissions from the total traffic is of interest equivalent continuous sound pressure levels ($L_{peq,T}$) may be evaluated for a suitable time window T. $L_{peq,T}$ is evaluated as A-weighted level and in third octaves.

4.9.2 Rail

Trains can be evaluated by a sound exposure level over the duration of a complete pass-by of a train.

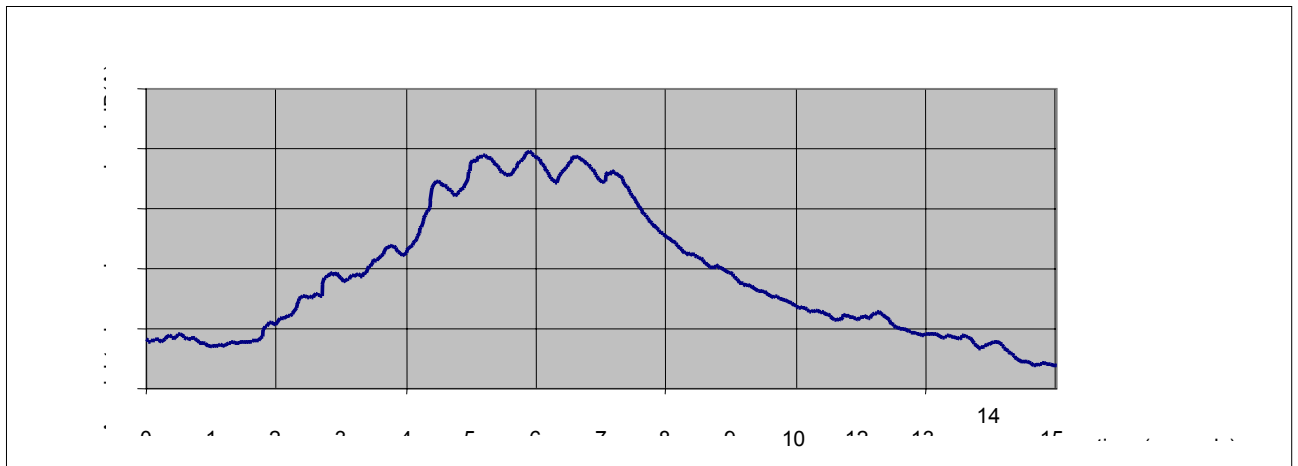


Figure A. 4: Example of the level-time history of a passing train

However the footprint requirement is to characterise the sound power of individual vehicles even if these are influenced by noise coming from adjacent vehicles. A typical measurement is shown in **Figure A. 5**.

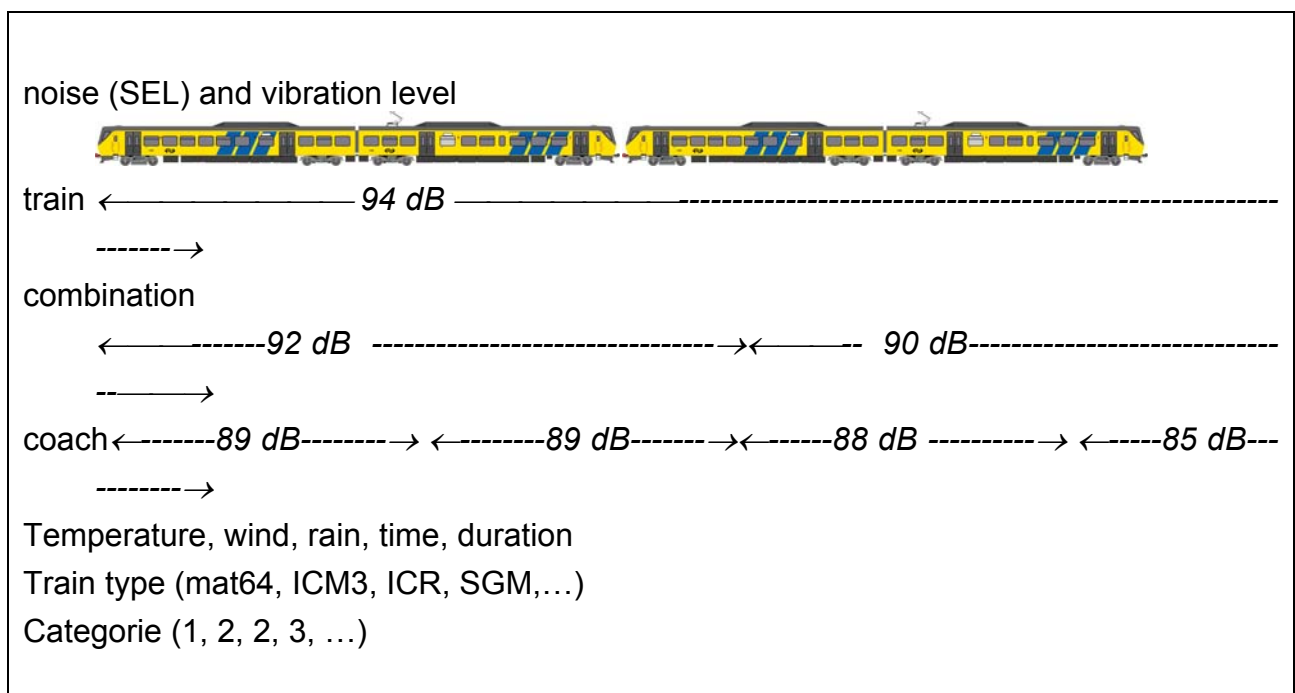


Figure A. 5: Outcome of noise measurements of a passing train

Measurement of individual vehicles will enable one to identify which vehicles are excessively noisy, which could be due one of the following reasons –

- wheel quality
- condition of damper or suspension
- condition of bearings
- dragging brakes which could lead to bearing failure, axle seizure and derailment
- internal combustion engines inadequately maintained

Suitable time windowing of the level-time history allows for detailed analysis of single vehicles.

Quality control and calibration

Extensive quality checking is required for reliable data as

- rail or pavement roughness can vary in time
- road surface noise is very dependent upon the properties of the surface layer e.g. porous asphalt
- weather conditions may be beyond ISO 3095 requirements
- microphone base levels may drift

This can be monitored by recording vibration measurements (refer Chapter 5) and installing a simple weather station to monitor rainfall, wind and temperature.

Calibration is required on a regular basis (at least once a year) to establish the relationship between the sound pressure and the electrical output of the microphone. Calibration can be undertaken at either 250 Hz or 1 kHz. 250 Hz is in the frequency range where the frequency response of almost all microphones is flat and will therefore give the most accurate calibration. If however the microphone is used with weighting filters then the 250 Hz signal will be attenuated by the weighting network and so calibration at 1 kHz might be better.

Calibration can either be undertaken by regular site visits at least once a month or by automated calibration through the passage of known vehicles.

Vehicle type and recognition

Vehicle type can be classified by identification of the number of the axles, their location and the mass of each axle. From this information, vehicle type can be identified using the classification schemes developed for both road and rail (refer chapter 8).

Train types can be identified by RFID tag readers provided at least one vehicle is fitted with a suitable transponder (refer chapter 8).

Microphone

Measurement microphones are sensitive to environmental factors like wind, rainfall or snow. By purchasing suitable outdoor and environmental microphones, it is possible to protect the microphone diaphragms against the influences of the environment.

The measurement direction should be horizontal in order to maximise the sound from

the passing vehicle and reduce background noise coming from other extraneous sources.

A sound calibrator is also required which will produce a constant level of sound at a specific decibel level and frequency.

Data input for environmental noise directive

The calculation of noise levels such as L_{den} or L_{night} in the community needs knowledge of the source strength as well as the sound attenuation from the source to the receiver points. Roads or railway lines can be treated as line sources. Modern models such as ISO 9613 or Harmonoise use the emitted sound power level of the average single vehicle in different categories as a basis for calculation and this is the contribution that Footprint can make to the source models.

The noise levels in the community are then calculated by taking into account

- the sound power of the average vehicle
- number of vehicles per unit time
- attenuation of the sound propagation from source to receiver

In Footprint each individual vehicle is characterised by its maximum by pass-by level. With the knowledge of the measurement geometry and the acoustical properties of the ground surface, it is then possible to determine the sound power of the vehicle. For that purpose the geometrical spreading and the effect of reflection at the ground have to be considered.

Alternative measurements may be performed by the evaluation of the equivalent continuous sound pressure level ($L_{peq,T}$) over a certain period of time (e.g. 30 minutes or 1 hour) to describe the emission of the total traffic.

Specification summary

Measurement parameters

- frequency range 20 hz to 10 kHz
- dynamic range 40- 110 dB(A)
- sampling rate 22 kHz
- trigger from start and end of signal from WIM or vibration sensor or acoustic signal above background level

- single microphone 7,5 metres from centre of nearest lane
- minimum height 1,2 metres above outside lane or track



- height to be adjusted so that there is no obstacle or shielding by any guard rail
- valid data may also be acquired from a second lane or track if space does not permit installation of a second microphone 7,5 m from the other outside lane
- to determine whether a measurement is valid, the location of any vehicles on any other lanes to be identified
- initial calibration to be undertaken by suitable acoustic calibrator at site
- subsequently calibration to be checked at least once a month either by a visit to the site or by passage of specific tagged vehicles at a known speed
- record weather conditions like rainfall, wind and temperature
- humidity of road surface and temperature of surface layer
- lane in which vehicle is travelling
- vehicle direction of travel
- vehicle speed
- axle number and spacing (to determine vehicle type)
- axle load (to determine vehicle mass)

Footprint vibration measurements

Introduction

Vibration is the oscillatory motion of an element in a medium with no net movement. This oscillation phenomenon is propagated forward in a wave movement and can be described in terms of its displacement, velocity or acceleration.

Vibrations are induced as a result of the presence of irregularities at the road surface and of characteristics of the vehicles themselves (**Figure A. 6**). The irregularities can be discrete, random or periodic and their presences lead to dynamic vehicle-pavement interaction forces that are the SOURCE of the vibration. These impact forces generate successive stress waves in the supporting soil, which act as a TRANSMISSION PATH. Stress waves propagate through the ground in the form of body waves (compression and shear waves), and in the form of surface or Rayleigh waves (**Figure A. 7**) and eventually reach the foundations of adjacent buildings or structures, which are the RECEIVER of the vibration.

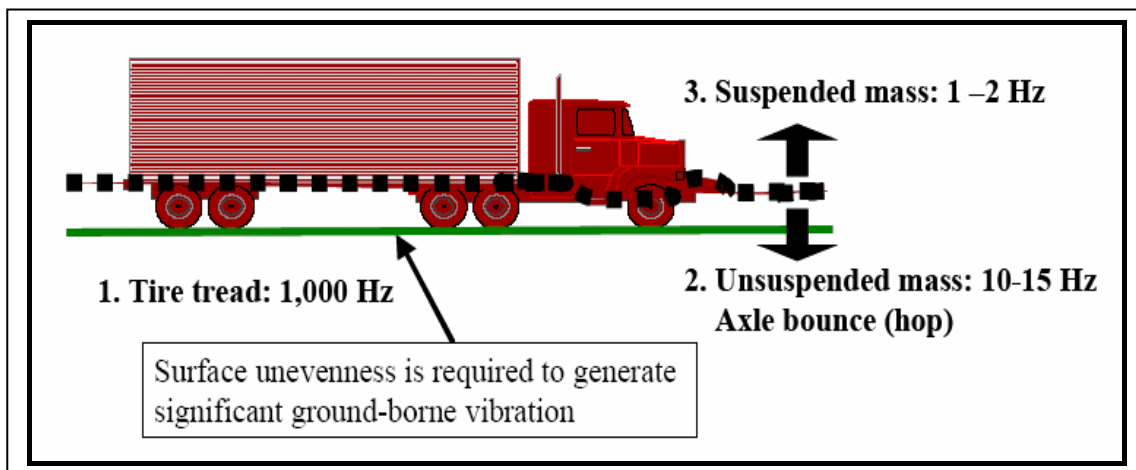


Figure A. 6: Vehicle as source of vibration of different frequencies

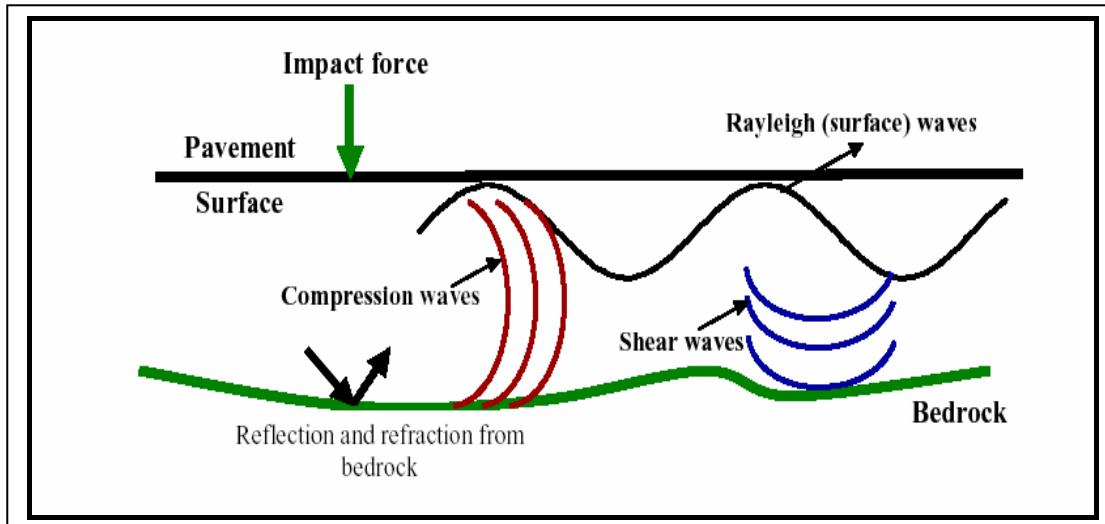


Figure A. 7: Propagation of the vibration in form of different waves

The amount of energy transmitted into the structure is strongly dependent on factors such as the smoothness of the surface, the vehicle characteristics in terms of suspension, tyres, load and speed. The energy is dissipated in the structure, sub structure and subgrade soil and reduce with distance and topography. All these factors influence the amount of ground borne vibration that can be experienced by the receiver (Table A. 2).

Table A. 2: Factors influencing ground borne vibration values

SOURCE	TRANSMISSION PATH	RECEIVER
Surface conditions	Distance	Building parameters
Vehicle parameters	Soil/ground absorption	Receiver location and coupling
Vehicle speed	Ground topography	

Figure A. 8 depicts the problem of measuring at different locations (1 to 5) as all measurements are influenced for the different factors enumerated above.

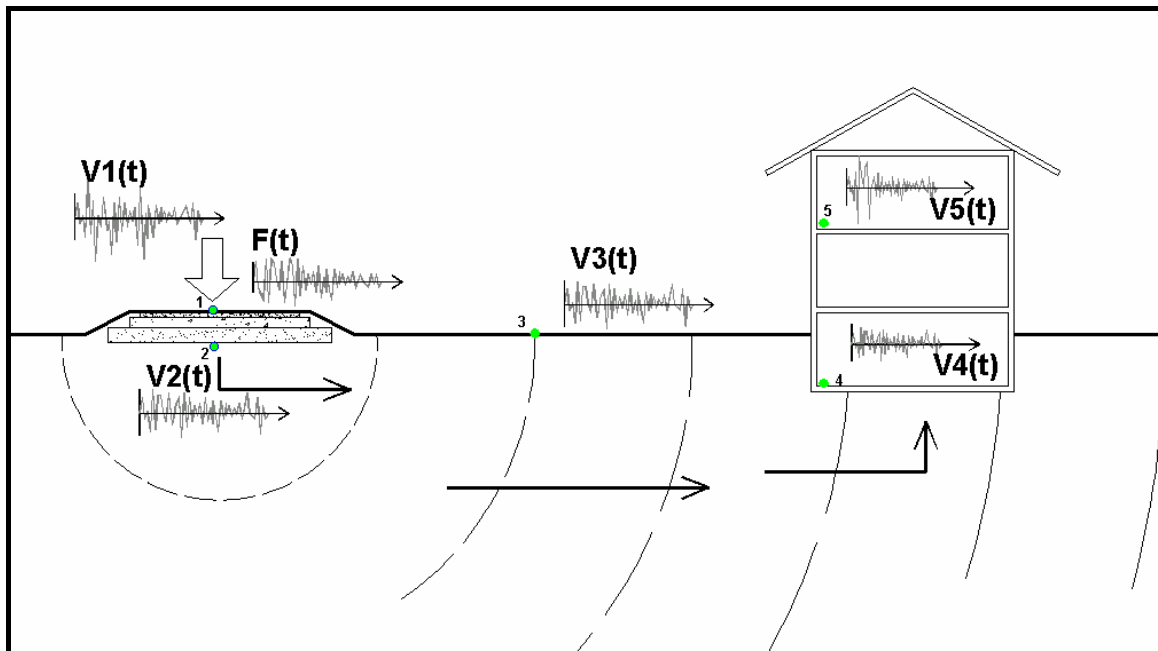


Figure A. 8: Transmission path from source to receiver

Ground vibration generated by traffic can be considered to be a random process. At the road or track side, this random process is clearly non-stationary since the level of vibration rises and falls with the passage of each individual vehicle. Away from the road, at a distance significantly greater than the mean vehicle spacing, an observer will be unable to distinguish the passage of individual vehicles, and the ground motion can be described as a statically stationary function of time [16].

Because of the rapid decrease of vibration with distance, trucks travelling close together often do not increase peak vibration levels substantially; rather more trucks will show up as more peaks, not necessarily higher peaks. Wave fronts emanating from several trucks travelling closely together may either cancel or partially cancel (destructive interference), or reinforce or partially reinforce (constructive interference) each other, depending on their phases and frequencies. Since traffic vibrations can be considered random, the probabilities of total destructive or constructive interference are extremely small. Coupled with the fact that two trucks cannot occupy the same space, and the rapid drop-off rates, it is understandable that two or more trucks normally do not contribute significantly to each other's peaks.

One of the environmental consequences of traffic is ground borne vibrations alongside the infrastructure. Any foundation of a structure near the source will be excited by the resultant waves, and then the maximum vibration amplitudes of floors and walls may occur at the resonance frequencies of various components of the building. As a consequence, traffic induced vibration may cause minor damages on buildings, malfunctioning of sensitive equipment or may cause discomfort to people living or

working near a track or roadway during a vehicle passage.

As with noise, vibration measurements can be used to populate source models.

Normative references

There are no standards about measurement of ground borne vibration from passing vehicles. Instead, there are guidelines prepared by different institutions based on their own experience, some research and standards about how vibration affects the human body. The most important guidelines used to write this chapter are:

US Department of Transportation, Federal Transit Administration. Transit noise and Vibration Impact Assessment, Report DOT-T-95-16, April 1995

California Department of Transportation, CALTRANS. Transportation Related Earth borne Vibrations, Technical Advisory, Vibration TAV – 02 – 01 –R9601

These guidelines and papers are partially based on the following norms that recognise discomfort to people, malfunctioning of sensitive equipment or damage to buildings:

ISO 2631-1:1997 Mechanical vibration and shock -- Evaluation of human exposure to whole-body vibration -- Part 1: General requirements

ISO 2631-2:2003 Mechanical vibration and shock -- Evaluation of human exposure to whole-body vibration -- Part 2: Vibration in buildings (1 Hz to 80 Hz)

ANSI S3.29-1983 (ASA 48-1983) Acoustic Society of America, "American National Standard: Guide to Evaluation of Human Exposure to Vibrations in Buildings",

DIN 4150/2 1999-02 Structural vibration - Effects of vibration on structures

Characteristic parameters

Most transducers measure either velocity or acceleration and these are quantified using the following parameters as illustrated in Figure 5.5

- the peak particle velocity (ppv) in mm/s;
- the root mean square velocity (rms velocity) in mm/s²;
- vibration velocity level in decibels

$$Lv = 20 \times \log_{10} \left(\frac{v}{v_{ref}} \right)$$

where Lv is the velocity level in decibels, v is the rms velocity amplitude and v_{ref} is the reference velocity amplitude (1×10^{-8} m/sec).

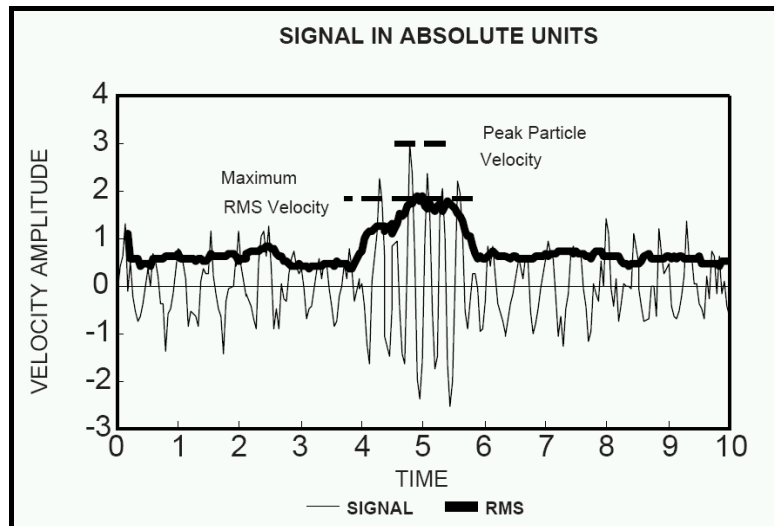


Figure A. 9: Measured signal, PPV and RMS (source (1))

Definition of terms

Vibration: Quantitative term describing movement of a building or part of a building

Whole-body vibration: Vibration acting on the body of a person, e.g. when lying in a bed, sitting on a chair, or standing on a vibrating floor.

Annoyance: Adverse response from persons, when subjected to an unwanted physical stimulus.

Environmental vibration: Vibration caused by vibration sources outside the habitation or house, from e.g. traffic or industry.

Acceleration signal: An electrical signal proportional to the instantaneous acceleration (of the measurement position).

RMS-value: Square-root of the average of the squared signal, an expression of the energy of the signal. The averaging time is an important parameter for the RMS-value.

Acceleration level: 20 times the logarithm (base 10) of the ratio between the RMS-value of the acceleration signal and the reference acceleration (= 10^{-6} m/s²).

Stationary vibration: Vibration with negligibly small fluctuation of level and frequency within the period of observation.

Intermittent vibrations: Vibration which suddenly changes between two or more stationary vibrations within the period of observation.

Sensor types

Vibration transducers only measure vibration along one axis. In this respect they are different from noise measuring microphones, which measure noise arriving from all directions simultaneously. Therefore, to obtain a measurement of the total vibration at a



point it is necessary to measure in three mutually perpendicular directions. These are normally: one in the vertical plane, and two in the horizontal plane.

Velocity sensors (geophones)

These are usually based on exciting a moving coil system, the most common types being electromagnetic, piezoelectric or cable extension potentiometers.

Electromagnetic velocity sensors use the principle of magnetic induction, with a permanent magnet and a fixed geometry coil, such that the induced (output) voltage is directly proportional to the magnet's velocity relative to the coil.

Piezo-velocity transducers (PVTs) are piezoelectric accelerometers with an internal circuit which produces a velocity signal.

Cable extension-based transducers use a multi-turn potentiometer (or an incremental/absolute encoder) and a tachometer to measure the rotary position and rotating speed of a drum that has a cable wound onto it. Since the drum radius is known, the velocity and displacement of the cable head can be determined.

Optical and microwave velocity sensors are non-contacting, and utilise the optical-grating or Doppler frequency shift principle to calculate the velocity of the moving target.

Accelerometers

Accelerometers use the mass of an element to convert force into acceleration in accordance with Newton's second law. The classification of the different kinds of accelerometers depends on the physical characteristic to be used for the measurement.

Piezo-electric - piezoelectric effect of quartz or ceramic crystals to generate an electrical output proportional to an applied force

Piezoresistive (Strain Gauge) - alter resistance in response to stress

Capacitive - the gap between two plates or electrodes changes under acceleration

Force-balance or servo accelerometers - close-loop devices in which the deflection signal is used as a feedback in a servo system that move the inertia mass back to the equilibrium position

Selection

The appropriate transducer type should be selected according to the frequency and



vibration amplitude ranges which are of interest or anticipated. Considering norm *ISO 2631-2*, the frequency range of interest is from 1Hz to 80Hz as they cover the frequency ranges of interest.

Many of the available accelerometers may not be satisfactory for measuring induced ground vibration from low-level traffic due to insufficient resolution and sensitivity. Those accelerometers with high resolution and sensitivity have usually a large mass, but nowadays force balance and some capacitive accelerometers have quite good resolution and high sensitivity using reduced mass. Geophones are more sensitive to low levels of vibrations although they are generally large and heavy.

The following example helps understand why geophones are more sensitive than accelerometers in the range of interest of ground borne vibrations.

Supposing that a point is vibrating following a sinus function with amplitude 0.05mm, if the maximum velocities and acceleration are plotted for a range of frequency from 1 to 100Hz at 1Hz the maximum displacement will be 0.05mm, the maximum velocity of the point will be 0.31mm/s and the maximum acceleration 200g. Few accelerometers possess such resolution. Figure 5.6 shows the maximum levels of acceleration and velocity for the given displacement, at different frequencies.

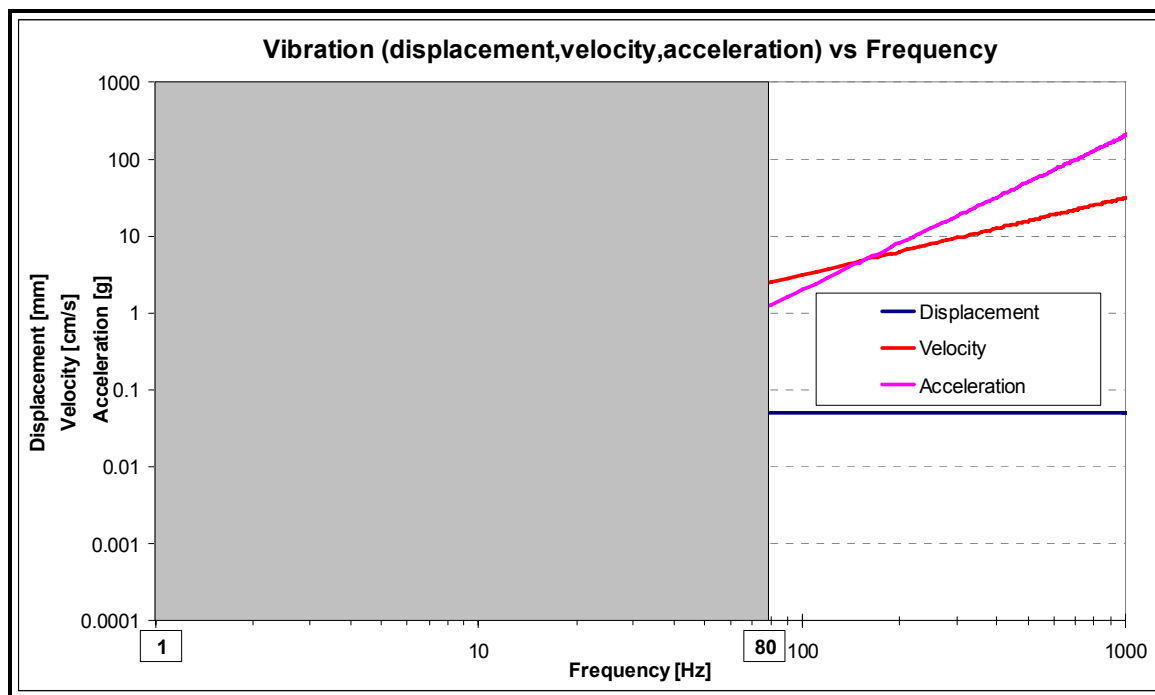


Figure A. 10: Vibration versus frequency

Sensor location

Transducers should be selected so that the vibration levels reflect the purpose of the measurement. Footprint has proposed the use of two sensors rather than one, so that it is possible to characterise both the source (vehicle) and the transmission of the signal through the supporting substructure and ground.

Source measurement

In order to try to avoid the factors of the transmission path and receiver influencing the vibration levels, the sensor should be placed so close to the vehicle as possible. EMPA have mounted the sensor (accelerometer) in a 50mm hole at 40mm depth below the pavement surface, when possible in the centre of the tyre trace (in the case of the A1 site, at 55cm from the border). The mounting was done by gluing a plate and screwing the sensor to the plate. ProRail have mounted the accelerometer on the foot of the rail whilst modelling by Holland Rail Consult shows that it is possible to locate the sensor adjacent to the track bed and still be able to characterise the source. In the UK, this sensor is mounted adjacent to the nearest lane.

Free field measurement

The sensor (geophone) should be located at a distance of 7.5 m from the centre of the nearest track or lane at the same distance as the microphone. As with the microphone, to save space this sensor can be positioned across the opposite track/lane from that being measured

Measurement method

Table A. 3: Specifications of the measurement equipment

Item	Sensor Ground Borne Vibrations
Sensor	accelerometer (source) geophone (free field)
Location	<u>rail</u> : 2.5m and 7.5m <u>road</u> : <i>free field geophone</i> : 7.5m from the centre line <i>source accelerometer</i> : under the wheel path (0.55m from the border line)
Placement	Geophone: Accelerometer:
Directions	3 dimensional
Frequency range	1-80 Hz
Resolution	Geophone: Accelerometer:
method processing	PPV; RMS; KB; v_{eff} - value
measurement parameters each event	Measured signal: maximum velocity-value ,dominant frequency Vehicle: geometry, axle load, speed
environmental impact	+/- 0.1 mm/s (perception level) +/- 2 mm/s (damage sensitive buildings)
filter	Ant aliasing filter, cut off frequency 100Hz

Additional data needed

For the evaluation of the vibration parameters the following additional data is needed:

- type of vehicle under investigation
- speed of vehicle under investigation
- type, position and speed of possible disturbing vehicles in the environment at the moment in time where the maximum value of the vehicle under investigation is reached.

Furthermore the following data should be recorded:

- air temperature and temperature of pavement (road only)
- air humidity and humidity of pavement (road only)

Processing the data



Calibration

Calibration of individual components of the complete measuring system should be performed periodically in accordance to instrument manufacturers; a minimum period of one month and a maximum of one year. Alternatively, in the case of accelerometers which extend down to DC, the system may calibrate systematically using gravitational field of Earth.

Quality control

Data collection and on-line analysis

Introduction

In each of the preceding chapters, there is a brief description of the available sensors and where and how they should be mounted on, beneath or adjacent to the pavement or track. In addition to these sensors, sensors that measure weather conditions like wind and rainfall are required in order to be able to interpret and record valid noise data.

These sensors provide data which have to be collected, collated and if possible, analysed on-line to reduce the data sets. The only real time data that will need to be retained are extreme events where sensor output exceeds preset levels.

The sensor outputs for measuring parameters like axle load, pavement deformation, vibration, noise, temperature and humidity need to be recorded simultaneously. Analogue and digital signals with quite different dynamics and sample rates can be processed using commercially available electronic devices. They range from quasi static signals like temperature and humidity to the highly dynamic signals of axle-load.

Almost all measurement systems are based on the inclusion of WIM sensors because these sensors can identify vehicle speed, length, direction of travel, axle configuration, lane location and vehicle type. Such information is vital to interpret the measurements from the other Footprint sensors like noise and vibration.

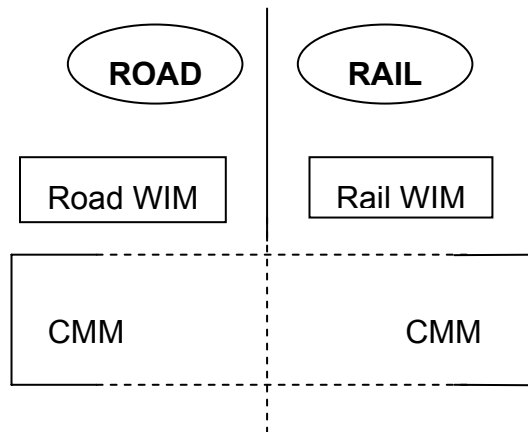
The example of two measurement systems is shown in Box 1

Box 1: Specification for footprint measuring system

Measurement system

The Footprint measurement station system configuration can be based on two separate and compatible systems. The first system comprises the existing measuring station i.e. WIM on road and rail. The second system comprises the Common Mode Measurement (CMM) system which will be the same for road and rail and will measure some or all of the following:

- Deformation strains in the supporting structures of road and rail
- Audible noise
- Ground borne vibration



Common mode measurements sensors specifications

Measurement	Channels	Bandwidth	Sample rate (kHz)	Resolution (bit)
Noise <i>Road</i>	2	20 kHz	50	16
<i>Rail</i>	2	20 kHz	50	16
Deformation	4	300 Hz	1	12
Vibration <i>Road</i>	4 (2x2axis)		1	12
Rail	9 (3x3axis)		1	12
Temperature	1			
Rain	1			

To gain readout speed, load measurement data can be stored in binary form and analysed offline. This provides a higher flexibility for the analysis and independency of the measurement system. Analysis methods can subsequently be implemented at the measurement station to gain an even higher data reduction. The WIM data form the master data for all other data sets.

Figure 7.1 gives an overview of the data acquisition system built for the Swiss Footprint station on the A1 motorway as a possible solution.

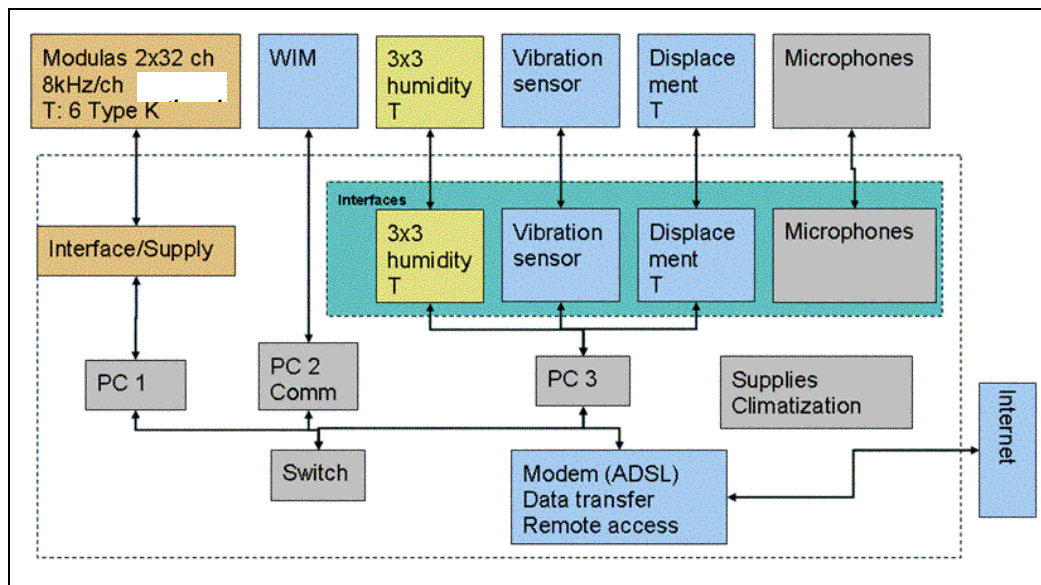


Figure A. 11: Overview of the Data Acquisition System on the Swiss Motorway

WIM data

The WIM data should log all vehicles above a certain weight. Axle load total weight, number of vehicles and axles as well as the speed should be recorded (depending on the number of truck passages daily a file of about 800 kB is generated). The WIM data can be used to identify single passages. All the other data can then be searched by time stamp according to this selected passage.

Vibration data

The vibration data require a minimum sample frequency of 2 kHz. A threshold value provides the possibility to reduce the amount of data, so only valid vibration data from a passage will be saved.

Noise data

The noise data require a sample frequency of 50 kHz and can be reduced after passage of the vehicle.

Pavement deformation data

The magnetostrictive sensors which measure the deformations within the pavement layers should be sampled at a frequency of 250-300 Hz. This is sufficient for speeds up to 100 km/h.

Temperature and humidity data

To correlate footprint data, temperature and humidity data are also required for each passage.



Tyre pressure

The system can measure the load distribution under the tyre by means of 64 piezo electric sensors. The raw data are stored in a binary file of 1 MB size (= 4096 points x 64 channels x 4 Byte) and can be subsequently reduced. A limit value defines the minimal force in a channel for a detection of a vehicle passage. If in a file the signals of all 64 channels are below this limit, the raw data will be deleted immediately. After a detection of a passage, a second limit value defines the noise level. All values below this limit will be deleted in order to reduce the measurement points to the relevant data of the vehicle passage. The size of this reduced array depends on the speed and the Tyre size. The reduced data will then be saved with the exact time stamp name as a binary file, together with a log file containing the information of the active channels. The raw data can then be deleted.